Government of **Western Australia**
Department of **Mines and Petroleum**

RECORD 2011/23

THE GEOLOGY OF THE EAST ALBANY–FRASER OROGEN — A FIELD GUIDE

by
CV Spaggiari, CL Kirkland, MJ Pawley, RH Smithies, MTD Wingate, MG Doyle, TG Blenkinsop, C Clark, CW Oorschot, LJ Fox, and J Savage


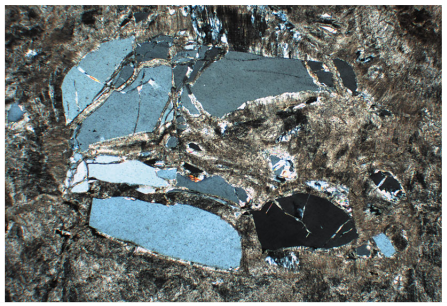


Geological Survey of Western Australia

Government of **Western Australia**
Department of **Mines and Petroleum**

Record 2011/23

THE GEOLOGY OF THE EAST ALBANY–FRASER OROGEN — A FIELD GUIDE

by
CV Spaggiari, CL Kirkland, MJ Pawley, RH Smithies, MTD Wingate, MG Doyle[1], TG Blenkinsop[2], C Clark[3], CW Oorschot[3], LJ Fox[1], and J Savage[1]

[1] **AngloGold Ashanti Ltd, Level 13, St Martins Tower, PO Box Z5046, Perth, WA 6831**
[2] **Economic Geology Research Unit, School of Earth and Environmental Science, James Cook University, Townsville, QLD 4811**
[3] **Department of Applied Geology, Curtin University of Technology, Perth, WA 6845**

Perth 2011

Geological Survey of Western Australia

MINISTER FOR MINES AND PETROLEUM
Hon. Norman Moore MLC

DIRECTOR GENERAL, DEPARTMENT OF MINES AND PETROLEUM
Richard Sellers

EXECUTIVE DIRECTOR, GEOLOGICAL SURVEY OF WESTERN AUSTRALIA
Rick Rogerson

REFERENCE
The recommended reference for this publication is:
Spaggiari, CV, Kirkland, CL, Pawley, MJ, Smithies, RH, Wingate, MTD, Doyle, MG, Blenkinsop, TG, Clark, C, Oorschot, CW, Fox, LJ and Savage, J 2011, The geology of the east Albany–Fraser Orogen — a field guide: Geological Survey of Western Australia, Record 2011/23, 97p.

National Library of Australia Card Number and ISBN 978-1-74168-411-7

Grid references in this publication refer to the Geocentric Datum of Australia 1994 (GDA94). Locations mentioned in the text are referenced using Map Grid Australia (MGA) coordinates, Zone 51. All locations are quoted to at least the nearest 100 m.

Published 2011 by Geological Survey of Western Australia
This Record is published in digital format (PDF) and is available online at <http://www.dmp.wa.gov.au/GSWApublications>.

Further details of geological products and maps produced by the Geological Survey of Western Australia are available from:
Information Centre
Department of Mines and Petroleum
100 Plain Street
EAST PERTH WESTERN AUSTRALIA 6004
Telephone: +61 8 9222 3459 Facsimile: +61 8 9222 3444
www.dmp.wa.gov.au/GSWApublications

Contents

Figures

Tables

Plates

The geology of the east Albany–Fraser Orogen — a field guide

by

CV Spaggiari, CL Kirkland, MJ Pawley, RH Smithies, MTD Wingate, MG Doyle[1], TG Blenkinsop[2], C Clark[3], CW Oorschot[3], LJ Fox[1], and J Savage[1]

Preface

The Albany–Fraser Orogen lies along the southern and southeastern margins of the West Australian Craton (WAC; Fig. 1). The orogen is dominated by Paleoproterozoic and Mesoproterozoic rocks that formed along, or close to, the margin of the Yilgarn Craton, resulting in successive episodes of reworking of that margin. Fragments of Archean crust, interpreted to be remnants of the Yilgarn Craton, are preserved within the Proterozoic crust that forms the bulk of the orogen. These fragments — present at the kilometre- to grain-scales, the latter indicated by the isotopic record preserved in zircon — may have contained sources of economic minerals or elements, such as gold. In addition, Paleoproterozoic and Mesoproterozoic events are likely to have provided opportunities for focusing or concentrating Yilgarn-sourced components into economic deposits, as well as enabling access to new sources during orogenic processes.

A preliminary version of this field guide was prepared for use during two, back-to-back, four-day excursions through the eastern part of the Albany–Fraser Orogen. The aim of these excursions was to provide a better understanding of the geological evolution of this largely greenfields region, and to present an overview of the recent geoscientific work carried out in the region by Geological Survey of Western Australia (GSWA) and its research partners. Much of the area described has had very little previous work, particularly the Tropicana region in the far northeast. There are also vast areas covered either by regolith, or by the younger cover rocks of the Gunbarrel and Eucla Basins. Because of this, large driving distances are required to reach areas with optimal outcrop in order to see most tectonic units and critical geological relationships. The large driving distances adds to time constraints, and limits the number of outcrops that can be visited during the excursions. For these reasons, this field guide includes extra details and illustrations of critical outcrops that lack good track access.

This field guide is presented in two parts: Part 1 is a review of the geology of the east Albany–Fraser Orogen and its tectonic setting, whereas Part 2 provides descriptions of each of the excursion localities, including relevant information about adjacent areas that are difficult to access. Part 2 also provides an overview of the geology of the Tropicana area, which is visited in Excursion 2. Note that much of the region covered by this guide is in remote country, and access restrictions apply in certain areas: these details are provided in the logistics section of Appendix 1 or at the beginning of individual locality descriptions. Also provided are three plates: Plate 1 is an interpreted bedrock geology map at 1:500 000 scale, which was simplified from the pre-Mesozoic, 1:250 000 scale, interpreted bedrock geology digital map layers in Geological Survey of Western Australia (2011). Plate 1A provides geophysical and remote sensing imagery of the area covered by Plate 1, and the geological reference for Plate 1. Plate 2 is an interpreted bedrock geology map, at 1:250 000 scale, of the Tropicana region, which was also extracted from the pre-Mesozoic, 1:250 000 scale, interpreted bedrock geology digital map layers in Geological Survey of Western Australia (2011).

The Albany–Fraser project: scope, collaborative work, and progress

The discovery of the >5 Moz gold deposit at Tropicana–Havana in the northeast of the Albany–Fraser Orogen highlighted the fact that very little was known about this orogen, particularly the more remote, eastern half. As a result, GSWA embarked on a program to rapidly gain an understanding of the whole orogen by 'mapping' the crust, primarily using geophysical (aeromagnetic and gravity) and isotopic (geochronological and geochemical) data. Unlike most mapping projects at GSWA, work on the Albany–Fraser project does not include systematic, regional, 1:100 000 scale geological mapping. This is

[1] AngloGold Ashanti Ltd, Level 13, St Martins Tower, PO Box Z5046, Perth, WA 6831

[2] Economic Geology Research Unit, School of Earth and Environmental Science, James Cook University, Townsville, QLD 4811

[3] Department of Applied Geology, Curtin University of Technology, Perth, WA 6845

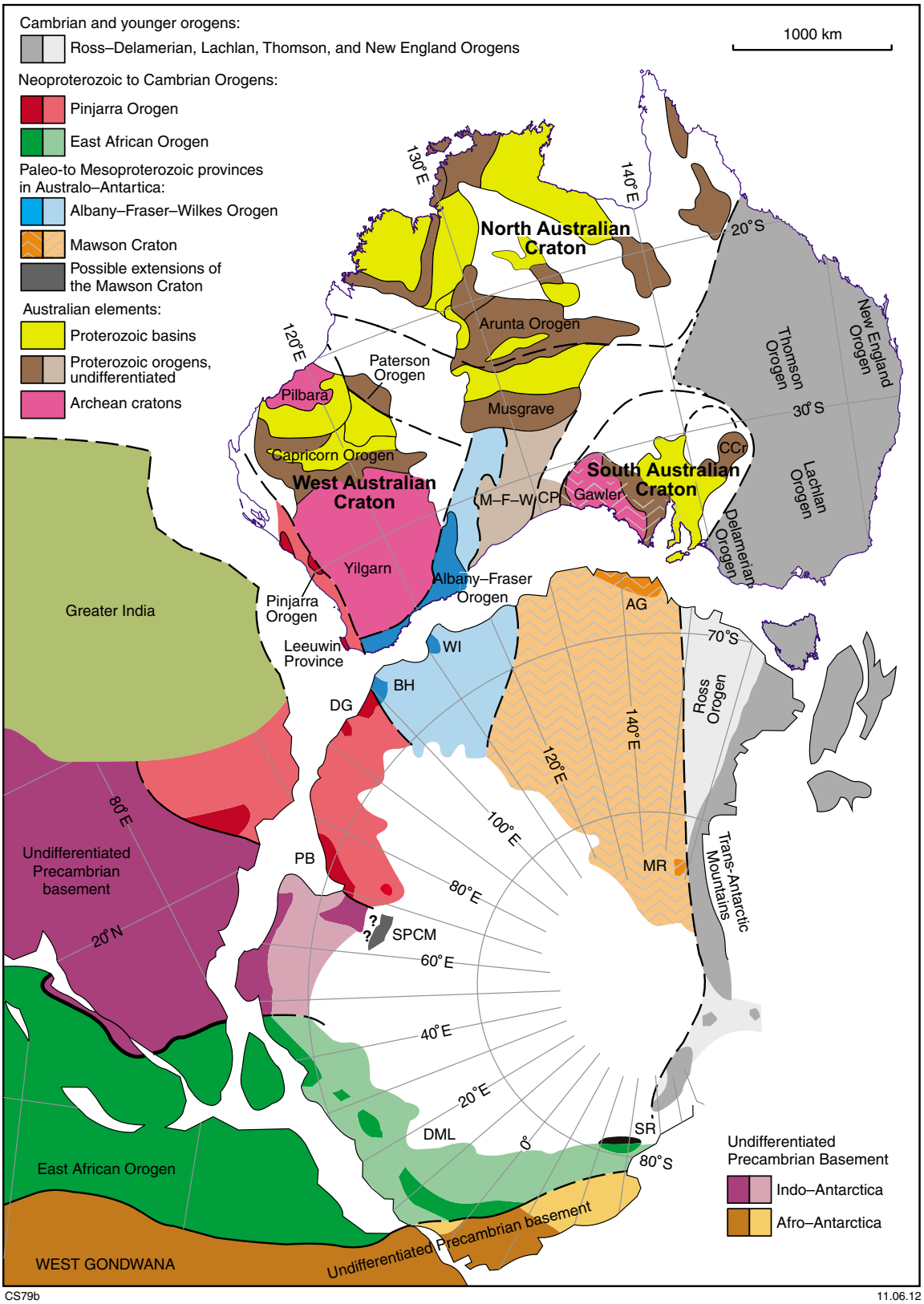

Figure 1. **Crustal elements of easternmost Gondwana (modified from Fitzsimons, 2003; Geoscience Australia, 1998; Tyler, 2005). Where lighter and darker shades of the same colour are shown, the lighter shade indicates large areas without outcrop, where the crustal element is inferred. Abbreviations used: AG = Terre Adélie – King George V Land; BH = Bunger Hills; CCr = Curnamona Craton; CP = Coompana Province (concealed by the Officer and Eucla Basins); DG = Denman Glacier region; DML = Dronning Maud Land; M–F–W = Madura, Forrest, and Waigen Provinces (undivided; concealed by the Gunbarrel, Officer, and Eucla Basins); MR = Miller Range; PB = Prydz Bay; SPCM = southern Prince Charles Mountains; SR = Shackleton Range; WI = Windmill Islands.**

due to the vast area that the orogen covers (Figs 1 and 2), and the minimal bedrock outcrop available in most regions. The project commenced in 2006 with the release of the South Yilgarn aeromagnetic dataset, focusing on the central part of the orogen (Geological Survey of Western Australia, 2007; Spaggiari et al., 2009). The project has since expanded to the eastern part of the orogen and includes the collection and interpretation of new geophysical datasets, collection and analysis of major- and trace-element geochemistry, and a more extensive geochronology/isotopic analysis (U–Pb, Lu–Hf, and Sm–Nd) program funded in part through the Exploration Incentive Scheme (EIS). The Co-funded Drilling Exploration Program of the EIS is also providing valuable drillcore for sampling, and information from the various companies involved. In the past two years, GSWA has worked in collaboration with research staff at the Department of Applied Geology, Curtin University, on understanding metamorphic P–T conditions and the timing of metamorphism using monazite geochronology. Two honours theses from this collaboration have been completed (Oorschot, 2011; Adams, 2011, 2012).

The project has focused on the Archean and Paleoproterozoic areas adjacent to the Yilgarn Craton margin in the eastern part of the Albany–Fraser Orogen, with the aim being to gain an understanding of the character of that margin and its relationship to gold mineralization. We are also currently moving further east, which includes looking at the Mesoproterozoic history, but as we do so, the Proterozoic rocks become increasingly obscured beneath the Eucla and Bight Basins (Figs 2 and 3). The aim in this eastern region is to produce an interpreted bedrock geology map of the basement beneath the Eucla Basin, utilizing drillcore and geophysical data to help define both the nature of that basement, and the extent of the orogen. Through EIS funding, and in addition to the co-funded drilling, several stratigraphic holes are planned to test interpretations and constrain the basement geology.

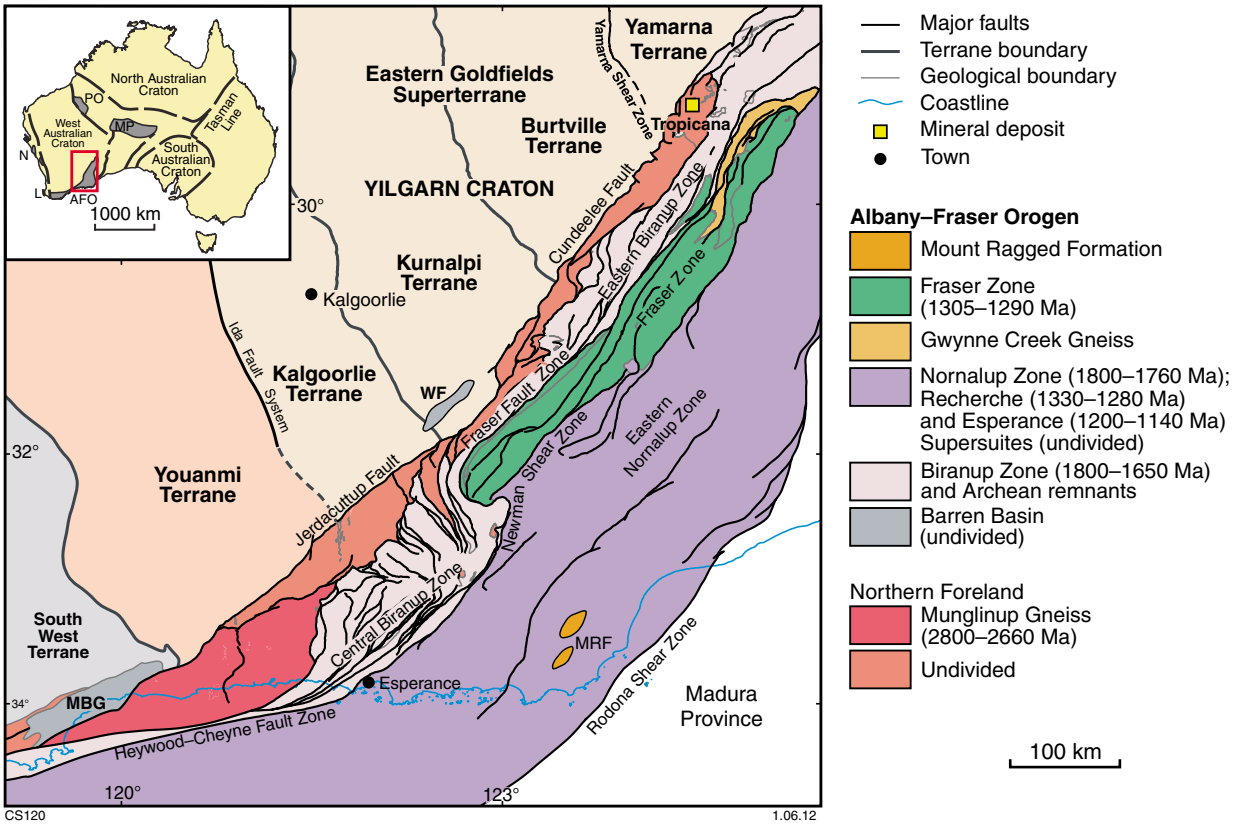

Figure 2. Simplified, pre-Mesozoic interpreted bedrock geology of the eastern Albany–Fraser Orogen and tectonic subdivisions of the Yilgarn Craton (modified from Cassidy et al., 2006; Spaggiari et al., 2009; Geological Survey of Western Australia, 2011; Pawley et al., in press). Abbreviations used: AFO = Albany–Fraser Orogen; L = Leeuwin Province; MBG = Mount Barren Group; MP = Musgrave Province; MRF = Mount Ragged Formation; N = Northampton Province; PO = Paterson Orogen; WF = Woodline Formation.

The geology of the east Albany–Fraser Orogen — a field guide: part 1

This section outlines the tectonic setting and current nomenclature for the Albany–Fraser Orogen, and defines and briefly describes its major tectonic units, lithological units, and events. A geological history of the orogen and interpreted tectonic models are also presented. Unless stated otherwise, all geochronological dates reported in this field guide are U–Pb age determinations from zircon grains dated by ion microprobe (SHRIMP), and are quoted with 95% confidence intervals. Published Geochronology Records for dated samples are referenced normally; uncited results should be considered as 'in preparation'.

Tectonic setting of the Albany–Fraser Orogen

The Albany–Fraser Orogen lies along the southern and southeastern margin of the Archean Yilgarn Craton, which is part of the West Australian Craton (Fig. 1). Apart from probable extensions in East Antarctica, all of the known tectonic units of the Albany–Fraser Orogen are located within Western Australia. The orogen is interpreted to be part of the larger Australo–Antarctic, Albany–Fraser–Wilkes Orogen that was linked prior to the breakup of Gondwana (Fitzsimons, 2003). The Wilkes Land coast in East Antarctica is part of East Gondwana, and has outcrops of ortho- and paragneisses with a similar Mesoproterozoic history, in terms of the timing of magmatism and metamorphism, to the Albany–Fraser Orogen. A potential Paleoproterozoic connection is denoted by the presence of granodioritic gneiss dated at 1699 ± 15 Ma (Sheraton et al., 1992; Fitzsimons, 2003).

To the west, the Albany–Fraser Orogen is truncated by the late Mesoproterozoic to Neoproterozoic Darling Fault Zone and Pinjarra Orogen. To the northeast, it is overlain by the Officer and Gunbarrel Basins, but shares a similar temporal Mesoproterozoic history with the Musgrave Province (Myers et al., 1996; Kirkland et al., 2010a). Although this temporal link suggests that the Albany–Fraser Orogen and Musgrave Province may once have been contiguous, there are distinct differences in their evolution that indicate otherwise. Alternatively, the Albany–Fraser Orogen may curve to the northwest beneath the Officer Basin, following the eastern Yilgarn Craton margin, and link with the Capricorn Orogen and/or the northern parts of the Paterson Orogen. The eastern margin of the Albany–Fraser Orogen is obscured by the Eucla Basin, and the orogen's margin in that direction is inferred to coincide approximately with the location of the Rodona Shear Zone (Fig. 3).

The Albany–Fraser Orogen is divided into a foreland component (the Northern Foreland), a younger, pre-Stage I amalgamation basement component (the Kepa Kurl Booya Province), the Recherche and Esperance Supersuites (formerly the Recherche Granite and Esperance Granite), and three major basins (Spaggiari et al., 2009). The Kepa Kurl Booya Province is further divided into the fault-bound tectonic units of the Biranup Zone (formerly the Biranup Complex), the Fraser Zone (formerly the Fraser Complex), and the Nornalup Zone (formerly the Nornalup Complex) (Fig. 2; Myers, 1985, 1990a, 1995b; Spaggiari et al., 2009). These units are described below in 'Tectonic subdivisions of the Albany–Fraser Orogen'.

The main tectonic events recognized so far in the Albany–Fraser Orogen (Fig. 4) are the newly defined Paleoproterozoic Biranup Orogeny, which includes the c. 1680 Ma Zanthus Event (Kirkland et al., 2011a), and the Mesoproterozoic Albany–Fraser Orogeny, which took place in two stages: 1345–1260 Ma (Stage I) and 1215–1140 Ma (Stage II) (Clark et al., 2000; Bodorkos and Clark, 2004a). Stage I has been interpreted to reflect the northwest-directed convergence and subsequent collision of the combined South Australian and Mawson Cratons with the West Australian Craton, whereas Stage II has been interpreted to reflect intracratonic orogenesis (Bodorkos and Clark, 2004b; Spaggiari et al., 2009). These events, and in particular Stage II, have formed the preserved crustal architecture, dominated by craton-directed, fault-bound thrust slices of largely mid-crustal, high grade-rocks (Spaggiari et al., 2009 and references therein; Geological Survey of Western Australia, 2007, 2011).

Eastern Goldfields Superterrane — subdivisions and geology

This section provides an overview of the Eastern Goldfields Superterrane. Understanding this superterrane is important because of its close relationship to the eastern Albany–Fraser Orogen along its northwestern margin (Plate 1; Fig. 2), and due to the potential for Eastern Goldfields Superterrane fragments to be preserved within the eastern parts of the orogen.

The Eastern Goldfields Superterrane (Fig. 2), which was previously known as the Eastern Goldfields Province (Gee et al., 1981), comprises four terranes — the Kalgoorlie, Kurnalpi, Burtville, and Yamarna Terranes — located to the east of the Ida and Waroonga Faults (Cassidy et al., 2006; Pawley et al., in press). Terrane divisions are based on geological, geophysical, geochemical, isotopic, and geochronological data. The region west of the Ida Fault, now called the Youanmi Terrane, forms the nucleus of the Yilgarn Craton, and has been interpreted as the proto-craton onto which the Eastern Goldfields Superterrane was accreted (Cassidy et al., 2006).

The lithostratigraphic sequence within the Kalgoorlie Terrane includes the 2715–2692 Ma mafic–ultramafic

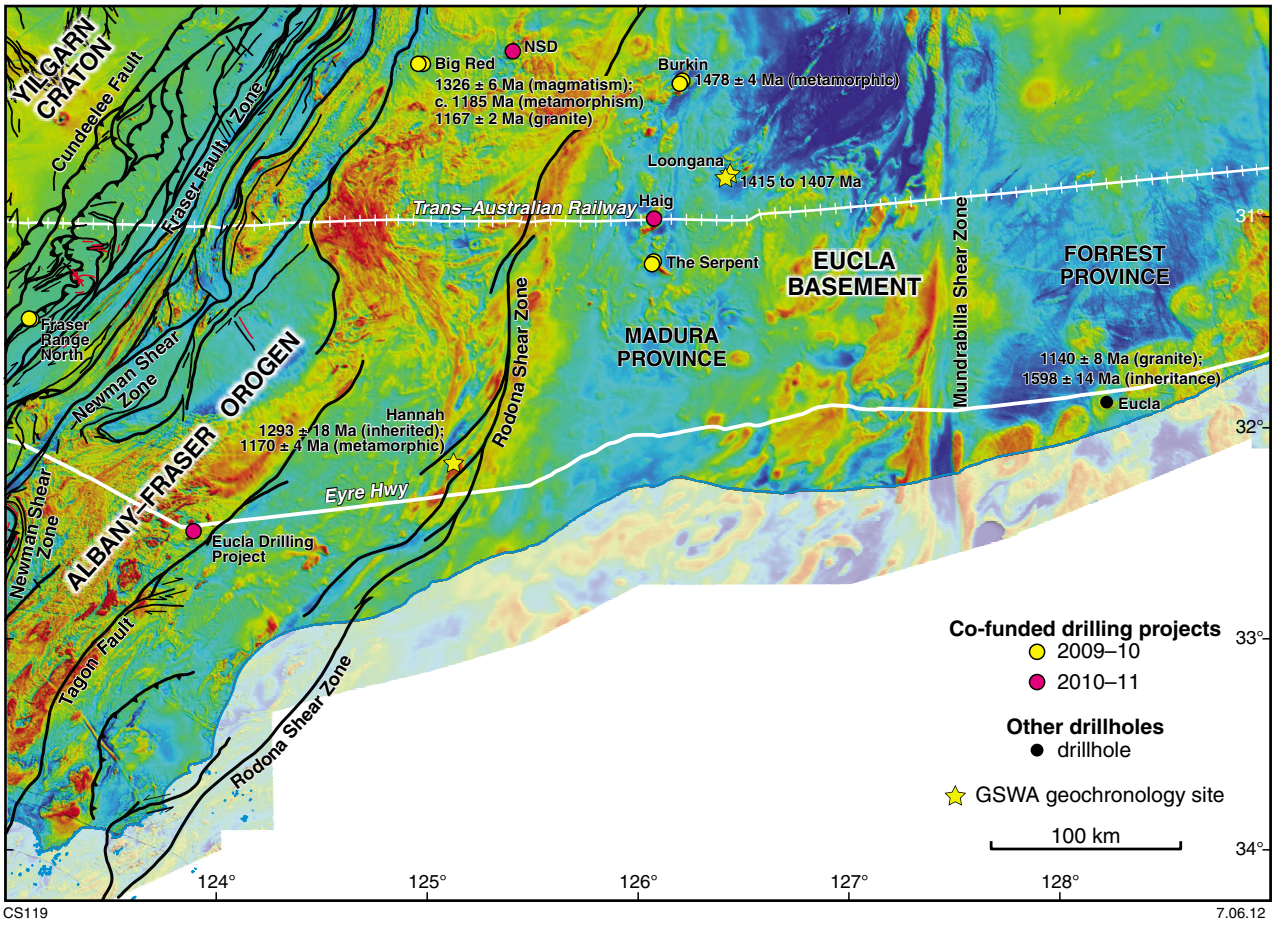

Figure 3. Aeromagnetic image, including preliminary Eucla data, covering the eastern Albany–Fraser Orogen and Eucla Basin, showing major tectonic units and structures, and the locations of drillholes and geochronology sites referenced in this guide.

Kambalda Sequence, which is overlain by felsic volcanic and volcaniclastic rocks of the 2686–2666 Ma Kalgoorlie Sequence (Kositcin et al., 2008; Swager, 1997). These rocks have been interpreted as having been deposited in an extensional back-arc setting (Krapež and Barley, 2008) and influenced by a mantle plume, as inferred by the widespread presence of ultramafic lavas (Campbell et al., 1989). The western Kurnalpi Terrane contains 2695–2675 Ma bimodal (basalt–rhyolite) volcanic rocks (Kositcin et al., 2008), which are interpreted to represent a rifted, mature-arc system (Barley et al., 2008). The eastern part of the Kurnalpi Terrane contains the 2715–2704 Ma calc-alkaline, andesite-dominated complexes of the Kurnalpi Sequence, which are interpreted as a series of intra-arc complexes (Barley et al., 2008). The rocks of the Kalgoorlie and Kurnalpi Terranes are overlain by a series of c. 2660 Ma, fault-related, late basins, interpreted to be associated with terrane amalgamation (Krapež et al., 2008).

Farther east, the northeast Yilgarn Craton comprises a number of greenstone packages, which fall into four periods, dated at 2970–2910 Ma, 2815–2800 Ma, 2775–2735 Ma, and 2715–2630 Ma (Pawley et al., in press). The distribution of these packages defines two terranes separated by the Yamarna Shear Zone (Fig. 2). The greenstones west of the Yamarna Shear Zone are older than 2735 Ma and form the Burtville Terrane, whereas the greenstones east of the Yamarna Shear Zone are younger than c. 2715 Ma and form the Yamarna Terrane. The greenstones in the Burtville Terrane are similar in age and character to older greenstones in the western Youanmi Terrane. In contrast, the greenstones of the Yamarna Terrane have age and lithological affinities with the rocks of the Kalgoorlie Terrane (in the western part of the Eastern Goldfields Superterrane), particularly the upper basalt of the Kambalda Sequence and the felsic rocks of the Kalgoorlie Sequence (Kositcin et al., 2008).

The age and rock distributions suggest that the Youanmi and Burtville Terranes had a similar greenstone history prior to c. 2735 Ma, and were most likely contiguous during this time. Extension after c. 2720 Ma produced two separate crustal blocks, and magmatism and sedimentation in the intervening Kalgoorlie and Kurnalpi Terranes, as well as in the outboard Yamarna Terrane (Pawley et al., in press). The presence of scattered 'basement' fragments and older inherited zircons in rocks of the Kalgoorlie and

Kurnalpi Terranes, which also have similar age patterns to the Youanmi and Burtville Terranes, suggests the incorporation of older crustal components into the rocks of the younger terranes.

Five main granite types have been recognized in the Eastern Goldfields Superterrane (Champion and Sheraton, 1997), with most felsic magmatism occurring between c. 2720 and 2630 Ma (older granites are scattered across the superterrane). Although there is overlap in their ages, the magmatism responsible for the different granite types 'peaked' at different times.

- High-HFSE granites are a minor phase (~5%) generally restricted to the Kurnalpi Terrane, and have a magmatic age peak between 2720 and 2680 Ma.
- Mafic granites are also a minor phase (~5%) with a magmatic age peak between 2720 and 2680 Ma, and lesser volumes until <2655 Ma.
- High-Ca granites are the dominant granite type (~60%), and intruded between 2720 and 2655 Ma.
- Syenitic granites are a minor phase (~1%) ranging in age from 2675 to <2655 Ma, and are generally restricted to the Kurnalpi Terrane.
- Low-Ca granites are common (~25%), are typically younger than 2655 Ma, and are interpreted to be derived from the recycling of the older granitoids.

All of these granite types, apart from the high-HFSE and syenitic granites, have been recognized across the Eastern Goldfields Superterrane. The high-HFSE and mafic granites decrease in age from east to west, which is consistent with the age pattern seen in felsic volcanic rocks of the Kurnalpi Terrane, indicating the volcanic rocks were most likely co-magmatic with the granitic rocks.

Structural history of the Eastern Goldfields Superterrane

Although published structural studies differ in nomenclature (Blewett et al., 2010 and references therein; Swager, 1997), up to six main deformation events are recognized in the Eastern Goldfields Superterrane. Extension between c. 2720 Ma and c. 2670 Ma (D_1) was accompanied by deposition of the Kambalda Sequence. This was followed by several cycles of episodic transpression and extension/transtension between c. 2665 and c. 2635 Ma (Blewett et al., 2010), including: D_2 north-northwesterly trending upright folding and reverse faulting at c. 2665 Ma; D_3 northeasterly directed extension at 2665–2655 Ma, which produced shear zones that reached the base of the crust, extensional granite doming, and deposition of clastic sedimentary 'late basins' adjacent to these domes; D_{4a} tightening of the north-northwesterly trending folds and reverse faulting at c. 2655 Ma; D_{4b} north-northwesterly trending sinistral shearing and thrusting at 2655–2650 Ma, interpreted as due to minor rotation of the stress field; and D_5 north-trending dextral strike-slip shearing at 2650–2635 Ma. This sequence of deformation events has been ascribed to tectonic switching at a convergent boundary (Czarnota et al., 2010). According to Blewett et al. (2010), the final deformation event, which occurred after c. 2630 Ma, produced locally developed, minor vertical shortening with variable extension vectors attributed to thermal relaxation.

A major feature of the Eastern Goldfields Superterrane is the development of north-northwesterly trending shears and faults. A deep-crustal seismic traverse across the central part of the Eastern Goldfields Superterrane (Goleby et al., 2004) showed that the terrane-bounding Ockerburry and Hootanui Fault systems, and the Yamarna Shear Zone, are large-scale, east-dipping, listric structures that extend to the base of the crust. Such structures can have long and complex histories. For example, the Yamarna Shear Zone preserves three phases of deformation, including dextral strike-slip shearing in the footwall; tight to isoclinal folding and layer-parallel strike-slip shearing in the greenstones adjacent to the footwall, which is demonstrably contemporaneous with the footwall deformation; and sinistral strike-slip shearing in the hangingwall to the east (Pawley et al., 2009). Based on the age of the syn-kinematic Point Salvation Monzogranite, located in the footwall of the shear zone, the dextral strike-slip shearing has been constrained to c. 2664 Ma (Pawley et al., in press). This age is older than the 2650–2635 Ma timing proposed for dextral transtension by Blewett et al. (2010), suggesting that deformation may have been diachronous across the eastern Yilgarn Craton.

Isotopic constraints of the Eastern Goldfields Superterrane

Both Sm–Nd and Lu–Hf isotope data have provided insights into crustal growth processes in the Yilgarn Craton. The significance of the Ida Fault is highlighted by the Sm–Nd isotopic data, which indicates a change from older average crustal ages in the Youanmi Terrane, to younger crustal ages in the Eastern Goldfields Superterrane (Champion and Cassidy, 2007). New Lu–Hf isotope data obtained by GSWA reveal that mantle extraction occurred in the central Yilgarn Craton at 4.2, 3.5, 3.1, and 2.7 Ga (Wyche et al., in press). The earliest of these episodes of mantle extraction is not well expressed in the Eastern Goldfields Superterrane, implying that crust formation in this region post-dated the earliest development of the Yilgarn Craton. The isotopic data also suggest that magmas in the Eastern Goldfields Superterrane had a substantial juvenile input, whereas those in the central Yilgarn Craton involved reworking of older crust. Furthermore, the widespread occurrence of the 3.5 and 3.1 Ga mantle extraction events indicate that several episodes of major, possibly plume-related, heating occurred across the craton (Wyche et al., in press). This supports the interpretation that the Burtville and Youanmi Terranes had a common history extending back to c. 2960 Ma.

Gold mineralization in the Eastern Goldfields Superterrane

The Eastern Goldfields Superterrane has world-class gold

endowment, with structurally controlled mineralization occurring throughout most of its deformation history, and with some deposits recording multiple gold events (Blewett et al., 2010 and references therein). Only minor gold deposition occurred during D_1 (c. 2720 Ma and c. 2670 Ma) and D_2 (c. 2665 Ma; e.g. the Tarmoola Deposit), but it is from D_3 onwards that the volume of gold mineralization increased significantly. The development of the D_3 extensional shear zones between c. 2665 and c. 2655 Ma provided crustal-scale conduits for the transfer of mantle-derived magmas, fluids, and metals, and sites for gold deposition (e.g. Sons of Gwalia at Leonora). Several gold deposits, such as New Holland near Agnew, formed during D_{4a} (c. 2655 Ma) reverse dip-slip faulting, but it was the change in shortening direction during D_{4b} (2655–2650 Ma) that led to the formation of the largest gold deposits (e.g. Kalgoorlie, Sunrise Dam, St Ives, Kanowna Belle, and Lawlers). Blewett et al. (2010) proposed that rotation of the stress axes at 2655–2650 Ma led to sinistral shearing and the development of a new network of contractional and dilational jogs, which were favourable sites for fluid flow and traps for gold deposition. D_5 (2650–2635 Ma) transtension resulted in northerly trending, dextral shearing and development of associated brittle structures, which host mineralization at Sunrise Dam, St Ives, and Wiluna.

Eucla basement

Much of the eastern part of the Albany–Fraser Orogen, and all of the Madura, Forrest, Waigen, and Coompana Provinces farther east (Shaw et al., 1996), are covered by the Officer, Gunbarrel, and Bight and Eucla Basins (Figs 1 and 3). Because of this, very little is known about these basement tectonic units, although recently acquired aeromagnetic data are now providing valuable information about their structure and lithology (Fig. 3). Within this region, two major structures stand out: the Rodona Shear Zone and the Mundrabilla Shear Zone. Based on geochronology from drillcore to the east in the Madura Province (see below), the Rodona Shear Zone is currently inferred to approximate the eastern edge of the Albany–Fraser Orogen. The Mundrabilla Shear Zone is a prominent north–south structure that appears to separate two blocks of crust with different aeromagnetic and gravity signatures, and corresponds to the boundary between the Madura and Forrest Provinces. It is a long, wide, straight shear zone — the latter indicative of a subvertical orientation — with drag fabrics indicative of a sinistral shear sense, at least during its more recent history. The Mundrabilla Shear Zone apears to be coincident with a surface fault and a small present-day scarp through Miocene limestone of the Eucla Basin. Some of the other basement structures also appear to cut the limestone, indicating that they may have been reactivated, or have at least had an effect on the topography. Continent-scale gravity inversion modelling suggests that the Mundrabilla Shear Zone offsets the Mohorovičić discontinuity (the 'Moho') by up to 10 km, with the thinner crust on the western side displaced upwards relative to the thicker eastern side (Aitken, 2010). The timing of sinistral movement on the Mundrabilla Shear Zone may correspond with sinistral movement on the Darling Fault on the western margin of the Yilgarn Craton, denoted by significant rotation drag of the westernmost part of the Albany–Fraser Orogen during the late Neoproterozoic (Beeson et al., 1995; Fitzsimons, 2003). This event has been correlated with other late-stage faults in the Albany–Fraser Orogen, such as the north-northeasterly trending sinistral mylonite zones that cut Biranup Zone rocks west of Esperance, and c. 1140 Ma Esperance Supersuite granites nearby (Bodorkos and Clark, 2004b).

Exploration drilling in the Madura Province has intersected ultramafic, metagabbroic, and metagranitic rocks at the Loongana prospect southeast of Haig Cave; variably to strongly magnetic metagabbro at the Serpent prospect; and heterogeneous gneissic rocks, iron-rich layered quartz–chlorite–garnet schist, metamorphosed banded-iron formation (BIF), and amphibolite at the Burkin prospect (Fig. 3). Medium-grained granite from the Loongana prospect yielded a date of 1415 ± 7 Ma, interpreted as the age of igneous crystallization of the granitic protolith that either intrudes, or is coeval with, the mafic protolith in the same section of core (hole LNGD0002, depth interval 363.52 – 364.00 m; GSWA 178070, Nelson, 2005a). Pinkish-white, fine- and even-grained, unfoliated biotite microtonalite from a nearby hole, LNGD0001, yielded a date of 1408 ± 7 Ma, interpreted as the age of igneous crystallization (depth interval 611.80 – 612.50 m; GSWA 178071, Nelson, 2005b). The date of this microtonalite is identical to the interpreted igneous crystallization age of 1407 ± 7 Ma of pinkish-white, medium- to coarse-grained, foliated biotite tonalite gneiss taken from the same core (hole LNGD0001, depth interval 637.60 – 640.00 m; GSWA 178072, Nelson, 2005c). There are no tectonic units of this age in the Albany–Fraser Orogen, which is consistent with the interpretation that the Madura Province is not part of the Albany–Fraser Orogen, although detritus of this age does occur in metasedimentary rocks of the Fraser Range Metamorphics and Malcolm Metamorphics (Fig. 4). Based on aeromagnetic data, rocks along-strike to the northeast of these drillsites are interpreted to be cut by the Mundrabilla Shear Zone (Fig. 3). The Serpent prospect lies to the southwest of Loongana (Fig. 3), and is defined by an elongate, northwesterly trending magnetic high perpendicular to the dominant northeast-trend of the Loongana magnetic features. Diamond cores from the Serpent prospect show that it is dominated by variably to strongly magnetic metagabbro.

Drilling at the Burkin prospect (Fig. 3), about 50 km northeast of Loongana, intersected heterogeneous gneissic rocks cut by quartz veins, and locally, brecciation zones. The gneisses are described as banded quartz–chlorite–garnet schists with hematite and magnetite (possibly impure chert), metamorphosed BIF, and mafic amphibolite (unpublished GSWA Petrological Report, no. 9838). Preliminary geochronology of migmatitic gneiss (hole BKD002, 270.38 – 270.48 m depth; GSWA 182485) yielded a date of 1478 ± 4 Ma, interpreted as the age of migmatization and high-grade metamorphism. This indicates that the protolith to the gneiss is older than the c. 1410 Ma granites of the Loongana prospect. Leucosomes in the dated gneiss from the Burkin prospect crosscut a folded fabric, which indicates deformation prior

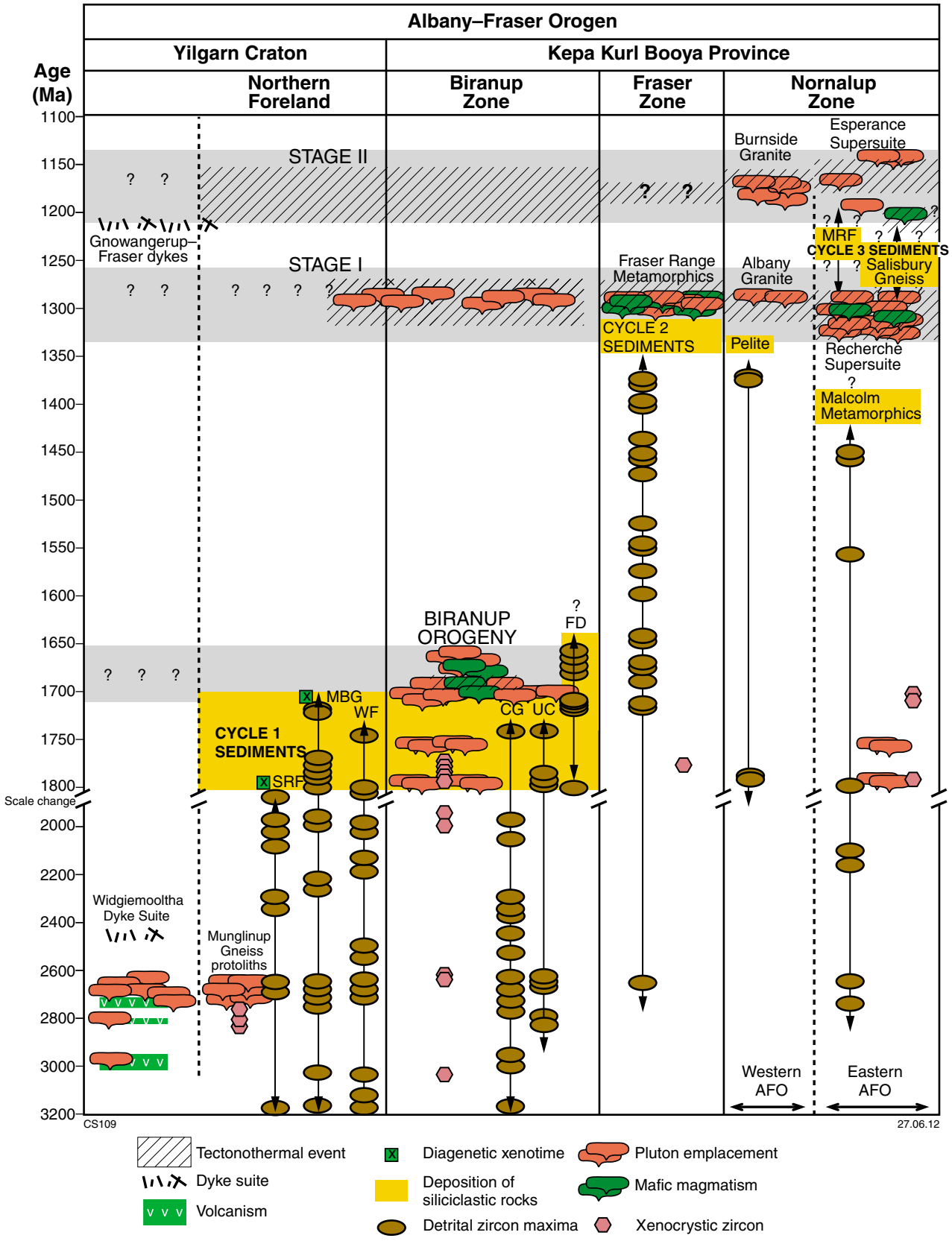

Figure 4. **Time–space diagram, showing age relationships between the Northern Foreland, Biranup Zone, Fraser Zone, and Nornalup Zone (modified from Spaggiari et al., 2009; age data from references therein, and given in text). Stages I and II are of the Albany–Fraser Orogeny. Cycle 1 sediments = Barren Basin; Cycle 2 sediments = Arid Basin (including the Gwynne Creek Gneiss); Cycle 3 sediments = Ragged Basin. Abbreviations used: AFO = Albany–Fraser Orogen; CG = Coramup Gneiss; FD = Fly Dam Formation; MBG = Mount Barren Group; MRF = Mount Ragged Formation; SRF = Stirling Range Formation; UC = unnamed conglomerate; WF = Woodline Formation.**

to migmatization. Three analyses of zircon cores from GSWA 182485 yielded dates of 2408–2293 Ma, possibly reflecting the ages of sedimentary detritus in the protolith, if the gneiss is interpreted as a metasedimentary rock. Four analyses of zircon cores from the same sample yielded a weighted mean date of 1538 ± 17 Ma, which could represent a maximum age of deposition.

East of the Mundrabilla Shear Zone, within the Forrest Province, the Alliance Petroleum Eucla No. 1 well lies over a distinctly ovoid geophysical feature with high magnetic intensity, interpreted as a late granitic intrusion (Fig. 3). It forms part of a set of northeasterly trending nested plutons with moderate to strong magnetic signatures. Small rock chips and mineral fragments from the base of the well (from 215–222 m; GSWA 194773) are interpreted to be derived from a granitic rock, and contain oscillatory zoned zircon grains that yielded a date of 1140 ± 8 Ma, interpreted as the magmatic crystallization age of the inferred granite protolith (Kirkland et al., 2011j). A single analysis on an unzoned zircon crystal yielded a date of 1598 ± 14 Ma, interpreted as either the age of an inherited component within the granite, or the age of zircon incorporated from another rock unit (e.g. a sedimentary rock) within the drillhole. The magnetic signature, together with the c. 1140 Ma age, suggests that the intrusion is related to the Esperance Supersuite of the Albany–Fraser Orogen. The nested plutons are cut by the Mundrabilla Shear Zone, indicating that at least one phase of movement on the structure post-dates these intrusions.

The Coompana Province, referred to as the Coompana Block in South Australia (Flint and Daly, 1993), lies adjacent to the western margin of the Gawler Craton, but is entirely covered by younger basin rocks. The only basement rock available for observation was obtained from the Mallabie 1 drillhole in South Australia, which intersected granitic gneiss at its base. The granitic protolith has been interpreted as an A-type granite that crystallized at 1505 ± 7 Ma, based on LA-ICP-MS dating of zircons (Wade et al., 2007). This is unlike any known ages of granitic rocks from the Albany–Fraser Orogen. However, the presence of a late Mesoproterozoic thermal overprint, shown by dating of the same drillcore (K–Ar hornblende and biotite ages of c. 1185 and 1159 Ma, respectively), does suggest a link to Stage II of the Albany–Fraser Orogeny (Webb et al., 1982; Fitzsimons, 2003; Wade et al., 2007).

Tectonic subdivisions of the Albany–Fraser Orogen

Northern Foreland

The Northern Foreland is defined as the portion of the Yilgarn Craton reworked during the Albany–Fraser Orogeny, thereby reflecting its proximity to the collisional orogenic belt (Figs 1 and 2; Myers, 1990a; Spaggiari et al., 2009). It includes the dominantly granitic rocks of the Munglinup Gneiss, which was previously included in the 'Biranup Complex' of Myers (1995b), but has been reassigned based on geochronological and isotopic data that indicate that much of it was originally part of the Yilgarn Craton (Spaggiari et al., 2009; Kirkland et al., 2011k). The Munglinup Gneiss is interpreted as a higher-grade, more strongly reworked component of the Northern Foreland, bound by major faults.

Reworking of the Yilgarn Craton in the Northern Foreland varied from moderate- to high-strain ductile deformation under amphibolite- to granulite-facies metamorphic conditions (Munglinup Gneiss and the southern part of the Mount Barren Group), to low- to moderate-strain, brittle to semi-brittle, greenschist to amphibolite conditions (Beeson et al., 1988; Myers, 1995a; Jones, 2006). This variation in conditions generally reflects lower strain conditions and lower metamorphic grade with increasing distance from the orogen (i.e. northwards), or the exhumation of shallower crustal levels of the Northern Foreland. In a section of the Pallinup River, west of Bremer Bay in the central Albany–Fraser Orogen, Beeson et al. (1988) described an increase in deformation intensity from north to south, with progressive overprinting of the regional, north-northwesterly trending Archean structures by Mesoproterozoic, Albany–Fraser Orogeny -related, west-southwesterly trending dextral shear zones and gneissic foliations. The northern limit of the Northern Foreland is defined by the presence of discontinuous and widely spaced shear zones (Beeson et al., 1988). Mafic dykes in the central Albany–Fraser Orogen also show the effects of increased deformation intensity, from north to south, within the Northern Foreland (Beeson et al., 1988; Spaggiari et al., 2009). In the north, magmatic textures and clear intrusive relationships are preserved, whereas towards the south, the dykes are metamorphosed and rotated parallel to the trend of the main, Albany–Fraser Orogeny -related fabric.

The Jerdacuttup and Cundeelee Faults are two linked, major, thrust faults separating Archean rocks of the Yilgarn Craton that show very minor to no Albany–Fraser Orogeny -related deformation effects, from the more strongly deformed, mixed Archean and Proterozoic rocks of the Northern Foreland (Plate 1; Fig. 2; Witt, 1997, 1998; Jones, 2006; Spaggiari et al., 2009; Geological Survey of Western Australia, 2011). In the northeastern part of the orogen near Tropicana, the Cundeelee Fault abuts a succession of Permian rocks that is at least 300 m thick (part of the Gunbarrel Basin), and which overlies the Yilgarn Craton. On the southeastern side of the fault, the Permian succession is much thinner, with small isolated remnants thinly overlying rocks of the Albany–Fraser Orogen (Plate 2). In this region, the Cundeelee Fault is interpreted as a thrust fault later reactivated as a normal fault, which probably acted as a paleo-fault scarp during the deposition of Permian glacial sediments (Geological Survey of Western Australia, 2011).

Munglinup Gneiss

The Munglinup Gneiss was first defined by Myers (1995b) as a gneissic unit derived from Archean granite, granodiorite, tonalite, and pegmatite, within the former Biranup Complex. The latter was interpreted as an allochthonous piece of Archean and Proterozoic crust accreted onto the Yilgarn Craton during the Albany–Fraser

Orogeny (Myers et al., 1996). The Munglinup Gneiss is now interpreted as a reworked part of the Yilgarn Craton based on similarities in lithologies, protolith ages (Fig. 5; Spaggiari et al., 2009), and Lu–Hf data (Kirkland et al., 2011k). It represents the southernmost exposures of the craton within elongate, craton-parallel, fault-bound packages of predominantly granitic gneiss. West of Ravensthorpe, in the central Albany–Fraser Orogen, the Munglinup Gneiss is part of the Northern Domain of Beeson et al. (1988), where it is bounded by the linked, south-dipping Boxwood Hill and Yungunup Pool Thrusts to the north, and the south-dipping Millers Point Thrust and Bremer Fault to the south (Geological Survey of Western Australia, 2007). The thrusts are high-strain zones that locally contain leucosomes, and are interpreted as oblique thrust faults with a component of dextral strike-slip movement (Beeson et al., 1988). South of the Mount Barren Group, the northern margin of the Munglinup Gneiss is bounded by the Jerdacuttup Fault (Fig. 2), which links with the Bremer Fault to the west. These faults are interpreted to form the northern edge of a separate, eastern fault-bound package of Munglinup Gneiss, with the Mount Barren Group contained within a separate thrust package between the two fault-bound slices of Munglinup Gneiss (cf. figs 2 and 15, Spaggiari et al., 2009).

The Jerdacuttup Fault has been interpreted as a major, south-dipping thrust accommodating a component of dextral strike-slip movement, and was partly responsible for the exhumation of the Munglinup Gneiss (Myers, 1990a; Witt, 1997, 1998). To the southeast, in the Esperance region, the Munglinup Gneiss is bounded by the Red Island Shear Zone, which is interpreted as the present-day expression of the boundary between the reworked component of the Yilgarn Craton (Northern Foreland) and Biranup Zone rocks of the Kepa Kurl Booya Province (Figs 2 and 6a; Geological Survey of Western Australia, 2011).

The Munglinup Gneiss comprises amphibolite- to granulite-facies orthogneiss interlayered with lenses of metamorphosed mafic rocks, some of which are interpreted as metamorphosed mafic dykes or sills. Minor banded metachert (jaspilite), amphibolitic schist, serpentinite, and metamorphosed ultramafic rocks are interpreted as remnants of Archean greenstone sequences (Thom et al., 1977; Beeson et al., 1988; Myers, 1990a). Isolated lenses of mafic and ultramafic rocks, including some with historic nickel deposits (e.g. the Young River Nickel prospect, east of Ravensthorpe), are also interpreted to be remnants of Archean greenstone intruded by the granitic precursors to the orthogneiss (Thom et al., 1977; Geological Survey of Western Australia, 2007).

Geochronological data (Nelson et al., 1995) have shown that the orthogneisses were derived from late Archean precursors, and more recent data (Spaggiari et al., 2009) have further refined these ages. The geochronological data indicate at least four phases of granitic magmatism: at c. 2709, 2680, 2660, and 2630 Ma. These are comparable to the typical ages of granite magmatism in the Yilgarn Craton (Cassidy et al., 2006 and references therein) and thereby support the interpretation that the granitic precursors to the Munglinup Gneiss were part of the Yilgarn Craton.

The oldest granitic phases recognized in the Munglinup Gneiss are a migmatitic granitic gneiss from the headland west of Quagi Beach (Stop 1 on Fig. 6a; GSWA 184334), and a medium- to dark-grey, strongly foliated monzogranitic gneiss with well-developed differentiated layering (GSWA 184120) outcropping along the Pallinup River, west of Bremer Bay, in the central Albany–Fraser Orogen (Spaggiari et al., 2009). The migmatitic granitic gneiss yielded an upper intercept date of 2709 ± 35 Ma, interpreted as the magmatic crystallization age of the granitic protolith (GSWA 184334, Kirkland et al., 2011b). The monzogranitic gneiss from the Pallinup River yielded an interpreted igneous crystallization date of 2681 ± 5 Ma (GSWA 184120, Bodorkos and Wingate, 2008a).

The most abundant phase in the Munglinup Gneiss is a leucocratic, banded, tonalitic to monzogranitic gneiss. The gneissic fabric appears to be intruded by sheets of a porphyritic monzodiorite, and both granitic phases pre-date at least two episodes of folding (Spaggiari et al., 2009). Zircons from the two phases, observed at Powell Point, about 70 km west of Quagi Beach in the central Albany–Fraser Orogen, give igneous crystallization dates that are within uncertainty of each other: 2660 ± 13 Ma for the leucocratic tonalitic gneiss (GSWA 184128, Bodorkos and Wingate, 2008c), and 2658 ± 21 Ma for the porphyritic monzodiorite (GSWA 184127, Bodorkos and Wingate, 2008b). These dates are also within uncertainty of a less well-constrained date, also interpreted to reflect igneous crystallization, of 2661 ± 5 Ma, which comes from a banded leucocratic granodioritic gneiss located approximately 70 km northeast of Powell Point on the Lort River (GSWA 184314, Bodorkos and Wingate, 2008d).

The Munglinup Gneiss includes at least one phase of granitic gneiss that has a Proterozoic protolith. Biotite granodioritic gneiss from near Bald Rock on the Lort River gave an igneous crystallization date of 1299 ± 14 Ma (GSWA 83690, Nelson, 1995g). This date corresponds with Stage I of the Albany–Fraser Orogeny (1345–1260 Ma; Clark et al., 2000), and is the only available data indicating that event's effect on the Munglinup Gneiss. It is also the only evidence of magmatism associated with the 1330–1280 Ma Recherche Supersuite as yet identified within the Northern Foreland. At this locality, the orthogneiss is well-lineated, and contains numerous millimetre- to centimetre-scale mafic layers, some of which are probably deformed and metamorphosed mafic dykes (Spaggiari et al., 2009). Both the mafic layers and orthogneisses contain folded felsic veins. Similar mafic horizons can be found throughout the Munglinup Gneiss and may represent deformed remnants of the Gnowangerup–Fraser Dyke Suite, which intruded at c. 1210 Ma (see 'Mafic dyke suites' section).

Although the data are sparse, dates indicating metamorphism in the Munglinup Gneiss fall within the interval for Stage II of the Albany–Fraser Orogeny (1215–1140 Ma; Clark et al., 2000). The leucocratic tonalitic gneiss from Powell Point yielded a group of eight analyses from within zircon grain edges and rims with very low Th/U ratios (mostly <0.15) that gave a weighted mean date of 1195 ± 17 Ma (GSWA 184128, Bodorkos and Wingate, 2008c; GSWA 184217, Bodorkos and

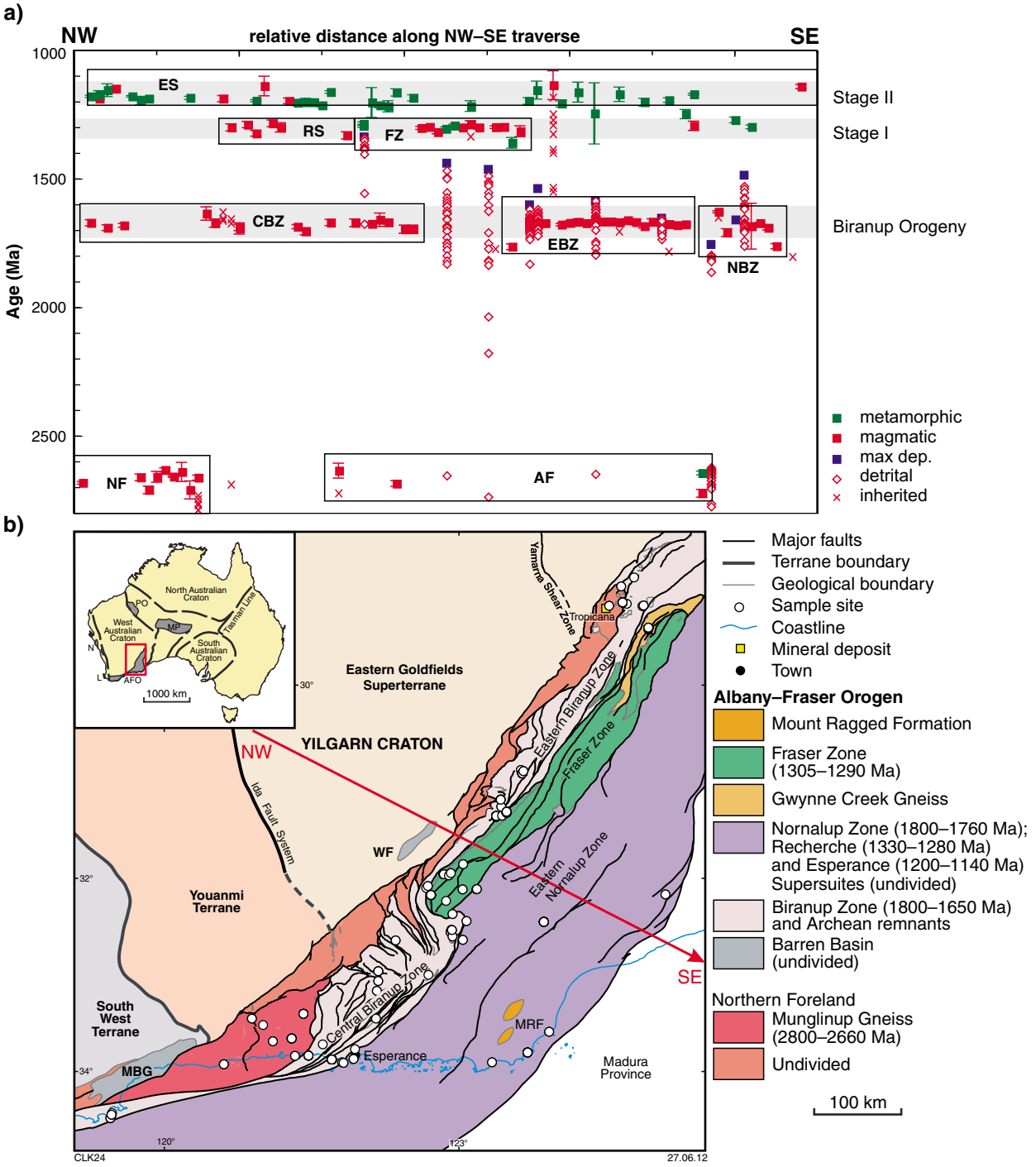

Figure 5. **a) Time–space diagram of U–Pb ages from the Albany–Fraser Orogen, arranged according to distance away from the Yilgarn Craton centre, towards the southeast. The diagram includes all ion microprobe (SHRIMP) U–Pb zircon and baddeleyite ages determined by the Geological Survey of Western Australia within the region. All of this data can be viewed at <http://www.dmp.wa.gov.au/geochron>; b) simplified interpreted bedrock geology map of the east Albany–Fraser Orogen and east Yilgarn Craton (modified from Spaggiari et al., 2009 and Geological Survey of Western Australia, 2011), showing the locations of the geochronology samples plotted in part a). Abbreviations used: AF = Archean fragments; AFO = Albany–Fraser Orogen; CBZ = central Biranup Zone; EBZ = eastern Biranup Zone; ES = Esperance Supersuite; FZ = Fraser Zone; L = Leeuwin Province; MBG = Mount Barren Group; MP = Musgrave Province; MRF = Mount Ragged Formation; N = Northampton Province; NBZ = northern Biranup Zone; NF = Northern Foreland; PO = Paterson Orogen; RS = Recherche Supersuite; WF = Woodline Formation.**

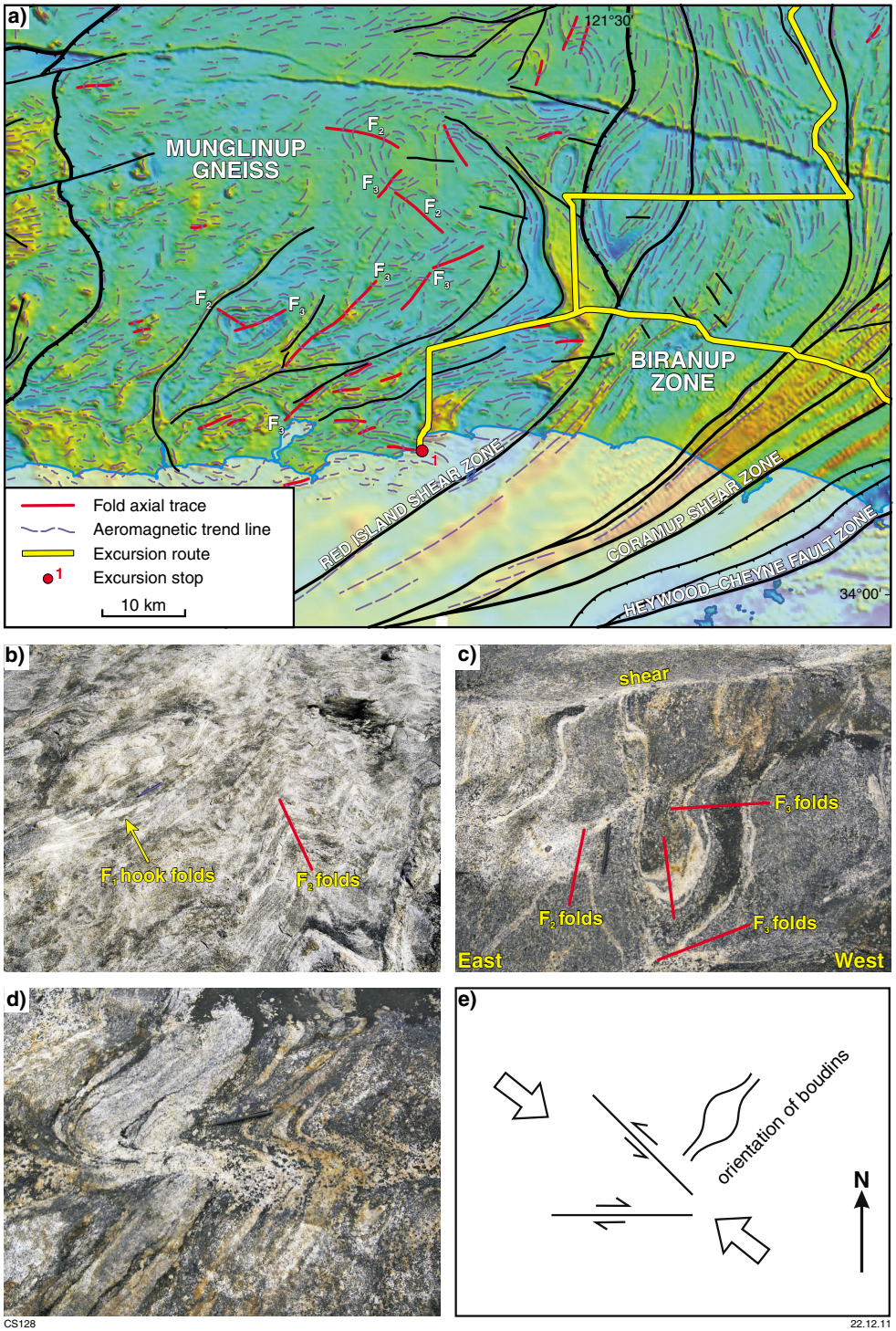

Figure 6. **a) Reduced-to-pole (RTP) aeromagnetic image and structural interpretation of the Munglinup Gneiss in the area around, and to the north of, Quagi Beach (Excursion 1, Stop 1). The image shows the area's magnetic character and large-scale refolded folds. The fold generations are denoted F_2 and F_3, accordingly. The Red Island Shear Zone marks a major boundary between the Munglinup Gneiss (Northern Foreland) and the Biranup Zone, which has a completely different magnetic character. Modified from Spaggiari et al. (2009); b) small-scale F_1 hook folds in layering of leucocratic Munglinup Gneiss, refolded by larger-scale, regional, north-trending F_2 folds; Powell Point (MGA 274527E 6243949N). The blue pen near the hook fold indicates the scale; c) northerly trending tight to isoclinal F_2 folds, refolded by easterly to east-northeasterly trending F_3 folds in both the leucocratic tonalitic and porphyritic monzodioritic parts of the Munglinup Gneiss; Powell Point (MGA 274527E 6243949N). The black pen in the centre of the image indicates the scale; d) asymmetric, northeasterly trending F_3 folds cut by leucosome-filled shears in the Munglinup Gneiss. These folds are developed in both the leucocratic tonalitic gneiss and the porphyritic monzodiorite at Powell Point (MGA 274527E 6243949N). The black pen in the centre of the image indicates the scale; e) interpretative sketch of conjugate shears in the Munglinup Gneiss, indicating northwest–southeast compression, with boudinage indicating orthogonal extension during Stage II of the Albany–Fraser Orogeny. In this interpretation, the shear crosscutting F_3 folds in part d) is an example of one half of a conjugate pair.**

Wingate, 2008b). Migmatitic gneiss from west of Quagi Beach (GSWA 184334, Kirkland et al., 2011b) yielded a date of 1184 ± 6 Ma from two analyses of zircon rims, indicative of high-grade metamorphism at this time.

The Munglinup Gneiss has been affected by at least three phases of folding, and is locally sheared and boudinaged (Spaggiari et al., 2009). Megascale structures are well-defined in aeromagnetic imagery, particularly as fold interference patterns, due to the presence of magnetite in the metamorphic fabrics (Fig. 6a). The fold patterns correspond to mesoscale structures in outcrop, where early hook folds (F_1) of gneissic banding in leucocratic tonalitic gneiss are refolded into approximately north-trending, open to tight folds (F_2; Fig. 6b). These are refolded by easterly to northeasterly trending tight folds, which are parallel to the dominant trend of the orogen (F_3; Fig. 6c). The F_2 and F_3 folds are interpreted to correlate with the megascale refolded folds visible in the aeromagnetic imagery (Fig. 6a). These folds are cut by shears that locally contain leucosomes, which indicates that this last phase of deformation took place at high temperatures, probably at the upper amphibolite to granulite facies (Fig. 6c,d). In outcrop, dextral shears trend predominantly in an easterly direction, whereas sinistral shears trend predominantly to the northwest. Both post-date the folding and can be interpreted as conjugates, indicative of northwest–southeast compression (Fig. 6e). The Munglinup Gneiss is also locally boudinaged, but the timing of the boudinage with respect to folding is not clear. The boudins mostly trend parallel to the orogen, and do not appear to be folded. This suggests they are relatively late-stage and may relate to extension of the orogen in a northeast–southwest orientation, perpendicular to the shortening direction indicated by the conjugate shearing (Fig. 6e).

Given that the late stages of deformation appear to have been in the upper amphibolite to granulite facies, it is likely that the shearing, and possibly the third phase of folding, which is parallel to the regional trend of the orogen, occurred during Stage II of the Albany–Fraser Orogeny. This is supported by the ages of 1210–1180 Ma for high-temperature metamorphism. Timing of the second phase of folding is less well-constrained and could have occurred during Stages I or II, or possibly during the Paleoproterozoic or Neoarchean. The northerly to northwesterly trend of these folds is consistent with Neoarchean structures in the Yilgarn Craton, and may correlate with the <2660 Ma regional D_4 event (D_2 of Swager, 1997) in the Eastern Goldfields Superterrane (Blewett et al., 2010). These folds are unlike those observed to the south within the Biranup Zone, such as in the Bremer Bay area (Spaggiari et al., 2009), further supporting a Neoarchean age. At Powell Point, the early hook-folds (F_1) and gneissic banding in the leucocratic tonalitic gneiss appear to pre-date intrusion of the porphyritic monzodiorite at 2658 ± 21 Ma, and therefore these folds are interpreted as Neoarchean structures.

Barren Basin — Cycle 1 sediments

The Albany–Fraser Orogen contains Paleoproterozoic metasedimentary rocks belonging to the Stirling Range Formation, Mount Barren Group, and Woodline Formation (Woodline Sub-basin; Plate 1; Fig. 2). These units overlie the Yilgarn Craton, and are interpreted to be the inboard remnants of a much larger basin system — here named the Barren Basin — that evolved along, or in the distal reaches of, the Yilgarn Craton margin during the late Paleoproterozoic (Fig. 4; Thom et al., 1977, 1984a; Hall et al., 2008; Spaggiari et al., 2009). Isolated occurrences of quartzite and metaconglomerate, and psammitic to semipelitic rocks in the northeastern and eastern Albany–Fraser Orogen are interpreted to be part of that same basin system. The higher grade pelitic and psammitic rocks of the Fly Dam Formation in the Biranup Zone (see below) are interpreted to be somewhat younger, more distal components of the Barren Basin, or alternatively, part of a separate, still younger, Mesoproterozoic basin system (Fig. 4). Together, the metasedimentary rocks of the Barren Basin are interpreted to form part of a series of related or linked basins formed prior to, and during, the Biranup Orogeny. They are here termed Cycle 1 sediments, to reflect the first major cycle of basin formation preserved in the Albany–Fraser Orogen (Fig. 4). These Cycle 1 sediments are interpreted to relate to active-margin, rift-, or back-arc processes that substantially modified the Yilgarn Craton margin during the Paleoproterozoic.

Stirling Range Formation

The Stirling Range Formation outcrops in the western Albany–Fraser Orogen approximately 100 km west of the Mount Barren Group, and consists of sub-greenschist to lower greenschist facies quartzite, shale, slate, and phyllite (Muhling and Brakel, 1985). The unit has been interpreted as a shallow-marine, tide-dominated, succession (Cruse, 1991; Cruse and Harris, 1994). It has a minimum age of 1800 ± 14 Ma, based on dating of authigenic xenotime of probable diagenetic origin (Rasmussen et al., 2004). This suggests a depositional age somewhat older than that of the Mount Barren Group. Detrital zircons and xenotime from the Stirling Range Formation indicate a maximum depositional age of 2016 ± 6 Ma (Rasmussen et al., 2002, 2004). Probability plots of detrital zircon ages from the Mount Barren Group and Stirling Range Formation show both similarities and differences and are therefore inconclusive, although data for the Stirling Range Formation are not abundant (Hall et al., 2008). Dating of monazite overgrowths from interbedded sandstone and shale sampled from the Stirling Range Formation yielded an interpreted metamorphic age of 1215 ± 20 Ma, which is consistent with previous Rb–Sr dating (Rasmussen et al., 2002 and references therein), and indicates that metamorphism occurred during Stage II of the Albany–Fraser Orogeny.

Discoidal and trace-like fossils discovered in sandstones of the Stirling Range Formation were initially thought to be of Ediacaran affinity, suggesting that the unit was Neoproterozoic (Cruse and Harris, 1994). However, geochronological data are not consistent with this interpretation; significantly, a 1800 ± 14 Ma authigenic xenotime date is now considered to provide a minimum age for these fossils (Rasmussen et al., 2004).

Mount Barren Group

The Mount Barren Group is exposed in the central Albany–Fraser Orogen, and consists of lower-greenschist to upper-amphibolite facies, Paleoproterozoic metasedimentary rocks, which overlie the southern edge of the Yilgarn Craton along a strike length of about 120 km, extending from Bremer Bay to east of Ravensthorpe (Fig. 2; Plate 1; Thom et al., 1977, 1984b; Witt, 1997). The group is divided into the Steere Formation, the Kundip Quartzite, and the Kybulup Schist (Thom and Chin, 1984; Thom et al., 1984a).

The Steere Formation is the lowermost unit of this group, and consists of a thin basal conglomerate with clasts of quartzite, chert, BIF, and felsic volcanic rocks, overlain by several metres of pebbly sandstone and 4 m of dolomitic limestone (Thom et al., 1977, 1984a; Witt, 1997). At its type locality in the Western Steere River, the Steere Formation non-conformably overlies the Archean Manyutup Tonalite of the Yilgarn Craton (Thom et al., 1977, 1984a).

The Kundip Quartzite consists predominantly of thickly bedded pure quartzite, which is interbedded with mica- and magnetite-bearing quartzite and mudstone, and minor thin lenses of metaconglomerate dominated by quartzite clasts (Thom et al., 1984a; Witt, 1997; Vallini et al., 2005). Sedimentary structures, such as cross-bedding and ripple marks, are common (Witt, 1997) and suggest deposition under shallow, near-shore marine to tidal-sandflat conditions. At Barrens Beach, thin, muscovite-rich layers contain rare kyanite (Witt, 1997). The quartzite is well exposed in a series of prominent rocky peaks such as West Mount Barren, which show its predominant southeasterly dip.

The Kybulup Schist consists predominantly of thinly bedded pelitic and psammitic rocks with variable metamorphic grade. In the northwest, the unit is dominated by slate and phyllite, plus low-grade, mudstone-dominant rhythmite and shale that coarsens upwards into siltstone, whereas amphibolite-facies kyanite-, staurolite-, and garnet-bearing schists are found in the southeast (Thom et al., 1984a; Witt, 1997; Fitzsimons and Buchan, 2005; Fitzsimons et al., 2005; Vallini et al., 2005). Rare outcrops of dolostone and calc-silicate schist are considered indicative of a facies variation, suggesting the presence of carbonate banks surrounded by deeper-water sediments (Witt, 1997). A mafic intrusion approximately 300 m thick, named the Cowerdup Sill, is broadly conformable with the Mount Barren Group, but cuts the stratigraphy regionally (Thom et al., 1977, 1984a; Thom and Chin, 1984; Witt, 1997).

The Mount Barren Group has been interpreted as a deltaic to shallow-marine sequence, with the Steere Formation representing fluvial or fluvial–deltaic sediments, the Kundip Quartzite representing a delta-plain or upper delta-front, and the Kybulup Schist representing a lower delta-front, possibly with an upper prograding section (Witt, 1998; Dawson et al., 2002; Vallini et al., 2002, 2005). In examining drillcore of a low-grade section of the Mount Barren Group, Vallini et al. (2002, 2005) described a 26 m thick phosphatic unit at the interface between the Kundip Quartzite and the Kybulup Schist. This phosphatic unit is thinly bedded and consists of alternating medium- to coarse-grained sandstone and carbonaceous shale, enriched in phosphatic minerals. Authigenic xenotime overgrowths on zircons obtained from the phosphatic unit yielded four age components of 1693 ± 4, 1645 ± 3, 1578 ± 10, and 1481 ± 21 Ma (Vallini et al., 2002, 2005). The dating showed no evidence of Stage I or II metamorphism, and the unit was interpreted as a shielded, low-strain envelope due to its low permeability and porosity (Vallini et al., 2005). Based on detailed petrography and geochemistry, Vallini et al. (2005) deduced a paragenetic sequence for the unit, which provided a framework for the geochronology. The 1693 ± 4 Ma date was interpreted to date early diagenesis of unconsolidated sediments, and therefore is closest to the depositional age of the unit. The onset of burial, and a possible change to anaerobic conditions, was interpreted to have commenced prior to c. 1654 Ma. The two younger age components of 1578 ± 10 and 1481 ± 21 Ma were interpreted to reflect periods of hydrothermal xenotime growth post-dating quartz cementation, and may reflect further burial. Detrital zircon studies of the Mount Barren Group are consistent with this xenotime dating, yielding a maximum depositional age of c. 1700 Ma, and significant detrital zircon age components of c. 2663, 2645, 2291, 2246, 2018, 1857, 1803, and 1773 Ma (Nelson, 1996a,b; Dawson et al., 2002; Hall et al., 2008).

Most structural studies of the Mount Barren Group have concluded that it is part of a northwest-vergent fold and thrust belt, although the amount of overall displacement on the thrust faults is unknown (Sofoulis, 1958; Thom et al., 1984a; Myers, 1990a; Witt, 1998). Several stages of folding and associated fabrics have been recognized within the Mount Barren Group, with the highest degree of complexity in the higher-grade rocks to the south and southeast (Witt, 1998; Wetherley, 1998; Dawson et al., 2003). Dating of peak metamorphism from kyanite-bearing, amphibolite-facies rocks of the Mount Barren Group yielded ion probe U–Pb dates of 1206 ± 6 and 1194 ± 8 Ma for xenotime and monazite, respectively (Dawson et al., 2003). Dawson et al. (2003) interpreted these dates to represent c. 1205 Ma peak thermal metamorphism, statically overprinting the S_1 and S_2 foliations. These dates are consistent with Stage II of the Albany–Fraser Orogeny, and indicate that formation of the fold and thrust system occurred during that period.

Woodline Formation

The Woodline Formation is exposed approximately 350 km northeast of the Mount Barren Group, and unconformably overlies granite and greenstone of the Eastern Goldfields Superterrane, near its southeastern margin (Plate 1; Fig. 2). The formation consists of weakly deformed, lower greenschist facies, mature sandstone interbedded with siltstone, and was interpreted as a remnant of a broader siliciclastic sequence (Hall et al., 2008). At its base is a quartz-rich sandstone to pebbly conglomerate, which is overlain by three quartz-rich sandstone units that include minor amounts of granular to pebbly conglomerates and are interbedded with a massive

siltstone tens of metres thick (Hall et al., 2008). Minor units consist of pebble and cobble conglomerates, and matrix- to clast-supported chert breccias. These rocks are folded into open, upright, northeasterly trending folds, and contain a weak to moderately developed, axial-planar spaced cleavage (Hall et al., 2008). Two dominant sets of paleocurrent directions were recorded, indicating both southeasterly and southwesterly directed flow. These paleocurrent readings have been interpreted either as transverse and axial components in a foreland-basin setting, or as fluvial to deltaic and barrier island sedimentary processes interacting with longshore currents (Hall et al., 2008). The depositional setting is interpreted as changing from a distal fluvial environment to a marine-dominated setting (Hall et al., 2008).

The Woodline Formation has a maximum depositional age of 1737 ± 28 Ma, permitting a similar depositional time as the Mount Barren Group (Fig. 4; Hall et al., 2008). However, detrital zircon age spectra from the Woodline Formation were interpreted as most similar to spectra from the upper section of the Earaheedy Group on the northeastern margin of the Yilgarn Craton (Hall et al., 2008). Although there are significant differences between the age components of the Woodline Formation and Mount Barren Group (Hall et al., 2008 and references therein), this may be due to the large geographical separation of the units during deposition, and the more distal original position inferred for the Mount Barren Group, before it was thrust towards the craton. This interpretation would be consistent with the relatively lower amount of Neoarchean material seen in the Mount Barren Group, and the significant component of 1810–1760 Ma detritus, which in turn fits with inheritance and granitic protolith ages from the Biranup Zone (Figs 4 and 5). The Woodline Formation is thus regarded as deposited during Cycle 1 in a separate sub-basin (the Woodline Sub-basin) from the Mount Barren Group, though still as part of the more extensive Barren Basin.

Unnamed metasedimentary units

Isolated ridges and outcrops of metaconglomerate, quartzite, and metasandstone occur in the northeastern part of the Albany–Fraser Orogen (Plate 2). Quartzite and metasandstone occurrences contain well-developed sedimentary structures such as cross-bedding and ripple marks, and are folded into northeasterly trending, open to tight folds (see Excursion 2, Stop 6).

Similar rocks have been described near Lindsay Hill (van de Graaff and Bunting, 1977). Preliminary geochronology of a sample from this quartzite (GSWA 182405) yields a maximum depositional age of 1990 ± 15 Ma, based on the weighted mean date from two analyses of a single zircon. A more conservative estimate of the maximum age of deposition can be based on the weighted mean date of 2641 ± 3 Ma for the next youngest 52 analyses. Fifty-eight analyses yield dates between 2735–2619 Ma, indicating a significant Neoarchean component, compatible with Yilgarn Craton provenance.

Northeast of Tropicana is a ridge of probable greenschist-grade, coarse quartz-pebble metaconglomerate with a quartz-rich, micaceous matrix, and distinctive iron-rich laminated metasiltstone beds throughout (Fig. 7a; denoted UC on Fig. 4). Above this is a pale-grey quartzite interbedded with metagritstone and metasandstone. Bedding in the metaconglomerate dips to the east, and is cut by a weak to moderate foliation that also dips east but at a shallower angle. This indicates that the fold vergence (direction to next antiform) is to the east, and that this locality is in the overturned limb of a gently northeast-plunging antiform. Preliminary geochronological data (GSWA 182416) indicate a maximum depositional age of 1752 ± 19 Ma (1σ), and older detrital zircon dates of 2835–1794 Ma, including significant age components at c. 2635 Ma and 1807 Ma. This suggests that the metaconglomerate, and by correlation the quartzites and metasandstones described above, are part of the same sedimentary cycle (Cycle 1) that links the Paleoproterozoic metasedimentary rocks of the Barren Basin (Stirling Range Formation, Mount Barren Group, and Woodline Formation) (cf. Bunting et al., 1976).

Along Ponton Creek, north of the Trans-Australian Railway, is a psammitic gneiss that locally contains evidence of anatexis such as thin leucosomes, and is intruded by coarse pegmatite. However, it also exhibits well-preserved laminations and cross-bedding (Fig. 7b). Petrographic analysis shows that it contains a micromosaic of K-feldspar (60%) and quartz (35%), with 2% garnet, 1–2% opaque oxide grains, and ~1% altered biotite. This psammitic gneiss (GSWA 194731, Kirkland et al., 2010d) yields a unimodal zircon age component of 1689 ± 6 Ma, which is interpreted as a maximum depositional age. A minimum age is provided by the crystallization age of c. 1667 Ma obtained for the metagranitic rocks that intrude the psammitic gneiss (GSWA 194732, Kirkland et al., 2010e; GSWA 194733, Kirkland et al., 2010f). The unimodal age component and high K-feldspar content relative to quartz are both suggestive of a proximal source, which could be interpreted to reflect volcanic activity related to widespread granitic magmatism of the Biranup Orogeny. The short time interval between deposition and intrusion is indicative of a dynamic setting.

Several other occurrences of amphibolite- to granulite-facies metasedimentary rocks, intruded by granitic rocks of Biranup Orogeny age, occur throughout the Biranup Zone, both north and south of the Trans-Australian Railway. Strongly deformed to mylonitic, schistose metasedimentary rock is interpreted as intruded by magmatic rocks of the Eddy Suite (see 'Eddy Suite' section, and Excursion 1, Stop 9). Geochronological data for this schist (GSWA 194722, Kirkland et al., 2010c) yielded significant age components at c. 2645, 1783, 1745, and 1650 Ma. The c. 1650 Ma component may reflect the intrusion of Eddy Suite pegmatitic or granitic material into the metasedimentary rocks that subsequently became disaggregated during deformation and metamorphism, forming rounded K-feldspar porphyroclasts. Dates of 1304–1185 Ma for 21 analyses of zircon rims are interpreted to reflect elevated temperatures and zirconium mobility during a metamorphic event between these dates, with the high dispersion either reflecting a prolonged process, or radiogenic Pb-loss (Kirkland et al., 2010c).


a)
b)
c)
d)
e)
f)
g)
h)
CS133
23.08.11

Within the eastern Nornalup Zone, preliminary geochronology of drillcore samples of migmatitic gneiss from the Big Red prospect (Fig. 3) (Hole BRDDH1, GSWA 182473 and 182475) yielded a large range of predominantly Archean detrital ages, and a maximum depositional age of 1729 ± 27 Ma (1σ). These migmatites are tentatively interpreted as Barren Basin Cycle 1 sediments, implying that some sediments from this basin system were deposited a substantial distance from the craton margin. Nonetheless, this interpretation is consistent both with the presence of Paleoproterozoic basement in the Nornalup Zone (see 'Nornalup Zone' section), and the interpretation of the Mesoproterozoic Fraser Zone as possibly developing in a rift setting within Archean to Paleoproterozoic crust (see 'Fraser Zone' section). The preliminary geochronology shows that the migmatitic gneisses from Big Red were metamorphosed under high-temperature conditions at 1193 ± 5 and 1176 ± 10 Ma, and were intruded by Esperance Supersuite granite at 1167 ± 2 Ma, during Stage II of the Albany–Fraser Orogeny (Fig. 4).

Fly Dam Formation

The Fly Dam Formation is exposed south of the Trans-Australian Railway, in the Biranup Zone of the eastern Albany–Fraser Orogen (Plate 1). It is comprised of a succession of amphibolite- to granulite-facies interlayered psammitic (Fig. 7c) to semipelitic (Fig. 7d) gneisses, which appear to be the metamorphosed equivalents of interbedded sandstones and mudstones. Semipelitic horizons are layered on the centimetre-scale with alternating quartzofeldspathic and more mafic, biotite-rich material, and also contain abundant garnets ranging 0.5 – 2 cm in diameter (Fig. 7d). The gneisses are mostly migmatitic, and contain both isoclinally folded leucosomes, and leucosomes parallel to the main, axial-planar foliation. These leucosomes are texturally continuous and probably belong to a single generation. The leucosomes are also locally boudinaged parallel to the foliation. Diatexitic textures occur locally.

Petrographically, the semipelitic rocks contain a foliation defined by biotite (dominantly), hornblende, titanite, K-feldspar, and quartz. This foliation wraps around abundant garnets that are inclusion-rich and partly resorbed. Inclusions are mostly K-feldspar, but also include epidote or zoisite, quartz, and titanite. The felsic bands comprise a mixture of K-feldspar, plagioclase, perthite, and quartz. These minerals have ragged to lobate grain margins, and there is some evidence of static recovery in smaller quartz grains. The psammitic gneiss contains a fine- to medium-grained matrix of quartz and K-feldspar (dominant), plagioclase, some perthite, and microcline. These all have ragged grain boundaries, but also show some evidence of recrystallization or recovery, and mostly have a granuloblastic texture. The foliation is predominantly defined by biotite. Abundant small garnets appear to be fragments of larger crystals that have been partly resorbed, and contain inclusions of quartz, epidote, and possibly K-feldspar. Small, euhedral epidote grains with sector zoning are scattered throughout the matrix, and some contain cores of probable allanite. Accessory titanite occurs as small, but fresh, crystals.

The Fly Dam Formation is exposed in an area of large-scale, open to tight folds that are well-defined in aeromagnetic imagery (Fig. 8). In outcrop, the latest folding phase (F_3) has a moderately east-dipping enveloping surface, which corresponds to a large-scale, easterly plunging synformal fold in the magnetic data. This latest phase refolds earlier, large-scale, tight folds (F_2), and early, small-scale intrafolial folds (F_1) defined by gneissic layers with parallel leucosomes (Fig. 7e). Where well-exposed in the northern limb of the large-scale F_3 fold (Fig. 8), the F_2 folds are inclined to the northwest in predominantly southeasterly dipping layering (Fig. 7f). Thin leucosomes define early, intrafolial folds that are refolded into the larger F_2 folds. The axial planar foliation to the F_2 folds is parallel to the main foliation throughout, and locally contains white mica.

Preliminary geochronological data from the Fly Dam Formation indicate maximum depositional ages (1σ) of 1535 ± 26 and 1598 ± 9 Ma (single analyses from two samples, GSWA 194742 and 194743, respectively), or the more conservative estimates of 1640 ± 12 and 1617 ± 26 Ma obtained from the weighted means of the youngest age group in each sample (Fig. 4). The two samples yield significant detrital zircon age components at c. 1679 and c. 1672 Ma. The datasets also include analyses of zircon rims, which yield metamorphic ages of 1196 ± 13 Ma (GSWA 194743) and a less well-constrained age of 1154 ± 35 Ma (GSWA 194742). These ages are consistent with Stage II of the Albany–Fraser Orogeny.

Figure 7. (right) a) Quartz-pebble metaconglomerate with iron-rich laminae, from northeast of Tropicana (MGA 663584E 6774594N). Note the change from metasandstone with iron-rich lamellae and sparse pebbles, to metaconglomerate with densely-packed, elongate pebbles, some of which are iron-rich; b) psammitic gneiss (GSWA 194731) from Ponton Creek, showing fine laminations and cross-bedding (MGA 561588E 6579876E); c) psammitic gneiss belonging to the Fly Dam Formation, occurring in the hinge of an antiform (MGA 535693E 6531025N); d) semipelitic, garnet-rich gneiss belonging to the Fly Dam Formation (MGA 535691E, 6530522N); e) psammitic to semipelitic gneiss of the Fly Dam Formation, showing folded leucosomes overprinted by diatexite texture (MGA 535063E 6539836N); f) F_2 folds with southeasterly dipping axial planes, inclined to the northwest, in psammitic to semipelitic gneiss of the Fly Dam Formation (MGA 535301E 6539918N). The white line drawn on this diagram shows the fold form; g) migmatitic, hornblende–biotite–garnet granitic gneiss with folded, centimetre-scale, layer-parallel leucosomes, from which GSWA 194730 was sampled; Ponton Creek, eastern Biranup Zone (MGA 562765E 6582098E); h) axial-planar leucosomes in migmatitic, hornblende–biotite–garnet granitic gneiss with folded, centimetre-scale layer-parallel leucosomes. The axial planar leucosome was chiselled out to provide material for GSWA 194729; Ponton Creek, eastern Biranup Zone (MGA 562765E 6582098E).

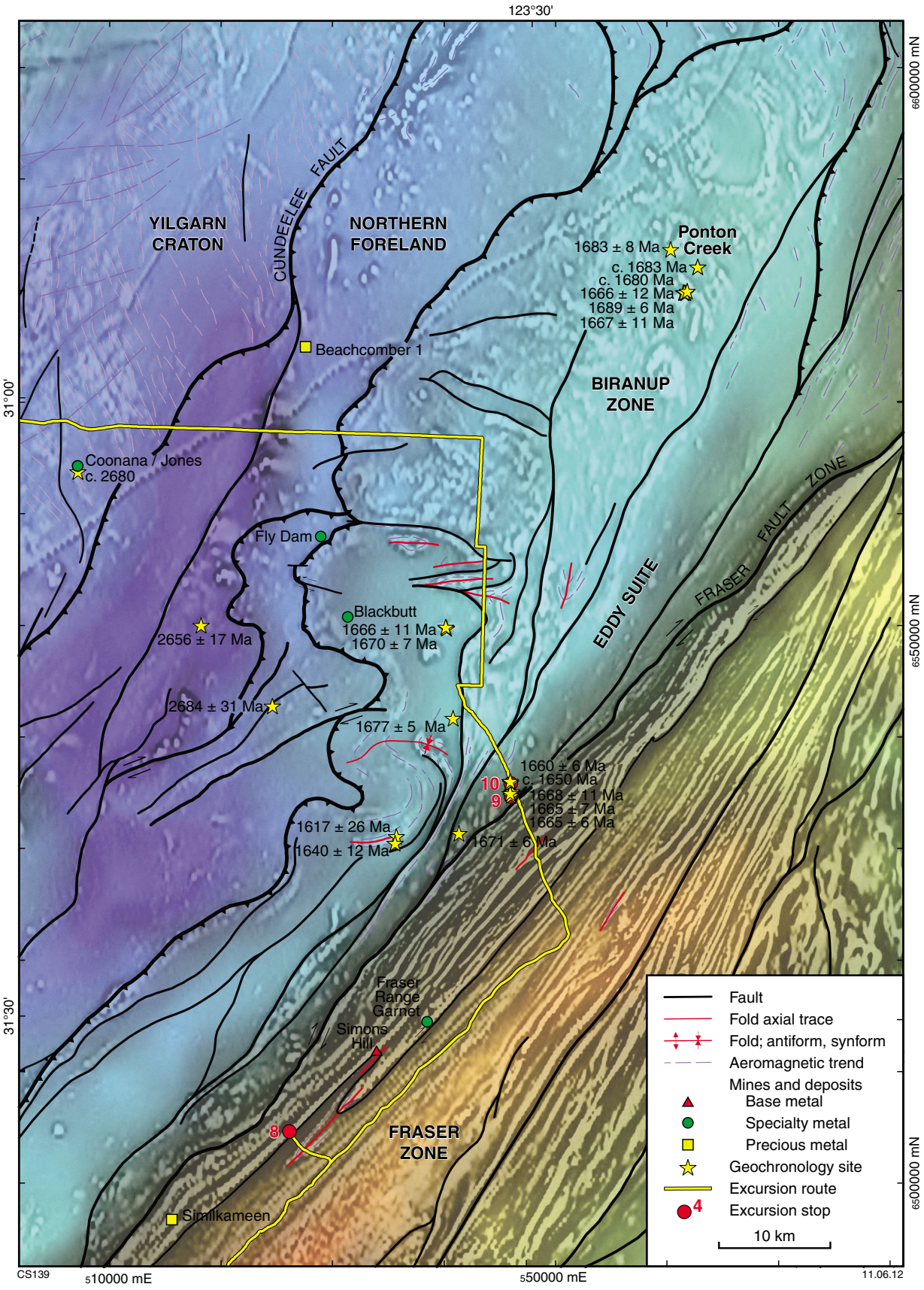

Figure 8. **Gravity image (colour) of the central part of the eastern Biranup Zone and Fraser Zone, and surrounding area, with a first vertical derivative, reduced-to-pole aeromagnetic data (greyscale) drape. The map shows interpreted structures (extracted from Geological Survey of Western Australia, 2011), published and preliminary GSWA geochronology, known mines and deposits, and excursion route and stops.**

Given the predominance of sandstone and mudstone protoliths, the metasedimentary rocks of the Fly Dam Formation could be interpreted as turbidites, possibly representing the youngest known, more distal, and deeper water component of the Barren Basin Cycle 1 sediments, deposited during the late stages of the Paleoproterozoic Biranup Orogeny. Alternatively, they could be much younger, Mesoproterozoic sediments, and therefore part of Cycle 2 (see 'Arid Basin — Cycle 2 sediments' section; Fig. 4). It is interesting to note that their provenance appears to be dominated by Paleoproterozoic Biranup Orogeny aged components, suggesting derivation from related volcanic sources, and/or the relatively rapid exhumation and exposure of the basement.

Kepa Kurl Booya Province

Myers (1990a) divided the Albany–Fraser Orogen into two major tectonic units: an inboard, intensely deformed component named the Biranup Complex, and an outboard component named the Nornalup Complex. In Myers' early definition, the Biranup Complex contained what were later called the Munglinup, Dalyup, and Coramup Gneisses (Myers, 1995b), as well as the Fraser Complex (Myers, 1985); however, the c. 1300 Ma Fraser Complex was later removed from the Biranup Complex (Myers, 1995b). In light of new data and interpretations, the Biranup Complex was recently renamed the Kepa Kurl Booya Province (Spaggiari et al., 2009), and defined as the crystalline basement of the Albany–Fraser Orogen; i.e. the various crustal components affected, and probably amalgamated by, Stage I tectonism. It includes three fault-bound geographical and structural zones (Biranup, Fraser, and Nornalup) that contain rocks with variable protolith ages and geological histories (Plate 1; Figs 2 and 4; Spaggiari et al., 2009). The southeastern part of the Biranup Zone and most of the Nornalup Zone contain granitic intrusions of the 1330–1280 Ma Recherche Supersuite and the 1200–1140 Ma Esperance Supersuite (Nelson et al., 1995; Clark, 1999). Various Mesoproterozoic cover rocks also locally overlie the Nornalup Zone.

The first tectonic subdivisions of the Fraser Zone (formerly the Fraser Complex) and surrounding rocks were presented in Bunting et al. (1976), where a transition zone of reworked Archean rocks was delineated along the southeastern margin of the Yilgarn Craton, bounded by the northeasterly trending Western Gneiss and Granite Zone consisting of Proterozoic igneous and metamorphic rocks with no recognizable remnants of the Yilgarn Craton. This zone was separated from the Fraser Zone by the Fraser Fault.

Biranup Zone

The Biranup Zone is a belt of predominantly mid-crustal rocks that lies along the entire southern and southeastern margin of the Yilgarn Craton (Fig. 2; Myers, 1990a; Spaggiari et al., 2009). In the eastern part of the orogen, the Biranup Zone is in fault contact to the southeast with the Mesoproterozoic Fraser and Nornalup Zones (Fig. 2). In an area denoted the 'S-bend', it is tectonically interlayered with reworked rocks of the Yilgarn Craton within the Northern Foreland (Figs 9 and 10; Spaggiari et al., 2009).

The Biranup Zone is dominated by intensely deformed orthogneiss, metagabbro, and paragneiss, with ages ranging from c. 1800 to 1625 Ma (Figs 4 and 5). The lack of evidence for a Paleoproterozoic magmatic or tectonothermal event in the southern Yilgarn Craton led to the suggestion that the Biranup Zone was an exotic terrane accreted onto the Yilgarn Craton margin during Stage I of the Albany–Fraser Orogeny (e.g. Nelson et al., 1995; Clark et al., 2000; Spaggiari et al., 2009). However, recent work has shown that the Biranup Zone was more likely to have formed autochthonously along the Yilgarn Craton margin (Kirkland et al., 2011a). Within the Biranup Zone, the presence of fragments of Archean granite with ages typical of Yilgarn Craton granites support this interpretation (Plate 1; Fig. 5). These fragments occur in the 'S-bend' area around, and to the southwest of, Mount Andrew, and possibly include rocks associated with the Splinter prospect (Figs 9 and 10; see Excursion 1, Stops 2, 3, and 4). This interpretation is further supported by Lu–Hf data from granitic rocks in the Biranup Zone (see 'Lu–Hf isotopes' section), which indicate that the Biranup Zone evolved on Archean Yilgarn Craton crust. Rocks in the vicinity of Tropicana (Plate 2; Fig. 2) are probably Archean granites and greenstones, and are likely to be part of another crustal fragment derived from the Yilgarn Craton, or part of the Northern Foreland. Preliminary geochronology results from a strongly altered metagranite sampled just northwest of Tropicana yielded an interpreted magmatic crystallization age of 2722 ± 15 Ma, whereas analysis of zircon rims yielded a date of 2643 ± 7 Ma, interpreted as the age of metamorphism (GSWA 182435).

The oldest dated intrusive rocks in the Biranup Zone are c. 1806 Ma granitic gneiss from south of Salmon Gums (preliminary geochronology, GSWA 192502), and a metasyenogranite from the far northeastern part of the orogen along McKay Creek (known as the McKay Creek Metasyenogranite; see Excursion 2, Stop 5). The McKay Creek Metasyenogranite has a preliminary interpreted magmatic crystallization age of 1761 ± 10 Ma (GSWA 182424). Mingling of this granite with gabbroic rocks has produced dioritic hybrid rocks. The McKay Creek Metasyenogranite is one of several phases of alkaline granite magmatism that produced various syenogranitic rocks throughout the eastern part of the Biranup Zone. The next oldest of these phases is the Bobbie Point Metasyenogranite, which also occurs in the northeastern part of the orogen (see Excursion 2, Stop 4). It has been dated at 1708 ± 15 Ma, interpreted as the age of magmatic crystallization (GSWA 194737, Kirkland et al., 2010i). All of these metasyenogranites occur in the eastern part of the Biranup Zone, and most fall within the age range of c. 1690 Ma to 1670 Ma, apart from one component of the Eddy Suite and the youngest Biranup Zone granite dated at 1627 ± 4 Ma (GSWA 194736, Kirkland et al., 2010h). Other metagranitic rocks of both the central and eastern Biranup Zone include metamonzogranite, metagranodiorite, and rare tonalitic gneiss, with most ages falling in the range of c. 1690 to 1660 Ma (Figs 4 and 5; Kirkland et al., 2011a; Spaggiari et al., 2009).

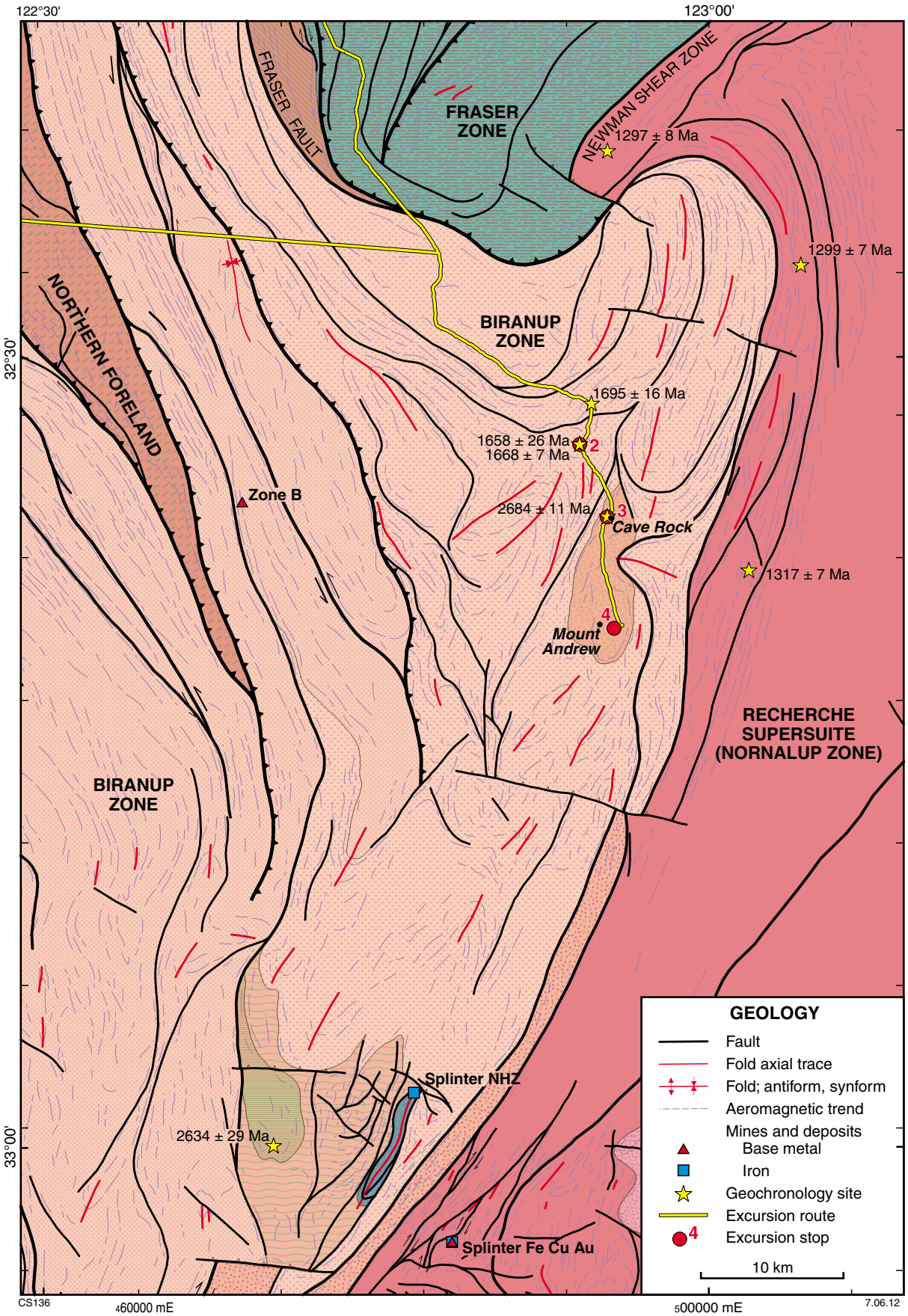

Figure 9. **Pre-Mesozoic interpreted bedrock geology map of the 'S-bend' area, including Mount Andrew, showing geology, structure, published and preliminary GSWA geochronology, known mines and deposits, and excursion route and stops. Modified from Geological Survey of Western Australia (2011); see Plate 1 for geological legend.**

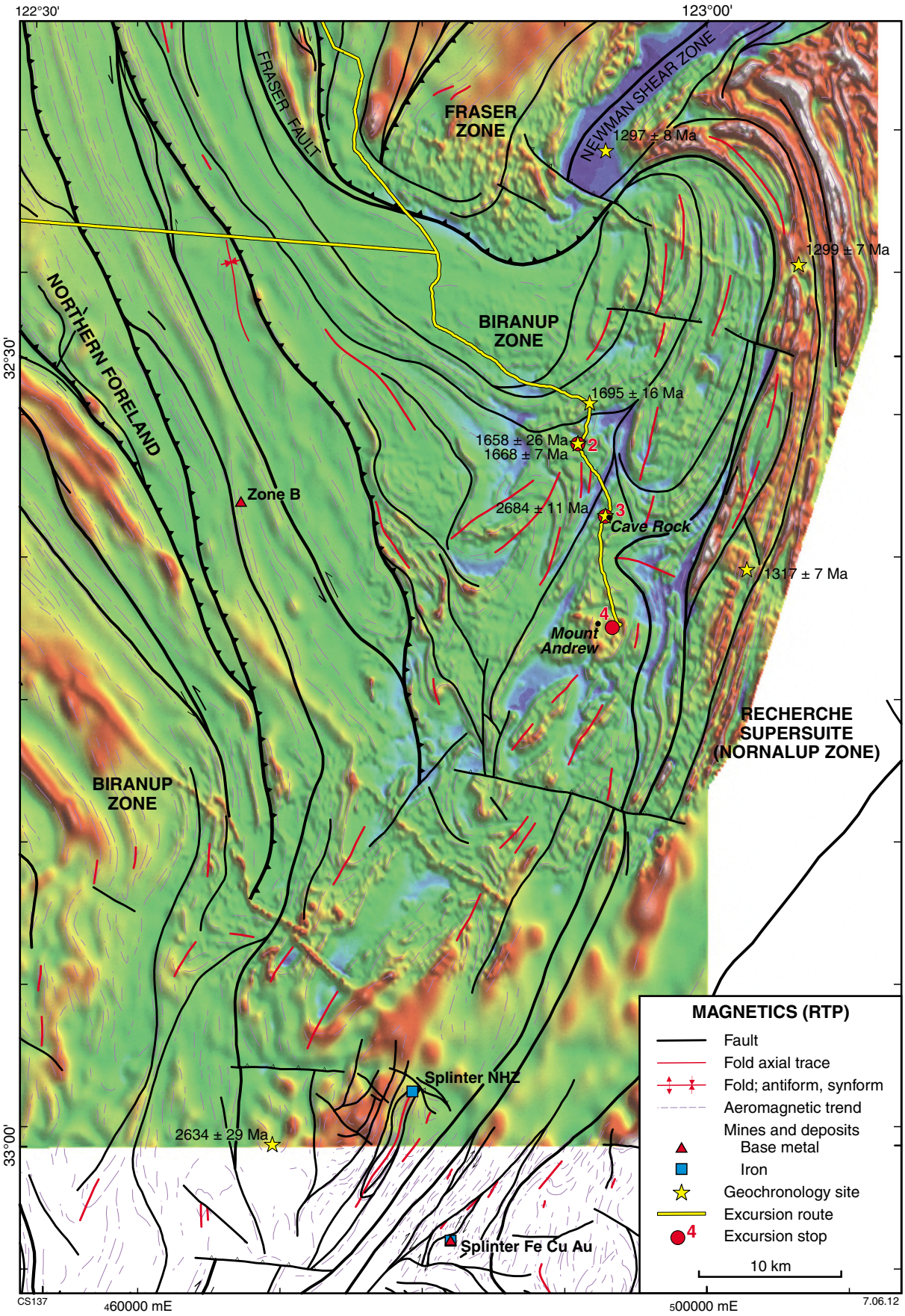

Figure 10. Reduced-to-pole aeromagnetic image of the 'S-bend' area shown in Figure 9, showing structure, published and preliminary GSWA geochronology, known mines and deposits, and excursion route and stops. Modified from Geological Survey of Western Australia (2011).

As described above, the Biranup Zone also contains metasedimentary rocks, most of which are migmatitic paragneisses (see 'Barren Basin — Cycle 1 sediments' section).

Eddy Suite

The Eddy Suite, which ranges from megacrystic metamonzogranite and equigranular metasyenogranitic gneiss, to rapakivi-textured metagranodiorite and metagabbronoritic rocks, occurs in the eastern Biranup Zone, and is well exposed west of Harris Lake (Fig. 8; see Excursion 1, Stop 9). These rocks have been dated at c. 1660 Ma, and represent the dominantly younger, more juvenile, component of Biranup Zone magmatic rocks (Kirkland et al., 2011a,k). The metagranodiorite contains ovoid K-feldspars up to 3 cm long, with a millimetre-wide mantle of more calcic feldspar, and rounded quartz phenocrysts up to 6 mm in diameter, within a medium-grained groundmass. These textures are typical of many Proterozoic A-type rapakivi granites (Rämö, 2005). The metagabbronorite is fine to medium grained, and forms irregular enclaves within the metagranodiorite. These enclaves have lobate, commonly gradational, boundaries with the metagranodiorite, suggesting that the two phases are co-magmatic and that a degree of mingling is likely to have occurred. In this respect, it is possible that the metagranodiorite is a hybrid of the megacrystic metamonozogranite and the metagabbronorite, indicating that magma mixing also occurred. Rocks of the Eddy Suite are heterogeneously deformed, such that mingling textures are preserved in some areas, although most exposures exhibit a pervasive gneissosity and localized mylonite zones. The magmatic rocks intrude metasedimentary rocks that are probably part of the same succession as the psammitic gneiss in the Ponton Creek area described previously in the 'Barren Basin — Cycle 1 sediments' section (Fig. 8; GSWA 194731, Kirkland et al., 2010d).

Fraser Zone

The Fraser Zone is bounded by the Fraser Fault Zone along its northwestern edge and southern tip, and by the Newman Shear Zone and Boonderoo Fault along its southeastern edge (Plate 1; Fig. 2). It is dominated by high-grade metagabbroic rocks that have a strong, distinct, geophysical signature in both aeromagnetic and gravity data (Figs 8 and 11). Most of the northeastern part of the Fraser Zone is obscured by younger rocks of the Eucla Basin, but geophysical data show that it is a northeasterly trending, fault-bounded unit that is approximately 425 km long and up to 50 km wide.

The Fraser Zone contains the 1305–1290 Ma Fraser Range Metamorphics (Spaggiari et al., 2009), which are dominated by sheets of metagabbroic rocks, interlayered with sheets of granitic material (Fig. 12a), and layers or slivers of pelitic, semipelitic, and calcic metasedimentary rocks of the Arid Basin. The metasedimentary rocks were deposited just prior to the intrusion of the mafic and felsic magmatic rocks, and all have been metamorphosed at high temperatures (granulite facies), with some locally retrogressed to amphibolite facies, and low to moderate pressures of about 6.5 – 8 kbars (Figs 4 and 5; Doepel, 1973; Myers, 1985; Clark et al., 1999; De Waele and Pisarevsky, 2008; Spaggiari et al., 2009; Oorschot, 2011). Metagranitic rocks range from metamonzogranite to metasyenogranite. The metasedimentary rocks mostly occur along the northwestern side of the Fraser Zone, and are typically intercalated with layers of mafic granulite or amphibolite (Fig. 12b) that were probably originally dykes, sills, or sheets related to the main gabbroic intrusions. Whereas pelitic and semipelitic rocks dominate the metasedimentary component in the southern part of the Fraser Zone (e.g. Gnamma Hill and Mount Malcolm; see Excursion 1, Stop 5), the northern exposed section of the Fraser Zone contains metasedimentary rocks that have calc-silicate affinities, and may represent metamorphosed marls, or volcaniclastic protoliths. In some localities, these rocks contain layers packed with unusual, orange-coloured, euhedral garnets up to 1 cm, set in a white, sugary matrix dominated by quartz and lesser plagioclase (Fig. 12c). There are also variable amounts of titanite, some epidote or zoisite, minor hornblende, and variable amounts of magnetite.

The Fraser Range Metamorphics are typically dominated by a well-developed, northeasterly trending, steeply dipping, foliation, although massive rocks can locally be found in the centre of the zone's exposed, southern part. The Fraser Range Metamorphics are strongly mylonitized and have a dextral shear sense along, and close to, the Fraser Fault Zone (Figs 8, 11, and 12d; see Excursion 2, Stop 10). Elsewhere, they are tightly to isoclinally folded along northeasterly trending axes, and are cut by thrust faults and shear zones. Kinematics along the Newman Shear Zone are complex, but there is some indication of subhorizontal sinistral shear, and locally, subvertical movement denoted by a strong vertical lineation. These kinematics, and the interpreted presence of numerous sinistral shears and thrust faults in the 'S-bend' area (Plate 1; Figs 9 and 10), are consistent with a model of exhumation of the Fraser Zone by extrusion to the southwest (Fig. 13).

Crystallization of gabbro within the Fraser Zone has been dated at 1291 ± 8 Ma (De Waele and Pisarevsky, 2008), and at 1291 ± 21 Ma by a whole-rock Sm–Nd isochron from olivine gabbronorite (MSWD = 0.25; Fletcher et al., 1991). The gabbronorite comes from approximately 1.3 km north-northeast of the Fraser Range Black dimension stone quarry (Fig. 11), and is most likely the same rock unit as that exposed in the quarry. A biotite whole-rock Rb–Sr isochron date of 1268 ± 20 Ma from the gabbronorite is interpreted to reflect the time of cooling below the isotopic closure temperature for biotite in this rock (Fletcher et al., 1991). Preliminary geochronology of a gabbro pegmatite from the Fraser Range Black dimension stone quarry (GSWA 194782) yielded a date of 1299 ± 6 Ma, interpreted as the age of magmatic crystallization of the gabbro. A minimum age for mafic rocks in the Mount Malcolm area is provided by an orthopyroxene–hornblende orthogneiss (charnokitic orthogneiss at Verde Austral dimension stone quarry; Fig. 11), which intrudes the gabbros at 1301± 6 Ma (Clark et al., 1999). Orthopyroxene-bearing orthogneiss just north of Mount Malcolm yielded a date of 1293 ± 9 Ma,

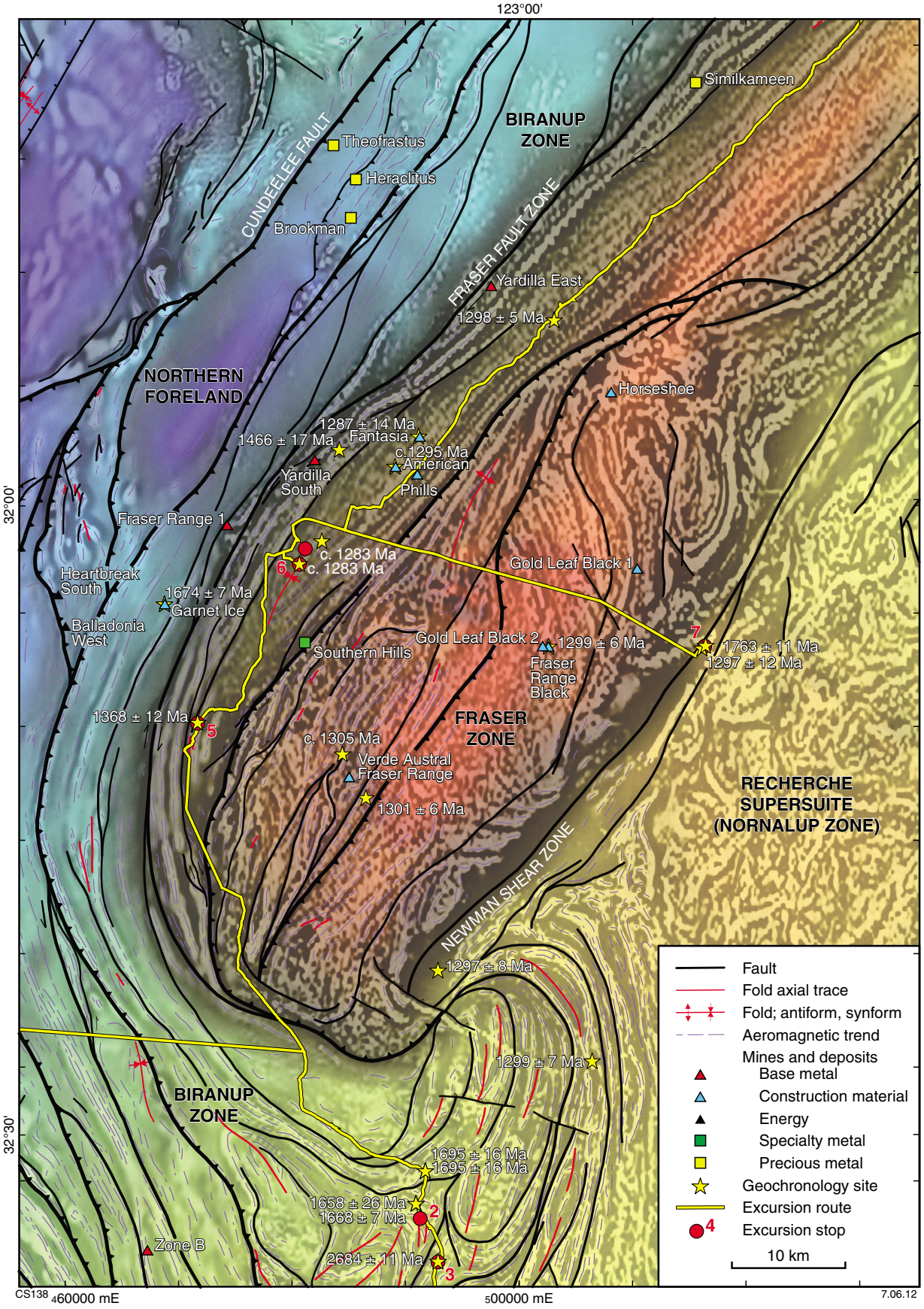

Figure 11. Gravity image (colour) of the southern Fraser Zone and surrounding area, with a first vertical derivative, reduced-to-pole aeromagnetic data (greyscale) drape. The map shows interpreted structures (extracted from Geological Survey of Western Australia, 2011), published and preliminary GSWA geochronology, known mines and deposits, and excursion route and stops.

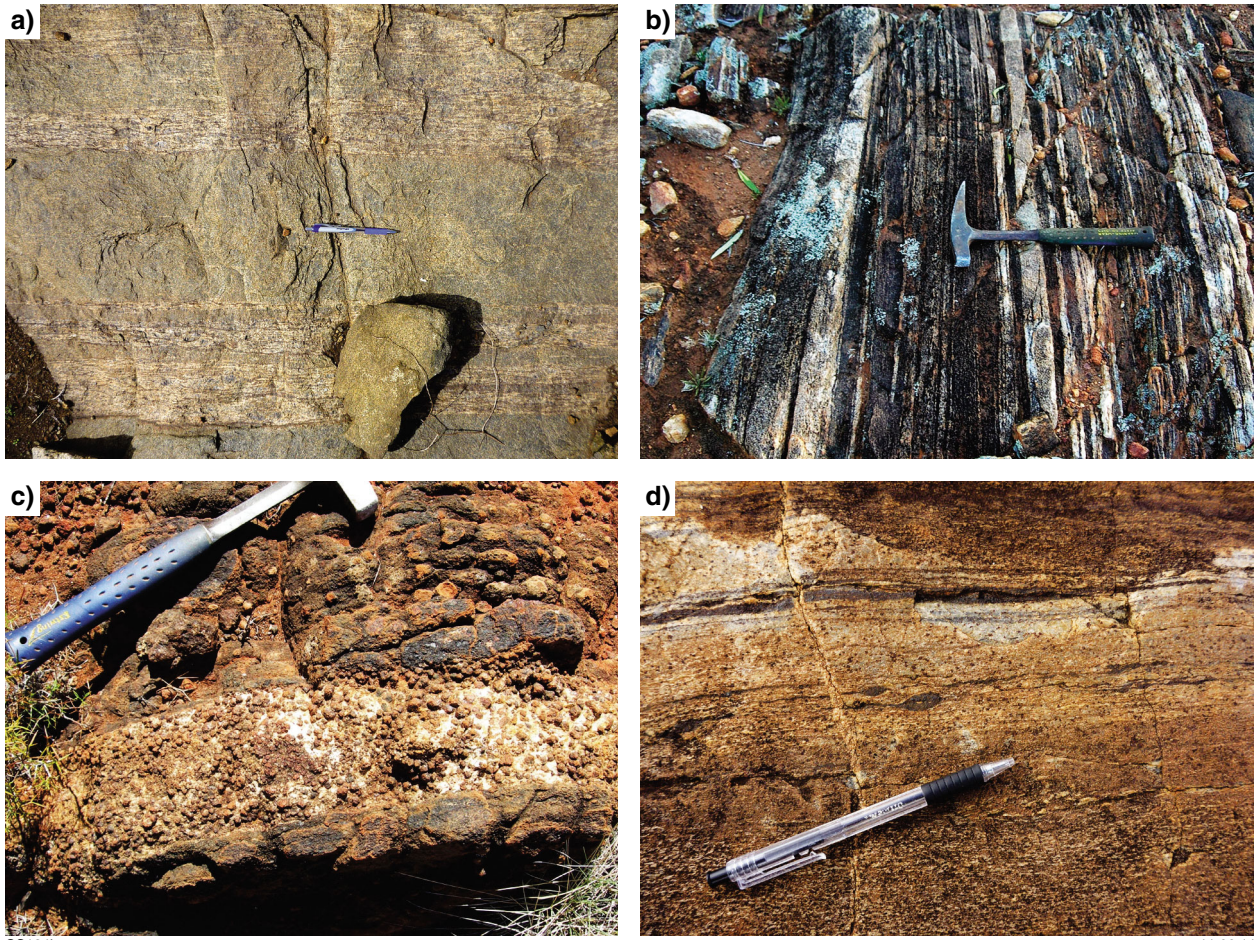

Figure 12. a) Metagabbroic rocks (dark) interlayered with sheets of granitic material (pale); Fraser Range Metamorphics, gully exposure at Wyralinu Hill, Fraser Range, Excursion 1, Stop 6; b) Fraser Range Metamorphics, showing interlayered mafic granulite with calcic metasedimentary rocks, from the northwestern exposed section of the Fraser Zone (MGA $_{5}$51580E $_{65}$35349N); c) Fraser Range Metamorphics, showing calcic metasedimentary rocks with large, orange-coloured garnets, from the northwestern exposed section of the Fraser Zone (MGA $_{5}$37121E $_{65}$22810N); d) strongly mylonitized metasedimentary rocks of the Fraser Range Metamorphics, showing porphyroblasts and fabric with dextral asymmetry; Excursion 1, Stop 8.

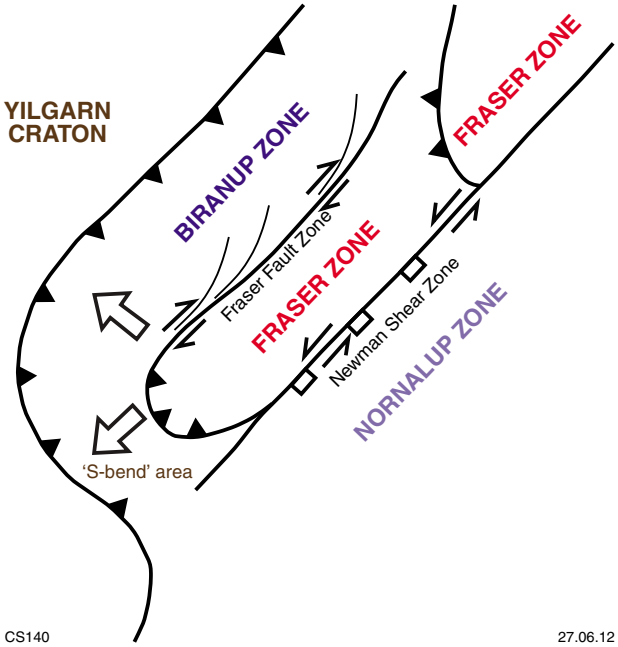

Figure 13. Interpretive model of exhumation of the Fraser Zone by extrusion to the southwest

which is also interpreted as an igneous crystallization age (Clark et al., 1999). The age is within uncertainty of the Verde Austral sample; however, the intrusion is interpreted as post-D_1 and pre-D_2 (Clark et al., 1999). Metasyenogranite from near Symons Hill yielded a similar crystallization age of 1298 ± 5 Ma (Kirkland et al., 2010b). Monzogranitic gneiss from the Fantasia dimension stone quarry (Fig. 11) yielded a date of 1287 ± 14 Ma, interpreted as a minimum age for igneous crystallization (GSWA 177909, Wingate and Bodorkos, 2007a). These dates show that the ages of mafic and felsic intrusions are indistinguishable throughout the Fraser Zone (Fig. 14).

Early metamorphism in the Fraser Zone, at 1304 ± 7 Ma, is recorded by zircon rims developed within quartz metasandstone, which is interlayered with amphibolite and pyroxene granulite, and which has a maximum depositional age of 1466 ± 17 Ma (GSWA 177910, Wingate and Bodorkos, 2007b). Other maximum depositional and metamorphic ages are presented in Part 2, Excursion 1, Stop 5. All isotopic results from the Fraser Zone indicate a short time interval for both mafic and felsic igneous crystallization, predominantly between 1305 and 1290 Ma, and essentially coeval granulite-facies metamorphism (Figs 5 and 14). The close correspondence between the age of mafic to felsic magmatism and the age of granulite-facies metamorphism implies that magmatism provided the thermal impetus for metamorphism. All of the geochronological data indicate tectonothermal activity during Stage I of the Albany–Fraser Orogeny, with no evidence of Stage II. The preservation of pre- 1250 Ma Rb–Sr cooling ages (Bunting et al., 1976; Fletcher et al., 1991) also indicates a lack of Stage II activity. This is curious, considering the extent of high-grade, Stage II metamorphism within the adjacent Biranup Zone and other units (Fig. 5). However, analyses of monazite rims from sheared leucosomes within pelitic rocks sampled from Gnamma Hill (see Excursion 1, Stop 5) have provided a younger age of 1236 ± 22 Ma, interpreted either as evidence of a younger metamorphic event, or as the influence of hydrothermal fluids (Oorschot, 2011). Therefore, it is possible that the juxtaposition of the Fraser Zone against the Biranup Zone along the Fraser Fault Zone occurred, at least in part, during Stage II.

Although several interpretations for the tectonic setting of the Fraser Zone rocks have been published, it remains enigmatic to some degree. Initially, both the metagranitic and metamafic components of the Fraser Zone were interpreted as an exhumed block of lower crust (Doepel, 1975). However, after detailed mapping, the mafic rocks of the Fraser Zone were interpreted as part of a large, layered mafic intrusion, with the granitic and metasedimentary rocks representing basement slivers belonging to the former Biranup Complex (Myers, 1985). Following analysis of trace-element data, it was argued that the mafic magmas were derived from a subduction-related source, and that the 'Fraser Complex' represented remnants of multiple oceanic magmatic arcs (Condie and Myers, 1999). Our current interpretation is that the Fraser Zone represents a structurally modified, mid- to deep-crustal 'hot zone', formed by the repeated intrusion of gabbroic magma into quartzofeldspathic country rock (see 'Whole-rock geochemical datasets' section). This could fit with a continental magmatic-arc, back-arc, or rift setting. An oceanic magmatic-arc setting is considered unlikely due

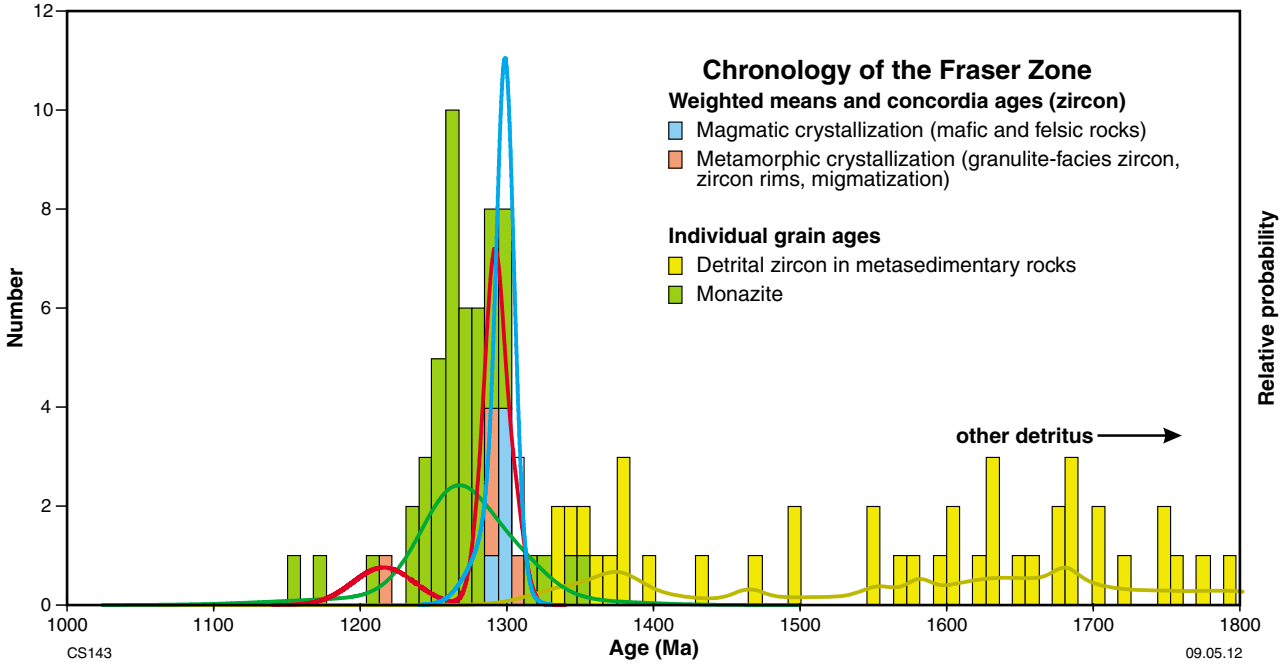

Figure 14. Probability density diagram of ion microprobe (SHRIMP) U–Pb geochronology from the Fraser Zone. All GSWA zircon geochronology can be can be downloaded from <http://www.dmp.wa.gov.au/geochron>. Monazite geochronology is from Oorschot (2011). Magmatic crystallization and metamorphic ages are weighted means or concordia ages for the rocks. Monazite and detrital zircon dates are based on individual spot ages.

to the presence of Paleoproterozoic basement rocks in the Nornalup Zone (see 'Nornalup Zone' below), and the Biranup-like Lu–Hf isotopic signature of the Fraser Zone igneous rocks (see 'Lu–Hf isotopes' section).

Nornalup Zone

The Nornalup Zone is the southern- and easternmost unit of the Albany–Fraser Orogen (Fig. 2; Myers, 1990a, 1995b). This zone is dominated and intruded by the voluminous Recherche and Esperance Supersuites, which mask much of the original basement. In the eastern Albany–Fraser Orogen, the Nornalup Zone is separated from the Biranup and Fraser Zones by the Newman Shear Zone and Boonderoo Fault, and from the Madura Province by the Rodona Shear Zone (Plate 1; Fig. 3). Supracrustal rocks in the Nornalup Zone comprise the Mesoproterozoic Malcolm Metamorphics (previously the Malcolm Gneiss) and paragneissic rocks that occur in the Albany region of the western Albany–Fraser Orogen. These supracrustal rocks belong to the Arid Basin, and are part of the Cycle 2 sedimentary sequence (see 'Arid Basin — Cycle 2 sediments' section). Younger cover rocks are Cycle 3 sediments, which form part of the Ragged Basin (e.g. Mount Ragged Formation; Fig. 4).

Recently dated metamorphic rocks from the Nornalup Zone have helped to identify its basement components. A migmatitic, monzogranitic gneiss containing angular mafic inclusions is exposed about 12 km east of Boingaring Rocks, and has yielded a preliminary date of 1809 ± 8 Ma (GSWA 194785), interpreted as the age of magmatic crystallization of the monzogranite. Granitic gneiss from Newman Rocks (Newman Shear Zone; Fig. 11; see Excursion 1, Stop 7) has a preliminary, interpreted magmatic crystallization age of 1763 ± 11 Ma (GSWA 194784). Together, these dates indicate that the basement to the Nornalup Zone contains Paleoproterozoic granitic rocks, and that the presence of Biranup Zone aged granites extends beyond the Biranup Zone itself, below the Fraser Zone. Zircon rims from the Boingaring Rocks sample (GSWA 194785) yielded a date of 1198 ± 11 Ma, which is interpreted as the age of metamorphism and migmatization, and which corresponds to Stage II of the Albany–Fraser Orogeny.

Arid Basin — Cycle 2 sediments

Several successions of metasedimentary rocks that have maximum depositional ages younger than the Biranup Orogeny, but have been affected by Stage I tectonism, occur within the Fraser and Nornalup Zones. These sedimentary successions are here termed Cycle 2 sediments of the Arid Basin. Their provenance provides a record of tectonothermal activity in the region, following the Biranup Orogeny. Most of the dated Cycle 2 sediments contain a substantial portion of detritus with Biranup Zone aged components, reflecting the proximity of the Biranup Zone as a source. The Arid Basin includes the Malcolm Metamorphics of the eastern Nornalup Zone (formerly the Malcolm Gneiss; Myers, 1995b), paragneissic rocks from the western Nornalup Zone (near Albany; Love, 1999), the Gwynne Creek Gneiss, and metasedimentary rocks of the Fraser Range Metamorphics (Fig. 4). Because of their close association with Fraser Zone magmatic rocks, the Fraser Range Metamorphics are covered in the 'Fraser Zone' section.

The Malcolm Metamorphics are dominated by siliciclastic metasedimentary rocks, including mafic amphibolitic schist and minor calc-silicate rocks that are likely to have had volcanic precursors (Plate 1; Fig. 15a). The former Malcolm Gneiss was reported to include c. 1450 Ma granitic gneiss (Myers, 1995b), but recent work by GSWA has not found any evidence of this. The metasedimentary rocks consist dominantly of muscovite–biotite psammite and quartzite, with subordinate garnet–biotite–sillimanite pelitic rocks that are locally migmatitic (Clark, 1999). Two recently dated samples of migmatitic semipelitic gneiss yielded maximum depositional ages of 1455 ± 16 Ma and 1456 ± 21 Ma (Adams, 2011, 2012). This shows that these rocks are substantially younger than the previously published maximum depositional age of 1560 ± 40 Ma (GSWA 112128, Nelson, 1995a), and also indicates that suggestions of the presence of c. 1450 Ma granitic gneiss in this area (Myers, 1995b) may reflect detrital, rather than intrusive, material. Sample GSWA 112128 also yielded an age component at 1807 ± 35 Ma, and single zircons with ages of c. 2033, 2175, and 2734 Ma (Nelson, 1995a).

The Malcolm Metamorphics were intruded by monzogranite and granodiorite of the Recherche Supersuite at 1330 ± 14 Ma (Poison Creek; GSWA 83662, Nelson, 1995d) and 1314 ± 21 Ma (Israelite Bay; GSWA 83663, Nelson, 1995e), during Stage I of the Albany–Fraser Orogeny (Clark et al., 2000). This was followed by formation of northwesterly verging folds, which were cut by a leucocratic microgranite dyke that has a SHRIMP U–Pb zircon age of 1313 ± 16 Ma (Clark et al., 2000). Low-pressure, high-temperature metamorphism (4–5 kbar, 750–800°C; Clark et al., 2000) of the Malcolm Metamorphics occurred either just prior to, or during, intrusion of the microgranite dyke at 1311 ± 4 Ma, recorded by monazite within migmatitic semipelite (Adams, 2011, 2012). Metadolerite dykes also cut the regional foliation in the Malcolm Metamorphics (Clark, 1999). A second period of metamorphism took place during Stage II, at 1180 ± 5 Ma (Adams, 2011).

Paragneiss in the western Nornalup Zone includes garnet–sillimanite migmatite and quartzite (Clark, 1995; Love, 1999). Migmatitic rocks contain detrital zircons with ages of 1750–1720 Ma, have a maximum depositional age of c. 1360 Ma (Whalehead Rock; Love, 1999), and were metamorphosed at 1314 ± 5 Ma (Whalehead Rock; Love, 1999) and 1304 ± 3 Ma (Ledge Point; Clark, 1995). This constrains the depositional age of the Whalehead Rock paragneiss to between c. 1360 and 1310 Ma, and the first episode of metamorphism in these rocks to Stage I (Fitzsimons and Buchan, 2005).

Gwynne Creek Gneiss

The Gwynne Creek Gneiss occurs in the northeastern part of the Albany–Fraser Orogen, between the Fraser and Biranup Zones, east of the Tropicana deposit (Plates 1

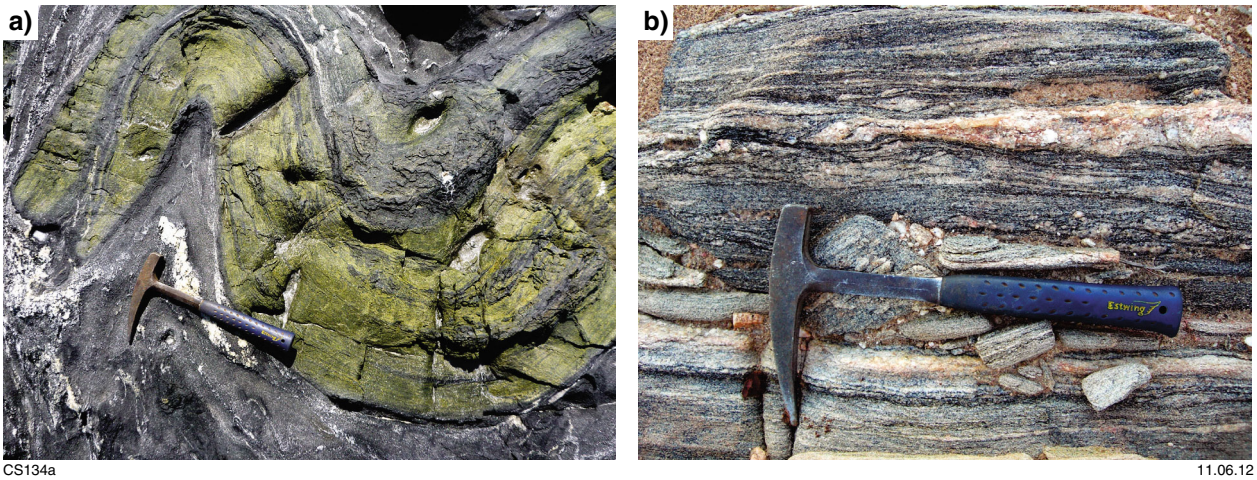

Figure 15. a) Folded calc-silicate (green) rocks interlayered with mafic amphibolite (black); Malcolm Metamorphics, Point Malcolm (MGA 570579E 6260226N); b) semipelitic gneiss with layer-parallel leucosome; Gwynne Creek Gneiss, Gwynne Creek (MGA 688969E 6743276N)

and 2). It outcrops along the far northeastern edge of the Fraser Zone and, although dominated by psammitic and semipelitic gneiss, this unit also includes layered, finely laminated, quartzofeldspathic gneiss with layer-parallel leucosomes and minor metagranitic, metamafic, and meta-ultramafic rocks (see Excursion 2, Stop 11). The paragneissic rocks are intruded by late, coarse to very coarse, K-feldspar-rich pegmatites.

Preliminary geochronology from the semipelitic gneiss (Fig. 15b) shows that these metasedimentary rocks have a maximum depositional age of 1483 ± 12 Ma (based on one analysis), with a more conservative estimate of 1533 ± 11 Ma, based on six zircons (GSWA 182432). This sample also includes a significant 1675 Ma detrital age component, and minor age components at c. 1739 and 1607 Ma. Garnet–biotite-bearing, quartzofeldspathic migmatitic gneiss (GSWA 194735, Kirkland et al., 2010g) yielded a concordia age of 1657 ± 5 Ma, interpreted as representing detrital material from a migmatitic precursor, based on the maximum depositional age described above. Two analyses of high-uranium overgrowths in two zircons yielded an age of 1270 ± 11 Ma, interpreted to date zircon growth during metamorphism. Three analyses, in three zircons, of low-uranium rims yielded an age of 1193 ± 26 Ma, interpreted to reflect zircon growth during a younger metamorphic event. Because the low-uranium rims heal brittle fractures that transect entire zircon crystals, including the high-uranium overgrowths, the timing of brittle deformation in this rock is constrained between 1270 and 1193 Ma (Kirkland et al., 2011a).

Recherche and Esperance Supersuites

The 1330–1280 Ma Recherche Supersuite (formerly the Recherche Granite of Myers, 1995b; Nelson et al., 1995; Clark, 1999) and the 1200–1140 Ma Esperance Supersuite (formerly the Esperance Granite of Myers, 1995b; Nelson et al., 1995) mark two major magmatic events that coincided with Stages I and II of the Albany–Fraser Orogeny, respectively (Figs 4 and 5; Clark et al., 2000). Igneous rocks belonging to the Recherche Supersuite are generally metamorphosed to amphibolite or granulite conditions, contain a gneissic fabric, and include synmagmatic mafic rocks (Myers, 1995b; Nelson et al., 1995). Deformation and metamorphism occurred during Stages I, II, or both (Nelson et al., 1995; Clark et al., 2000). Igneous rocks belonging to the Esperance Supersuite are generally metamorphosed up to greenschist or amphibolite facies, and are generally less pervasively deformed than rocks of the Recherche Supersuite, but may locally contain a foliation or be mylonitic (Myers, 1995b; Nelson et al., 1995). Strongly magnetic, variably deformed granitic bodies in aeromagnetic images are correlated with the Esperance Supersuite (Plate 1).

At least two distinct varieties of granitic rocks belonging to the Recherche Supersuite have been recognized in the eastern Nornalup Zone (Clark, 1999); the most common is a biotite–hornblende monzogranitic gneiss that contains rare calc-silicate boudins (e.g. GSWA 83662 from Poison Creek, dated at 1330 ± 14 Ma; Nelson, 1995d). The other variety is a peraluminous, garnet-bearing granodiorite gneiss that lacks hornblende (e.g. GSWA 83663 from Israelite Bay, dated at 1314 ± 21 Ma; Nelson, 1995e). The Recherche Supersuite contains synplutonic mafic dykes and intrusions that show extensive back- and net-veining and disaggregation by granite, and hybrid zones that indicate magma mingling (Myers, 1995b; Clark, 1999). These rocks are intruded by equigranular microgranite dykes, one of which yielded an interpreted igneous crystallization age of 1313 ± 16 Ma (Clark et al., 2000). Granitic rocks belonging to the Recherche Supersuite are much less abundant in the western Nornalup Zone, which is dominated by Stage II granitic rocks (Fitzsimons and Buchan, 2005).

In the northeastern Nornalup Zone, core from the Big Red prospect (Fig. 3) contains interlayered granitic gneiss, metasedimentary gneiss, and mafic amphibolite,

which are similar to rocks of the adjacent Fraser Zone. Migmatitic gneiss (hole BRDDH2, GSWA 182476), interpreted as a probable metagranitic rock, yielded a magmatic crystallization age of 1326 ± 6 Ma, consistent with the age of early Recherche Supersuite intrusions. The same sample also yielded a date of 1187 ± 9 Ma, interpreted as Stage II high-temperature metamorphism. Mafic granulite (hole BRDDH2, GSWA 182477) yielded a date of 1188 ± 4 Ma, also interpreted as the age of high-temperature metamorphism.

Recherche Supersuite meta-igneous rocks are also present in the southeastern parts of the Biranup Zone, and one occurrence is exposed within the Munglinup Gneiss of the Northern Foreland. This suggests a spatial connection between the Northern Foreland and the Kepa Kurl Booya Province, and between the Biranup and Nornalup Zones, during Stage I of the Albany–Fraser Orogeny. However, the Northern Foreland spatial connection is rather tenuous, being based solely on one example of biotite granodioritic gneiss from near Bald Rock, which has an igneous crystallization age of 1299 ± 14 Ma (see 'Munglinup Gneiss').

In the southeastern Biranup Zone, biotite monzogranitic gneiss from Mount Burdett, hornblende–biotite syenogranitic gneiss from Coramup Hill (north of Esperance), and foliated leucogranite from Observatory Point (west of Esperance) all have c. 1300 Ma ages, and as such are assigned to the Recherche Supersuite (Fig. 16). The biotite monzogranitic gneiss from Mount Burdett yielded an interpreted igneous crystallization age of 1299 ± 18 Ma (GSWA 83697, Nelson, 1995h). The Coramup Hill syenogranitic gneiss (GSWA 83700A, Nelson, 1995i) yielded an igneous crystallization age of 1283 ± 13 Ma. This metasyenogranite contains layers of metamafic rock, is strongly foliated, and intrudes a grey, biotite-rich metagranite. Foliated leucogranite from Observatory Point yielded a date of 1288 ± 12 Ma, interpreted as the igneous crystallization age (GSWA 83659, Nelson, 1995c).

The Esperance Supersuite represents magmatism associated with Stage II of the Albany–Fraser Orogeny. Although originally defined as having occurred in the late stages of that event, at c. 1140 Ma (Nelson et al., 1995; Clark et al., 2000), Esperance Supersuite magmatism is now thought to have extended from c. 1200 to 1140 Ma. The Esperance Granite of Myers (1995b) was defined as comprising relatively undeformed, low metamorphic grade granitic rocks that intruded the Recherche Granite, based on dating from Wireless Hill (Esperance) and Balladonia Rock (east of Newman Rocks).

Unmetamorphosed, porphyritic, biotite granite sampled from Balladonia Rock has an imprecise date (based on five analyses) of 1135 ± 56 Ma, interpreted as the age of igneous crystallization (GSWA 83667, Nelson, 1995f). An interpreted minimum age of igneous crystallization of 1138 ± 38 Ma was obtained from unmetamorphosed, porphyritic, biotite monzogranite quarried from Wireless Hill in Esperance (GSWA 83657A, Nelson, 1995b), but sampled from Esperance Harbour jetty.

The spatial extent of Esperance Supersuite rocks across the Albany–Fraser Orogen is not well constrained, although the supersuite appears to be most voluminous in the Nornalup Zone. Preliminary geochronology from monzogranite at Mount Ridley (GSWA 184374; Fig. 16) yielded a magmatic crystallization age of 1196 ± 11 Ma. Although the monzogranite appears undeformed in outcrop, aeromagnetic imagery indicates that its margins are deformed, and that the central, more competent core of the granitic body defines a strain shadow within the strongly deformed gneissic rocks of the Biranup Zone. A similar granitic body, also interpreted to be part of the Esperance Supersuite, occurs to the southwest (Fig. 16), suggesting that the magmatism that produced the Esperance Supersuite was not confined to the late stages of Stage II, but extended from at least c. 1200 Ma to 1140 Ma.

Ragged Basin — Cycle 3 sediments

In the eastern Albany–Fraser Orogen, the Mount Ragged Formation was not deposited until after Stage I tectonism, and is therefore interpreted as a cover unit overlying the Kepa Kurl Booya Province, here termed Cycle 3 sediments of the Ragged Basin (Figs 2 and 4). Although situated within the Madura Province, the Salisbury Gneiss is also inferred to be part of the Ragged Basin.

The Mount Ragged Formation comprises upper-greenschist to lower-amphibolite facies, massive grey quartzites, muscovite quartzites, and sporadic thin layers of pelitic rocks (Clark, 1999). The mature quartzose sediments are interpreted as deposited in shallow intracratonic basins (Clark et al., 2000). SHRIMP U–Pb analysis of these rocks identified an older detrital zircon component (seven analyses) with a weighted mean age of 1783 ± 12 Ma and a maximum depositional age, defined by 12 analyses, of 1321 ± 24 Ma. This age is consistent with local derivation from the unconformably underlying Recherche Supersuite and, in conjunction with the angular relationship between the Mount Ragged Formation and the complexly deformed gneissic rocks that it overlies, suggests that the eastern Nornalup Zone was uplifted and eroded between Stages I and II of the Albany–Fraser Orogeny (Clark et al., 2000). Such an interpretation is supported by the presence of amphibolite-facies metamorphism (4–5 kbar, 550°C) and growth of 1154 ± 15 Ma rutile in the rocks of the Mount Ragged Formation, which shows that these rocks were buried and metamorphosed during Stage II (Clark et al., 2000). The interpretation is further supported by the dating of zircons from metasedimentary rocks of the Gwynne Creek Gneiss, which showed that high-uranium zircon overgrowths were fractured and overgrown with a later phase of metamorphic zircon, indicating a period of crustal uplift and cooling between c. 1270 and 1197 Ma (GSWA 194735, Kirkland et al., 2010g; Kirkland et al., 2011a).

A similar origin and depositional setting is likely for the pelitic protoliths of the Salisbury Gneiss (Bodorkos and Clark, 2004b). The Salisbury Gneiss is exposed on a series of islands offshore to the southeast of Esperance, and is separated from the Malcolm Metamorphics to the northwest by the Rodona Shear Zone (Fig. 3; Clark et al., 2000). On Salisbury Island, the Salisbury Gneiss comprises pelitic gneisses and mafic granulite, porphyritic

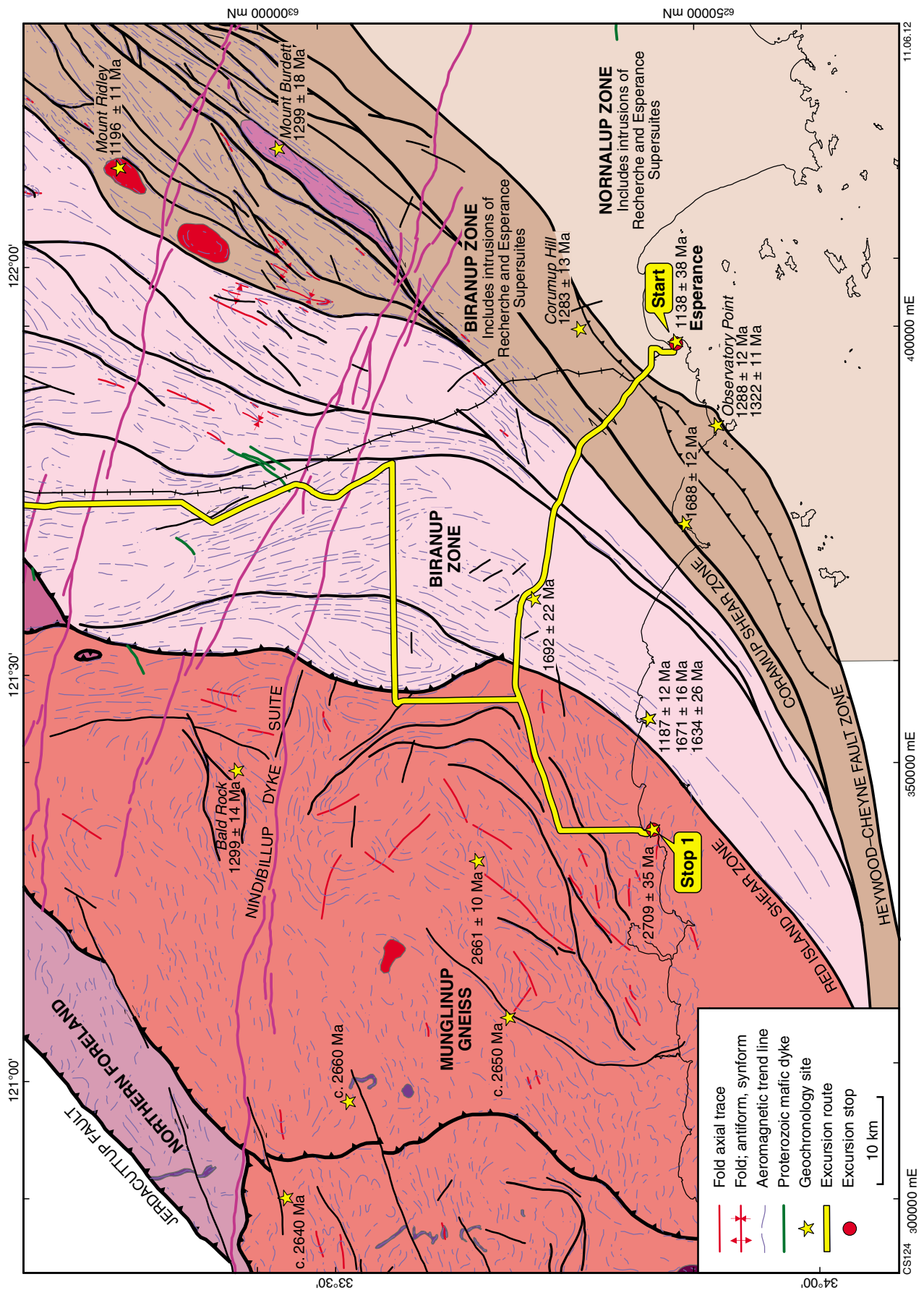

Figure 16. Interpreted bedrock geology of the region around, and to the west of, Esperance, showing published and preliminary GSWA geochronology, and excursion route and stops.

granitic gneiss, and a two-pyroxene metagabbro that is undeformed in its core but deformed and amphibolitic at its margins (Clark, 1999). Outcrops of migmatitic pelitic gneiss contain mesosomes of biotite–sillimanite–garnet–cordierite–feldspar–quartz(–spinel), and leucosomes that are K-feldspar-rich with localized garnet(–cordierite). These gneisses record granulite-facies metamorphic conditions of approximately 800°C and >5 kbar (Clark, 1999; Clark et al., 2000). The depositional age of the Salisbury Gneiss is unknown, although a lack of evidence for Stage I metamorphism suggests deposition after this event, and therefore that the unit is distinct from the Malcolm Metamorphics (Clark, 1999). Migmatitic leucosome derived from partial melting of the pelitic gneiss yielded dates of 1214 ± 8 (18 core analyses) and 1182 ± 13 Ma (six rim analyses; Clark et al., 2000). The older date is interpreted as the age of crystallization of the leucosome, whereas the younger date is interpreted to reflect zircon growth during decompression from peak metamorphic conditions (Clark et al., 2000).

In the Malcolm Metamorphics, a late-stage pegmatite yielded a SHRIMP U–Pb monazite age of 1165 ± 5 Ma. This was interpreted as the age of crystallization of the pegmatite, the age of shearing related to thrusting of the Salisbury Gneiss to the northwest along the Rodona Shear Zone (Fig. 3), and the age of related deformation in the Mount Ragged Formation (Clark et al., 2000).

Mafic dyke suites

Four mafic dyke suites can be recognized within the Albany–Fraser Orogen, based on orientation, magnetic character, and previous work: the Widgiemooltha, Gnowangerup–Fraser, Nindibillup, and Beenong Dyke Suites (Plate 1). A fifth suite, the Cosmo Newbery Dyke Suite, is only recognized in aeromagnetic data, and is interpreted both in the northeast of the Albany–Fraser Orogen and the adjacent Eastern Goldfields Superterrane (Plates 1 and 2).

Dykes belonging to the Widgiemooltha Dyke Suite are mostly recognizable in the Yilgarn Craton, where they are mostly undeformed. They trend easterly to east-northeasterly, are mostly 10–50 m wide, but can be up to 2 km wide, and have lateral extents up to hundreds of kilometres (Sofoulis, 1966; Myers, 1990b; Wingate, 2007). The Binneringie Dyke and the Jimberlana Norite are the largest intrusions of this suite. In general, dykes belonging to the Widgiemooltha Dyke Suite are composed of olivine gabbro and dolerite, and include cumulate textures and granophyric differentiates (Campbell et al., 1970; Elias and Bunting, 1982; Griffin, 1989). An extension of the Binneringie Dyke to the west has isotope-dilution thermal ionization mass spectrometry (IDTIMS) and ion microprobe (SHRIMP) U–Pb baddeleyite ages of 2418 ± 3 Ma and 2420 ± 7 Ma, respectively (Nemchin and Pidgeon, 1998). These ages are within uncertainty of Rb–Sr and Sm–Nd isochron ages of 2411 ± 52 and 2411 ± 55 Ma, respectively, for the Celebration Dyke and Jimberlana Norite (Turek, 1966; Fletcher et al., 1987). The baddeleyite ages reported above are slightly older than an IDTIMS baddeleyite age of 2410 ± 2 Ma from the Binneringie Dyke (French et al., 2002), and precise SHRIMP baddeleyite and zircon ages of 2403 and 2407 Ma from the Jimberlana Norite (Wingate et al., unpublished data). Dykes belonging to the Widgiemooltha Dyke Suite crosscut Archean structures in the Yilgarn Craton, but are in turn cut by structures formed during the Mesoproterozoic Albany–Fraser Orogeny.

The Gnowangerup–Fraser Dyke Suite is one of the largest of the five mafic dyke suites, extending across the southern and southeastern parts of the Yilgarn Craton, and forming part of the c. 1210 Ma Marnda Moorn Large Igneous Province (Wingate et al., 2005). It includes northeasterly trending dykes from the eastern Albany–Fraser Orogen and southeastern Yilgarn Craton, informally named the Fraser dykes, which appear to be continuous with those in the central Albany–Fraser Orogen and southern Yilgarn Craton. Most dykes belonging to the Gnowangerup–Fraser Dyke Suite are moderately to strongly magnetic. Their trend changes from dominantly east-northeasterly in the west, to northeasterly in the east — parallel to the craton margin. In aeromagnetic images, the dykes are visible as multiple intrusions, with the two dominant trends overlapping each other where they meet in the central Albany–Fraser Orogen and southern Yilgarn Craton margin (Geological Survey of Western Australia, 2007). East of Ravensthorpe the dykes are particularly numerous. Dykes belonging to the Gnowangerup–Fraser Dyke Suite typically consist of dolerite or gabbro (Wingate et al., 2005). Two dykes from the Gnowangerup–Fraser Dyke Suite have zircon ages of 1203 ± 15 Ma and c. 1238 Ma (Evans, 1999), and three others (in the Stirling Ranges) have zircon, baddeleyite, and zirconolite ages of 1215 ± 10, 1217 ± 39, and 1218 ± 3 Ma, respectively (Rasmussen and Fletcher, 2004). A northeast-trending Fraser dyke exposed in the Victory Gold Mine at Kambalda yielded a baddeleyite age of 1212 ± 10 Ma (Wingate et al., 2000). This dyke has identical paleomagnetic directions to four dykes near Ravensthorpe, supporting the interpretation that the Fraser and Gnowangerup dykes are part of the same suite (Giddings, 1976; Pisarevsky et al., 2003; Wingate et al., 2005). In the central Albany–Fraser Orogen (within the Kepa Kurl Booya Province and most of the Munglinup Gneiss), dykes from this suite are mostly strongly deformed, and therefore are not discernable in aeromagnetic images (Spaggiari et al., 2009).

In the Tropicana region of the northeastern part of the Albany–Fraser Orogen, abundant northeasterly trending mafic dykes are evident in aeromagnetic images, but are not exposed (Plate 2). Based on their orientation, these dykes may be part of the c. 1210 Ma Gnowangerup–Fraser Dyke Suite, but because they crosscut all structures in the region, this interpretation would only be valid if that part of the orogen has not been affected by Stage II (1215–1140 Ma) of the Albany–Fraser Orogeny. This seems unlikely, given the prevalence of Stage II metamorphism and fabrics throughout the rest of the orogen (Figs 4 and 5). Therefore, it is possible that these dykes may post-date Stage II. One interpretation is that they may be part of the widespread c. 1075 Ma Warakurna Supersuite (Wingate et al., 2004).

The Nindibillup Dyke Suite comprises mafic (dolerite) dykes with an east-southeasterly trend (Spaggiari et al., 2009). These dykes vary from strongly magnetic and extensive — some up to hundreds of kilometres long — to moderately or nonmagnetic varieties that are less extensively developed. The dykes of this suite clearly crosscut major structures of the Albany–Fraser Orogen, and post-date Stage II (1215–1140 Ma) of the Albany–Fraser Orogeny. Preliminary geochronology, based on a sample from one of the largest (over 400 km long), strongly magnetic dykes of this suite, has yielded a date of c. 750 Ma, although additional geochronology will be required to confirm this age.

The Beenong Dyke Suite comprises a set of northwesterly trending dykes (Spaggiari et al., 2009), which are mostly moderately magnetic and tend to be relatively short in length, especially in comparison to dykes of the Nindibillup Dyke Suite. Their age is presently unknown, although they clearly crosscut structures in the Albany–Fraser Orogen. Their composition is also unknown. Although these dykes have the same trend as the c. 1210 Ma Boyagin dykes, which are part of the Marnda Moorn Large Igneous Province in the western Yilgarn Craton (Wingate et al., 2005), they are probably younger as they crosscut Stage II structures within the Kepa Kurl Booya Province.

Tectonic events

Three major tectonic events have been recognized in the Albany–Fraser Orogen (Fig. 4). Widespread magmatism, the formation of sedimentary basins, and high-temperature metamorphism and deformation, including the Zanthus Event, are here collectively termed the Biranup Orogeny. Based on current geochronology, this orogeny covers the period 1710–1650 Ma (Figs 4 and 5). However, it is now clear that this was not the first event to take place during the Paleoproterozoic along the southern and southeastern Yilgarn Craton margin. The presence of c. 1806 Ma and c. 1760 Ma granitic rocks in the Biranup and Nornalup Zones, c. 1800 Ma zircon inheritance in younger magmatic rocks, and the deposition of the Stirling Range Formation at c. 1800 Ma (Figs 4 and 5), all indicate tectonic activity prior to the Biranup Orogeny, marking the onset of modification to the southern and southeastern Yilgarn Craton margin by at least 1800 Ma. This also indicates active margin processes during Paleoproterozoic times, encompassing rocks of the Northern Foreland, Biranup, and Nornalup Zones. The c. 1650 Ma lower age limit for the Biranup Orogeny is a conservative estimate, and does not include the youngest known Biranup Zone metagranite — a single metasyenogranite dated at 1627 ± 4 Ma (GSWA 194736, Kirkland et al., 2010h). As such, the timing of completion of the Biranup Orogeny is not constrained.

The Zanthus Event occurred at c. 1680 Ma, and is constrained by the dating of folded migmatitic leucosomes in Biranup Zone hornblende–biotite–garnet granitic gneiss at 1676 ± 6 Ma, and crosscutting axial planar leucosomes in the same granitic gneiss at 1679 ± 6 Ma (Ponton Creek area; Fig. 8; Kirkland et al., 2011a). Gneisses along Ponton Creek contain an early gneissic fabric with centimetre-scale, layer-parallel leucosomes (Fig. 7g), folded into northwesterly trending isoclinal folds that have an axial-planar foliation. The axial planes were locally injected by a second generation of leucosomes, one of which was sampled for dating by chiselling out the leucosome material along the axial plane (Fig. 7h). The dating shows that the two generations of leucosomes are within uncertainty of one another. The structural observations indicate that leucosome injection occurred during a period of northeasterly–southwesterly directed shortening (present coordinates), the age of which is constrained by the zircon U–Pb results from these samples. The characteristic northwesterly trend of the gneisses in the Ponton Creek area is consistent with the trends in aeromagnetic data within the large fault slice that contains the gneisses (Fig. 8). This fault slice preserves evidence of both the shortening event and the migmatization that accompanied it; i.e. the Zanthus Event. The northwesterly trending fabric is truncated by the northeasterly trending fabric of the Fraser Fault Zone, which bounds the Mesoproterozoic Fraser Zone to the southeast.

The Albany–Fraser Orogeny is divided into two tectonic events: Stage I (1345–1260 Ma) and Stage II (1215–1140 Ma) (Clark et al., 2000; Bodorkos and Clark, 2004a). Stage I of the orogeny is widely assumed to have been caused by the collision of the West Australian Craton with the combined Mawson and South Australian Cratons, whereas Stage II is interpreted to represent intracratonic reworking (e.g. Myers et al., 1996; Clark et al., 2000; Giles et al., 2004; Spaggiari et al., 2009). Stage I is dominantly represented by voluminous mafic and felsic magmatism forming both the Recherche Supersuite and magmatic rocks of the Fraser Zone, and was accompanied by high-temperature metamorphism and deformation (e.g. Clark, 1999; Bodorkos and Clark, 2004a,b). The presence of c. 1300 Ma granitic intrusions within each of the Northern Foreland, and Biranup, Fraser, and Nornalup Zones suggests a spatial link, or stitching, of these tectonic units by the end of Stage I. This in turn indicates that high-temperature metamorphism during Stage II — which was widespread in both the central and eastern Biranup Zone, and is recorded in the Munglinup Gneiss, Gwynne Creek Gneiss, and Recherche Supersuite — took place within an intracratonic setting. Major, dominantly thrust faults (e.g. Jerdacuttup Fault, Cundeelee Fault, Red Island Shear Zone), which juxtapose different tectonic units and internal fault-bound sequences, are also interpreted to have been active during Stage II. The development of fold and thrust sequences in the central and western parts of the orogen during Stage II are evident in the structural sequence documented and dated at Bremer Bay (Spaggiari et al., 2009; Barquero-Molina, 2010), in the Mount Barren Group (Dawson et al., 2003), and in the Stirling Range Formation (Rasmussen et al., 2002; Black et al., 1992).

Whole-rock geochemical datasets

Obtaining representative geochemical data for all exposed igneous rock units in the Albany–Fraser Orogen is critical for understanding the crustal evolution of the orogen. With sufficient data, and in association with

geochronological data, age-constrained 'suites' may be recognized both chemically and geographically. These data not only help us to understand the petrogenesis of the specific magmatic units, but can form a powerful mapping tool and provide critical information on the geodynamic evolution of the orogen itself. Although our geochemical database is not extensive enough for rigorous interpretation, the data currently available confirm that a larger and geographically more extensive dataset will greatly contribute to the understanding of the evolution of the Albany–Fraser Orogen.

Granitic rocks of the Biranup and Fraser Zones

Based on the geochemistry of a limited number of samples, granitic rocks from specific tectonic regions and of particular ages appear to form relatively distinct groups, permitting, as yet very cautious, petrogenetic interpretations. For example, the 1700–1650 Ma granites of the eastern Biranup Zone are sodium-poor calc-alkaline rocks (Fig. 17a). Their major and trace-element compositions, and their continuous range of silica values, are perhaps suggestive of an arc-setting. In contrast, the c. 1300 Ma granites of the Fraser Zone have restricted high-silica and ferroan compositions (Fig. 17b) more suggestive of very high temperature melting of dry, quartzofeldspathic crust.

The composition of the Munglinup Gneiss from the Northern Foreland is entirely consistent with geochronological and isotopic evidence that this unit contains a significant component of reworked Archean (Yilgarn Craton) crust. This gneiss is typically sodic (Fig. 17a), is highly enriched in large-ion lithophile elements such as strontium (Fig. 17c), and combines very low ytterbium concentrations with high La/Yb ratios (Fig. 17d,e) — a signature of Archean granites that reflects the high-pressure (garnet-present) melting of mafic crust. Interestingly, the metasyenogranite from Cave Rock in the southeastern Biranup Zone (Fig. 9; see Excursion 1, Stop 3), interpreted to be a fragment of the Yilgarn Craton (red asterix on plots in Fig. 17), also has these 'Archean granite' signatures — supportive of that interpretation. In addition, the same signature is seen in several granites from the central part of the Biranup Zone (Fig. 17), and it is possible that these also contain a significant component of reworked Archean crust.

Metagabbroic rocks of the Fraser Range Metamorphics

Metagabbros have been sampled over a wide area of the exposed southern part of the Fraser Zone. These metagabbros typically form closely sheeted sills separated by quartzofeldspathic layers that represent either metasedimentary layers, granites, or both. Melting of the quartzofeldspathic gneiss was synchronous with gabbro emplacement, an interpretation consistent with the occurrence of hybridization along contact zones.

The most primitive gabbros are low- to medium-potassium tholeiites (Fig. 18a,b; green dots) with trace-element patterns showing small to moderately negative niobium anomalies (not shown), which is consistent with an early-arc, oceanic-arc, or fore-arc setting — or more simply, with minor crustal contamination. The quartzofeldspathic rock between the gabbro sheets is compositionally diverse, but can essentially be subdivided into two end-members: one with high thorium, lanthanum, and ytterbium concentrations (Fig. 18c–e; red dots with black margin, and field with yellow shade), consistent with fractionation of a mafic magma (possibly the gabbro itself); and the other with low lanthanum and ytterbium concentrations, and high La/Yb ratios (Fig. 18f; red dots, and field with blue shade), perhaps reflecting high-temperature partial melting of dry quartzofeldspathic material. Interestingly, gabbros that show field evidence for mingling or hybridization, or that were sampled very close to lithological contacts (Fig. 18c–e; blue dots), show trends consistent with mixing between primitive gabbro magmas and both felsic end-member compositions (i.e. three-component mixing). This type of mixing is thought to be typical of a deep crustal 'hot-zone'. In such zones, repeated gabbro intrusion eventually raises ambient temperatures above the solidus of both the gabbro and the quartzofeldspathic country rock. This means that the gabbro sills retain an evolved (i.e. granitic) liquid fraction (i.e. incompletely crystallize) and the quartzofeldspathic country rocks partially melt (to produce granite), and that both of these granite fractions are available to mix with remaining or newly emplaced gabbroic melts to form a range of hybrid compositions.

Lu–Hf isotopes

Understanding the geological evolution of a region is enhanced by knowledge of the timing of extraction of material from the mantle to form the crustal substrate. It also requires an understanding of how this process occurred: either by direct extraction from the mantle into the crust, or through several reworking steps. Zircon Lu–Hf isotope measurements, when coupled with U–Pb geochronology on the same crystals, provide time-integrated information about the relative roles of juvenile mantle input or reworking of older continental crust (e.g. Kinny and Maas, 2003), and can characterize the source of magmatism (e.g. Kemp et al., 2009, 2010). Such information is important in constraining geological models, and in defining zones of juvenile material that are known to be prospective for mineralization. Lu–Hf isotopes are also a useful tool for constraining geodynamic models, as they can indicate temporal trends in source composition that may be related to the tectonic setting (Kirkland et al., 2011a; Collins et al., 2011).

The evolution of hafnium in a sample can be referred to models of solid-Earth evolution (e.g. Chondritic Uniform Reservoir (CHUR) or Depleted Mantle (DM)). Due to the low Lu/Hf ratio in zircon, there is relatively little production of radiogenic hafnium in zircon and, following a small time-correction, this can accurately record the value in the magma source at the time of crystallization

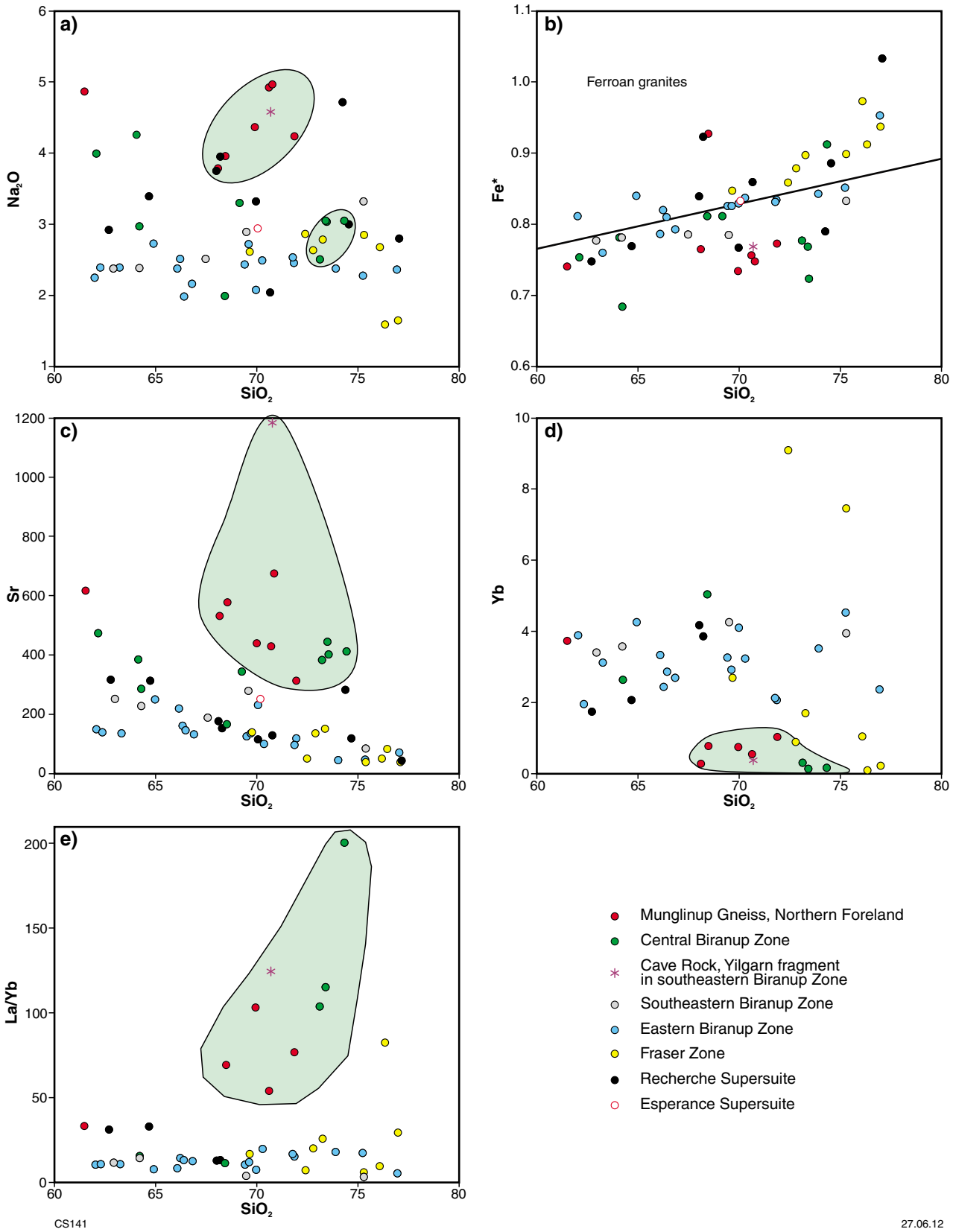

Figure 17. Whole-rock geochemistry plots for granitic rocks from the Northern Foreland, and Biranup and Fraser Zones, showing Na_2O (a), Fe* (b), Sr (c), Yb (d), and La/Yb (e) against SiO_2. Green shading shows the field for rocks with compositions similar to Archean granites. See text for explanation.

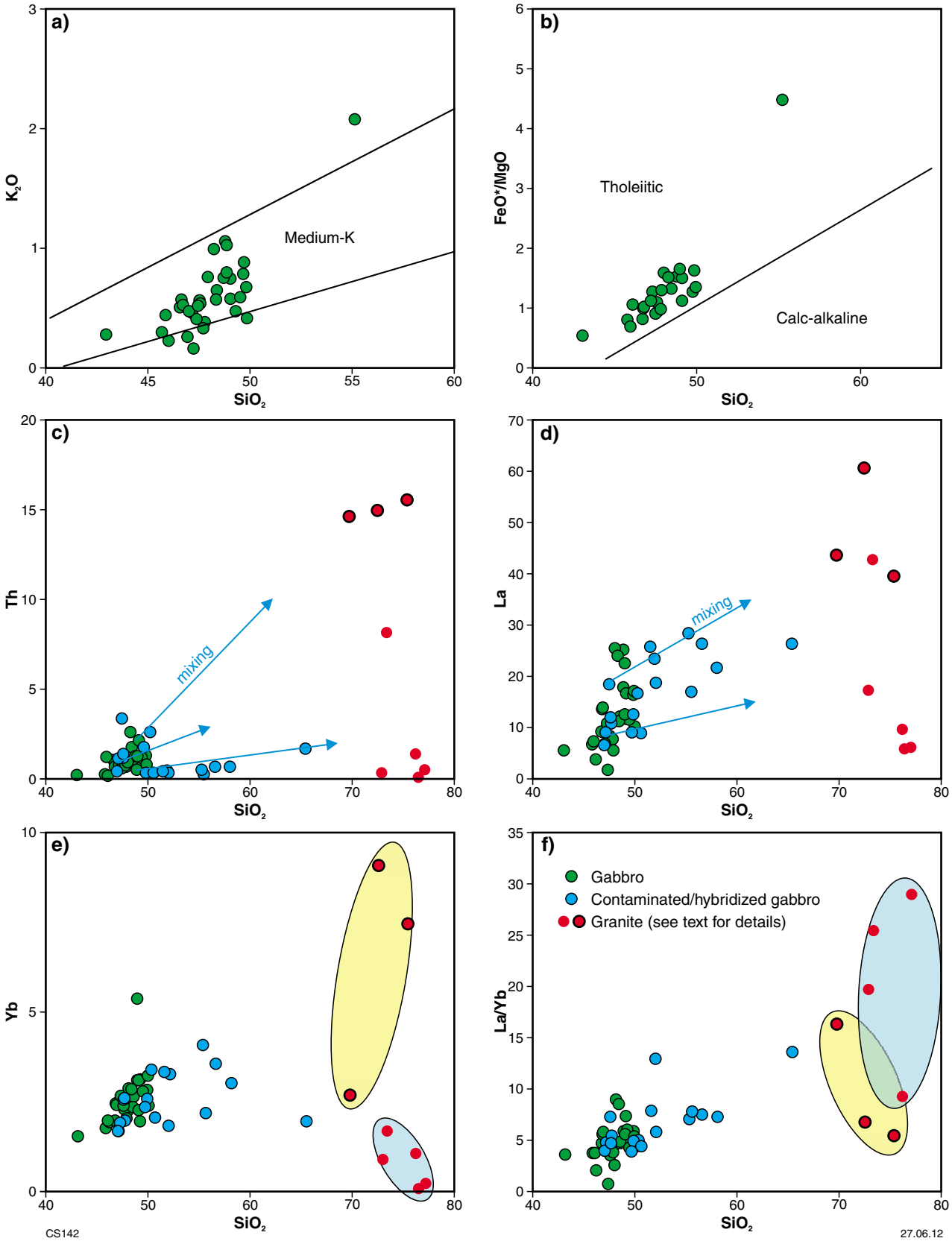

Figure 18. Whole-rock geochemistry plots for gabbroic rocks from the Fraser Zone, showing K_2O (a), FeO*/MgO (b), Th (c), La (d), Yb (e), and La/Yb (f) against SiO_2. See text for explanation.

(Kinny and Maas, 2003). To use this information to constrain the time of extraction of the hafnium from the mantle (crustal residence time) an assumption on the Lu/Hf ratio of the precursor hafnium reservoir is required (i.e. the material in which the hafnium resided prior to being incorporated into the zircon). Based on this assumption (e.g. a Lu/Hf ratio of typical crust is 0.015), the time at which hafnium retained in the zircon was extracted from the mantle can be estimated (e.g. Griffin et al., 2002).

Sm–Nd model ages (T_{DM}) of 2930–2920 Ma obtained from the rocks of the Munglingup Gneiss in the Northern Foreland (Fig. 2; see above) are similar to those from felsic units within the Eastern Goldfields Superterrane (Nelson et al., 1995). Hafnium analyses from the Northern Foreland define a relatively restricted range of initial-hafnium values, indicating extraction from the mantle at about 3.4 Ga (Fig. 19). The Eastern Goldfields Superterrane yields hafnium model ages of 4.2 – 2.9 Ga. The model ages from the Northern Foreland are broadly similar to those from the Eastern Goldfields Superterrane and support the interpretation that the Munglingup Gneiss is a component of the craton that was intruded by granitic rocks during Stage I, and metamorphosed to granulite facies during Stage II of the Albany–Fraser Orogeny (Spaggiari et al., 2009).

A regional compilation of Lu–Hf isotopes across the Yilgarn Craton (Wyche et al., in press) indicates at least four episodes of mantle extraction in the central and eastern Yilgarn Craton — at c. 4.2, c. 3.5, c. 3.1, and c. 2.7 Ga. The earliest episode of mantle extraction is not recorded in the Eastern Goldfields Superterrane, indicating that crust formation in this region post-dated the earliest development of the Yilgarn Craton. Subsequent, broadly contemporaneous episodes of mantle extraction and crustal reworking are indicated by the datasets for both the Eastern Goldfields Superterrane and the Southern Cross

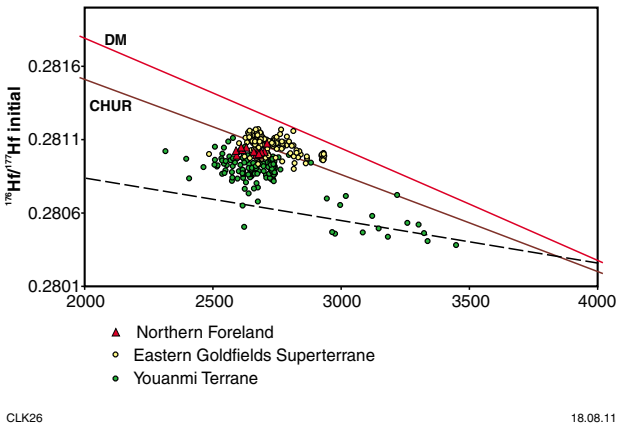

Figure 19. Initial-hafnium evolution plot for magmatic zircons from the Northern Foreland compared to the Youanmi Terrane and Eastern Goldfields Superterrane of the Yilgarn Craton. The dashed line represents the evolution of a reservoir with a Lu/Hf ratio of 0.015. Individual ages are based on $^{207}Pb/^{206}Pb$ ratios. Abbreviations used: DM = Depleted Mantle; CHUR = Chondritic Uniform Reservoir.

Domain of the Youanmi Terrane. However, a connection between the crustal sources of the central and eastern Yilgarn Craton is implied by the overlap of the most radiogenic values in the Youanmi Terrane with the most evolved analyses in the Eastern Goldfields Superterrane. This overlap is consistent with an autochthonous origin for the Eastern Goldfields Superterrane (i.e. formed on the margin of the Youanmi Terrane), and a horizontally layered crustal architecture for the craton.

Hafnium values for the Northern Foreland fall within the area of overlap between the values for the Eastern Goldfield Superterrane and Youanmi Terrane (Fig. 19). A non-parametric statistical test (Kolmogorov–Smirnov test; Fasano and Franceschini, 1987) of the hafnium components in zircon between the individual domains and terranes of the Yilgarn Craton and the Northern Foreland reveals a weak correlation between the Eastern Goldfields Superterrane hafnium components, but no correlation between the Northern Foreland and Youanmi Terrane with other regions (Fig. 20; Table 1). The lack of correlation does not imply a total absence of coeval mantle extraction events across this region, but indicates either some unique events in specific areas, or more likely, the mixing of different magma sources (e.g. a juvenile component together with different evolved crustal sources) across the region. Based on hafnium isotopes alone, it is not possible to associate the Northern Foreland with a specific domain or terrane of the Yilgarn Craton (Fig. 20).

Magmatic zircons in rocks of the Paleoproterozoic Biranup Zone display a distinctive continuous increase towards more radiogenic εHf values over time, commencing at approximately -12 at 1700 Ma and increasing to +2.6 at 1655 Ma (Fig. 21). Hafnium isotope data from c. 1700 Ma magmatic zircons from the eastern Biranup Zone encompass Yilgarn Craton -like values, but also extend to more juvenile signatures (Fig. 21; see also Kirkland et al., 2011a). Magmatic rocks in the Biranup Zone show increasingly radiogenic (depleted) εHf values with decreasing age (Fig. 22). Mixing textures, whole-rock chemical evolution, and neodymium and hafnium isotopes all support a model of melt production from mixed sources — an evolved component with crustal residence ages of less than c. 3100 Ma, and a juvenile component. Scale independence in the relationship of juvenile addition through time (i.e. from individual crystals to entire intrusions) can be recognized in the Biranup Zone. The outer edges of magmatic zircons consistently indicate higher εHf values than the grain centres, when outside of analytical uncertainty (Kirkland et al., 2011a). This implies incorporation of material with higher Lu/Hf ratios through time, which is consistent with either cratonic rifting or back-arc formation on an active margin.

In situations where a single crustal source has been reworked for several hundred million years without the addition of new crust, the slope of the evolution array defined by zircons with the highest εHf will define the source Lu/Hf ratio (Hawkesworth et al., 2010). However, in the case of the Biranup Zone, the indication of increasingly juvenile addition through time is strongly supported by the steep positive slope of the array through the most radiogenic data. This array cannot be interpreted as evolution of a consistent source, because it would

Table 1. Table of K–S P-values used to test the hypothesis that the hafnium isotope model-age distributions in zircons are identical between samples from individual Yilgarn Craton terranes and the Northern Foreland. A P-value of greater than 0.05 indicates a 95% confidence that the model-age components are similar. A conservative 50 Ma uncertainty is assumed for each model age. The samples highlighted in bold have a statistically identical Hf isotopic signature in their zircon components (at the 95% confidence level).

	Kalgoorlie Terrane	*Kurnalpi Terrane*	*Yamarna Terrane* [a]	*Burtville Terrane*	*Youanmi Terrane*	*Northern Foreland*
Kalgoorlie Terrane	-	**1.000**	0.012	**0.683**	0.000	0.000
Kurnalpi Terrane	**1.000**	-	0.033	**0.465**	0.000	0.002
Yamarna Terrane [a]	0.012	0.033	-	**0.060**	0.000	0.000
Burtville Terrane	**0.683**	**0.465**	**0.060**	-	0.000	0.000
Youanmi Terrane	0.000	0.000	0.000	0.000	-	0.000
Northern Foreland	0.000	0.002	0.000	0.000	0.000	-

NOTES: (a) indicates a low number of analyses and therefore uncertain significance.

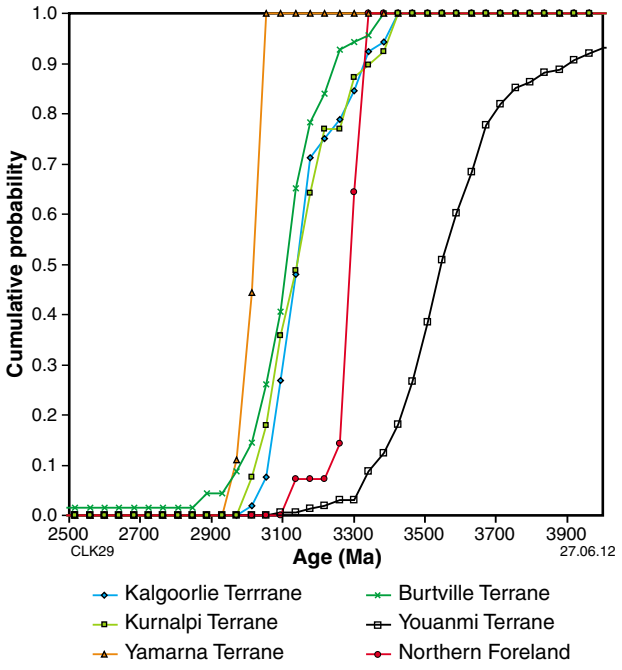

Figure 20. Probability density diagram comparing model-age distributions between the Northern Foreland and potential correlative terranes in the Yilgarn Craton. Similarity between the cumulative density curves is compared statistically using a K–S test (Table 1).

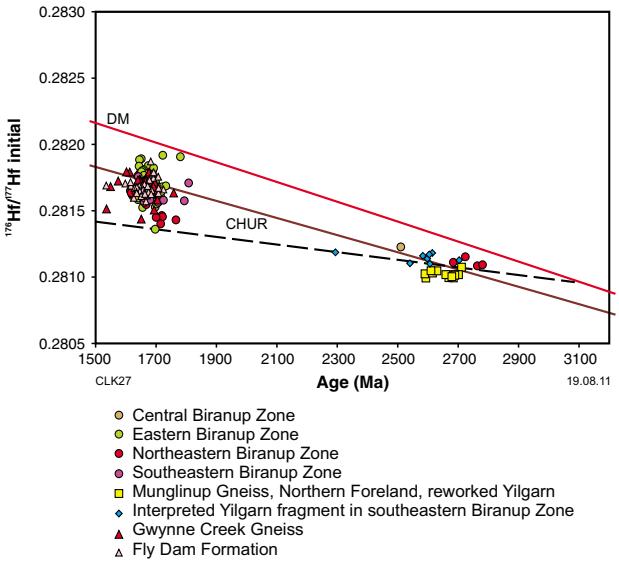

Figure 21. Initial-hafnium evolution plot for magmatic zircons from the Biranup Zone compared to the Northern Foreland and Archean fragments (no results for metamorphic or hydrothermal zircons are included). Reworking of unradiogenic Archean crust can account for the most evolved Biranup Zone hafnium compositions. The dashed line represents evolution of a 3100 Ma reservoir with a Lu/Hf ratio of 0.015. Individual ages are based on $^{207}Pb/^{206}Pb$ ratios. Abbreviations used: DM = Depleted Mantle; CHUR = Chondritic Uniform Reservoir.

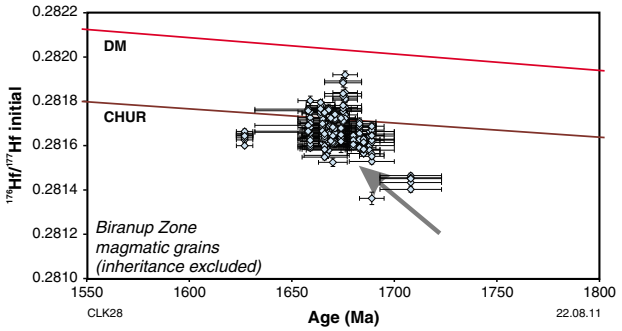

Figure 22. (left) The 1800–1550 Ma hafnium evolution of the Biranup Zone. The grey arrow represents the increasing influence of radiogenic material within younger intrusions. Individual ages are based on preferred ages of intrusion (e.g. weighted mean $^{207}Pb/^{206}Pb$ dates or concordia age). Abbreviations used: DM = Depleted Mantle; CHUR = Chondritic Uniform Reservoir.

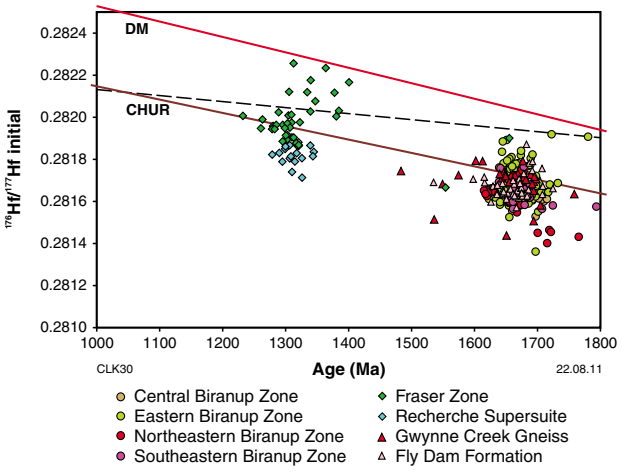

Figure 23. Initial-hafnium evolution plot for magmatic zircons from the Fraser Zone and Recherche Supersuite compared to the Biranup Zone (no results for metamorphic or hydrothermal zircons are included). Reworking of Biranup Zone crust can account for the most evolved Fraser Zone and Recherche Supersuite hafnium compositions. Detrital zircons from metasedimentary rocks in the Fraser Zone indicate additional juvenile input into the orogen, prior to Stage I of the Albany–Fraser Orogeny. The dashed line represents evolution of a c. 1850 Ma reservoir with a Lu/Hf ratio of 0.015. Individual ages are based on $^{207}Pb/^{206}Pb$ ratios. Abbreviations used: DM = Depleted Mantle; CHUR = Chondritic Uniform Reservoir.

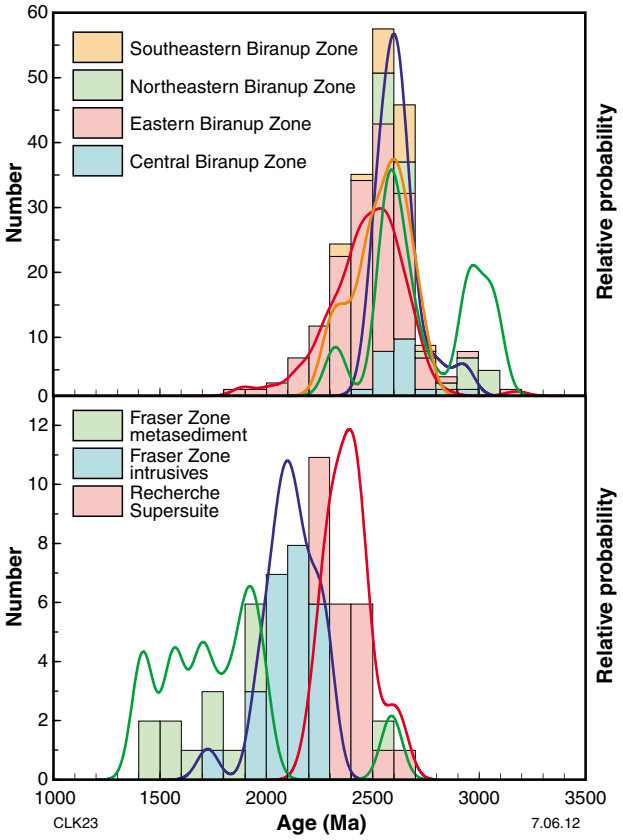

Figure 24. Probability density diagrams of crustal model ages from the Fraser Zone and Recherche Supersuite (bottom) compared to those for geographic divisions of the Biranup Zone (top). Much of the range of data for the Fraser Zone and Recherche Supersuite can be explained by reworking of Biranup Zone compositions; however, detritus from the Fraser Zone metasedimentary rocks shows the addition of a younger, more juvenile component.

imply an unrealistically mafic protolith with a Lu/Hf ratio much greater than 0.1 (Fig. 22) — thus, additional juvenile input is required. The slope of the array therefore appears to represent very constant juvenile input until a magmatic pulse at c. 1670 Ma, followed by a return to a similar constant input. In a geodynamic perspective, such constant juvenile input could be seen as an indication of stable back-arc rifting rates prior to a period of enhanced spreading. Episodic spreading is characteristic of back-arc settings, where plate rotations can enhance rifting (Wallace et al., 2008).

The age of the crustal component in the Mesoproterozoic Fraser Zone and Recherche Supersuite magmas is indicated by limited inherited zircons (Figs 4 and 5), which, for example, have ages of c. 1770 Ma (GSWA 194719, Kirkland et al., 2010b) and c. 1670 Ma (GSWA 83690, Nelson, 1995g). Such Paleoproterozoic ages are also recognized within the Biranup Zone. Hafnium evolution through a normal crustal reservoir of Biranup Zone material is able to account for practically the entire range of hafnium compositions observed within the c. 1300 Ma Fraser Zone and Recherche Supersuite intrusions (Fig. 23); that is, crustal reworking alone is sufficient to explain the variation in hafnium compositions in the igneous rocks of these units. However, the Fraser Zone intrusions appear to be consistently more juvenile than those of the Recherche Supersuite, which implies that Fraser Zone magmatism was influenced by a more juvenile source.

The Biranup Zone exhibits geographic variation in hafnium isotopic signatures, with T_{DM} (crustal) model ages typically ranging between 2.1 and 2.8 Ga, but extending up to 3.1 Ga in the older intrusions of the northeastern Biranup Zone (Fig. 24). However, no portion of the Biranup Zone is solely dominated by juvenile signatures. An additional juvenile, and potentially mantle, source appears to be necessary to mix with an original Biranup Zone composition to satisfactorily account for the tendency towards more juvenile values in the Fraser Zone. Furthermore, the average hafnium isotope composition of the Biranup Zone rocks is more evolved than that of the Recherche Supersuite, which suggests some degree of juvenile input into Recherche Supersuite granites was required.

The youngest detrital zircon sampled from metasedimentary rocks of the Fraser Range Metamorphics yielded a date of 1334 ± 20 Ma (1σ), indicating deposition just prior to Stage I magmatism. Epsilon-Hf values from detritus in this metasedimentary rock are the most juvenile within the Fraser Zone, ranging mainly between +11.3 and +3.4 for detrital zircons dated at 1400–1300 Ma

(Fig. 23). This juvenile signature indicates new crust generation prior to Stage I. Although speculative, the variation through time towards more evolved values in the Fraser Zone granites could imply oceanic subduction prior to crustal thickening, and melt interaction with a larger volume of unradiogenic crustal material. This in turn could imply that active margin processes associated with the Fraser Zone could be extended back in time from c. 1345 Ma (the beginning of Stage I) to at least 1400 Ma, although more data are needed to constrain this. Given that the Biranup Zone may have developed in a back-arc setting during the late Paleoproterozoic (Kirkland et al., 2011a), this may suggest a nearly continuous active margin along the southern West Australian Craton (in present coordinates) during most of the late Paleoproterozoic to Mesoproterozoic.

Tectonic models

Based on current geochronological constraints, the tectonic evolution of the Albany–Fraser Orogen encompasses an interval from at least 1800 Ma, through to 1140 Ma (Fig. 5). One of the difficulties in constraining tectonic models is the fact that the eastern extent of the orogen and the adjoining Eucla basement (Fig. 3) are entirely covered, up to depths of about 500 m, by the sedimentary rocks of the Eucla Basin. Although good progress has been made in defining tectonic units in the exposed parts of the orogen, their eastward extents, and the potential for undiscovered tectonic units, means that current tectonic models are effectively incomplete. Nevertheless, we have attempted to integrate the present knowledge into models of the tectonic setting in time slices through the orogen's history. These models will become better constrained as work on the Eucla basement progresses.

Formation of the Biranup Zone and the Biranup Orogeny

As stated previously (see 'Tectonic events'), it is now clear that tectonic activity along the southern and southeastern Yilgarn Craton margin began at least as early as c. 1800 Ma, and that there were pulses of magmatism at c. 1800 and c. 1760 Ma. Granitic rocks of these ages form basement components of both the Biranup and Nornalup Zones. These magmatic events were followed by the Biranup Orogeny between c. 1710 and 1650 Ma, which included deformation and metamorphism during the c. 1680 Ma Zanthus Event (Fig. 4). Magmatic rocks of Biranup Orogeny age were first described by Bunting et al. (1976), Myers (1995b), and Nelson et al. (1995), although interpretations of their extents, sources, and origins varied. It is now clear that the Paleoproterozoic rocks of the Biranup Zone span the entire exposed length of the southern and southeastern Yilgarn Craton margin, although their northeastward extents beneath the Officer and Gunbarrel Basins remain interpretative. A lack of evidence for tectonothermal or magmatic activity of Paleoproterozoic age within the Yilgarn Craton itself, and the apparent absence of Archean zircon inheritance in the Biranup Zone, led to suggestions that this zone was composed of exotic crust, with possible links to either the Gawler Craton (Myers et al., 1996) or the Warumpi Province of the southern Arunta Orogen (Spaggiari et al., 2009). These suggestions were also consistent with the interpretation that the southern and southeastern Yilgarn Craton margin was passive at that time (e.g. Hall et al., 2008). However, more recent work has led to autochthonous models of the formation of the Biranup Zone by modification of the Yilgarn Craton margin by active-margin processes (Kirkland et al., 2011a). Possible connections to the Yilgarn Craton were previously recognized in GSWA mapping and Rb–Sr geochronology (Bunting et al., 1976), in limited U–Pb geochronology (Black et al., 1992), and in limited Sm–Nd analysis (Nelson et al., 1995).

The presence of Archean crustal fragments with Yilgarn-like ages, the extensive formation of related sedimentary basins (Barren Basin), hafnium and neodymium isotopic signatures that indicate Yilgarn-like sources for the Paleoproterozoic magmas, and a progressive increase of juvenile material into Archean unradiogenic crust, are all indicative of a continental-rift style of tectonic setting. This setting could have been part of a back-arc system, although the distance (to the southeast in present coordinates) to any former subduction zone is not clear, nor is the extent of attenuated Yilgarn Craton crust. Current work on the Nornalup Zone and Eucla basement may help resolve these issues. Nonetheless, we propose a provisional model for formation of the Biranup Zone within an evolving arc- to back-arc setting (Fig. 25).

At c. 1710 Ma, west-dipping subduction (present coordinates) led to extensive magmatism, with granitic intrusions interpreted to have been emplaced at shallow levels in crust of the Yilgarn Craton margin. Subsequent slab roll-back away from the margin led to back-arc spreading, and a greater contribution from the asthenosphere to the magmatic source. Associated basins were filled by Cycle 1 sediments. Younger magmas produced within the back-arc region incorporated a greater mantle component, as increasing extension enhanced upwelling and partial melting of asthenospheric mantle. The majority of magmas appear to have crystallized between 1690 and 1680 Ma, producing granites that were rapidly migmatized and deformed during the Zanthus Event at c. 1678 Ma (Kirkland et al., 2011a). The Zanthus Event was associated with northeast–southwest compression (present coordinates) that may represent a period of tectonic switching when slab roll-back stalled, possibly driven by plate reorganization, or rotation, or by seamount arrival. The youngest intrusive rocks of the c. 1665 Ma Eddy Suite show an increase in Mg#, εHf, and εNd, reflecting a progressively more juvenile influence that might signify renewed back-arc extension.

The interpreted effect of back-arc extension and slab roll-back was to rift Archean fragments from their original location on the Yilgarn Craton margin and isolate them within Paleoproterozoic intrusive rocks of the Biranup Zone (see Excursion 1, Stops 3 and 4). Granite from one of these isolated Archean fragments has a magmatic crystallization age of 2684 ± 11 Ma (Fig. 9; GSWA 194709, Kirkland et al., 2011e). To the southwest of that locality, another Archean granite is dated imprecisely

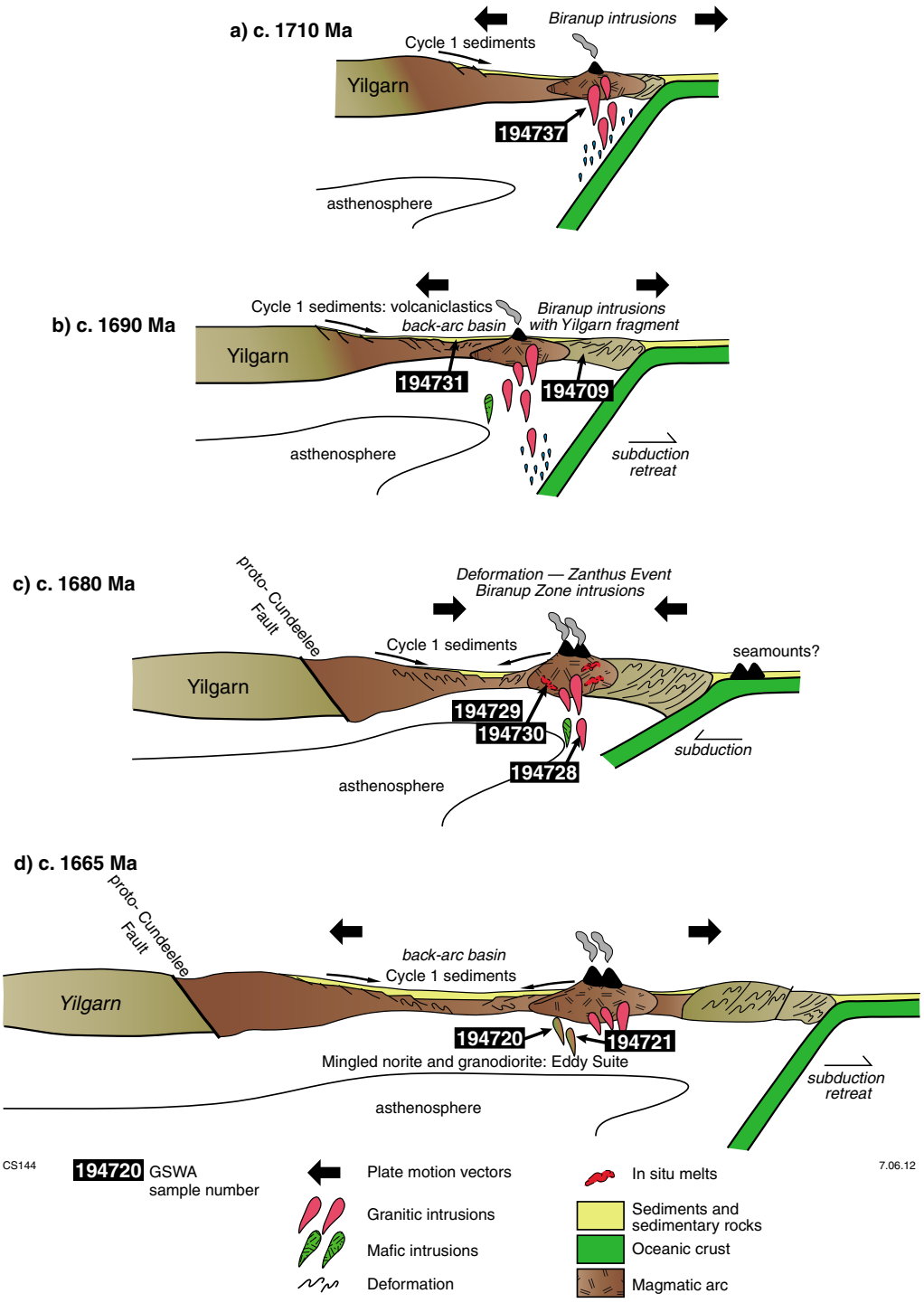

Figure 25. Schematic tectonic diagram, showing a model of the evolution of the Biranup Zone (modified from Kirkland et al., 2011a). GSWA sample numbers refer to examples that contribute to the interpretation of events: 194737 = Bobbie Point Metasyenogranite; 194731 = psammitic gneiss (Ponton Creek); 194709 = Cave Rock Archean metasyenogranite; 194729 = axial planar leucosomes in migmatitic granitic gneiss (Ponton Creek); 194730 = migmatitic granitic gneiss (Ponton Creek); 194728 = migmatitic granitic gneiss (Ponton Creek); 194720 = rapakivi metadiorite (Eddy Suite); 194721 = metagabbronorite (Eddy Suite). a) At c. 1710 Ma, rifting, extension, and attenuation of the Yilgarn Craton margin, here shown to be related to subduction, produced marginal basins filled with Cycle 1 sediments of the Barren Basin; e.g. the Woodline Formation, Mount Barren Group, and unnamed metasedimentary rocks in the Tropicana region; b) during the period 1700–1690 Ma, continued slab roll-back with voluminous felsic magmatism widened the back-arc basin, and isolated Yilgarn Craton fragments from the margin. Deposition of Cycle 1 sediments mixed with near-coeval volcanic detritus continued; c) tectonic switching during the Zanthus Event at c. 1680 Ma compressed and deformed the back-arc region. The reason for this is unknown, but the event may have been due to plate reorganization, rotation, or seamount arrival; d) intrusion of relatively more juvenile magmas (mingled norite and granodiorite of the Eddy Suite) into the back-arc region may have been due to renewed extension and back-arc widening, resulting in asthenospheric upwelling, possibly associated with slab roll-back.

at 2634 ± 29 Ma, and interpreted to be part of another Archean fragment (Plate 1; Fig. 9; GSWA 179644, Wingate and Bodorkos, 2007c). Granitic rocks with c. 2680 Ma ages are widely recognized within the Yilgarn Craton, including the high-Ca granites within the Eastern Goldfields Superterrane (Cassidy et al., 2006; Champion and Cassidy, 2007), the Southern Cross Domain of the Youanmi Terrane (e.g. GSWA 168963, Nelson, 2001), and within the Northern Foreland of the Albany–Fraser Orogen (Spaggiari et al., 2009).

East of Tropicana, the presence of rapakivi feldspar -bearing metasyenogranite with a magmatic crystallization age of 1627 ± 4 Ma (GSWA 194736, Kirkland et al., 2010h) suggests back-arc extension may have continued until about that time. After this, there is no record of any tectonic activity within the present bounds of the Albany–Fraser Orogen (west of the Rodona Shear Zone) until the commencement of the Albany–Fraser Orogeny at c. 1345 Ma (Fig. 4). However, in the adjacent Madura Province, the migmatization of gneissic rocks from the Burkin prospect, dated at 1478 ± 4 Ma (see 'Eucla basement' section; Fig. 3), indicates tectonic activity at that time, and the presence of pre- 1478 ± 4 Ma crust beneath the Eucla Basin. Furthermore, there are suggestions of juvenile crust formation between c. 1450 and 1330 Ma, based on detritus of this age in the Arid Basin, and on Lu–Hf analysis of detrital zircons from the Fraser Range Metamorphics (see 'Lu–Hf isotopes' section). This could suggest eastward stepping-out of the subduction system through time, or the development of a new rift system at c. 1450 Ma. East of the Rodona Shear Zone (Fig. 3), and within the Madura Province, amphibolite, tonalitic gneiss, and microtonalite were sampled from drillcore from the Loongana prospect, and the granitic rocks yielded dates of c. 1410 Ma (see 'Eucla basement' section). It is possible that the Loongana rocks form part of the source of 1450–1330 Ma detritus in the Arid Basin, including the new juvenile material.

Albany–Fraser Orogeny

The Albany–Fraser Orogeny has been divided into two stages of tectonic activity, based on geochronological, structural, and petrographic information (Clark et al., 2000; Spaggiari et al., 2009; Kirkland et al., 2011a). Stage I tectonism, at 1345–1260 Ma, has been attributed to convergence and collision of the combined West Australian – North Australian Craton and the combined Mawson – South Australian Craton (Clark et al., 2000; Fitzsimons, 2003), with the Nornalup Zone interpreted as the western margin of the Mawson Craton (Bodorkos and Clark, 2004b). Due to the presence of 'stitching plutons' of the Recherche Supersuite across the orogen, collision has been interpreted to have occurred during Stage I (Myers et al., 1996), although in the Northern Foreland the evidence for this is based solely on the Bald Rock occurrence (see 'Northern Foreland' section). Stage I is characterized by voluminous additions of both mafic and felsic magmatic rocks, accompanied by high-temperature metamorphism (Fig. 5). In contrast, 1215–1140 Ma Stage II tectonic activity was dominated by widespread, high-temperature metamorphism throughout much of the orogen, except for the Fraser Zone. Magmatism during Stage II was more limited, although exceptions include the Gnowangerup–Fraser Dyke Suite, emplaced at c. 1210 Ma (Wingate et al., 2000, 2005), and the Esperance Supersuite (Figs 4 and 5). Stage II tectonic activity has been interpreted as intracratonic reactivation during the assembly of the Rodinia supercontinent (Clark et al., 2000; Fitzsimons, 2003).

Stage I (1345–1260 Ma)

Stage I marks the time when the Northern Foreland, and Biranup, Fraser, and Nornalup Zones underwent synchronous tectonothermal or magmatic activity (Fig. 4). In previous models, this was taken as the best estimate for the timing of the amalgamation of the various components of the Kepa Kurl Booya Province, and of their suturing onto the Yilgarn Craton margin, in part via northwest-directed thrusting (Myers et al., 1996; Clark et al., 2000; Bodorkos and Clark, 2004b; Spaggiari et al., 2009). However, issues with these models included a poor understanding of the spatial relationships between the different tectonic units over time, particularly for the early parts of their histories, and the question of whether to place the Biranup Zone adjacent to the West Australian Craton, the combined Mawson and South Australian Craton, or elsewhere.

Previously, collision was thought to have been driven by southeast-directed subduction and ocean closure during convergence, based on the presence of pre- 1313 Ma magmatic and tectonothermal activity identified within the Nornalup Zone (interpreted as the margin of the Mawson Craton; Bodorkos and Clark, 2004b). The Fraser Zone was interpreted to be derived from oceanic-arc material (Condie and Myers, 1999), with a possible link to sediments containing 1460–1350 Ma detrital age components derived from the adjacent Nornalup Zone (Bodorkos and Clark, 2004b). As convergence continued and the ocean closed, the Fraser 'proto-arc' and Nornalup Zone were interpreted to have accreted onto the margin of the West Australian Craton, followed by localized extension, and then crustal thickening and thrusting (Bodorkos and Clark, 2004b). From about 1280 Ma, extension and erosion led to the deposition of the Ragged Basin and Cycle 3 sediments of the Mount Ragged Formation and Salisbury Gneiss (Clark et al., 2000; Bodorkos and Clark, 2004b). However, in light of new data suggesting spatial connections between the Fraser Zone and both the Nornalup and Biranup Zones (and therefore the Yilgarn Craton), it is feasible that none of these tectonic units were related to the Mawson Craton. Therefore, the timing of any collision, and the question of which of the crustal components were involved, remain unknown.

The presence of detrital and xenocrystic zircons with Biranup Zone ages (1800–1650 Ma) in metasedimentary and metagranitic rocks of the Fraser Range Metamorphics, Lu–Hf isotopic data consistent with reworking of Biranup-like source material, and the presence of Biranup-age metagranitic rocks on the western side of the eastern Nornalup Zone (c. 1760 Ma, Newman Rocks; Excursion 1, Stop 7; Fig. 11), all indicate that the Fraser Zone evolved on Biranup Zone crust. This indicates a spatial connection between Fraser Zone rocks and combined Biranup Zone and rifted Yilgarn Craton margin rocks, with the potential for the Fraser Zone to have formed in a rift-style setting on attenuated Yilgarn/Biranup crust. Although more geochemical, geochronological, and isotopic analyses are needed for confirmation, the Recherche Supersuite,

which is most voluminous in the Nornalup Zone, most likely encompasses the same event, with Fraser Zone magmas representing a shorter pulse. Within the Biranup Zone, occurrences of Recherche Supersuite granites are concentrated in, or possibly restricted to, the southeastern exposed part (Plate 1; Fig. 16), suggesting that Stage I magmatism was focused along the Mesoproterozoic southern and southeastern margins of the West Australian Craton (present coordinates), but some distance from the Yilgarn Craton component; i.e. within the outer parts of the Biranup Zone, as well as within the Nornalup Zone.

This scenario is seemingly at odds with models of craton collision during Stage I, although if the rift setting occurred within a back-arc environment (as for the Biranup Orogeny), the collision (or suture zone) may have been much farther outboard. Any model of collision with the combined Mawson and South Australian Craton must also account for the presence of the Madura, Forrest, Waigen, and Coompana Provinces (Figs 1 and 3), which are poorly understood (see 'Eucla basement' section). In the scenario outlined above, the c. 1410 Ma rocks of the Madura Province could be interpreted as part of a magmatic arc. A dynamic back-arc setting for the Fraser Zone would be consistent with the rapid burial of isotopically juvenile Cycle 2 sediments, followed almost immediately by intrusion of mafic and felsic magmas into these sediments and their substrate, and followed, shortly thereafter, by granulite-facies metamorphism (Fig. 14).

However, the progression towards more evolved magmas through time, albeit currently based on limited data (see 'Lu–Hf isotopes' section), is difficult to reconcile with a simple model in which the back-arc was actively extending during the formation of the Fraser Zone. Increasing incorporation of Biranup-like crust is one way to explain the Lu–Hf signature, suggesting the continued presence of Biranup-like crust. The presence of Biranup Zone aged metagranites on either side of the Fraser Zone is consistent with this interpretation, although all of the factors above could equally fit with a simple rift environment. Much more work, particularly on the Nornalup Zone and Recherche Supersuite, is needed before more robust tectonic models for Stage I can be presented.

It is interesting to note the varied nature of Cycle 2 sedimentary rocks within the Arid Basin, particularly those that are part of the Fraser Range Metamorphics. They range from pelitic, to semipelitic, to iron-rich, through to calcic varieties, and are mostly interlayered with mafic amphibolites or granulites, some of which may potentially have been of volcanic origin (cf. Bunting et al., 1976). This suggests some sort of restricted basin environment, rather than an open ocean.

Stage II (1215–1140 Ma)

In the interval between Stages I and II (1260–1215 Ma), the sedimentary protoliths of the Mount Ragged Formation and the Salisbury Gneiss were deposited into shallow intracratonic basins (Clark et al., 2000; Bodorkos and Clark, 2004b), marking Cycle 3 sedimentation. If we accept that Stage I marks the collision and stitching of the West Australian and combined Mawson – South Australian Cratons, then Stage II must represent repeated intracontinental reworking of the orogen over approximately 75 m.y. at high temperatures (amphibolite to granulite facies), on a major scale. Alternatively, Stage II could represent the effects of final collision (cf. Barquero-Molina, 2010), although, as noted above, the suture zone may have been a substantial distance away from the margin of the West Australian Craton. In either case, the structure of the orogen would have been significantly modified during Stage II, and it is this event that appears mostly responsible for the large-scale, northwest-vergent fold and thrust architecture preserved throughout most of the orogen.

The commencement of Stage II was marked by high-temperature metamorphism of the Salisbury Gneiss in the eastern Nornalup Zone and the southeastern Biranup Zone between c. 1225 and c. 1215 Ma (Clark et al., 2000; Spaggiari et al., 2009). Metamorphic dates of c. 1225 Ma, recorded in the southeastern Biranup Zone (at Butty Head), suggest that Stage II may have commenced slightly earlier than previously proposed by Clark et al. (2000). This was followed by the widespread emplacement of the c. 1210 Ma Gnowangerup–Fraser Dyke Suite (Clark et al., 2000; Wingate et al., 2000, 2005). From the geochronological data (Fig. 5), it is evident that high-temperature metamorphism and associated deformation was widespread during Stage II. However, in most cases it is difficult to assign particular structures to Stages I or II without the facility to date specific fabrics or crosscutting elements.

In the eastern Biranup Zone, many orthogneisses contain zircons with zircon overgrowths formed during high-grade metamorphism (Kirkland et al., 2011a). The metamorphism is mostly related to crystallization of leucosomes and migmatization, much of which either pre-dated, or was synchronous with, deformation. At Bremer Bay in the central Albany–Fraser Orogen, high-temperature metamorphism and intermediate- and large-scale boudinage related to two phases of extension occurred at c. 1180 Ma, and bracket large-scale, northwest-vergent F_3 folding (Spaggiari et al., 2009; Barquero-Molina, 2010). Further to the east in the southeastern Biranup Zone, upright folding and dextral shearing in the Coramup Shear Zone (Fig. 6a) is also interpreted to have occurred at about this time, or just after it (Bodorkos and Clark, 2004b). Major lithotectonic unit-bounding faults, such as the Red Island Shear Zone (Fig. 6a), mostly crosscut the main structures and fabrics and must have been active during the late stages of Stage II. Thrusting along the Rodona Shear Zone, and deformation of the Mount Ragged Formation in the eastern Nornalup Zone, are interpreted to have taken place between 1170 and 1150 Ma (Clark et al., 2000), along with intrusion of the Burnside Granite and related metamorphism of the host pelitic rocks in the western Nornalup Zone (Clark, 1995).

The Esperance Supersuite represents widespread granitic magmatism in the Nornalup Zone, and is characterized by plutons with moderate to high magnetic signatures (Plate 1). Plutons with similar magnetic signatures, including a granite dated at 1140 ± 8 Ma (Fig. 3; Kirkland et al., 2011j), occur in the Forrest Province (Fig. 3). This suggests that the Esperance Supersuite, or at least magmatism of about this age, is not limited to the bounds of the orogen, implying a spatial and temporal link between the Albany–Fraser Orogen and the Forrest Province, and most likely the intervening Madura Province.

The geology of the east Albany–Fraser Orogen — a field guide: part 2

Excursion 1: highlights of the geology of the east Albany–Fraser Orogen

This four-day excursion starts in Esperance and finishes in Kalgoorlie, covering a total distance of about 1040 km. The geological sites in this excursion have been chosen because of their relative ease of access, quality of outcrop, and coverage of tectonic units, with the aim of providing an overview of the current work on the geology of the east Albany–Fraser Orogen. To achieve this, large driving distances are necessary.

A general view of the excursion route is shown in Figures 26–29. Access to stops is via highways, shire roads, and four-wheel drive (4WD) tracks over a combination of crown land, pastoral leases, and lands managed by the Department of Environment and Conservation (DEC) (i.e. Nature Reserves), the largest being the Dundas Nature Reserve. Although this guide provides location details and driving directions, which can be used by anyone wishing to independently follow the excursion route, it must be noted that access to pastoral leases (Fraser Range Station and Southern Hills Station) requires permission from the station owners, and that restrictions, such as on the collection of samples, apply on DEC-managed lands. Please contact the relevant authorities before proceeding, especially as track conditions are subject to change, and may be damaged or impassable in wet weather. Topographic maps and a GPS for navigation are also recommended. Please refer to the Appendix for further information on logistics.

Day 1

The excursion assembly point is the carpark of the Esperance Civic Centre (Council Place, Jane Street, Esperance). From here, proceed to Pink Lake Road and turn right (west), then drive 600 m to the intersection with Harbour Road and turn right (north). Drive approximately 6 km along Harbour Road to the intersection with the South Coast Highway. Turn left onto this highway and follow it for 66 km to the intersection with Farrell's Road (at MGA 342358E 6265550N or 33°44′18.2″S 121°17′53.7″E), then turn left (note: this is a gravel road). Proceed for approximately 10 km to the picnic and camping area on the coast. From here, walk south along the beach and then a further ~700 m south along the rocky coastal headland.

Stop 1. Quagi Beach headland — Munglinup Gneiss

This locality provides an opportunity to view a well-exposed section of the Munglinup Gneiss, which is bound by major faults. The Munglinup Gneiss is an amphibolite- to granulite-facies, reworked component of the Yilgarn Craton, and forms part of the Northern Foreland (see 'Munglinup Gneiss' section; Spaggiari et al., 2009). Southeast of the exposure, structures within the Munglinup Gneiss are cut by the Red Island Shear Zone (Figs 6a and 16). The Red Island Shear Zone — named after a small rocky island, visible from the coast at this locality, that the shear zone passes through — is interpreted to be the present-day expression of the boundary between the Northern Foreland and the Biranup Zone of the Kepa Kurl Booya Province (Geological Survey of Western Australia, 2007).

The Munglinup Gneiss comprises amphibolite- to granulite-facies granitic gneiss interlayered with lenses of metamorphosed mafic rocks, and with minor banded metachert (jaspilite), amphibolitic schist, serpentinite, and metamorphosed ultramafic rocks (Thom et al., 1977; Beeson et al., 1988; Myers, 1990a). Isolated lenses of mafic and ultramafic rocks, including some hosting historical nickel deposits (e.g. the Young River Nickel prospect, east of Ravensthorpe), are interpreted to be remnants of Archean greenstone intruded by the granitic precursors to the Munglinup Gneiss (Thom et al., 1977; Geological Survey of Western Australia, 2007).

Along the headland south of Quagi Beach, both porphyritic gneiss and leucocratic, granitic, layered gneiss occur. Each contains mafic lenses. Centimetre-scale leucocratic layers locally grade into more diffuse patches, some of which occur in the necks of boudins. The layering defines the earliest recognized foliation (S_1), and is tightly to isoclinally folded into gently east-plunging folds. A well-developed mineral lineation plunges about 30° to the west. The folds, and the generally easterly trending fabric, correlate with the regional fabric and F_3 folds in aeromagnetic data (Fig. 6). Crosscutting shear zones also contain leucosome patches, some of which are cut by younger leucosome containing biotite selvedges, indicating successive generations of leucosome formation. Approximately 700 m south along the headland, an east-northeasterly trending sinistral shear zone about 50 cm wide is cut at high angles by small pegmatite veins. The sinistral shear zone and veins are in turn cut by conjugate sets of northwesterly trending dextral and north-northeasterly trending sinistral shear zones, both of which contain leucosomes.

Dating of migmatitic granitic gneiss from this headland (at MGA 342339E 6254715N) yielded an upper intercept date of 2709 ± 35 Ma, interpreted as the magmatic crystallization age of the granitic protolith (GSWA 184334, Kirkland et al., 2011b). The granitic gneiss is inequigranular, granuloblastic, and foliated, and is composed of 40% orthoclase, 32% quartz, 26% plagioclase, 1.5% biotite, and 0.5% garnet, plus

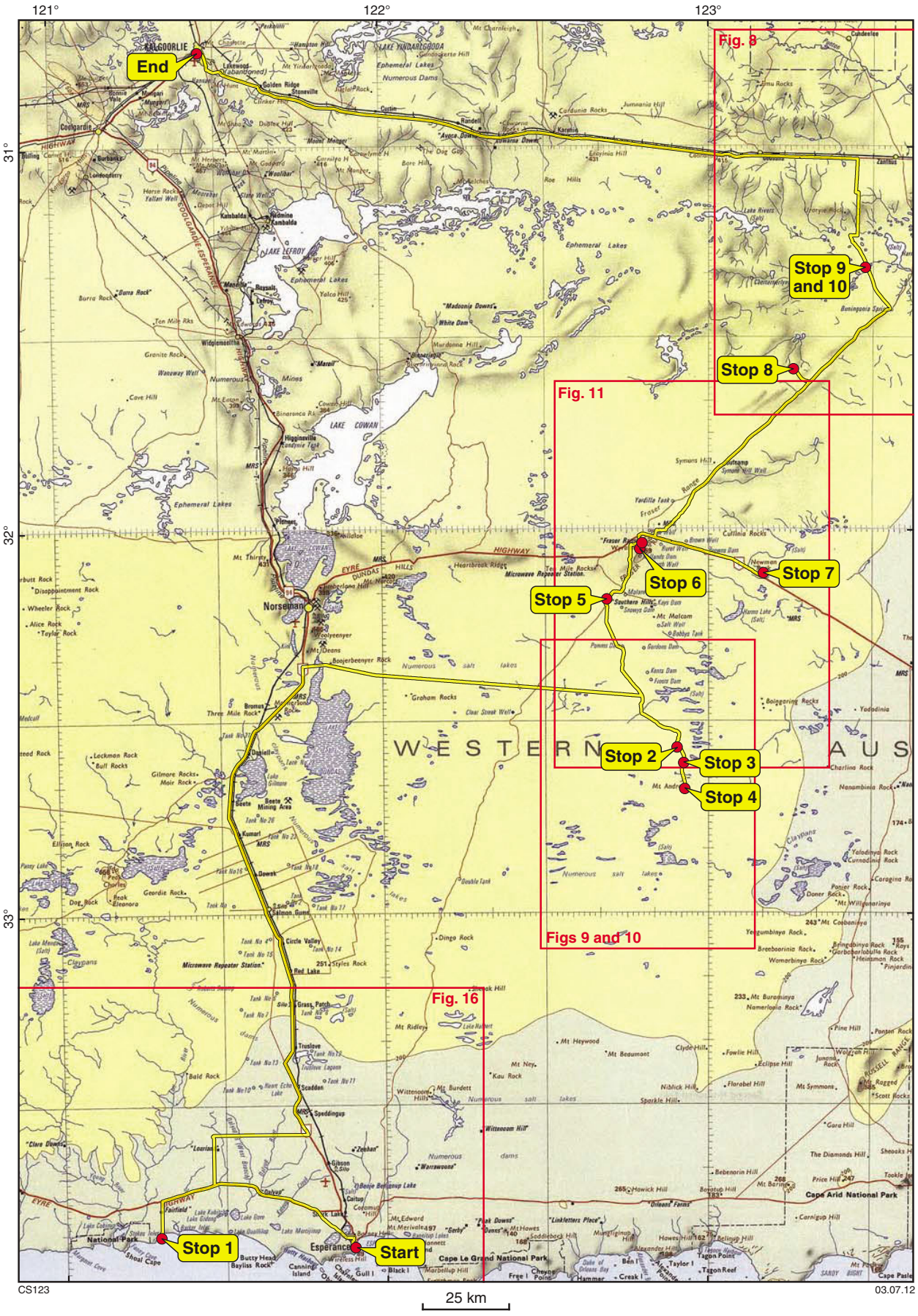

Figure 26. Route and stops for Excursion 1

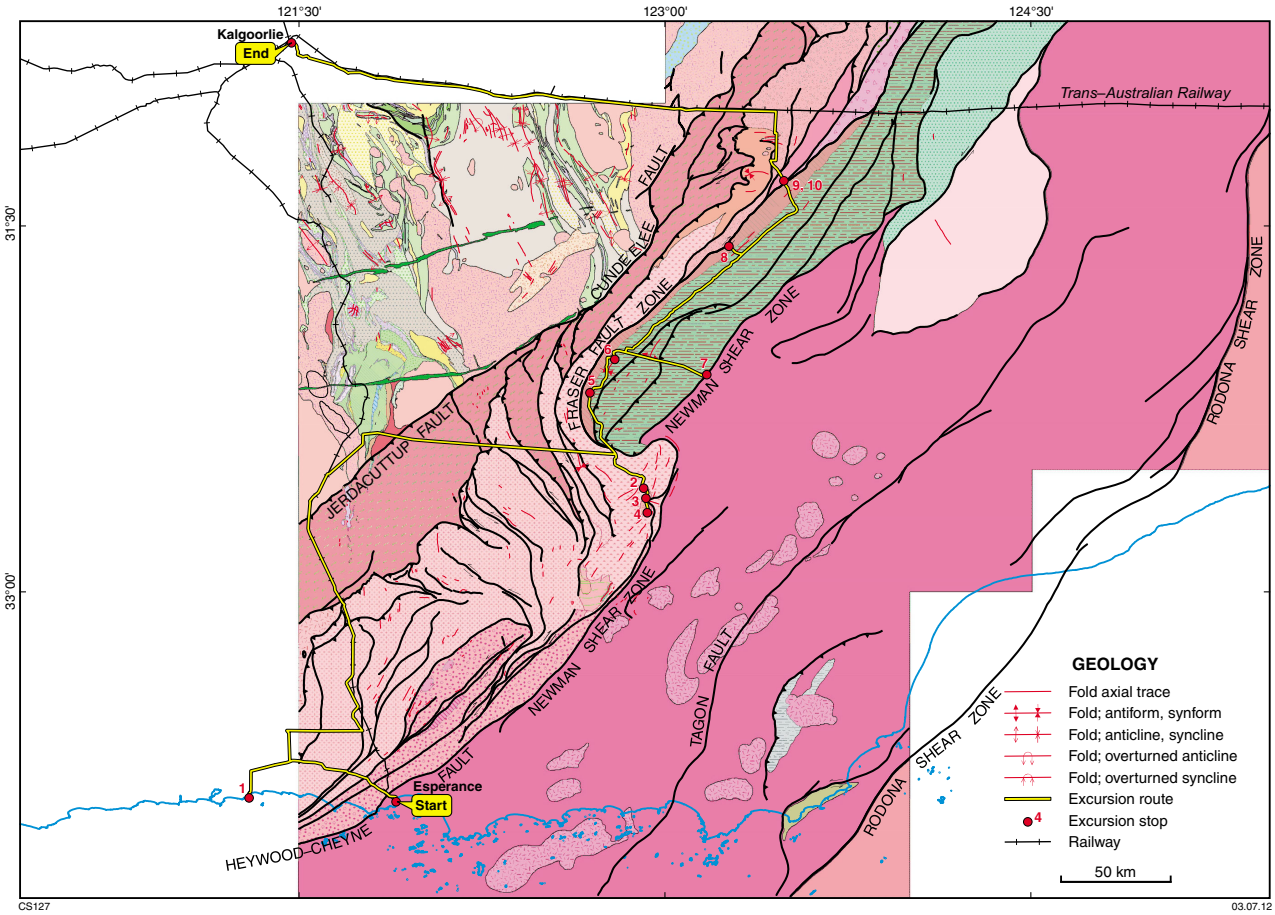

Figure 27. Route and stops for Excursion 1, superimposed on the pre-Mesozoic interpreted bedrock geology. Modified from Geological Survey of Western Australia (2011); see Plate 1 for geological legend.

traces of opaque oxide grains, apatite, and zircon. Large, anhedral orthoclase porphyroclasts are up to 10 mm long, and lobate interstitial quartz grains are up to 5 mm long. Plagioclase is mostly anhedral and less than 2 mm in size, is associated with smaller grains of quartz and orthoclase, and relatively common in small patches of myrmekite. Biotite is mostly foliated and dark brown (iron-rich), and up to 1 mm in grain size. Anhedral garnets are 0.2 – 1 mm in diameter.

Garnet-bearing mafic lenses of various size occur throughout the granitic gneiss, commonly parallel to, and locally folded with, the main fabric (Fig. 30a). These lenses probably represent mafic dykes, and may be part of the c. 1210 Ma Gnowangerup–Fraser Dyke Suite, metamorphosed and deformed during Stage II of the Albany–Fraser Orogeny. This would be consistent with Stage II metamorphic zircon ages of 1200–1180 Ma recorded elsewhere in the Munglinup Gneiss (see 'Munglinup Gneiss' section). Farther south along the headland, a 10–15 m wide mafic dyke, now a garnet-bearing, locally banded, coarse amphibolite to mafic granulite gneiss, cuts leucocratic granitic gneiss. The margins of the dyke show good evidence, in the form of crenulate margins and extensive back-veining of the country rock into the mafic dyke, that the country rock gneisses were deformed by hot mafic magma as the dyke was emplaced (Fig. 30b). To the southwest, a similar mafic dyke is crosscut by a felsic dyke (Fig. 30c).

Late, east-southeasterly trending mafic dykes of unknown age crosscut the earlier mafic dykes (Fig. 30d). Although these late dykes contain a substantial portion of secondary amphibole, they are undeformed. However, they locally contain leucosomes and show evidence of back-veining, cutting both the dykes themselves and their granitic host, indicating that the granitic host was hot enough to partially melt. This suggests that the late mafic dykes may have formed during the late stages of Stage II of the Albany–Fraser Orogeny, after deformation within the Munglinup Gneiss had ceased, but before it cooled, perhaps between c. 1160 and c. 1140 Ma.

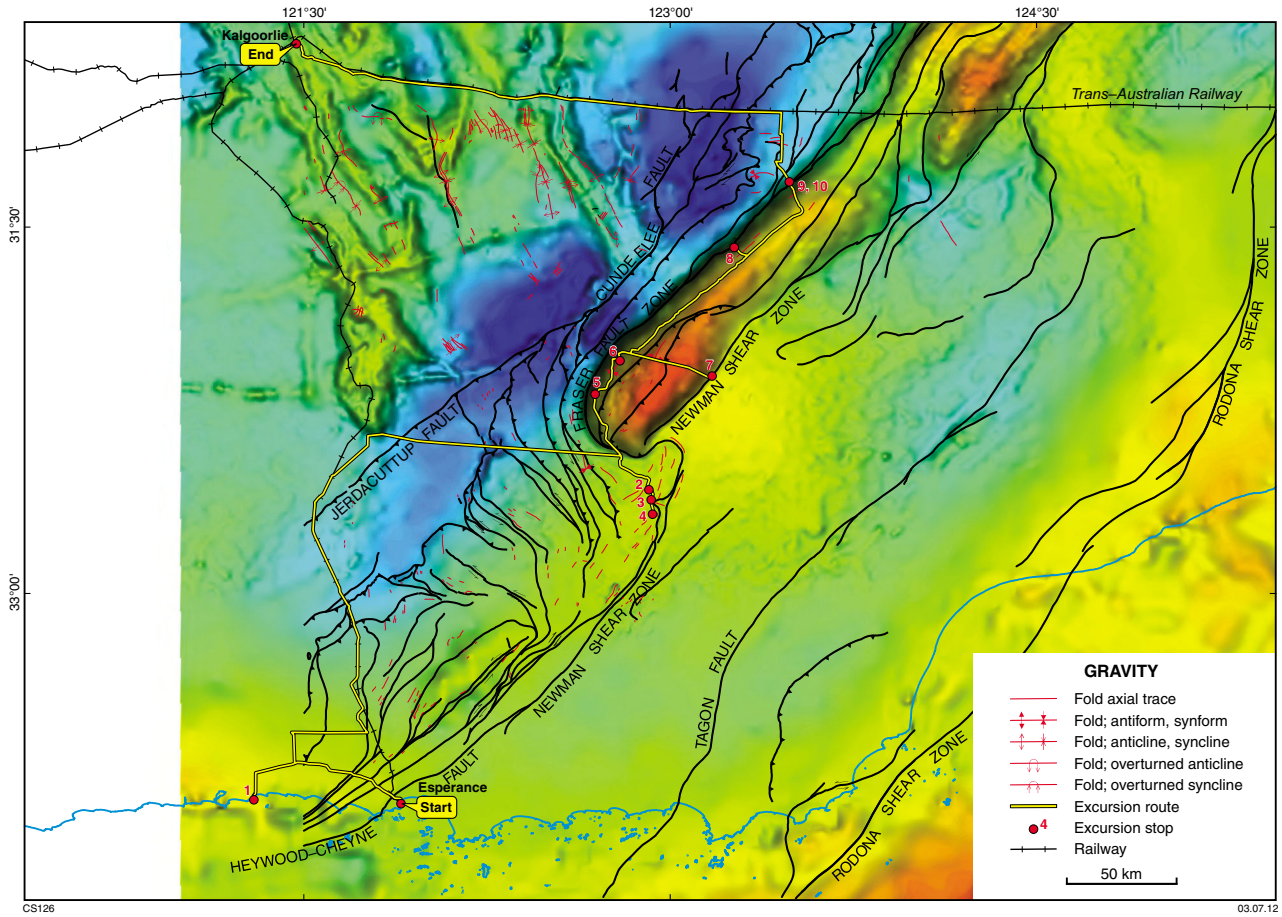

Figure 28. Route and stops for Excursion 1, superimposed on a gravity image, showing major structures. Modified from Geological Survey of Western Australia (2011).

Directions to Stop 2:

Drive 10.2 km to the intersection of Farrell's Road and the South Coast Highway (at MGA 342358E 6265550N; 33°44′18.2″S 121°17′53.7″E), then turn right. Drive 15.4 km, and turn left into Cascades Road (at MGA 357248E 6270248N or 33°41′53.3″S 121°27′34.9″E). Drive 13.7 km to Boydell Road (MGA 356766E 6284074N or 33°34′24.3″S 121°27′24.2″E), turn right, and drive 27.1 km to the Coolgardie–Esperance Highway (MGA 384350E 6284769N or 33°34′13.8″S 121°45′14.2″E). Turn left, drive 146.1 km to the turnoff for the Telegraph Track (MGA 383272E 6419587N or 32°21′16.4″S 121°45′34.0″E) and turn right.

Excursion participants should assemble after turning off the highway. Note that not far along the Telegraph Track there is a salt lake that may be boggy to cross; use 4WD if necessary. Continue for 3.5 km, then take the left fork in track. Drive an additional 95 km along the Telegraph Track to the intersection with the Mount Andrew Track, and turn right (south). Camp along the Telegraph Track, or just past the Mount Andrew Track turnoff.

Day 2

Drive 22 km south from the Mount Andrew Track turnoff to Stop 2, an area of extensive platform outcrops on the west side of the track (MGA 491055E 6397440N).

Stop 2. Biranup Zone migmatitic gneiss

This locality and nearby rock platforms provide excellent exposures of migmatitic monzogranitic and syenogranitic gneisses of the Biranup Zone (Fig. 9). These granitic gneisses occur within a regionally structurally complex area south of the Fraser Zone, and adjacent to the Newman Shear Zone, which marks the boundary with the Nornalup Zone (Figs 9 and 10). Aeromagnetic data show that rocks of the Biranup Zone are folded into open to tight, variably oriented but dominantly north-northeasterly trending folds, cut by numerous shear zones of various scales. The Newman Shear Zone is itself folded into a large S-fold, with the northeastern limb marking the boundary between the Fraser and Nornalup Zones. This structure most likely formed by the structural emplacement of the Fraser Zone,

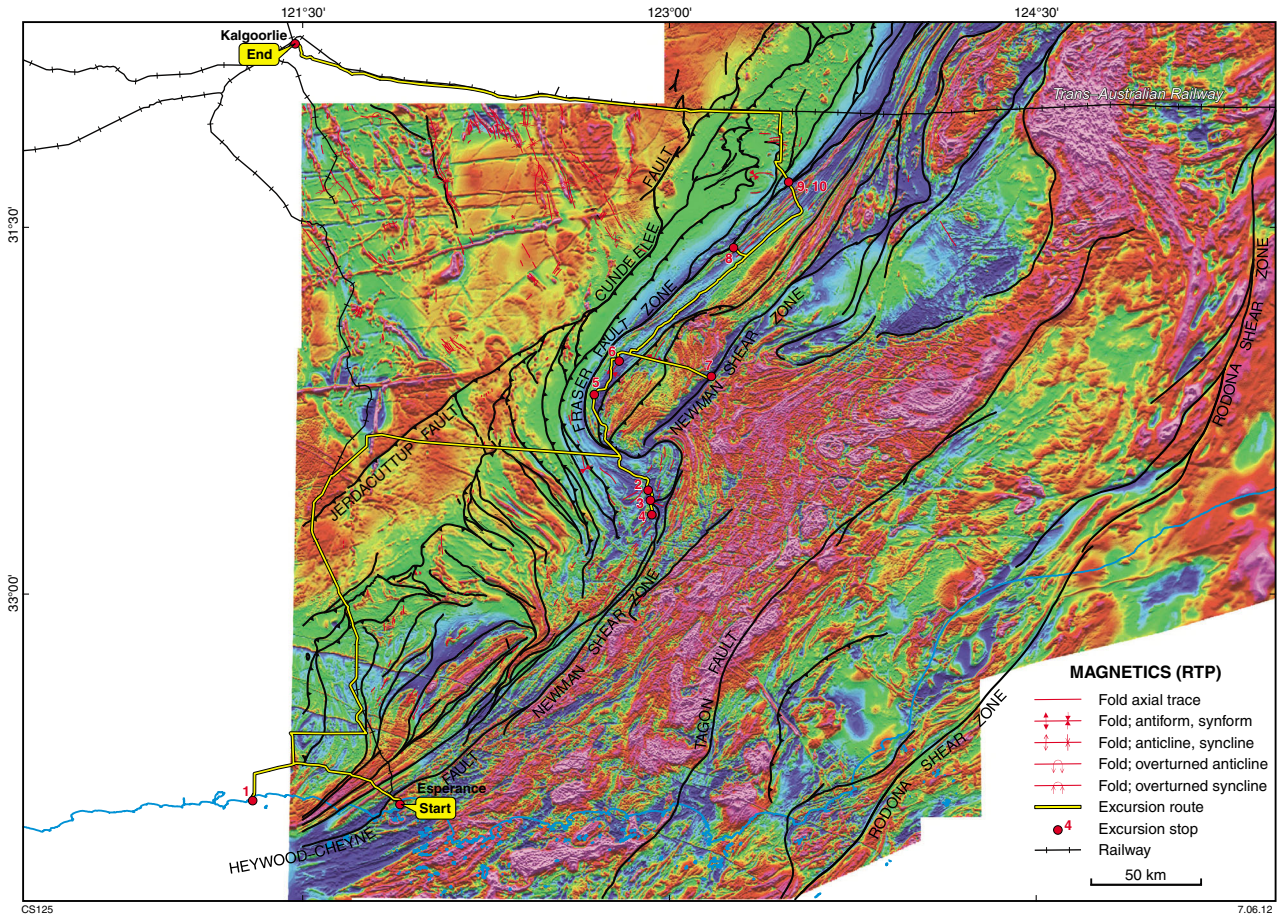

Figure 29. Route and stops for Excursion 1, superimposed on a reduced-to-pole aeromagnetic image, showing major structures. Modified from Geological Survey of Western Australia (2011).

possibly by extrusion to the southwest (Fig. 13). To the east and northeast of this locality, the Newman Shear Zone contains megascale sheath folds, interpreted from aeromagnetic data (Fig. 10). Metagranitic rocks exposed in the vicinity of these folds are L-tectonites, form part of the Recherche Supersuite, and have been dated at 1299 ± 7 Ma (GSWA 194712, Kirkland et al., 2011g) and 1317 ± 7 Ma (GSWA 194710, Kirkland et al., 2011f) (Figs 9 and 10).

Granitic gneisses at Stop 2 contain both metatexitic and diatexitic textures. Metatexite domains preserve coherent structures that pre-date secondary partial melting. The gneisses are medium to coarse grained, and contain K-feldspar porphyroclasts (average size 0.5 – 1 cm) in a strong to mylonitic foliation. This fabric and layer-parallel leucosomes (S_1) are folded into small-scale, open to tight, northeasterly trending, mostly asymmetric folds (Fig. 31a,b). Leucosomes along the axial planes of these folds (S_2) are locally dextrally offset. Younger crosscutting leucosome patches have biotite selvedges indicative of in situ partial melting, as do many of the layer-parallel leucosomes (Fig. 31b,c). Some leucosomes also contain abundant garnet.

At the northern end of this series of platforms (about 500 m to the north-northwest), a sample of monzogranitic gneiss yielded a magmatic crystallization age of 1658 ± 26 Ma (GSWA 194707, Kirkland et al., 2011c). A date of 1213 ± 10 Ma for seven zircon rims was interpreted as the age of metamorphism, and is within uncertainty of the 1217 ± 22 Ma magmatic crystallization age of a leucosome that intrudes this monzogranitic gneiss, ponded within a small-scale, easterly trending, dextral shear zone (GSWA 194708, Kirkland et al., 2011d). The dated monzogranitic gneiss (GSWA 194707) has a granoblastic texture, and contains 30–35% plagioclase, 30% microcline, 30% quartz, 7–8% biotite, 1% opaque oxide grains, accessory apatite, and rare titanite.

Directions to Stop 3:

Continue driving 5.3 km along the Mount Andrew Track to Cave Rock. Access this granite hill from the south side and walk up to the geochronology site (MGA 492878E 6392895N).

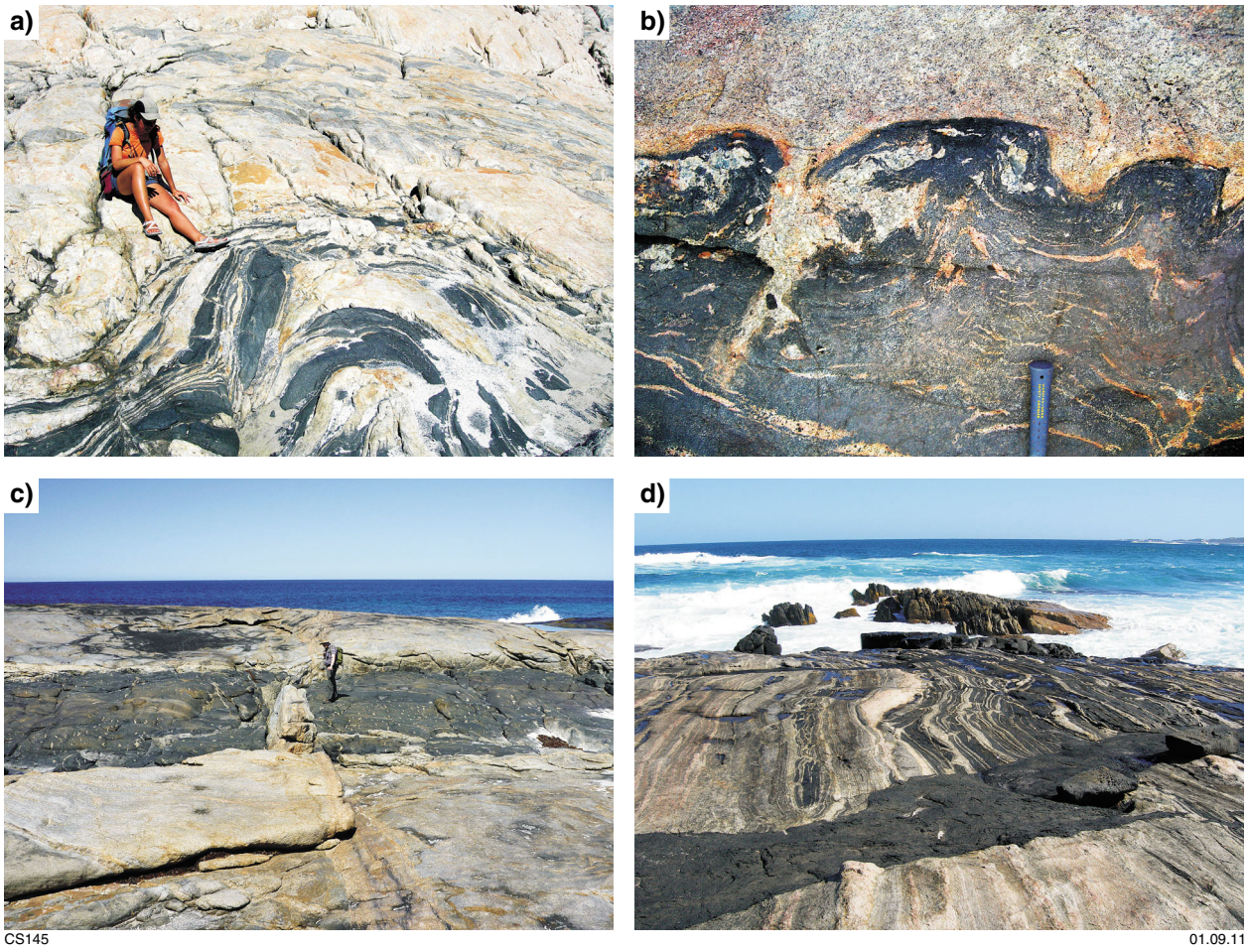

Figure 30. a) Folded mafic lenses, which are probably disaggregated mafic dykes, within the Munglinup Gneiss; southwest of Quagi Beach and southwest of Excursion 1, Stop 1; b) lobate and crenulate contact of a mafic dyke containing wispy leucosomes with granitic gneiss within the Munglinup Gneiss; southwest of Quagi Beach and southwest of Excursion 1, Stop 1; c) mafic dyke with wispy leucosome patches crosscutting granitic gneiss, and in turn crosscut by a felsic dyke, within Munglinup Gneiss; south of Quagi Beach and south of Excursion 1, Stop 1; d) late, undeformed mafic dyke crosscutting granitic gneiss with abundant disaggregated mafic lenses, inferred to be earlier mafic dykes that are possibly part of the Gnowangerup–Fraser Dyke Suite; Munglinup Gneiss; southwest of Quagi Beach, southwest of Excursion 1, Stop 1.

Stop 3. Cave Rock — Archean fragment

The Cave Rock area preserves evidence for the presence of Archean metagranite, located about 80 km southeast of the Jerdacuttup Fault that marks the boundary with the Yilgarn Craton (Figs 2 and 27). Based on lithological character and aeromagnetic data, the metasyenogranite exposed here is interpreted as part of a large fragment of Archean rocks, incorporating Mount Andrew to the south, which are completely surrounded by Paleoproterozoic granitic gneisses of the Biranup Zone (Figs 9 and 10; see also Excursion 1, Stop 4). At this locality, a large hill of pink, homogeneous, medium-grained, equigranular metasyenogranite is weakly foliated to unfoliated, and does not appear to contain any veins or intrusions. Where present, the foliation dips gently to the east-southeast. South of the main hill, an area of outcrop encompassing about 1 km^2 contains homogeneous, moderately foliated metasyenogranite, which is inferred to be the same granite. It is also equigranular, but locally porphyritic, with K-feldspar phenocrysts about 1–2 cm in size. The foliation trends to the northeast, and dips moderately to the southeast. The outcrops also contain minor, thin pegmatite veins parallel to the foliation, and minor, thin quartz veins. About 2 km southwest of this locality, in an area of scattered outcrop, is a strongly foliated, medium-grained metasyenogranite with leucosomes containing biotite clots and selvedges crosscutting the foliation (Fig. 31d). The foliation is defined by biotite wisps and elongate quartz and feldspar. This indicates that the relatively undeformed metasyenogranite at Cave Rock occupied a strain shadow during deformation.

The metasyenogranite from Cave Rock yielded a magmatic crystallization age of 2684 ± 11 Ma (GSWA 194709, Kirkland et al., 2011e). The dated metasyenogranite

contains about 60% mesoperthite, 30% quartz, 4.5% hornblende, 2.5% plagioclase, 2% clay–limonite altered ?pyroxene, and 1% biotite, magnetite, titanite, and apatite. Subparallel grains and lenses of hornblende, altered ?pyroxene, opaque oxide grains, and titanite up to 2 mm long together define a weak foliation, with individual grains up to 7 mm long. Some quartz and mesoperthite grains are also elongate parallel to the foliation and are up to 4 mm long. The quartz and plagioclase grains are anhedral, with some plagioclase intergrown with mesoperthite, and some as discrete grains. Most titanite has been altered to leucoxene.

Directions to Stop 4:

Continue driving 9 km along the Mount Andrew Track to Mount Andrew (MGA 493910E 6385287N). From here, walk west for approximately 700 m to the outcrop area of Stop 4 (MGA 493278E 6385090N).

Stop 4. Mount Andrew — Archean fragment

The Mount Andrew area contains several large granitic hills and sloping rock platforms, which are interpreted to be composed of the same metasyenogranite as Cave Rock (Excursion 1, Stop 3), and to form part of the same Archean fragment (Fig. 9). Most of the area comprises homogeneous, medium-grained, pink to grey, foliated metasyenogranite.

At this locality, the foliation is steeper and stronger than elsewhere at Mount Andrew, and the metasyenogranite is variably layered. The layering and foliation are folded into tight, metre-scale, northeasterly plunging folds with moderately to steeply southeast-dipping axial planes. Lenses of mafic amphibolite in the metasyenogranite are also folded (Fig. 31e). Locally, leucosomes are found in the fold hinges forming a saddle-reef geometry, which suggests that leucosome formation post-dates folding (Fig. 31f). Leucosome veins also crosscut the fold limbs. These folds do not appear to have an axial-planar foliation. The folded foliation contains biotite, local magnetite, plus quartz and feldspar. The latter two minerals locally have a granoblastic texture indicative of recrystallization, which may have occurred synchronously with crystallization of the leucosomes. The presence of northeasterly trending folds at this locality is consistent with the larger-scale, northeasterly trending folds evident in the aeromagnetic data (Fig. 10). The effects of low to moderate strain and variable metamorphism are clearly evident within the Archean fragment, and contrast markedly with the strongly deformed, migmatitic granitic gneisses of the Biranup Zone surrounding the fragment (e.g. at Excursion 1, Stop 2).

Directions to Stop 5:

Return along the Mount Andrew Track to the intersection with the Telegraph Track (34.6 km).Continue northwest along the Mount Andrew Track. Camp approximately 6 km along this track, west of Frost's Dam.

Day 3

Continue northwest on the Mount Andrew Track. At 13.9 km from the Telegraph Track intersection, bear right as you enter Southern Hills Station. Drive 1.8 km, bear left. Drive 1.9 km, bear right. Drive 12 km, continue straight ahead (slight left) to follow fenceline. Drive 800 m to reach the intersection with the Fraser Range Track. Turn right. Drive 4 km to Gnamma Hill.

Stop 5. Gnamma Hill — Fraser Range Metamorphics

The purpose of this stop is to examine a sliver of metasedimentary rocks within the Fraser Zone, which has been subject to detailed metamorphic and geochronological investigation (Oorschot, 2011; GSWA 194714, Kirkland et al., 2011h; GSWA 194715, Kirkland et al., 2011i). The field descriptions of these rocks are largely based on Oorschot (2011).

Lithologies

Rocks at Gnamma Hill comprise psammitic gneiss interlayered with semipelitic gneiss, garnet- and sillimanite-bearing pelitic gneiss, iron-rich metasedimentary gneiss, and locally, mafic amphibolite and metagranite. Southeast of the track at Gnamma Hill, medium- to coarse-grained semipelitic gneiss with a strong gneissic foliation accounts for much of the outcrop. The semipelitic gneiss contains the mineral assemblage quartz – K-feldspar – garnet – iron–titanium oxides – sillimanite – biotite – cordierite (–plagioclase). Quartz–K-feldspar leucosomes are interpreted to represent crystallized melt derived from the semipelitic gneiss. The gneissic foliation is defined by compositional variations between garnet-rich residue and quartz-rich leucosome. Sillimanite-rich bands are also preserved locally within the foliation and lineation. Mesosomes comprised of garnet and iron–titanium oxides have been interpreted as the product of a heterogeneous protolith with iron-rich zones (Oorschot, 2011), or an early differentiated fabric (Clark, 1999).The majority of leucosomes are subparallel to the regional foliation, although a small number of discordant leucosomes occur locally (see also the geochronology from a garnet-bearing leucosome at Excursion 1, Stop 6). Asymmetric folding suggests north- to northwest-directed vergence. In thin section, garnet porphyroblasts exhibit neocrystallized tails consistent with a component of dextral shear.

Southwest of the track, towards the westernmost extent of the outcrop, sparse occurrences of mafic granulite are characterized by the assemblage orthopyroxene–plagioclase–oxides–biotite(–clinopyroxene–garnet). On the northern side of the track is a strongly foliated quartzite containing K-feldspar and biotite-rich bands, as well as bands rich in garnet and iron oxide. Elsewhere at Gnamma Hill, several small granitic bodies include a strongly deformed variety of microgranite, an undeformed microgranite with no clear contact relationships, and a K-feldspar porphyritic granite that appears to intrude the semipelitic gneiss, and is discordant to the regional foliation.

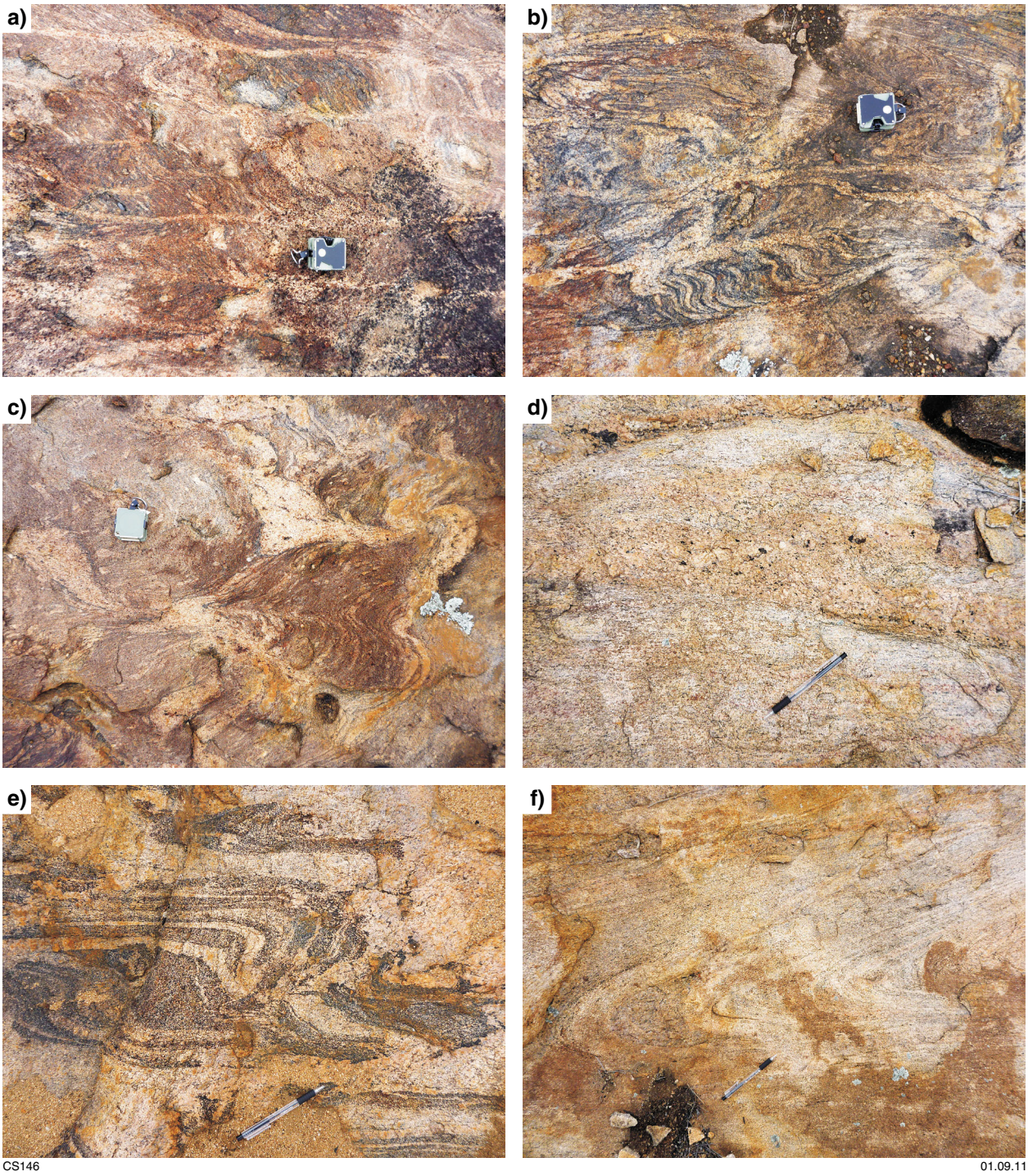

Figure 31. a) Strong to mylonitic folded fabric with axial planar leucosomes in granitic gneiss of the Biranup Zone. The axial planar leucosomes contain garnets and have biotite selvedges, indicative of in situ melting; Excursion 1, Stop 2; b) coherent (metatexitic) to more chaotic (diatexitic) folded fabric in granitic gneiss of the Biranup Zone. Here, both early folded leucosome and younger, more ponded leucosome have well-developed biotite selvedges, indicative of in situ melting; Excursion 1, Stop 2; c) strong to mylonitic folded fabric with layer-parallel leucosome, crosscut by coarser, ponded leucosome with well-developed biotite selvedges. Note that some of the coarser leucosome also appears to be folded, suggesting ongoing deformation during metamorphism; Excursion 1, Stop 2; d) coarse-grained leucosome vein crosscutting foliation in Archean metasyenogranite, southwest of Cave Rock (MGA 492022E 6390297N); e) folded mafic lenses in inferred Archean metasyenogranite west of Mount Andrew; Excursion 1, Stop 4; f) tightly folded fabric in inferred Archean metasyenogranite, with leucosome ponded in the hinge; west of Mount Andrew; Excursion 1, Stop 4.

Thermobarometry

Gnamma Hill semipelitic gneisses contain a peak metamorphic assemblage consisting of quartz–garnet–sillimanite–ilmenite–K-feldspar–liquid–biotite. Petrological and phase-equilibria modelling of these rocks constrain peak metamorphic conditions to 800–850°C and 8–9 kbar (Fig. 32; Oorschot, 2011). The presence of quartz, sillimanite, opaque minerals, and minor K-feldspar and biotite preserved in garnet, plus the absence of prograde cordierite or kyanite, together indicate a prograde path along a geotherm of approximately 1250°C / GPa. Post-peak isobaric cooling at approximately 9 kbar has previously been documented by Clark et al. (1999).

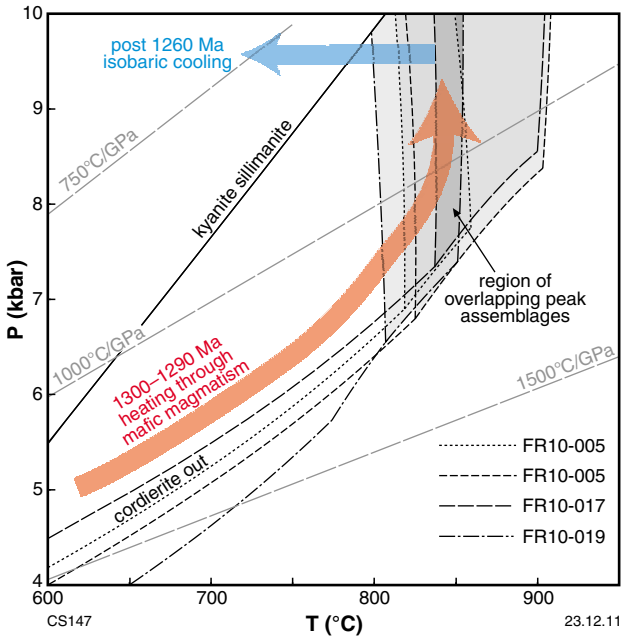

Figure 32. Compilation of pseudosections from semipelites of the Fraser Range Metamorphics from Gnamma Hill and Mount Malcolm, constraining the prograde, peak, and cooling conditions of the rocks in these areas. FR10-005 = Gnamma Hill; FR10-017, FR10-019 = Mount Malcolm.

Geochronology and isotope geochemistry

Psammitic gneiss sampled just north of Gnamma Hill has provided a maximum depositional age constrained by the youngest detrital zircon date of 1334 ± 20 Ma (1σ; GSWA 194714, Kirkland et al., 2011h). A more conservative estimate is provided by the weighted mean of 12 analyses at 1368 ± 12 Ma. A significant detrital age component is defined at c. 1374 Ma, with minor components at c. 1671 Ma and c. 1553 Ma. The youngest detritus (between c. 1400 to 1330 Ma) has the most juvenile hafnium signature of all material within the Fraser Zone, indicating the emplacement of juvenile magmatic rocks just prior to Stage I. The psammitic gneiss was metamorphosed at a high temperature, resulting in zircon rim growth at 1292 ± 5 Ma (GSWA 194714, Kirkland et al., 2011h). This date is within uncertainty of the 1285 ± 7 Ma age determined for the crystallization of leucosomes within the same psammitic gneiss (GSWA 194715, Kirkland et al., 2011i).

Monazite from the granulite-facies semipelitic gneiss at Gnamma Hill was dated in thin section by ion microprobe (SHRIMP) and yielded ages of 1285–1274 Ma (Fig. 33; Oorschot, 2011). This age range was interpreted to reflect metamorphism, although not necessarily the time of peak metamorphism. No difference was observed between monazite from different mineralogical contexts in this sample (e.g. included in garnet, versus in the matrix). Large monazites from a sample of leucosome yielded an age of 1274 ± 9 Ma, interpreted as the age of leucosome crystallization (Oorschot, 2011). Analyses of monazite rims from the same crystals provided a younger age of 1234 ± 17 Ma, interpreted as evidence of a younger metamorphic, or fluid-related, event (see also Clark, 1999).

The difference between slightly older ages for zircon growth during metamorphism and slightly younger monazite crystallization ages is consistent with empirical and theoretical considerations of zircon and monazite growth behaviour (Kelsey et al., 2008; Kirkland et al., 2009a). Zircon is refractory and tends to grow on pre-existing inherited zircon templates, whereas monazite is susceptible to rapid dissolution in small volumes of melt, and tends to regrow in entirety, unless shielded from fluids or melt.

Directions to Stop 6:

Continue on the same track for 5 km, then bear left. Drive 700 m to the intersection with Southern Hills Road; cross this road, and continue northeastwards on the track on the other side. Drive 14 km, bear right. Drive approximately 1.5 km to the northwestern corner of a paddock. Follow the track along the fence south for about 500 m, then turn left at the gate and head east about 250 m to the corner of the paddock. From here, head east-southeast across country for about 800 m, taking care to avoid the large crevasses in the field. Park at a water-worn rocky gully in Wyralinu Hill; walk up the gully over a distance of about 200 m (MGA 480664E 6454348N).

Stop 6. Wyralinu Hill, gully exposure — Fraser Range Metamorphics

The water-worn exposure in this gully provides an excellent across-strike section through the sheeted metagabbroic and metagranitic rocks typical of the exposed central portion of the Fraser Range Metamorphics. These rocks form the central spine of the range, and provide an informative view of the primary and secondary processes that formed these high-grade metamorphic rocks.

The sheets of metagabbroic and metagranitic rocks range in width from about 1–5 m (Fig. 34a). Although they occur as separate sheets, it appears that some of the lithologies are hybrids and may be the products of

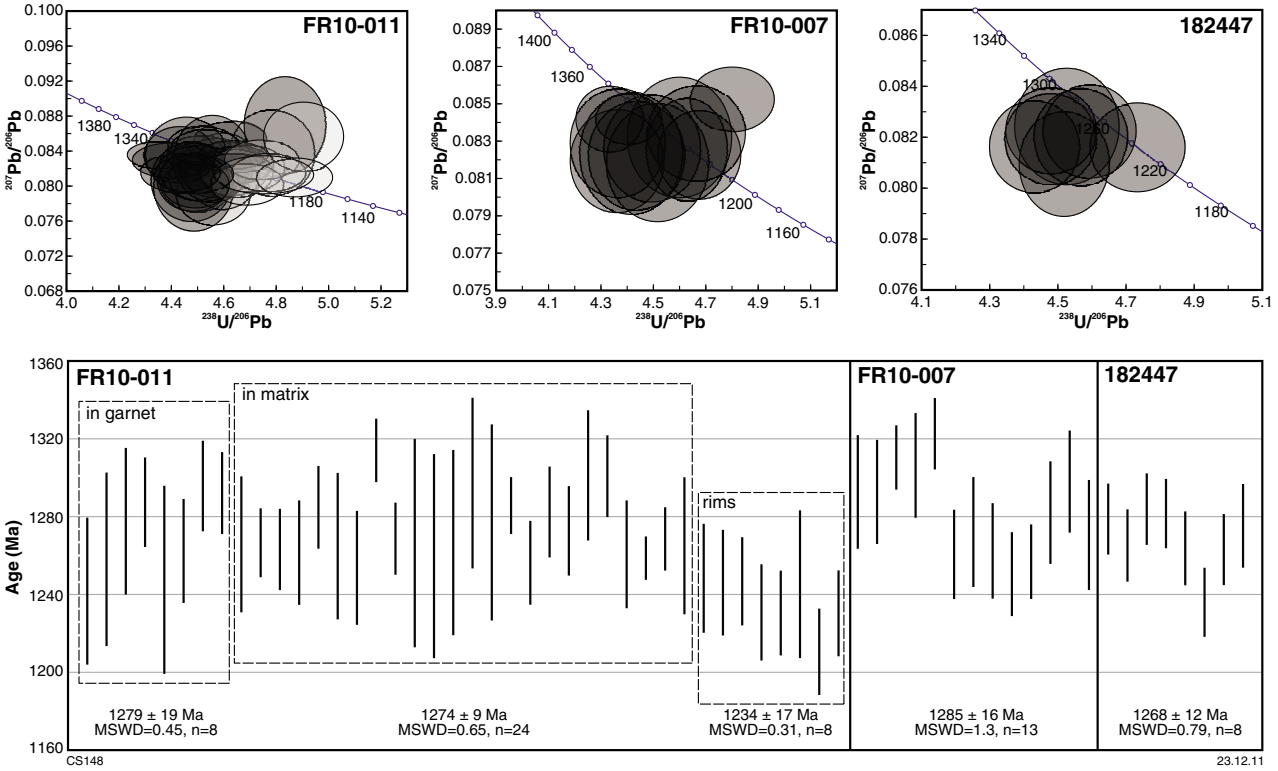

Figure 33. Tera–Wasserberg concordia plots and $^{207}Pb/^{235}U$ ages of monazite analyses from samples FR-10-011 and FR-10-007 (Gnamma Hill) and GSWA 182447 (Mount Malcolm), constraining the timing of monazite crystallization to between c. 1285 and 1268 Ma. Note how monazite inclusions in garnet display no difference to those from the matrix in sample FR-10-011; however, the eight rim analyses yielded a slightly younger age.

mixing between the gabbroic and granitic magmas. For example, large K-feldspar porphyroclasts and stringers of granitic material occur in some of the more gabbroic sheets (Fig. 34b), although the latter may be due to the effects of high-temperature metamorphism. The formation of hybrids by magma mixing is consistent with the whole-rock geochemistry, from which mixing trends could be interpreted in the magmatic products of the Fraser Range Metamorphics (see 'Whole-rock geochemical datasets', above). The sheets are overprinted by a strong to mylonitic foliation parallel to sheet contacts, and by high-temperature metamorphism, which has produced leucosome wisps and veins, some of which contain abundant garnet. Late leucosome veins locally contain large euhedral garnets (Fig. 34c). Although the strong fabric and high-temperature metamorphic overprint masks some of the primary magmatic features, the close timing between magmatism and high-temperature metamorphism in these rocks (Fig. 14) suggests a probable link between these processes.

The strong foliation dips approximately 80° to the southeast, and is locally tightly folded into northeasterly trending folds. These folds also fold the early leucosomes. A mineral lineation plunges approximately 40° to the northeast. Interpretation of aeromagnetic data shows that this exposure occurs on the eastern limb (but close to the hinge zone) of a large-scale (4–6 km wide), northeasterly plunging synform (Fig. 11; Geological Survey of Western Australia, 2011). The fold is interpreted to be bracketed by a northeasterly trending shear zone to the west, and by a northeasterly trending thrust fault with a dextral strike-slip component to the east. The Fraser Fault Zone is located about 6 km across strike to the west, and is interpreted to have predominantly dextral kinematics (see Excursion 1, Stop 8).

Metagranite from this locality has yielded a preliminary date of 1283 ± 6 Ma, interpreted as the age of magmatic crystallization (GSWA 194779). Approximately 2.8 km northeast of this locality, in a similar gully section, a garnet-bearing granitic pegmatite that appears to crosscut the foliation at a low angle has yielded a preliminary date of 1283 ± 7 Ma, interpreted as the age of magmatic crystallization of the pegmatite (GSWA 194780). These dates indicate a short time-span for the intrusion and subsequent metamorphism of the granitic rocks.

Directions to Stop 7:

Retrace the route back to the track, turn right (northeast), and drive 1.8 km to Fraser Range Station Caravan Park. Turn left and drive 1.8 km to the Eyre Highway (note that at this point you will be coming onto a sealed road). Turn right (east on the highway) and drive 39 km to the turnoff to Newman Rocks (on the left-hand side of the road). Follow this turnoff to the farthest, lower car park and picnic area.

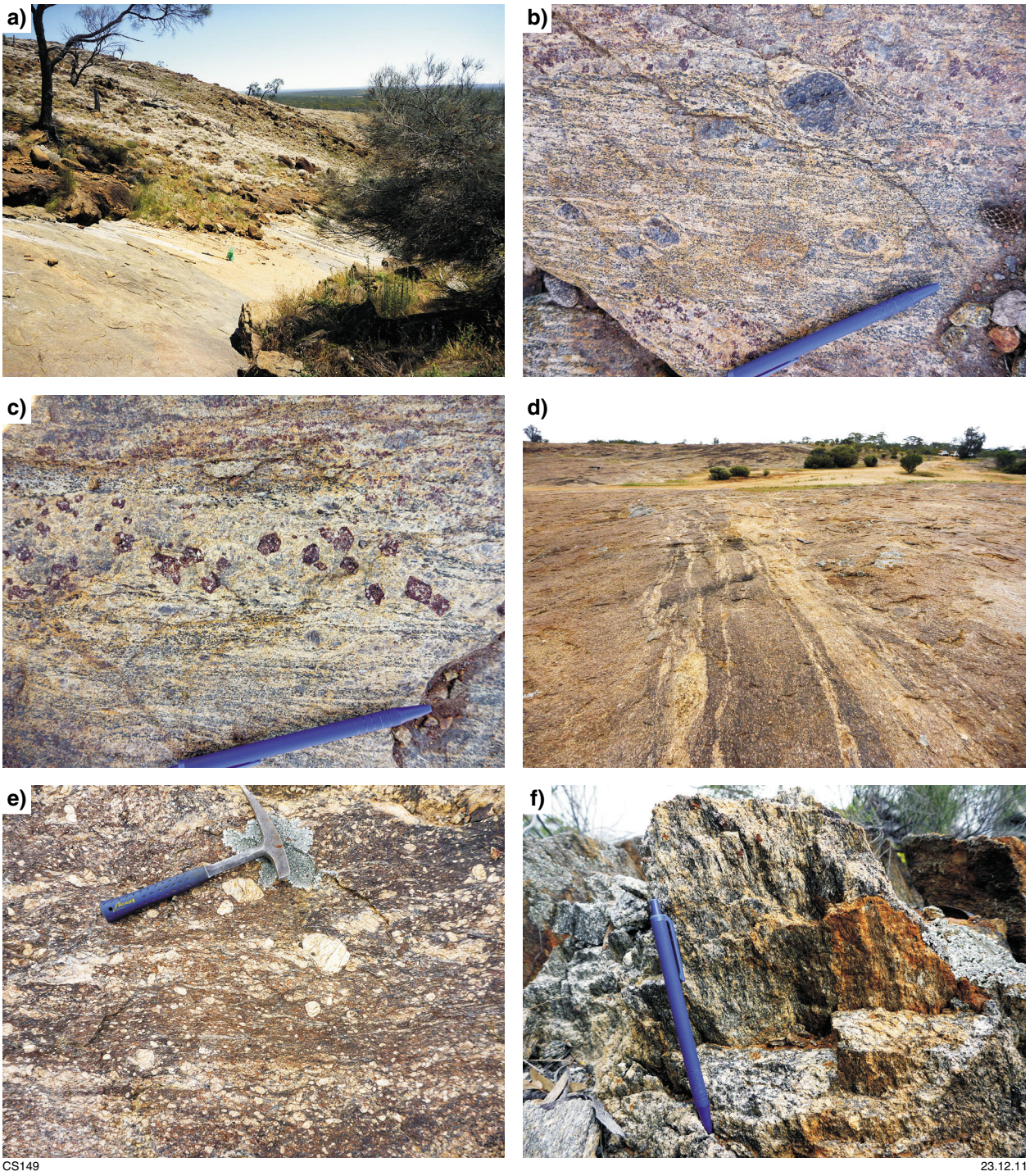

Figure 34. a) Sheeted metagabbroic (dark) and metagranitic (light) rocks in a well-exposed gully section; Fraser Range Metamorphics, Wyranilu Hill; Excursion 1, Stop 6; b) K-feldspar porphyroclasts in hybrid metagabbroic to metagranitic rocks; Fraser Range Metamorphics, Wyranilu Hill; Excursion 1, Stop 6; c) large euhedral garnet crystals in a coarse, late leucosome that is slightly discordant to the fabric in sheeted hybrid rocks; Fraser Range Metamorphics, Wyranilu Hill; Excursion 1, Stop 6; d) discrete high-strain zone of coarse-grained, K-feldspar megacrystic metagranite; Newman Shear Zone, Newman Rocks; Excursion 1, Stop 7; e) detail of high-strain zone of coarse-grained, K-feldspar megacrystic metagranite, showing grain-size reduction areas rich in biotite and garnet; Newman Shear Zone, Newman Rocks; Excursion 1, Stop 7; f) strongly deformed, c. 1763 Ma metagranite; Newman Shear Zone, Newman Rocks; Excursion 1, Stop 7.

Stop 7. Newman Rocks — Newman Shear Zone

The purpose of this stop is to observe mylonite and high-strain zones related to the formation of the Newman Shear Zone, and to examine both Paleoproterozoic and Mesoproterozoic metagranitic rocks within the shear zone. The Newman Shear Zone is a major structure that marks the boundary between the Fraser and Nornalup Zones, and in this region is defined by a prominent demagnetization zone that is at least 70 km long in aeromagnetic data (Figs 10, 11, and 29). The Newman Shear Zone is also defined by a distinct change in gravity data, from a high (dense) signature related to Fraser Zone rocks to the west, to a moderate (less dense) signature related to Recherche Supersuite and Nornalup Zone rocks to the east (Figs 11 and 28).

Approximately 36 km southwest of Newman Rocks, near the southwesternmost part of the demagnetization zone and in the hinge of the large-scale S-fold described above (Excursion 1, Stop 2), coarse-grained monzogranitic gneiss with a strong gneissic fabric has yielded a preliminary date of 1297 ± 8 Ma, interpreted as the age of magmatic crystallization of the monzogranite (GSWA 194711; Figs 9–11). The monzogranitic gneiss contains garnet and hornblende in millimetre- to centimetre-scale mafic layers and clots, and centimetre-scale K-feldspar phenocrysts. The fabric varies from an S-tectonite to an L-tectonite; dipping between 75° to the northwest through to vertical (S-layers), and plunging about 4° to the northeast (L-rods). Localized S–C fabric and shear bands indicate sinistral kinematics.

Here at Newman Rocks, coarse-grained, K-feldspar megacrystic (2–5 cm) metagranite has yielded an identical preliminary date of 1297 ± 12 Ma, interpreted as the age of magmatic crystallization of the granite (GSWA 194783; MGA 516133E 6446900N). Dating of this megacrystic metagranite has also yielded a preliminary date of 1305 ± 15 Ma from zircon rims, interpreted as the age of metamorphism. The megacrystic metagranite is well exposed in a series of platforms at this locality, and is variably strained, ranging from relatively undeformed to discrete, anastomosing high-strain and mylonite zones (Fig. 34d). There is a well-developed mineral lineation in these zones that is subvertical, which suggests subvertical movement. This is in contrast to the subhorizontal lineation in monzogranitic gneiss 36 km to the southwest. One example of the subvertical mineral lineation suggests east side up, but the relative movement sense is difficult to discern overall. The foliation in the high-strain zones is subvertical and mostly trends northeast, but some high-strain zones trend east-southeast. Garnet-bearing microgranite dykes about 5–20 cm wide are cut by the high-strain zones. One example is offset with apparent sinistral sense. Metagranite in the high-strain zones has undergone grain-size reduction, and is rich in biotite and garnet (Fig. 34e). The metagranite also contains localized remnants of quartz veins and small enclaves of mafic material.

Approximately 300 m to the northeast, away from the main exposures, strongly deformed metagranite with an L–S tectonite fabric (Fig. 34f) has yielded a preliminary date of 1763 ± 11 Ma, interpreted as the age of magmatic crystallization of the granite (GSWA 194784; MGA 516435E 6447139N). This indicates the presence of Paleoproterozoic granitic rocks on the eastern side of the Fraser Zone, probably related to granitic rocks in the Biranup Zone. Metasyenogranite of this age has been dated in the northeastern Biranup Zone, northeast of Tropicana at McKay Creek (see 'Biranup Zone' section, or Excursion 2, Stop 3). The metagranite represented by GSWA 194784 is different from the main exposure of megacrystic metagranite seen here at Newman Rocks in that it does not contain large K-feldspar phenocrysts.

Retrace the route back to Fraser Range Station Caravan Park.

Day 4

Directions to Stop 8:

From Fraser Range Caravan Park, drive 1.8 km to the Eyre Highway and turn right (east). Drive 4.8 km to the turnoff for the Symons Hill Track (on the left-hand side of the road) (at MGA 484633E 6457385N or 32°01′10.4″S 122°50′14.2″E). Follow this track for 2.1 km, then turn right onto another track. Drive 2.5 km, bear left at the fork, and drive another 1.2 km. Bear right at a fork, and drive 2.5 km to a gated crossroad; continue straight ahead 22.3 km to Symon's Well. From the well, drive 21.3 km, then bear right. Drive another 15.9 km, and bear left to head west at the track intersection. Drive an additional 6.1 km to reach Stop 8 (MGA 525328E 6505726N).

Stop 8. Fraser Fault Zone

The purpose of this stop is to examine mylonitic rocks associated with the Fraser Fault Zone, which marks the boundary of the Fraser and Biranup Zones, 1.5 km across-strike (northwest) from this locality. The rocks exposed along the Fraser Fault Zone have a steeply dipping foliation, and variably plunging mineral lineation. Where discernable, kinematic indicators mostly indicate a dextral shear-sense, but the fault zone is interpreted to also include a northwest-vergent thrust component (cf. Myers, 1985). Dextral kinematics are evident in aeromagnetic data, particularly to the northeast, where large-scale, displaced lozenges of interpreted Fraser Zone rocks have dextral asymmetry (Plate 1). The aeromagnetic data also shows distinct striped layering consistent with a high-strain fabric, and localized isoclinal folding of this fabric (Figs 8 and 35).

It is interesting to note that much of the outcrop along the northwestern margin of the Fraser Zone, and in the vicinity of the Fraser Fault Zone, comprises interlayered mafic amphibolite (possibly retrogressed from granulite facies) and metasedimentary rocks including semipelitic and psammitic to calc-silicate varieties (see 'Fraser Zone' section). The mafic amphibolite mostly forms uniform layers 3–10 cm wide (e.g. Fig. 12b), and probably represents mafic sills associated with gabbroic intrusions of the Fraser Range Metamorphics. The rocks at this locality (Stop 8) comprise quartzofeldspathic gneiss,

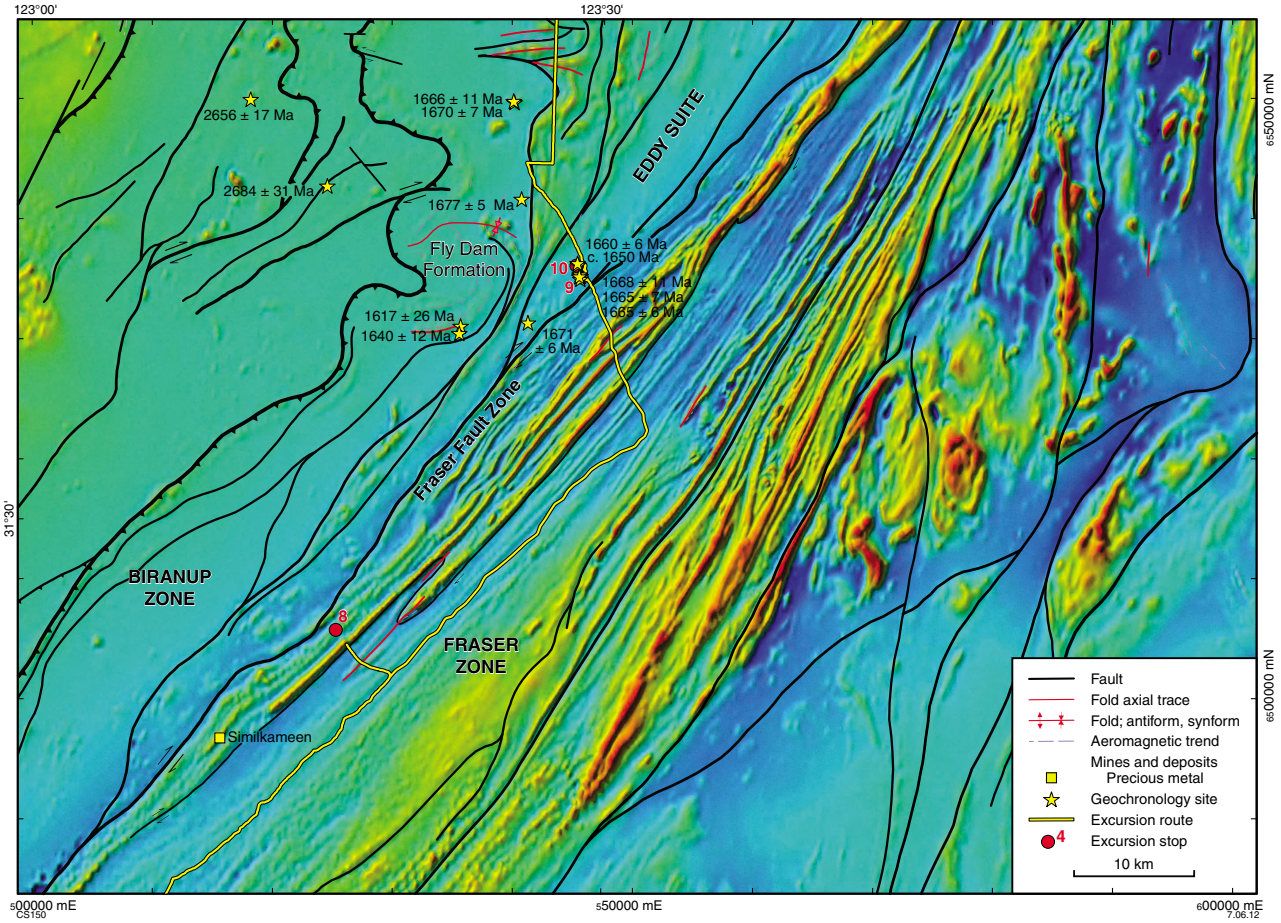

Figure 35. Aeromagnetic image of part of the Fraser Zone showing strong to mylonitic fabric (striped layers with northeasterly trend), and localized isoclinal folds of this fabric.

psammitic to calc-silicate gneiss (Fig. 36a), and mafic amphibolite. All are garnet-bearing, with some layers particularly garnet-rich.

The mylonitic foliation trends to the northeast and is subvertical (Fig. 36b). Locally, this fabric is isoclinally folded on a millimetre- to centimetre- scale, showing the same relationship as larger-scale folds evident in aeromagnetic data. The mineral lineation plunges about 12° to the northeast, suggesting subhorizontal movement. Kinematic indicators, such as tails on garnet–biotite porphyroblasts (Fig. 36c) and strung-out mafic lenses (Fig. 12d), mostly indicate dextral asymmetry or offset.

The timing of movement along the Fraser Fault Zone remains problematic, although to help resolve this issue, the rocks at this locality were recently sampled for in situ monazite dating. So far, all of the geochronology from rocks of the Fraser Zone indicate Stage I metamorphic dates (Fig. 5; cf. Clark et al., 1999; Oorschot, 2011). Stage I dates include a biotite – whole-rock Rb–Sr isochron date of 1268 ± 20 Ma, interpreted to reflect the time of cooling below the isotopic closure temperature for the biotite in the sample (Fletcher et al., 1991), and monazite dating from Gnamma Hill and Mount Malcolm (see Excursion 1, Stop 5; Oorschot, 2011), although rim analyses from one of the Gnamma Hill samples also provided a younger date of 1234 ± 17 Ma. This was interpreted as evidence for a younger metamorphic or fluid-related event. The Rb–Sr date obtained by Fletcher et al. (1991) comes from relatively massive metagabbroic rocks in the eastern part of the Fraser Zone (their sample 74777), and therefore this date is most likely unrelated to the timing of movement along Fraser Fault Zone.

The lack of Stage II ages recorded in the Fraser Range Metamorphics is problematic, as those ages are abundant in granulite-facies Biranup Zone rocks to the west of the Fraser Fault Zone (Fig. 5) and, indeed, throughout much of the rest of the orogen (see 'Tectonic events' section). However, the Biranup Zone rocks on the western side of the Fraser Fault Zone lack Stage I ages, suggesting that the Fraser Zone must have been structurally emplaced into its current position after Stage I. In addition, Stage II metamorphic dates have been recorded in metasedimentary schist intruded by the Eddy Suite (see Excursion 1, Stop 9) within 1 km of the Fraser Fault Zone, and adjacent to the Fraser Zone in the northeastern part of the Albany–Fraser Orogen, in the Gwynne Creek Gneiss (see Excursion 2, Stop 11).

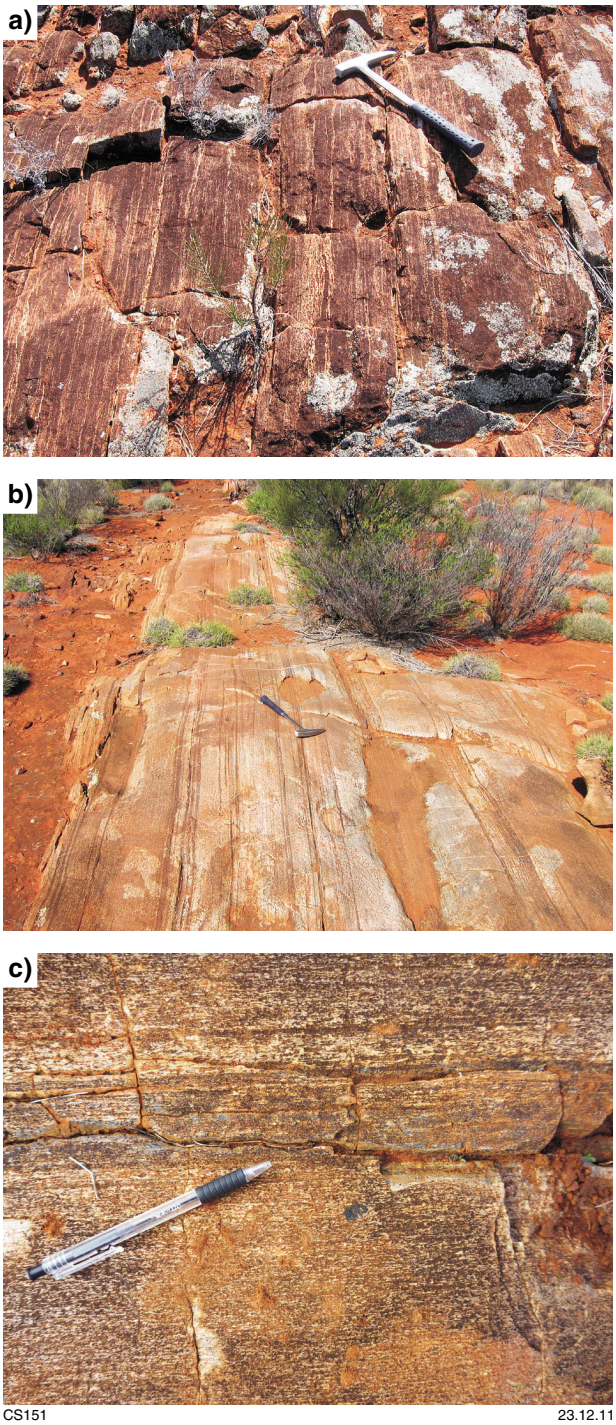

Figure 36. a) Platform exposure of mylonitic psammitic to calc-silicate metasedimentary gneiss with layers of mafic amphibolite; Fraser Fault Zone, Excursion 1, Stop 8. The hammer head points north; b) platform exposure of subvertical mylonitic foliation in metasedimentary gneiss with layers of mafic amphibolite; Fraser Fault Zone, Excursion 1, Stop 8. The hammer head points north; c) metasedimentary gneiss with garnet–biotite porphyroblast (to the right of the pen) showing dextral asymmetry; Fraser Fault Zone, Excursion 1, Stop 8.

Directions to Stop 9:

Retrace the track 6.1 km to the intersection with the Symons Hill track, and turn left (northeast). Continue on this track for approximately 30 km; at the fork, take the track on the left (MGA 551220E 6522137N). Drive 12 km to the next track intersection and continue straight ahead. Drive 2.1 km to Stop 9 (MGA 546153E 6534950N). Walk along the northwestern edge of the salt lake for a good view of the different lithologies here. If time permits, it is worth walking over the northeasterly trending, approximately 700 by 400 m wide ridge that flanks the salt lake.

Stop 9. The Eddy Suite

This locality has excellent exposures of rocks belonging to the c. 1665 Ma Eddy Suite (part of the Biranup Zone), a sequence of mingled and mixed metagranodiorite and metagabbronorite and their inferred hybrid products. The metagranodiorite contains rounded quartz phenocrysts up to 6 mm wide, and ovoid rapakivi K-feldspars up to 3 cm long with a mantle of more calcic feldspar, within a medium-grained groundmass (Fig. 37a). The metagabbronorite is fine to medium grained, and forms irregular enclaves that have lobate, commonly gradational, boundaries with the metagranodiorite, suggesting that the two phases were co-magmatic (Fig. 37b). Hybrids of these rocks contain variable amounts of both the rapakivi feldspars and rounded quartz phenocrysts. These rocks are interpreted to intrude semipelitic schist, exposed at the southwestern end of the salt lake at this locality (Fig. 37c).

The Eddy Suite occurs within a wedge-shaped, northeasterly trending fault slice, bound to the southeast by the Fraser Fault Zone (Figs 8, 27, and 35). Outcrops of the Fraser Range Metamorphics and the Fraser Fault Zone occur approximately 800 m to the southeast of this location. West of the Eddy Suite, in separate fault slices, are Biranup Zone granitic gneisses and rocks of the Fly Dam Formation (see 'Barren Basin — Cycle 1 sediments' section).

Exposures of the Eddy Suite seen at this locality are heterogeneously deformed, so that in some areas magmatic textures are well preserved (e.g. along the salt lake), whereas in other areas, the rocks contain a pervasive foliation and localized mylonite zones. The foliation is mostly northeasterly trending and steeply dipping, and locally mylonitic (Fig. 37d). A good example of this can be found in a small gully on the hillside to the north (MGA 545966E 6534945N), where a small, northeasterly trending shear zone, about 3 m wide and 500 m long, is exposed. On the margins of the shear zone, rapakivi feldspars in metagranodiorite are progressively deformed, and the associated fabric is curved into the shear zone with dextral sense (Fig. 37e). Layering in the metagranodiorite, defined by more mafic hybrid rocks and garnet-rich segments, is folded into gently southwesterly plunging, tight to isoclinal folds that have axial planes that dip moderately to the southeast (Fig. 37e,f). Nearby delta-porphyroclasts are interpreted to have dextral shear sense (Fig. 37f), although both dextral and sinistral kinematics are seen in other high-strain zones at this locality. The

garnet-rich segments and layers are interpreted to be intruded remnants of the semipelitic schist exposed at the southwestern end of the salt lake.

Metagranodiorite from this locality yielded a date of 1665 ± 6 Ma, interpreted as the age of magmatic crystallization (GSWA 194720, Kirkland et al., 2010j). The sample contains ovoid rapakivi feldspars, tabular euhedral feldspars, and rounded quartz phenocrysts, all within a fine- to medium-grained groundmass. Visually estimated, the sample's mineralogy includes about 35% plagioclase, 30% quartz, 25% microcline, 6–8% biotite, 1–2% garnet, and 1–2% hornblende–epidote; accessory minerals include apatite and zircon. The rapakivi texture is defined by grains up to 15 mm long and 10 mm wide, with cores of microcline (up to 10 by 6 mm) rimmed by aggregates of quartz and inequigranular, coarse-grained plagioclase. Discrete euhedral plagioclase grains are also present in this sample, and contain small inclusions and interstitial patches of microcline and quartz. Some plagioclase grains contain needles of epidote and minor sericitized cores. Aggregates of biotite(–hornblende) are developed within some plagioclase-rich rims on K-feldspar grains, but can also form discrete clots. Garnet, epidote, and hornblende are associated with the biotite aggregates. Large biotite grains, up to 2 mm long, occur outside the polycrystalline clots, and possess fringes of fine-grained biotite at each end of the crystal. Parts of the groundmass are rich in microcline, with less abundant quartz, plagioclase, and biotite, whereas other areas are largely composed of quartz and biotite aggregates. In some areas, there is evidence for garnet formation through the replacement of biotite aggregates.

Metagabbronorite was sampled about 100 m north of the dated metagranodiorite described above; baddeleyite grains isolated from this sample yielded a weighted mean (SHRIMP) $^{207}Pb^*/^{206}Pb^*$ date of 1664 ± 7 Ma (MSWD = 0.74), interpreted as the age of magmatic crystallization (GSWA 194721, Kirkland et al., 2009b). This date is within uncertainty of that from the metagranodiorite, supporting the interpretation that the mingling textures represent co-magmatic phases (Fig. 37b). The mafic sample dated is an ophitic biotite–augite norite, with a visually estimated mineralogy of about 45% plagioclase, 25% orthopyroxene, 15% clinopyroxene, 10% biotite, 2% olivine, 2% oxide minerals (magnetite > spinel), 0.5% hornblende, and minor spinel-bearing symplectites occurring between olivine and plagioclase grains. Olivine appears as rounded residual grains up to 0.7 mm long, and is mainly enclosed within orthopyroxene. Spinel-bearing symplectites and individual olive-green spinels occur as small grains attached to opaque oxide grains. Ophitic orthopyroxene grains up to 8 mm long, and clinopyroxene grains up to 5 mm long, exhibit complex exsolution textures. Inclusions of opaque oxide grains define a schiller texture within the clinopyroxene; minor exsolution also occurs in the orthopyroxene grains. Pyroxene grains enclose zoned plagioclase crystals up to 1.5 mm long; biotite encloses opaque oxide grains (–spinel), and also exists as an interstitial phase to both pyroxene and plagioclase. Biotite is partially replaced by olive-brown hornblende. Accessory phases include apatite, baddeleyite, and rare fine-grained sulfide minerals.

Semipelitic, garnet–micaceous schist interlayered with metagranodiorite, exposed at the southwestern end of the salt lake (MGA 546046E 6534694N), is folded into a moderately north-northeasterly plunging, tight antiform with metagabbronorite in the core. The antiform is inclined with a southeast-dipping axial plane, and also folds a strong foliation (S_1). A mineral lineation developed on the S_1 plane has the same orientation as the fold axis. The southeastern limb of the fold is truncated by a northeasterly trending shear zone containing L-tectonite and boudinaged rocks. A mineral lineation in the high-strain zone plunges 62° towards 005. A quartz vein also cuts the fold parallel to the hinge. In some layers, the schist contains rounded porphyroclasts of K-feldspar similar to those in the rapakivi metagranodiorite (Fig. 37c). The rounded K-feldspar porphyroclasts are interpreted to have been derived from pegmatitic veins associated with intrusions of Eddy Suite magmas, and subsequently dispersed throughout the schist during high-strain deformation. Late granitic to pegmatitic veins cut the foliation and folding, both here and elsewhere at this locality.

A sample collected from the sheared semipelitic schist (GSWA 194722, Kirkland et al., 2010c) yielded significant age components at c. 1650, 1745, 1783, and 2645 Ma. The c. 1650 Ma component may reflect the intrusion of pegmatitic or granitic material into the schist. Dates of 1304–1185 Ma for 21 zircon-rim analyses are interpreted to reflect elevated temperatures and zirconium mobility during a metamorphic event between these dates, with the large dispersion either reflecting a prolonged process, or radiogenic-Pb loss.

Although not clearly defined, it is likely that some of the deformation seen at this locality is related to movement along the adjacent Fraser Fault Zone, particularly where dextral kinematics can be inferred. The metamorphic rim analyses that yielded dates as young as c. 1185 Ma suggest the possibility of Stage II metamorphism and deformation along the Fraser Fault Zone.

Directions to Stop 10:

Continue another 1.2 km to the northwest, along the same track (MGA 546022E 6535898N).

Stop 10. Granitic gneisses — Eddy Suite?

This locality is about 1.5 km north of Stop 9, and comprises Biranup Zone granitic gneisses of about the same age. These gneisses occur northwest across-strike from the rocks of Stop 9, and although of similar age, may be of higher metamorphic grade (they contain abundant leucosome), and are much more felsic in composition. The rocks of Stops 9 and 10 appear to be separated by a northeasterly trending shear zone approximately 60 m wide, in which evidence is preserved of extreme flattening and a localized, well-developed rodding lineation that plunges 24° to the east-northeast (Fig. 38a). Large quartz veins also occur in this shear zone. Northwest of the shear zone, the granitic gneisses are folded into open,

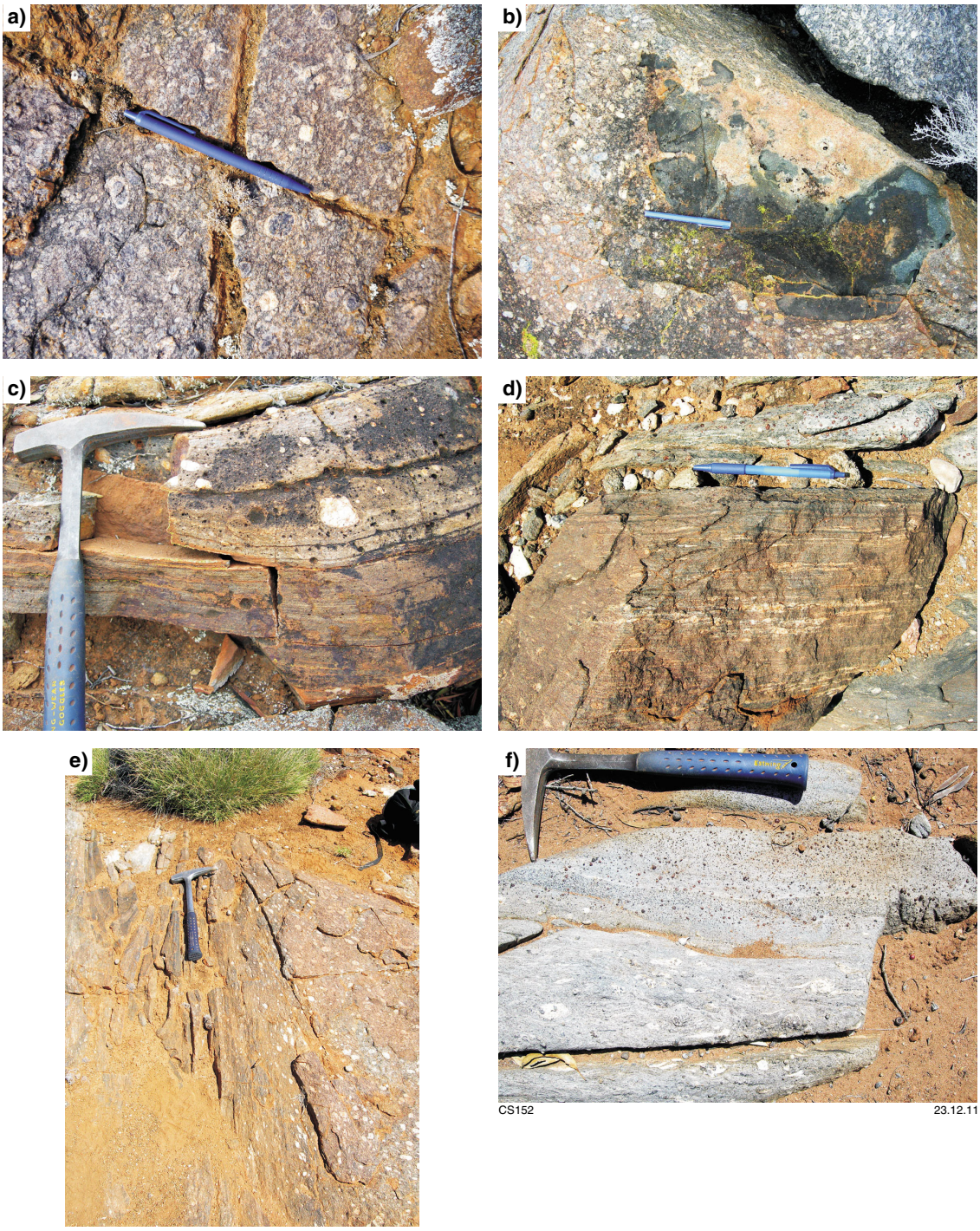

Figure 37. a) Rapakivi feldspars with well-developed calcic mantles in metagranodiorite of the Eddy Suite; Excursion 1, Stop 9; b) irregular and lobate boundaries of metagabbronorite in contact with metagranodiorite. These textures suggest mingling between the two phases; Eddy Suite; Excursion 1, Stop 9; c) strongly deformed metasedimentary schist, intruded by magmatic rocks of the Eddy Suite. The K-feldspar porphyroclasts are interpreted to have been derived from pegmatitic veins associated with Eddy Suite intrusions, and subsequently dispersed throughout the schist during high-strain deformation; Excursion 1, Stop 9; d) mylonitic fabric in hybrid metadiorite, with strung-out rapakivi feldspars. The layer at the top of the photograph is rich in garnet, and is interpreted to be a remnant of the same schistose metasedimentary rocks as those shown in part c) and represented by GSWA 194722; small gully in a hillside (MGA 545966E 6534945N), Excursion 1, Stop 9; e) folded layering (left of the hammer in the photograph) in a small shear zone within metagranodiorite and hybrid rocks of the Eddy Suite. Note the increasingly deformed rapakivi feldspars and increasing strain from the right side of the photograph towards the limb of the fold and into the shear zone (where the hammer lies). The deflection of the fabric into the shear zone is consistent with dextral kinematics. Small gully in hillside (MGA 545966E 6534945N), Excursion 1, Stop 9; f) sheared rapakivi-textured metagranodiorite interlayered with garnet-rich phase, interpreted to be a remnant of the same schistose metasedimentary rocks as those shown in part c). The delta-porphyroclast in the lower right of the photograph is interpreted to have dextral kinematics; Excursion 1, Stop 9.

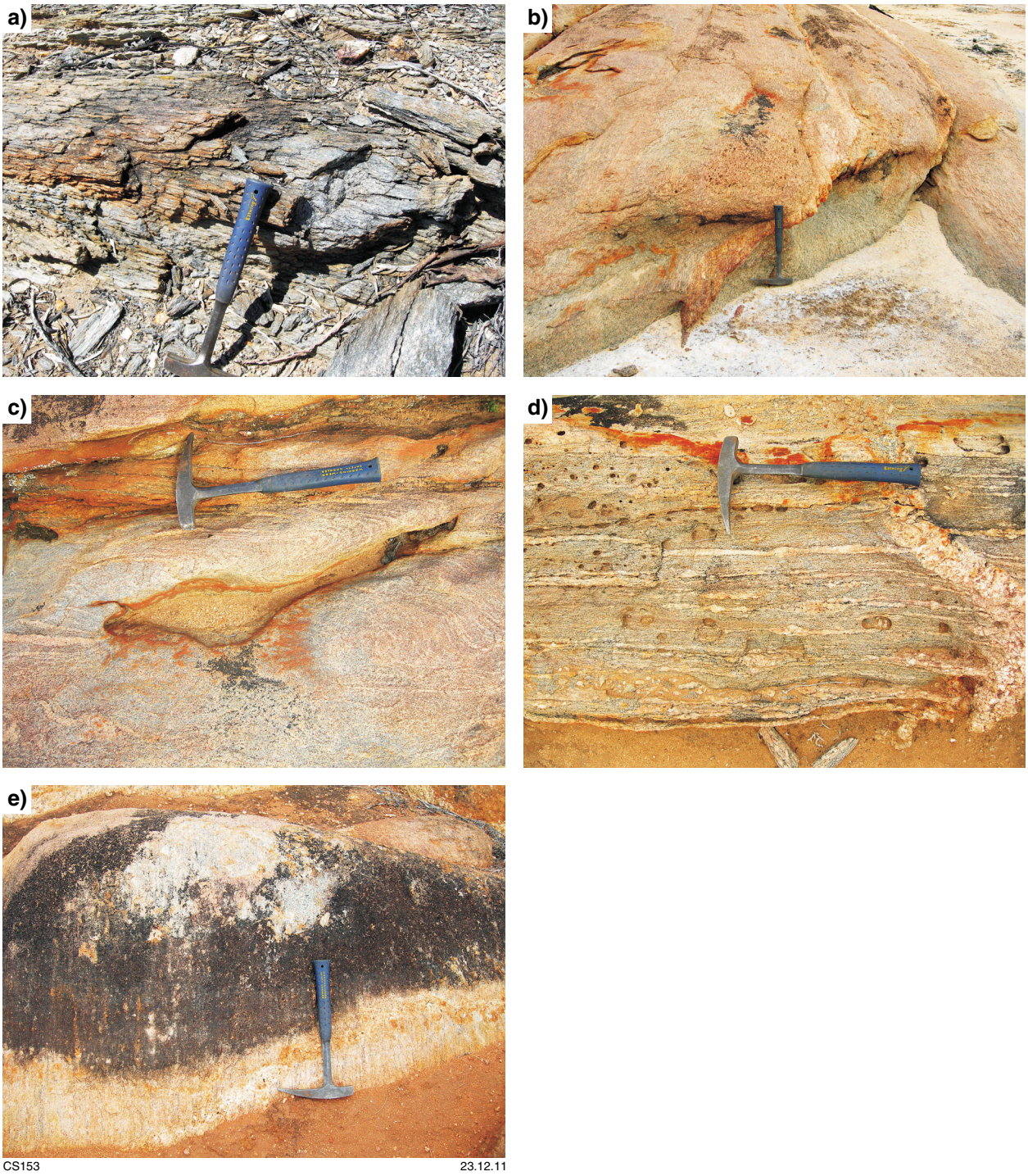

Figure 38. a) Strongly rodded granitic gneiss (possibly metagranodiorite of the Eddy Suite) in the shear zone between Stops 9 and 10 of Excursion 1; b) southeast-dipping gneissic layering and low-angle leucosome veins in monzogranitic gneiss; Excursion 1, Stop 10; c) folded gneissic fabric and leucosome in syenogranitic gneiss, looking down-dip to the southeast; Excursion 1, Stop 10; d) stretched K-feldspars and leucosome in sheared monzogranitic gneiss, with a crosscutting leucosome vein. View looking down-dip to the southeast; Excursion 1, Stop 10; e) down-dip mineral lineation on southeast-dipping gneissic foliation surface on monzogranitic gneiss. View looking northwest; Excursion 1, Stop 10.

decametre-scale folds with moderately southeast-dipping axial planes. Within the hinges are small-scale tight folds with a similar trend, which fold both the gneissic fabric and thin leucosome layers. The tighter angle of these folds suggests they may represent an earlier phase of co-axial folding. The gneissic fabric is cut by pegmatitic veins 5–10 cm wide.

Along strike to the northeast at this locality (Stop 10; MGA 545986E 6535986N), are two phases of granitic gneiss with a well-developed gneissic foliation that dips consistently and moderately to the southeast (Fig. 38b). As at the locality described above, thin leucosome veins are tightly folded with this foliation (Fig. 38c). Locally, however, the folded leucosomes have an axial-planar foliation that is parallel to the main foliation. Younger, coarser leucosome veins are slightly discordant to the gneissic foliation (Fig. 38b) or crosscut it at high angles (Fig. 38d). Apart from the late, high-angle leucosome veins, the sequence suggests the possibility of continued leucosome formation before and after folding, with the injection of new (low angle) leucosome following folding. Coarse, late pegmatite also crosscuts the gneissic fabric and folding, as do quartz veins.

The predominance of southeasterly dipping layering, and presence of inclined folds at this locality and at Stop 9, are suggestive of a northwest-vergent fold-and-thrust architecture. This architecture has also been interpreted on a larger scale from the aeromagnetic data (Figs 8 and 35). In the northwestern part of the exposure at Stop 10, a strong down-dip mineral lineation measuring 38° to 113 is well developed on the gneissic foliation plane in monzogranitic gneiss (Fig. 38e). This mineral lineation overprints the leucosome veins, suggesting it is relatively late. Mineral steps developed on the same gneissic foliation surface indicate southeast-side up, which suggests a thrust sense. This geometry would place the granitic gneisses seen here at Stop 10 structurally below rocks of the Eddy Suite (Stop 9 rocks), and possibly below the Fraser Zone rocks. This could explain the apparent increase of metamorphic grade, or at least the greater abundance of leucosome, in these granitic gneisses.

As indicated above, the granitic gneisses at this locality are of similar age to the Eddy Suite, which raises the question of whether they represent a felsic end-member in terms of mixing processes. K-feldspar monzogranitic gneiss yielded a date of 1660 ± 6 Ma, interpreted as the age of magmatic crystallization of the monzogranite (GSWA 194723, Kirkland et al., 2010k). The monzogranitic gneiss locally contains megacrysts, some of which are stretched parallel to the foliation, along with layer-parallel leucosome (Fig. 38d). It also locally contains medium-sized garnets. A strong lineation, locally with rodded megacrysts, is developed in high-strain zones.

Visually estimated, the sample dated has a mineralogy including 36% quartz, 31% microcline, 23% plagioclase, 8% biotite, 1% garnet, a brownish isotropic grain, and accessory titanite, epidote, apatite, and zircon. The biotite, which is up to 2 mm long, is very dark (iron–titanium rich) and foliated, and is accompanied by garnet, epidote, titanite, apatite, and zircon. Rare microcline and plagioclase grains are as much as 5 mm long, whereas most of the quartz and feldspar grains are less than 3 mm long. Some of the plagioclase grains have inclusions of disseminated fine-grained epidote.

The other granitic phase at this locality is an equigranular syenogranitic gneiss with sparse localized garnet and leucosomes, both of which are subparallel to the gneissic foliation, and are folded with it. The gneiss yielded a date of 1668 ± 11 Ma, interpreted as the age of magmatic crystallization of the syenogranite (GSWA 194724, Kirkland et al., 2010l). The sample consists of about 45% microcline, 36% quartz, 12% plagioclase, 5–6% biotite, <1% hornblende, and accessory opaque oxide grains, titanite, apatite, and zircon. Most grains are less than 2 mm long, with a foliation defined by dark yellow-brown biotite and very minor dark-green hornblende. Rare plagioclase contains patches of sericite and fine-grained muscovite of secondary origin, and some titanite grains are largely altered to leucoxene.

Directions to Kalgoorlie:

Continue another 10.2 km along the same track heading northwest, to an intersection with an east–west track, and turn right (to the east). Drive 2.1 km to a sharp left turn (to the north). Continue 12.4 km to another sharp corner, and bear left (to the west). Drive 800 m, bear right (north), and follow this track 9.6 km northwards to the Trans-Australian Railway Road, a major gravel road. At this road, turn left (west) towards Kalgoorlie, a total distance of about 194 km. After about 165 km, you will come to a T-intersection; turn right towards Kalgoorlie. The sealed road starts not far from here.

Excursion 2: Tropicana in a regional context

This four-day excursion starts and finishes at Tropicana, covering a total distance of about 300 km, not including driving times and distances from Kalgoorlie. The geological stops described in this excursion have been chosen based on their relative ease of access, quality of outcrop, coverage of the various tectonic units, and to provide an understanding of our current interpretations of the geology of the Tropicana region.

A general view of the excursion route is shown in Figures 39–42. All access is via 4WD tracks situated on crown land or DEC-managed lands (i.e. Plumridge Lakes Nature Reserve). Some tracks are located within an active exploration and mining area (Tropicana Joint Venture, or JV), and access via drilling tracks requires an escort by staff from the Tropicana Gold Project. Although this guide provides location details for use by anyone wishing to independently follow the excursion route, it must be noted that restrictions apply to DEC-managed lands. Please contact the relevant authorities before proceeding, especially as track conditions are subject to change, and may be damaged or impassable in wet weather. Topographic maps and a GPS are also recommended for navigation. Please refer to Appendix 1 for further information on logistics.

Directions to Tropicana:

The assembly point for this excursion is the carpark of the Tower Hotel (corner of Bourke and Maritana Streets), Kalgoorlie. From the carpark, turn right onto Bourke Street, and then right at the roundabout onto Maritana Street. Drive two blocks before turning left onto Piccadilly Street (there is a hospital on the corner). Drive approximately 1 km, until you come to a T-intersection with the Goldfields Highway. Turn right, and follow the highway for approximately 1.5 km, then turn left onto Sutherland Street, just south of the Mount Charlotte headframe. Drive for 1.3 km, then turn left onto Yarri Road. Drive a further 25.2 km, turn right onto Pinjin Road (towards Kurnalpi, heading east). Follow this road for 137 km (to Pinjin). At the fork, bear right towards Tropicana (this is the Nippon Highway), drive for 18.3 km, then bear left. Drive another 74 km to Argus Corner; this is a good place to take a break.

From Argus Corner, continue 38.5 km on the same road, then continue straight across the PNC Baseline Road. Drive 12.5 km to Snake Corner (a distinctive sharp right-hand bend), then drive for 14.4 km to the AngloGold Ashanti sign. Bear left and drive 40.7 km to a crossing with a major new road (haul road); go straight across. Continue 9.1 km to another intersection and turn right (east). Drive 40.4 km to another intersection, and turn left (north) towards Tropicana. From here, it is approximately 55 km to Tropicana, and an escort will be required as it is a major resource area on mining leases. Please observe all notices and restrictions.

Please note that substantive new infrastructure for the Tropicana JV is currently in development, including the replacement of the existing access tracks, airstrip, and exploration camp, and the provision of the power, water, and communications requirements for a mining operation. ***Access to the Tropicana mine site, airfield, and mine access roads requires prior written approval from the General Manager, Tropicana Mine***.

Geological overview

The Tropicana region covers the northeasternmost exposures of the Albany–Fraser Orogen (Plate 2; Figs 2 and 40). It comprises rocks of the Northern Foreland, Biranup Zone, and Gwynne Creek Gneiss (Arid Basin Cycle 2 sediments). In this region, the Fraser and Nornalup Zones are entirely under the cover of the Eucla Basin. Outcrop is sparse throughout much of the region, including around the Tropicana Deposit, and there are large areas with no outcrop at all.

The Carboniferous to Permian Paterson Formation locally overlies this part of the orogen with irregular unconformable contacts, mostly preserved in topographic depressions (van de Graaff and Bunting, 1977). It has an estimated thickness of 40–50 m (van de Graaff and Bunting, 1977). Conglomerates, sandstones, and mudstones of the Paterson Formation are undeformed, and based on the presence of faceted and striated clasts whose provenance is mostly unrecognizable in the basement rocks, the lack of sorting, and the general lack of recognizable bedding, the conglomeratic components are interpreted as glacigene rocks (i.e. tillites; van de Graaff et al., 1975; Van de Graaff and Bunting, 1977).

A major structure, the Cundeelee Fault, separates the Albany–Fraser Orogen from the Eastern Goldfields Superterrane of the Yilgarn Craton, and in the Tropicana region from the Yamarna Terrane (Plate 2; Fig. 40). The Cundeelee Fault is interpreted as a major, southeasterly dipping thrust, but drillcore indicates that its footwall contains glacigene rocks of the Paterson Formation down to at least 300 m depth (R. Hocking, 2009, written comm.). This suggests that although the Cundeelee Fault was originally a thrust fault, it later became the site of a paleo- fault scarp, possibly accompanied by a component of normal movement. This fault scarp probably formed by glacial activity during the Permian, thereby producing a deep glacial valley filled with Paterson Formation sediments. Aeromagnetic data shows that northeasterly trending mafic dykes that crosscut the Cundeelee Fault are deeply buried under the Paterson Formation on the western side of the fault, but are close to the surface on the adjoining eastern side, indicating a substantial west-side down offset (Fig. 42).

The Tropicana region was originally mapped in the 1970s during GSWA's 1:250 000 mapping campaign (van de Graaff and Bunting, 1975, 1977; Bunting et al., 1976). At this time, rocks with Archean affinities, such as BIF, and mafic and ultramafic rocks were

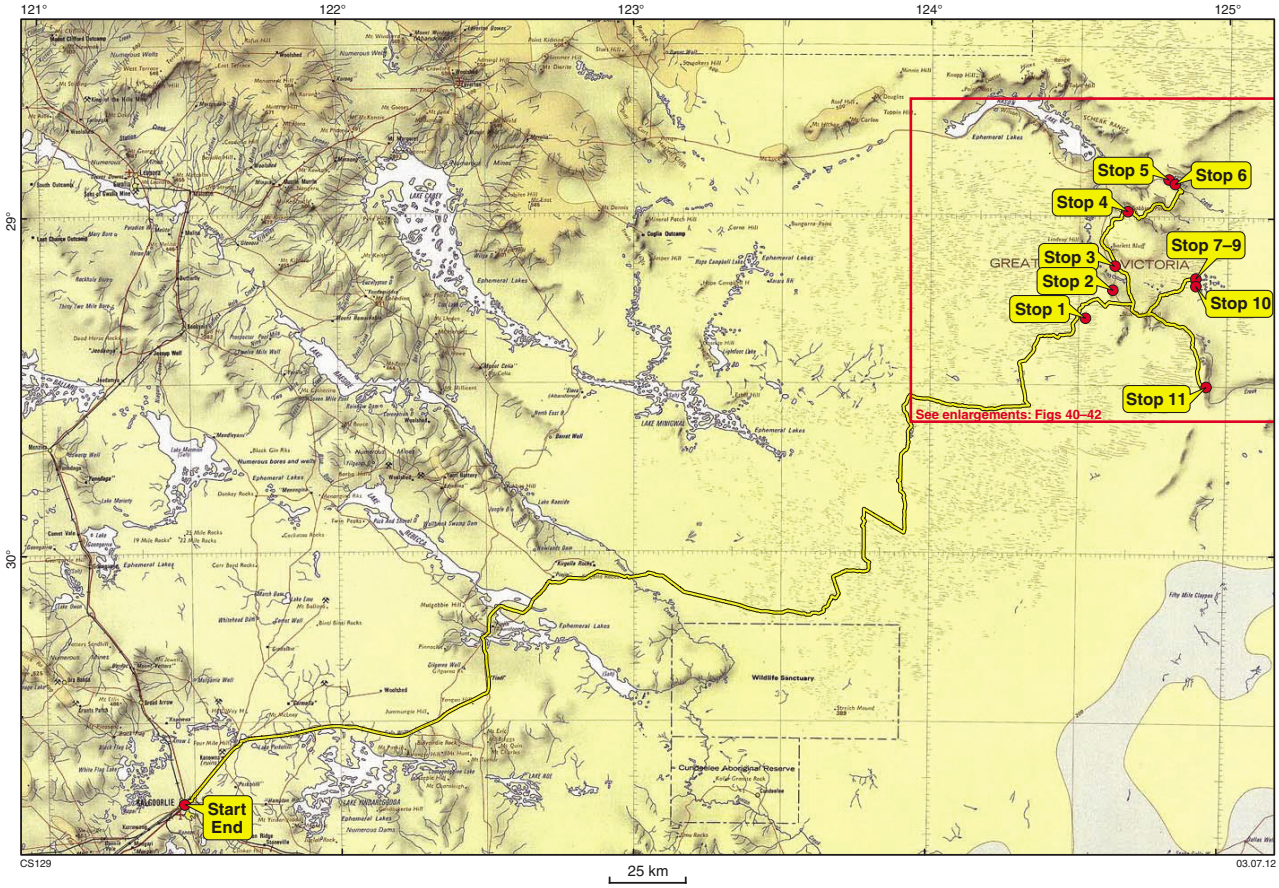

Figure 39. Route and stops for Excursion 2

identified and inferred to be Yilgarn Craton remnants, intruded by Archean or Proterozoic granites. Dating of metagranitic rocks has shown that although some are Archean, most metagranites exposed in the region are Paleoproterozoic in age. Strongly altered metagranite, sampled approximately 7 km north of the Tropicana Deposit (GSWA 182435; Fig. 43a) yielded a preliminary date of 2722 ± 15 Ma from zircon cores, interpreted as the age of igneous crystallization of the granite, and a date of 2643 ± 7 Ma from zircon rims, interpreted as the age of metamorphism. This granite intrudes mafic to ultramafic rocks, including metapyroxenite, indicating that those rocks are also Archean (Fig. 43b). The metagranite contains a moderately developed, northeasterly trending, subvertical foliation, which is cut by both K-feldspar rich veins and thin epidote veins; epidote and chlorite alteration give this metagranite a distinctive green colour. The dates obtained from this sample suggest that other mafic to ultramafic rocks, and meta-iron formation in the Hat Trick Hill area (see Excursion 2, Stops 3 and 4), are probable Archean greenstone remnants derived from the Yilgarn Craton. However, it should be noted that Paleoproterozoic mafic rocks are also present in the region, and are interpreted to be the products of mingling and mixing with the Paleoproterozoic granitic magmas (cf. Bunting et al., 1976 and van de Graaff and Bunting, 1977).

Outcrops of metagranitic rocks northeast and east of Tropicana have yielded Paleoproterozoic dates (see Excursion 2, Stops 4, 5, 7, 8, and 9) and were emplaced during, or prior to, the Biranup Orogeny. Based on the interpretation of high-resolution aeromagnetic data (including company data) and gravity data (Plate 2; Figs 41 and 42), these metagranites are interpreted to intrude the Archean rocks in the vicinity of Tropicana. Interpretations of solely faulted (non-intrusive) contacts between Archean and Paleoproterozoic rocks are difficult to map from these geophysical datasets.

Gold in the Tropicana Deposit is hosted by Archean rocks (Doyle et al., 2009), which suggests that if the gold was also originally Archean in age, it was probably reworked during Paleoproterozoic events. Alternatively, magmatism, followed by metamorphism and deformation associated with Paleoproterozoic events such as the Biranup Orogeny, may have been responsible for producing the deposit. This would fit with the gold deposit being described as not of typical Archean lode-gold type (see 'Discovery and project history' section). The presence of gold northeast of McKay Creek (Hercules Prospect), interpreted to occur within c. 1760 Ma metagranitic rocks (Plate 2), suggests a post-Archean age for mineralization, and all known events, including the Mesoproterozoic Albany–Fraser

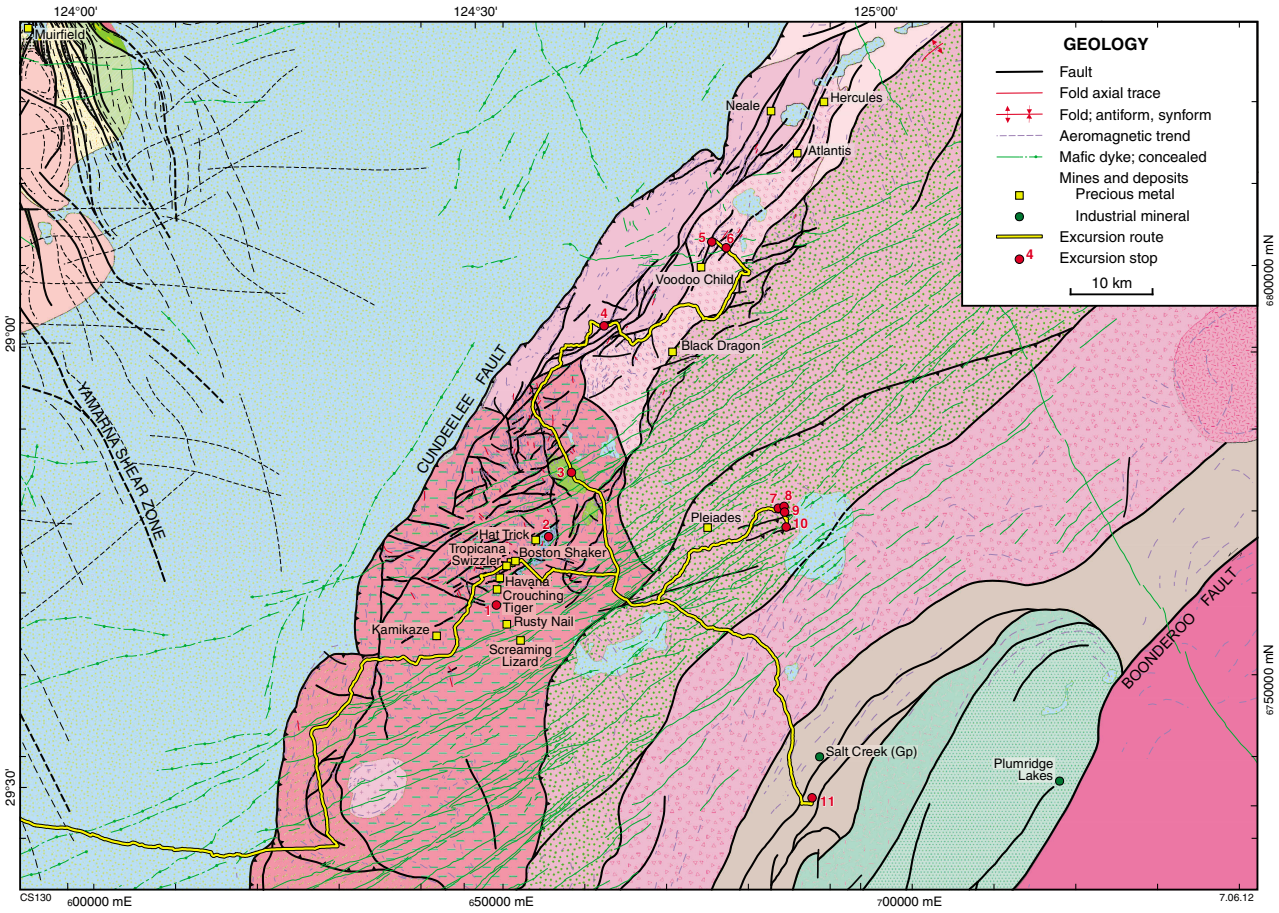

Figure 40. Route and stops for Excursion 2, superimposed on the pre-Mesozoic interpreted bedrock geology. Modified from Geological Survey of Western Australia (2011); see Plate 2 for geological legend.

Orogeny, remain as possible periods of gold deposition or enrichment. The presence of gold mineralization to the southwest of the Tropicana region (e.g. Corvette, Mustang, and Roadrunner Deposits), which occurs along northeasterly trending shear zones in interpreted Biranup Zone rocks adjacent to interpreted Fraser Zone rocks (Plate 1), is also suggestive of Proterozoic mineralization.

Mineralization at Tropicana is reported to be crosscut by mafic dykes ascribed to the c. 1210 Ma Gnowangerup–Fraser Dyke Suite (Doyle et al., 2009; see 'Mafic dyke suites' and 'Host rocks' sections), which suggests that mineralization pre-dates Stage II, unless it occurred in the earliest part of this stage, prior to 1210 Ma. The mafic dykes are reported to be unfoliated to schistose, and metamorphosed at greenschist facies, which, if their inferred age of c. 1210 Ma is correct, indicates relatively minor Stage II effects in this part of the orogen. A suite of northeasterly trending mafic dykes that crosscut all structures are prominent in aeromagnetic data (Plate 2; Fig. 42) but do not outcrop, and it is unclear whether they are the same dykes as those reported in Doyle et al. (2009). The northeasterly trending dykes also occur southwest of the Tropicana region, and are distinct from the more north-northeasterly trending mafic dykes ascribed to the c. 1210 Ma Gnowangerup–Fraser Dyke Suite (Plate 1; Fig. 8). In the Tropicana region, on the western side of the Cundeelee Fault beneath the Paterson Formation, north-northeasterly trending mafic dykes are also interpreted as part of the Gnowangerup–Fraser Dyke Suite, consistent with those to the southwest (Plate 2). This indicates the presence of at least two mafic dyke suites with north-northeasterly or northeasterly trends in the eastern Albany–Fraser Orogen. The northeasterly trending mafic dykes of unknown age clearly crosscut all structures, including those bounding Biranup Zone rocks (e.g. Ponton Creek area; Fig. 8) that have yielded post-1210 Ma Stage II metamorphic dates (Fig. 5), which suggests that these mafic dykes post-date Stage II. Although highly speculative, they may be related to the Giles Event in the Musgrave Province, and hence part of the 1085–1040 Ma Warakurna Large Igneous Province (Wingate et al., 2004; Howard et al., 2009).

Most of the Tropicana region is dominated by northeasterly trending faults, folds, and shear zones, although in some instances these structures appear to overprint earlier, northerly to northwesterly trending structures (Plate 2; Fig. 40). Much of the earlier structure is apparent in aeromagnetic and gravity data, although

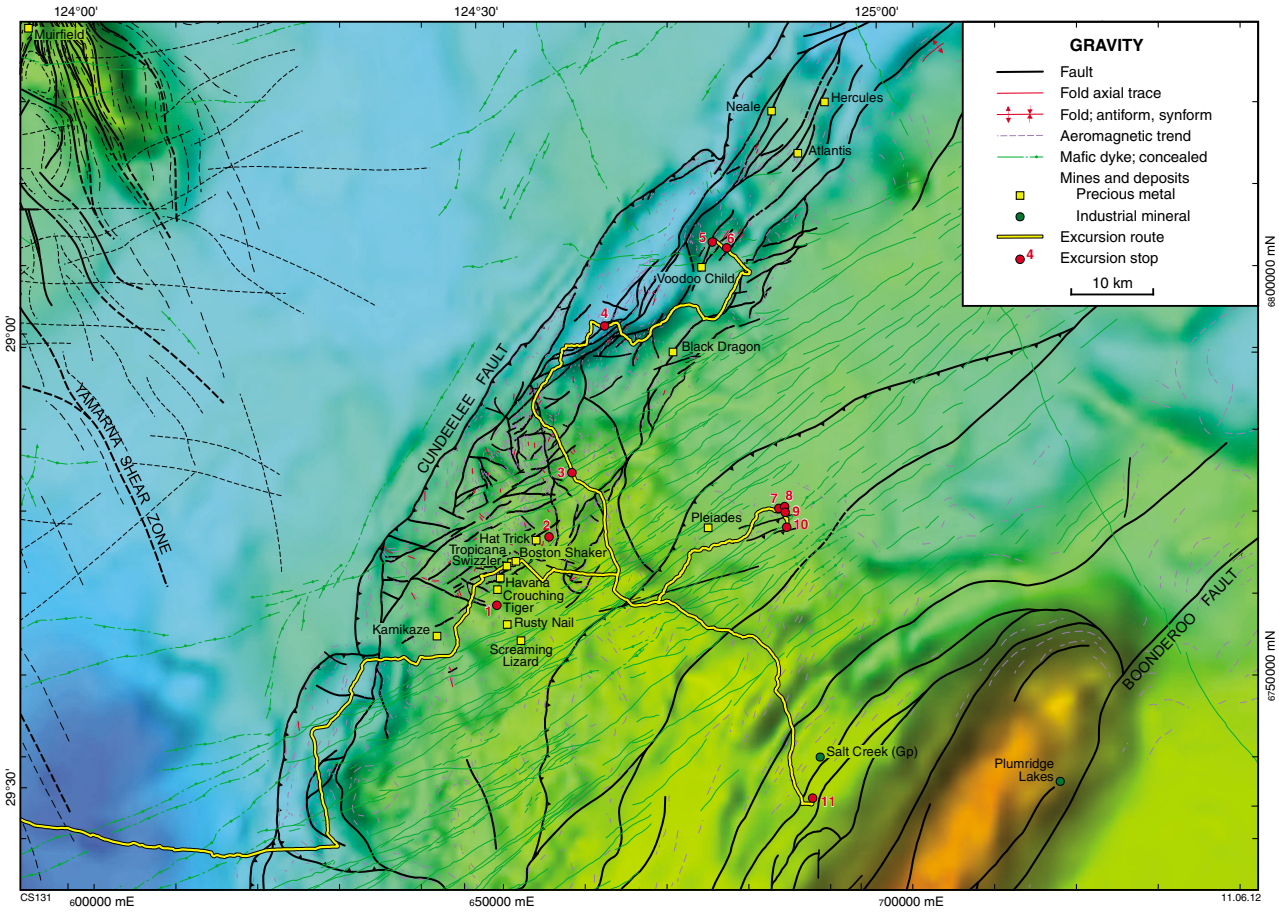

Figure 41. Route and stops for Excursion 2, superimposed on gravity data, showing major structures. Modified from Geological Survey of Western Australia (2011).

there are some areas of outcrop that contain northwesterly structural trends, or evidence of complexly reworked structures (e.g. the Hat Trick Hill area; Excursion 2, Stop 2). In some instances, the northwesterly trending fabrics appear to be rotated to the northeast, and cut by northeasterly trending shear zones (Fig. 42). These patterns are similar to those observed in the Ponton Creek area (Fig. 8), where northwesterly trending structures are interpreted to be related to the c. 1680 Ma Zanthus Event (see 'Tectonic events' section). The youngest structures in the Tropicana region appear to be east-northeasterly trending shear zones, mostly with apparent dextral offset. These are likely to be related to the same shearing event that offset the mineralization in the Tropicana Deposit (e.g. in the Boston Shaker Shear Zone; see 'Mineral deposit architecture' section).

Tropicana Gold Project

Tropicana joint venture ownership

Tropicana is an unincorporated joint venture (JV) between AngloGold Ashanti Australia Limited (70%) and Independence Group NL (30%). AngloGold Ashanti is the manager of the JV, which encompasses a total tenure area of approximately 13 000 km², located over a distance of approximately 330 km on the southeastern margin of the Yilgarn Craton (Fig. 44). The Tropicana Gold Project is a subset of the Tropicana JV, and encompasses all of the mining areas, plant, and infrastructure required to implement the Project.

Discovery and project history

The discovery and project history of the Tropicana Gold Project provided here is based on Kendall et al. (2007), amended to include the discovery history of the Boston Shaker Deposit and the progression of the project into development.

In early 2002, AngloGold signed a joint venture with Independence to investigate an untested gold-in-soil anomaly, with a peak value of 31 ppb gold, evident in historical Western Mining Corporation (WMC) data in open-file reports held by the Department of Mines and Petroleum. Prior to the JV, the WMC soil program represented the only gold exploration activity within

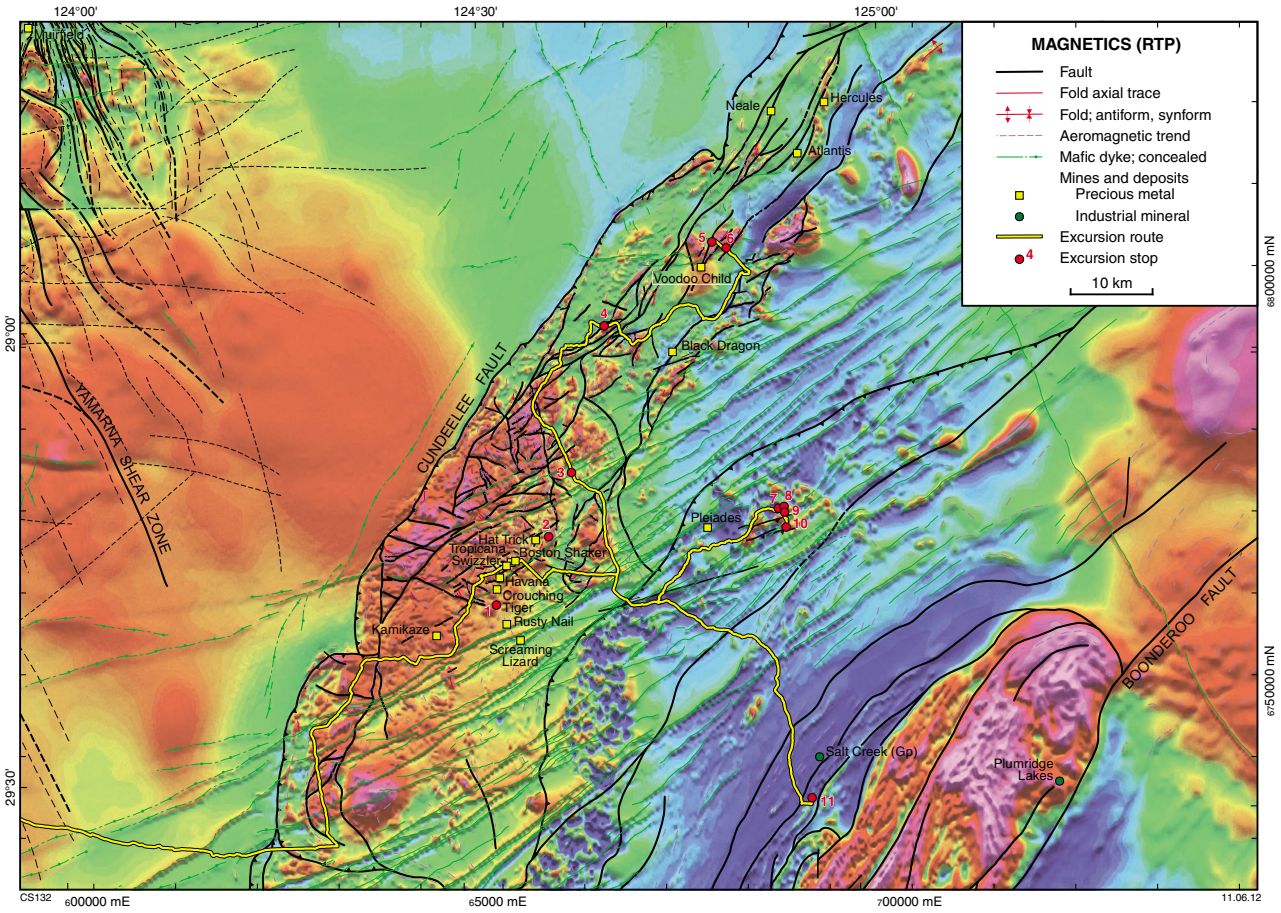

Figure 42. Route and stops for Excursion 2, superimposed on reduced-to-pole (RTP) aeromagnetic data, showing major structures. Modified from Geological Survey of Western Australia (2011).

the project tenure, and there were no other exploration datasets covering the area other than regional government magnetic and gravity data, which had resolutions too coarse for specific targeting.

Despite the sparse outcrop in the vicinity of the Tropicana Deposit, reconnaissance mapping by AngloGold geologists, as part of the JV property appraisal, identified BIF outcrops 30–40 km north of the Tropicana Deposit. This led to the interpretation that the area represented an enclave of Archean greenstone within the Proterozoic Albany–Fraser Orogen. On this basis, the area was considered to be prospective for deposits with Yilgarn lode-gold style affinities and the JV was signed, with AngloGold managing and earning up to 70% of the project. Subsequent work has demonstrated that the mineralization and host rocks are atypical of greenstone-hosted gold systems, and the revised exploration model has guided the pegging of an extensive tenement portfolio.

Broad-spaced, first-pass aircore drilling (1 km by 200 m) over the peak of the WMC soil anomaly was completed immediately after the tenement was granted in late 2002. This program returned several encouraging results, including 1 m @ 2.2 g/t and 7 m @ 2.0 g/t. Due to budget constraints and the paucity of regional datasets, only limited aircore and slimline RC drilling was carried out in 2003–04. Slimline RC drilling, which uses a small face sampling hammer on a boosted aircore rig, was chosen as a relatively low cost method that could be implemented using the aircore contractor, and which could provide information from fresh rock without having to mobilize heavy RC drillrigs to site. Drilling by this method is limited to a maximum depth of approximately 100 m at Tropicana. Encouraging results continued to be returned including 10 m @ 2.4 g/t, 8 m @ 1.2 g/t, and 13 m @ 1.9 g/t. The significance of these first-pass drilling results was immediately recognized, and during 2003, the JV applied for additional tenements extending around 330 km along the Albany–Fraser and Yilgarn Craton margin. Subsequent tenure acquisitions by AngloGold and Independence have expanded the tenure holdings to approximately 12 000 km^2.

The majority of the mineralized intercepts from this drilling program occurred at the base of the saprolite zone, and were interpreted at the time to be supergene mineralization. Primary mineralization, intersected in the

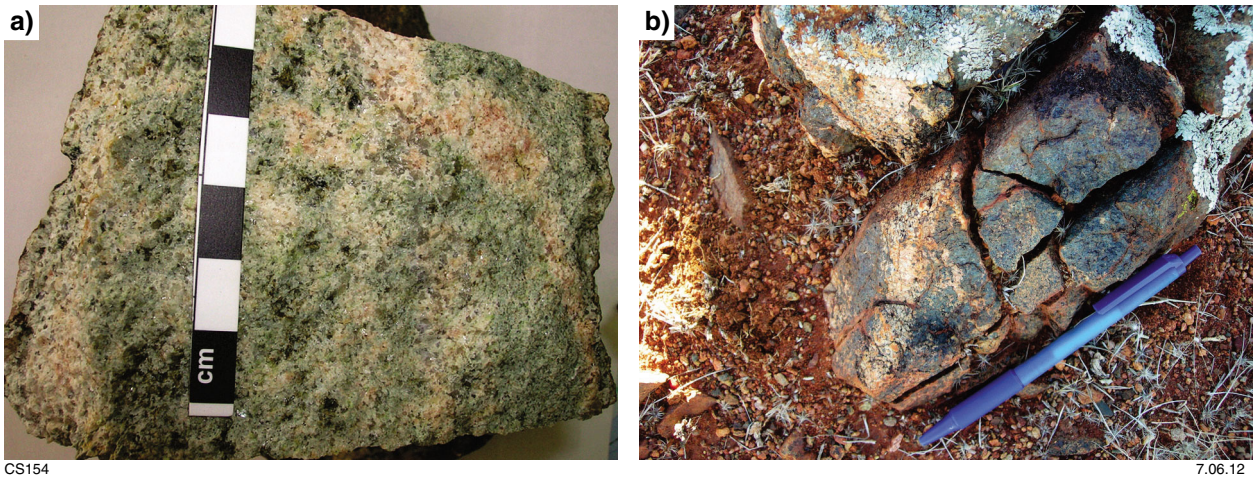

Figure 43. a) Strongly altered metagranite, sampled approximately 7 km north of Tropicana, which yielded an Archean magmatic age (GSWA 182435, see text for details); b) mafic to ultramafic rocks intruded by the same metagranite as in part a), at the same locality.

deepest slimline RC holes, was interpreted to be associated with a southeast-dipping shear zone transecting sericite-altered granite. The primary mineralization was also observed to coincide with a weak chargeability anomaly from a gradient-array induced polarization (IP) survey completed in mid 2003.

These initial results justified deeper drilling to determine the extent of primary mineralization. A program of RC holes was designed in 2004, but access issues forced the drilling contractor to abandon mobilization of the RC drillrig on the way to site. As a result, in late 2004, a program of five diamond holes were drilled instead using a smaller rig, although a planned follow-up program of another five diamond holes was not drilled due to budget cuts. The best result from this diamond program was 14 m @ 2.2 g/t.

The early availability of oriented diamond drillcore proved invaluable in confirming the east to southeast dip of the mineralized zones, and in clarifying the nature of the host-rock sequence, mineralization style, alteration mineralogy, and gold distribution. It also demonstrated that the immediate host for the mineralization was foliated gneiss, not sheared granite, and that the mineralization style contrasted markedly with Archean lode-gold deposits of the Yilgarn Craton. Although at the time it was thought that significantly better results would be required for the mineralization to be economic, these results and the difference in mineralization style justified further work.

In early 2005, AngloGold undertook a review of its global exploration activities. Like many global gold explorers at the time, exploration budgets were under pressure, gold exploration in Australia was considered to be relatively mature, and greener pastures existed overseas. Fortunately, the Australian exploration team motivated an ongoing exploration effort at Tropicana, although a decision was made to divest or exit the rest of the Australian exploration portfolio and retrench exploration personnel. Clearly, the five diamond holes planned for Tropicana in the last half of 2005 represented the last roll of the dice for AngloGold Ashanti exploration in Australia.

Diamond drilling commenced in July 2005. The diamond holes focused on areas where significant aircore results were associated with anomalous magnetic signatures, a slightly different targeting approach from the previous drilling. During this program, and before assay results were received, ten staff were retrenched, including two geologists, leaving a team of three geologists for Tropicana. Results from this diamond drilling program were received in mid August, a mere ten days after the retrenchments. Of the five holes drilled, three intersected significant mineralization, with standout results of 10 m @ 4.1 g/t and 19 m @ 4.7 g/t (including 16 m @ 5.45 g/t).

The higher-grade intercepts from this drilling indicated that Tropicana had the potential to be a significant economic resource. Furthermore, they indicated the potential for the discovery of an entirely new gold belt. On the basis of these results and the indicated potential, an additional budget was sought for wide-spaced RC drilling to define the potential scale of the gold system. The proposal was strongly supported by a new global exploration management team. A program of 10 000 m of RC with holes was approved in early September 2005. Drill testing, at 200 by 100 m centres, initially focused on three lines north of the Tropicana zone, testing the peak of a geophysical (chargeability) anomaly, and following up on both aircore results and a narrow intercept returned in diamond drillhole TPD012 (4 m @ 1.4 g/t Au). These holes intersected only weak alteration, and there were no significant assay results with the exception of one hole drilled down-dip of TPD012 that included 3 m @ 4.24 g/t (TPRC059).

Drilling has since shown that some of these holes intersected the up-dip tip of the Boston Shaker zone mineralization (Fig. 45), with the gradient array anomaly

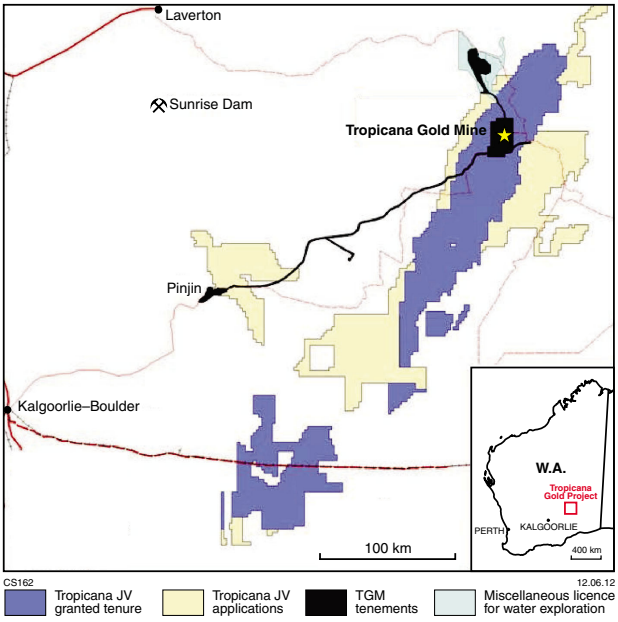

Figure 44. Tropicana Gold Project: location, tenements, and access routes. Figure courtesy of AngloGold Ashanti; abbreviations used: JV = joint venture; TGM = Tropicana Gold Mine.

probably in part due to groundwater. In contrast, drilling on lines south of the Tropicana discovery holes intersected significant mineralization and the focus of subsequent drilling programs moved progressively south. Significant mineralization was intersected, including 9 m @ 6.3 g/t, 23 m @ 2.1 g/t, 44 m @ 1.4 g/t, 24 m @ 2.8 g/t, and 32 m @ 6.6 g/t. By the end of 2005, significant mineralization had been identified in broad-spaced (>200 m spaced centres) RC and diamond drillholes over a strike length of 1 km. Assessment of geochemical datasets from auger sampling and rotary air blast (RAB)/aircore drilling of prospects within a 10 km radius of Tropicana highlighted the strongly depleted character of gold in the saprolitic zone within the weathering profile, indicating that there is little or no supergene enrichment. The data were consistent with the low tenor of geochemical anomalism in WMC soil (peak 31 ppb gold) and AngloGold auger data at Tropicana. Thus, the low-level gold values in first-pass aircore drilling are potentially very significant, especially in wide-spaced drilling. Subsequent refinement of the threshold values for gold and associated pathfinder elements identified an auger soil-geochemical anomaly extending south from Tropicana.

In the first quarter of 2006, aircore drilling on 200 by 200 m centres over this anomaly identified the Havana zone 1.5 km to the south-southeast of the Tropicana zone (Fig. 45), with peak values of 4 m @ 3.3 g/t, 3 m @ 5.1 g/t, and 6 m @ 3.0 g/t. The Havana zone comprises two distinct zones defined by the >1 g/t gold contour. An RC program of about 70 holes at 200 by 100 m centres was planned over both zones of the Havana anomaly, with drilling commencing in May 2006. Access issues meant

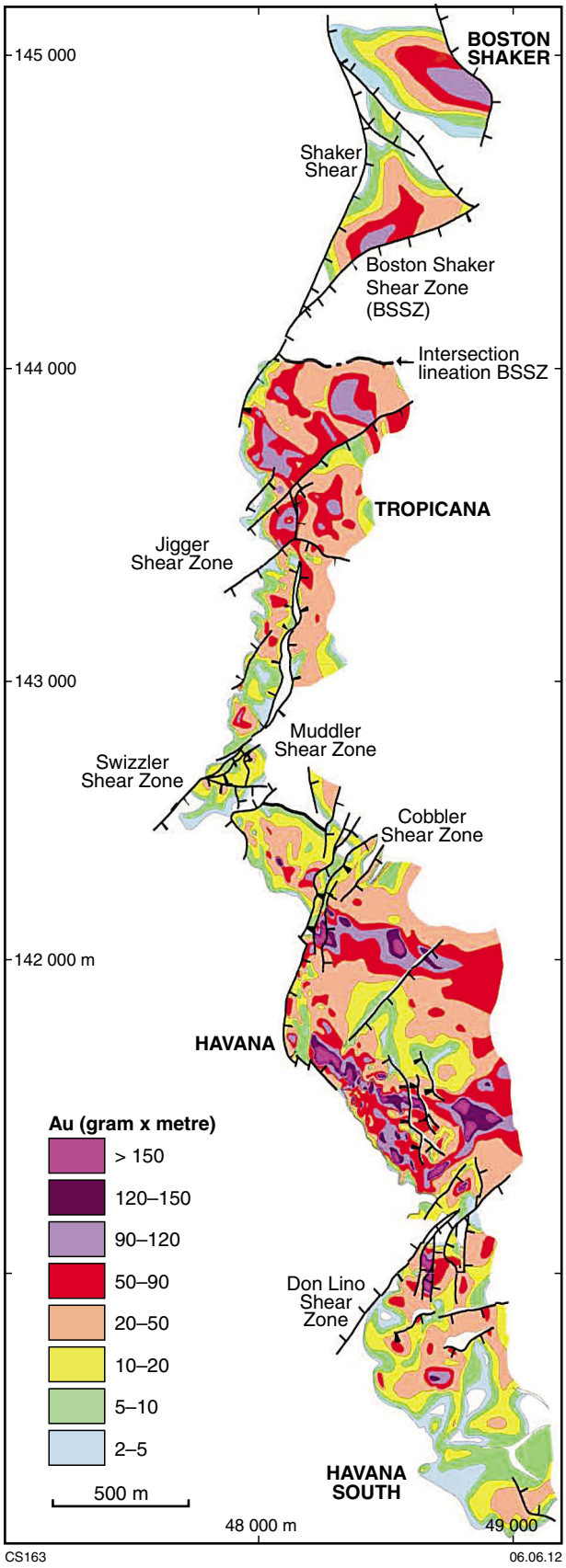

Figure 45. Grams of gold (ppm) times thickness (metres) contours for the Tropicana Deposit, comprising the Boston Shaker, Tropicana, Havana, and Havana South zones. Figure courtesy of AngloGold Ashanti.

that the stronger northern zone was not drilled first. As with the initial RC program at Tropicana, the first RC results received were disappointing, despite the strong biotite–pyrite alteration noted in most of the holes. Later results from the northern zone indicated that Havana had the potential to be both larger and higher grade than Tropicana. Better results from this program included 26 m @ 2.0 g/t, 11 m @ 3.1 g/t, 21 m @ 4.0 g/t, 32 m @ 2.5 g/t, 30 m @ 4.4 g/t, 41 m @ 3.7 g/t, and 18 m @ 6.0 g/t. Furthermore, several sections at Havana showed two mineralized zones, whereas only one zone was identified at Tropicana. The project now moved rapidly into a phase of resource delineation drilling. A project scoping study completed in April 2007 indicated the potential for a viable project and led to the commencement of pre-feasibility studies in mid 2007. Approval to commence the bankable feasibility study (BFS) was obtained in 2009.

During the fourth quarter of 2009, a program of six holes was drilled to test for potential extensions along the northern margin of the Tropicana zone. Detailed 3D modelling of the geology, combined with structural analysis of drillcore, suggested that the mineralization may have been offset along a major bounding shear, now known as the Boston Shaker Shear Zone (Fig. 45). Modelling suggested that blocks north of the shear zone were displaced to the northeast (local grid). Diamond and RC drilling were aimed to test positions north of the Boston Shaker Shear Zone, within the footwall of the structure. Two holes tested the down-dip continuity and tenor of narrow intercepts returned during 2005; both holes returned broad mineralized intercepts, including 14 m @ 3.49 g/t and 15 m @ 1.71 g/t, that warranted further drill testing.

Follow-up drilling during the first quarter of 2010 focused on scoping the strike extent and down-dip continuity of known intercepts, which could form part of an open-pit resource. The northern part of the mineralized zone was intersected in a diamond tail drilled as an extension to a vintage (2005) RC hole. The RC hole had failed at 135 m (planned 150 m) and returned assays below detection limit at the base of the hole. Economic mineralization (12 m @ 4.13 g/t) was intercepted 3 m into the diamond tail.

The Boards of AngloGold Ashanti and Independence approved development of the Tropicana Gold Project in November 2010. Based on Mineral Resource and Ore Reserve estimates at that time, the approved project was predicted to produce 470 000–490 000 ounces of gold per annum in its first three years of production, with an average of 330 000–350 000 oz per annum produced over the life of the operation, estimated to be at least ten years. Cash costs were forecast to be A$580–600/oz in the first three years. The Mineral Resource and Ore Reserve at Tropicana was subsequently updated as at 30 June 2011 to reflect recent increases in the gold price, and changes to the resource model through increased drill density in the Havana South and Boston Shaker zones. The Measured, Indicated, and Inferred Mineral Resource estimate increased slightly to 78.6 Mt grading 2.12 g/t gold, and containing 5.36 Moz of gold (Table 2), whereas the Ore Reserve estimate increased more significantly to 56.4 Mt grading 2.16 g/t gold containing 3.91 Moz of gold (Table 3).

Drilling is continuing in the Swizzler area (between the proposed Tropicana and Havana pits) and at Havana Deeps. A pre-feasibility study is being carried out on open-pit and underground mining options for the Havana Deeps mineralization, and this is anticipated to add to the Project's Mineral Resource. The project remains on schedule to pour its first gold in the December quarter of 2013.

Project geology

The Tropicana Deposit has a known strike length of about 5 km, and defines a northeast-trending mineralized corridor approximately 1.2 km wide (note: all grid references are relative to true north unless stated otherwise; the Tropicana local grid north is rotated 45° east of true north). The deposit comprises four known mineralized zones — from north to south, the Boston Shaker, Tropicana, Havana, and Havana South zones (Fig. 45). The deposit as a whole is located within a more extensive mineralized system, which extends for at least 10 km along strike.

Neither the immediate metamorphic host rocks nor mineralized zones are exposed at the surface due to the presence of widespread Recent to Cretaceous cover sequences (0.5 – 15 m thick), making aeromagnetic data essential for geological interpretation. Recent eolian sands locally manifest in the area as stabilized dunes up to 12 m high, and these overlie an incised sequence of siltstone, sandstone, and pebbly conglomerate units interpreted as Permian and Cretaceous based on historical regional mapping and proprietary paleontology. Contacts between the Phanerozoic rocks and underlying Tropicana host succession are unconformable and typically marked by a layer of quartz-pebble conglomerate. Both sequences have been overprinted by a Cenozoic lateritic weathering profile extending to depths of 40–50 m. Geochemical analyses of auger sampling, RAB, and aircore drilling samples highlights the strongly depleted character of gold in the saprolitic zone of the weathering profile. The observation is consistent with the low tenor of geochemical anomalism in the initial WMC soil (peak 31 ppb Au) and AngloGold Ashanti auger data within the project area (Kendall et al., 2007).

Host rocks

The rocks hosting the Tropicana Deposit can be grouped into seven distinct associations (Table 4). These associations have genetic significance with respect to formative processes and depositional environment, superimposed metamorphism, and timing relative to gold mineralization (Doyle et al., 2009). Six of the associations — garnet gneiss, quartzofeldspathic gneiss, amphibolite, granulite, metasedimentary rocks, and pegmatite — are characterized by mineral assemblages that imply metamorphism at amphibolite- to lower granulite-facies temperatures and pressures (Table 4). When combined, the similar mineralogy, the gradational texturally destructive contacts with the enclosing gneiss, locally discordant relationships, and interleaving of thin pegmatoidal and sub-pegmatoidal bands with finer-grained gneiss, all suggest that the pegmatites are products of partial melts formed during peak metamorphism.

Table 2. Tropicana Gold Project: mineral resource estimates, 31 December 2010 versus 30 June 2011. Table courtesy of AngloGold Ashanti.

		31 December 2010			*30 June 2011*		
Mineral resource	*Classification*	*Tonnes (millions)*	*Grade (g/t Au)*	*Ounces (millions)*	*Tonnes (millions)*	*Grade (g/t Au)*	*Ounces (millions)*
Open pit	Measured	25.8	2.18	1.80	28.4	2.15	1.97
	Indicated	28.8	2.04	1.89	43.9	1.89	2.67
	Inferred	16.6	1.81	0.96	1.0	3.06	0.10
Total — open pit		71.2	2.03	4.65	73.3	2.01	4.73
Underground	Measured	0.00	0.00	0.00	0.00	0.00	0.00
	Indicated	0.00	0.00	0.00	0.00	0.00	0.00
	Inferred	5.3	3.65	0.63	5.3	3.65	0.63
Underground — Havana Deeps		5.3	3.65	0.63	5.3	3.65	0.63
Total Tropicana	Measured	25.8	2.18	1.80	28.4	2.15	1.97
	Indicated	28.8	2.04	1.89	43.9	1.89	2.67
	Inferred	21.9	2.26	1.59	6.3	3.56	0.72
Project Total		**76.5**	**2.15**	**5.28**	**78.6**	**2.12**	**5.36**

Table 3. Tropicana JV: ore reserve estimates, 30 November 2010 versus 30 June 2011. Table courtesy of AngloGold Ashanti.

	30 November 2010			*30 June 2011*		
Classification	*Tonnes (millions)*	*Grade (g/t Au)*	*Ounces (millions)*	*Tonnes (millions)*	*Grade (g/t Au)*	*Ounces (millions)*
Proven	24.1	2.26	1.75	25.8	2.30	1.90
Probable	23.9	2.11	1.62	30.6	2.04	2.01
Total	**47.9**	**2.19**	**3.37**	**56.4**	**2.16**	**3.91**

Table 4. Principal lithofacies associations hosting the Tropicana Deposit (after Doyle et al., 2007).

Lithofacies	*Characteristics*	*Interpretation*
Basalt–dolerite	Crystalline interior; chilled margins (1–2 cm) locally sheared	Gnowangerup–Fraser Dyke Suite (c. 1210 Ma). Post-date mineralization.
Garnet gneiss	Feldspar–amphibolite–garnet–leucoxene(–quartz); equigranular (1–4 mm)	Metamorphosed basaltic to gabbroic volcanic and intrusive units
Quartzofeldspathic gneiss	Feldspar–quartz–biotite–rutile–titanite–apatite–zircon; recrystallized; banded	Metamorphosed felsic volcano-sedimentary and intrusive units
Amphibolite	Leucocratic/mesocratic bands; amphibole–feldspar–biotite–muscovite	Crystalline facies of metamorphosed basaltic to gabbroic intrusive units; some may be metasedimentary (mudstone)
Meta-ferruginous chert	Finely laminated, massive or planar to folded banding; intervals 0.1 – 3 m thick; coarse quartz(–amphibole (grunerite)–biotite–sericite–chlorite–magnetite–garnet) bands; semi-massive pyrite–pyrrhotite replacement	Grunerite-bearing units are metamorphosed iron-rich siliceous sediments; sericite/chlorite-rich divisions interpreted as former turbidites; pre-metamorphic suspension sedimentation in a deep and/or quiet water environment
Pegmatite	Intervals 1–30 cm; feldspar–quartz–biotite(–garnet–amphibole); coarse grained (5–10 mm)	Anatectic segregations formed during amphibolite- to granulite-facies metamorphism
Mafic granulite	Clinopyroxene–orthopyroxene–hornblende(–garnet); patchy chalcopyrite–pyrrhotite–magnetite	Lower-granulite facies metamorphosed medium- to coarse-grained ?dolerite

The metamorphic rock associations and mineralized zones are cut by younger, syn- to post-peak metamorphic mafic intrusions. The dolerite intrusions display the effects of greenschist-facies metamorphism and range from nonfoliated to schistose. Mafic dykes with crystalline interiors and thin (1–2 cm) chilled or weakly sheared margins are ascribed to the c. 1210 Ma Gnowangerup–Fraser Dyke Suite, providing a minimum age for mineralization.

Stratigraphic architecture

The immediate host rocks to the mineral deposit have undergone polyphase deformation resulting in a complex arrangement of lithofacies and significant thickening of the package. Nevertheless, the distribution of lithofacies associations remains predictable at the deposit scale, and serves as a useful guide for planning drilling and proposed mining operations. The garnet gneiss facies association dominates the immediate hangingwall of the mineralized zones, forming a structurally thickened stratigraphic interval up to 200 m thick at Havana (Figs 46 and 47).

Chert and former ferruginous chert units (metasedimentary facies association), are interleaved with the garnet gneiss, and locally occur at the base of the stratigraphic horizon, providing a useful marker and suggesting that the Tropicana and Havana mineralized zones occupy a similar stratigraphic position. Intervals of amphibolite, granulite, and quartzofeldspathic gneiss form subordinate, laterally discontinuous to continuous intervals within the hangingwall sequence.

The mineralized zones are principally hosted within rocks of the quartzofeldspathic gneiss and pegmatite facies associations. This stratigraphic horizon (referred to herein as the 'favourable horizon') thickens and thins along the strike length of the deposit. The favourable horizon is underlain by a mixed stratigraphic package comprising rocks of the quartzofeldspathic gneiss, garnet gneiss, granulite, and amphibolite associations. The top of the footwall package is marked by the first appearance of garnet gneiss, amphibolite, or granulite. Gold mineralization, generally of low grade, occurs in both the footwall and hangingwall stratigraphic packages as thin (typically <3 m) lenses within rocks of the metasedimentary facies, garnet gneiss, or quartzofeldspathic gneiss associations. In some drillholes, thin intercepts up to 10 g/t gold have been reported; however, the continuity of these zones is less than the current drillhole spacing (typically 25–50 m).

Mineral deposit architecture

Together, the Boston Shaker, Tropicana, Havana, and Havana South zones define a northeast-trending mineralized corridor approximately 1.2 km wide by 5 km long that has been tested to a vertical depth of up to 700 m (Fig. 45). Mineral resources remain open down-dip for both the Tropicana and Havana zones. Although the Boston Shaker and Havana South zones are truncated by large-scale shears along their northern and southern margins, respectively, 3D reconstructions using aircore, RC, and mapping data suggests that the favourable stratigraphic package may be replicated outside the area of intensive drill testing.

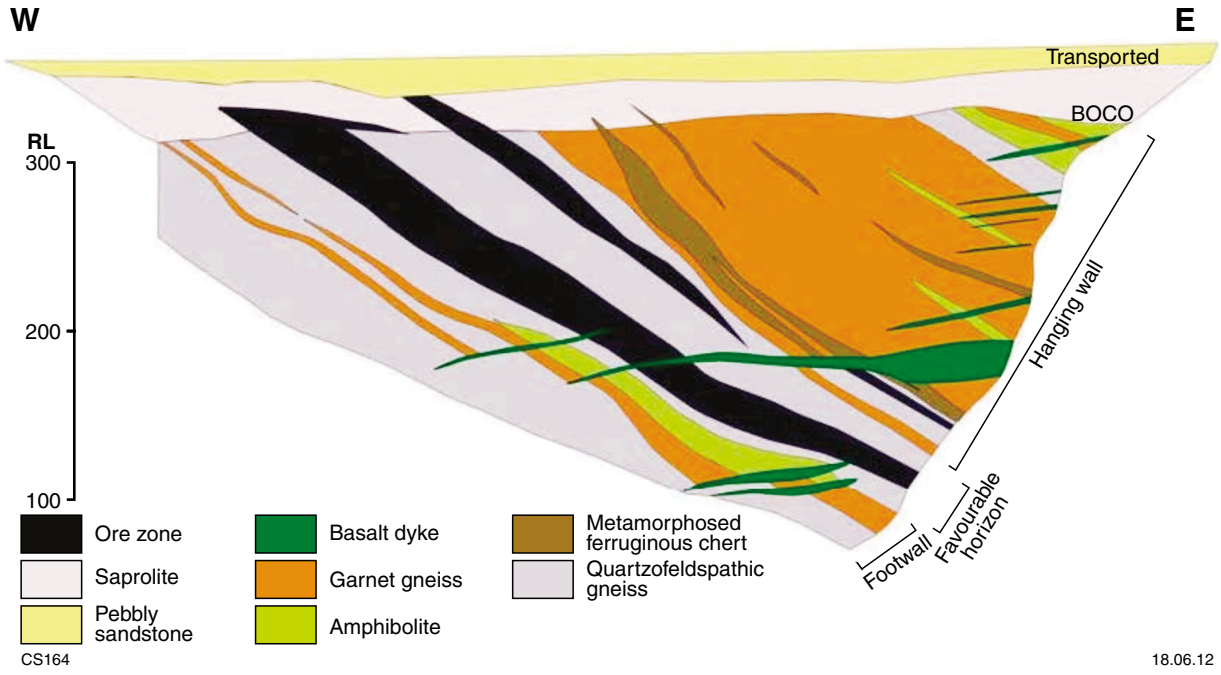

Figure 46. Representative stratigraphic section, Havana zone (local grid 141650N). Figure courtesy of AngloGold Ashanti.

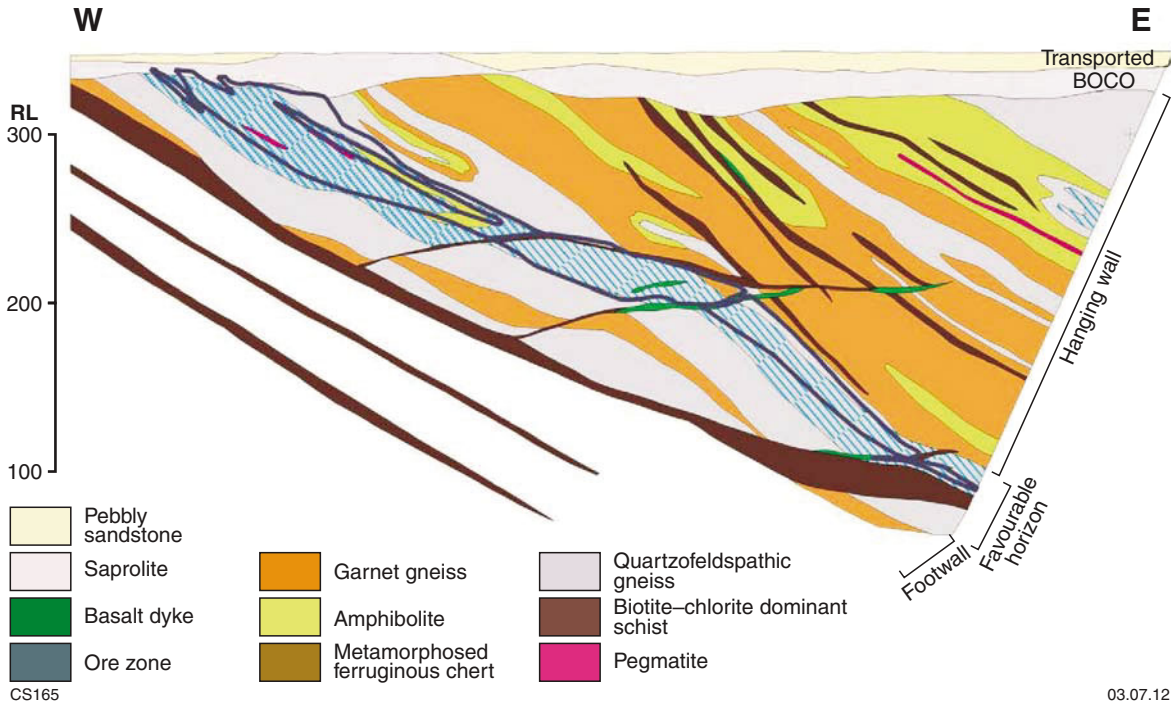

Figure 47. Representative stratigraphic section, Tropicana zone (local grid 143750N). Figure courtesy of AngloGold Ashanti.

In the Boston Shaker zone, mineralization zones dip 15–35° southeast and cut the enclosing garnet gneiss and quartzofeldspathic gneiss package at a low angle. Interpretations based on RC drilling suggest that mineralization may be hosted by discrete faults with damage zones that pinch and swell both down dip and along strike. In contrast, the Tropicana, Havana, and Havana South zones are grossly 'stratiform' within the enclosing gneissic package at the scale of the resource model. Models of the mineralized envelope (at ≥0.3 g/t gold) define a wavy, asymmetric foliation that is broadly subparallel to the dominantly east- to southeast-dipping gneissic banding and local stratigraphic divisions. This foliation is deflected upon approaching discrete high-strain sericite–biotite–chlorite(–graphite) shears that are anomalously high in gold.

Four distinct structural domains can be identified in the Tropicana Deposit: Boston Shaker, Tropicana, Havana, and Havana South (Fig. 45). The northern margin of the Tropicana domain is defined by the east-northeasterly striking, southerly dipping Boston Shaker Shear Zone, along which the Boston Shaker mineralization zone has been displaced by approximately 270 m to the northeast (local grid). The Tropicana and Havana zones are separated by northeasterly to easterly striking, variably dipping, structural discontinuities defined by the Muddler, Swizzler, and Cobbler Shear Zones. The southern portion of the Tropicana mineralization zone has been displaced approximately 300 m to the west between two major shear zones: the Swizzler Shear Zone to the north, and the Muddler Shear Zone to the south. Bounding shear zones consist of a strong S- to LS-fabric defined by quartz and feldspar grains and a biotite grain-shape fabric.

The Tropicana zone comprises one main ore zone and subordinate, thin (3–5 m), discontinuous mineralized lenses that typically return intercepts <0.5 g/t gold, hosted within the garnet gneiss dominated hangingwall package. The main ore zone is 2–50 m thick, with an average thickness of 30 m over a strike length of approximately 1.5 km, dipping between 20–45° to the southeast (Fig. 48).

The Havana zone comprises a lower, laterally continuous, higher-grade lode that is 2–50 m thick, with an average thickness of 30 m over a strike length of approximately 2 km. It also dips between 20–45° east-southeast, and is overlain, in the central and southern parts of the proposed pit, by stacked, typically lower-grade, thinner (5–25 m) ore zones dominantly hosted by quartzofeldspathic gneiss (Fig. 49). Although Havana South and Boston Shaker display a similar arrangement of stacked lodes, the lodes tend to be thinner and more discontinuous, in part due to displacement on post-mineralization shears.

In detail, single lodes comprise multiple, stacked, higher-grade (about 3 g/t gold) lenses within a lower grade (about 0.3 g/t gold) envelope. Single high-grade lenses and their medium-grade halos locally converge to form thicker, composite mineralized zones. High-grade lenses in the Havana structural domain dip between the south and east, and intersect in lines plunging to the south-southeast. This contrasts with the east- to southeast-dipping high-grade lodes in the Tropicana structural domain, which intersect

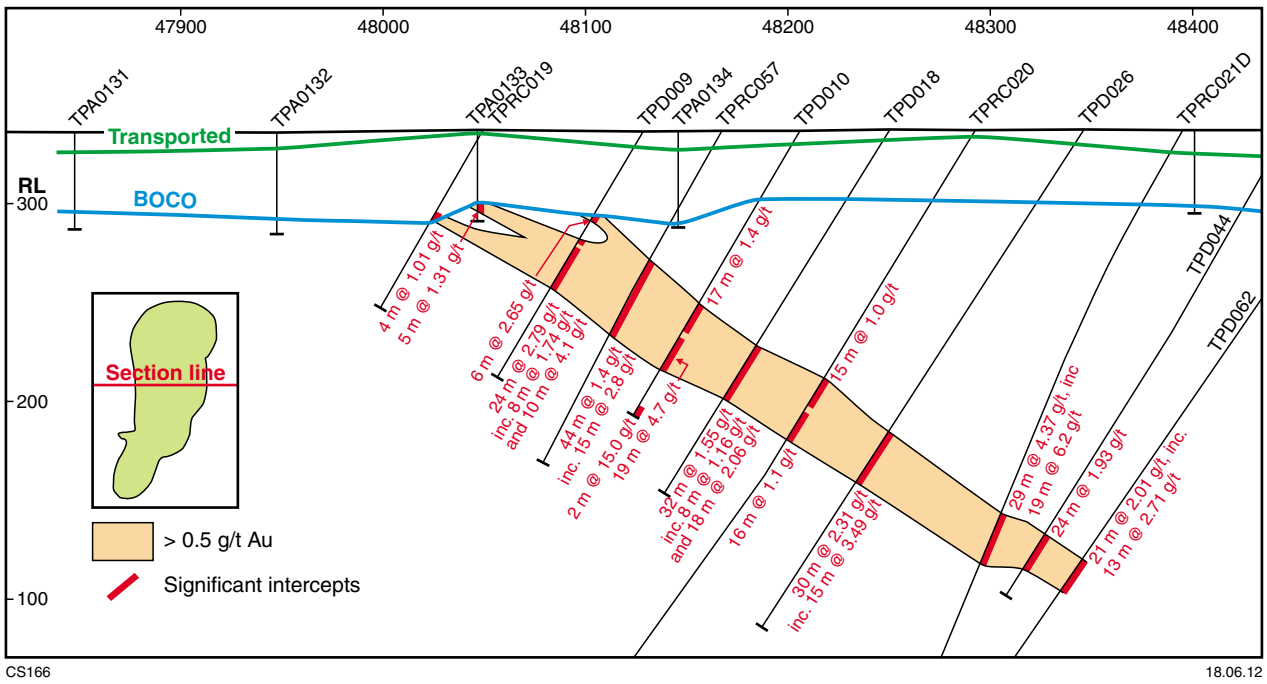

Figure 48. Simplified cross section, Tropicana zone (local grid 143500N). Figure courtesy of AngloGold Ashanti.

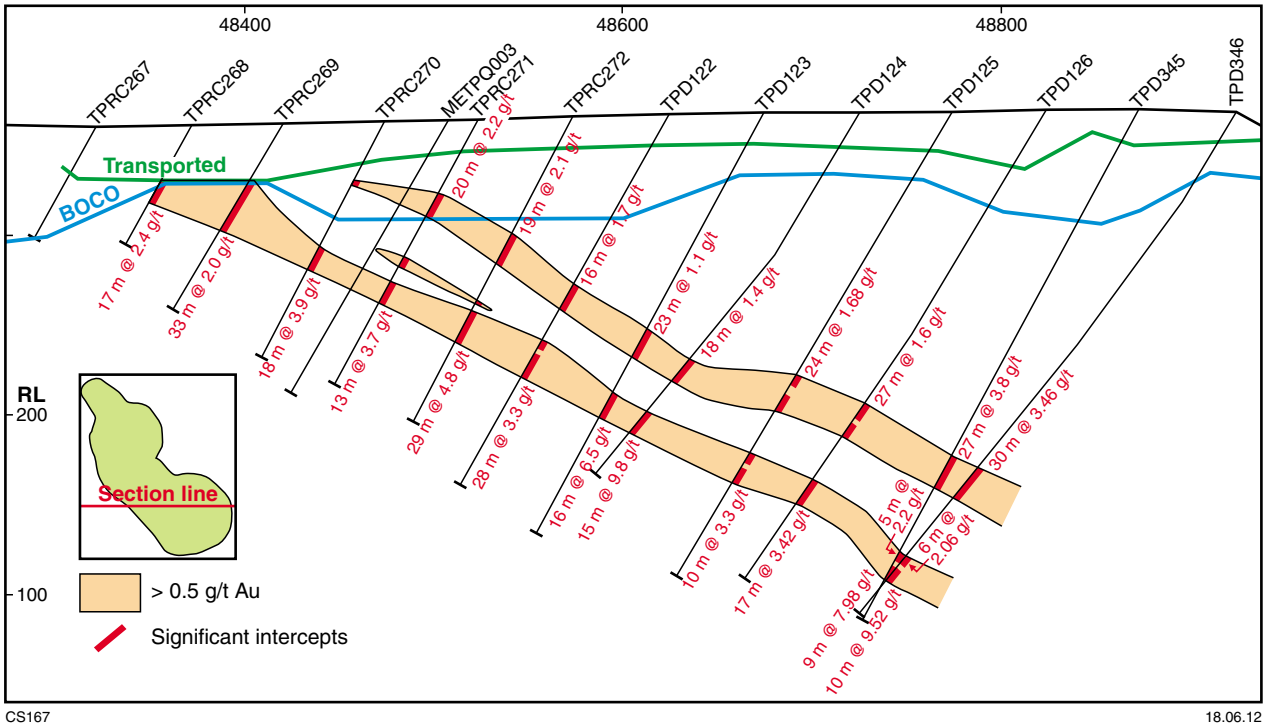

Figure 49. Simplified cross section, Havana zone (local grid 141550N). Figure courtesy of AngloGold Ashanti.

a generally east-plunging line. Higher-grade lodes in the Havana South and Boston Shaker structural domains are laterally discontinuous and many are displaced on shears, making interpretation of the RC drillholes difficult.

In sections parallel to the plunge direction, higher-grade (about 3 g/t gold) lodes are enveloped by lower-grade shells and are oriented at a slightly steeper angle than the modelled approximately 0.3 g/t gold envelope (Fig. 50). In sections orthogonal to the plunge direction, approximately 3 g/t gold lodes comprise steeper bounding domains and flatter linking segments, the intersection of which defines the principal lineation (Fig. 51). The resultant geometry is interpreted as a linked shear system that manifests in drillcore as discontinuous biotite–sericite–pyrite shears developed on the millimetre to centimetre scale, and are characterized by asymmetric S–C fabrics and sigma porphyroclasts.

Mineralization

Two mineralization styles are identifiable in the Tropicana Deposit, based on sulfide mineral occurrence and host rock type. They are:

- Biotite–sericite–pyrite-dominant disseminations, bands, and crackle-mosaic breccia units and veins, within altered quartzofeldspathic gneiss and rare garnet gneiss associations.
- Patchy and vein style pyrite–pyrrhotite incompletely replacing shear zones, cataclasite, and thin intervals of the metasedimentary association, interleaved with, and at the base of, the hangingwall garnet gneiss association.

The second mineralization style has not returned economic gold concentrations in drilling to date, and grades within single intercepts are typically ≤1 g/t gold. As such, the following description is limited to discussion of the biotite–sericite–pyrite-dominant mineralization style.

Mineralization hosted by the quartzofeldspathic gneiss association was strongly influenced by the character of the precursor metamorphic assemblages, at scales ranging from single grains and crystal clusters (millimetre to centimetre scale) to the preferential concentration of gold in rheologically and/or chemically favourable K-feldspar rich facies of the quartzofeldspathic gneiss association (deposit scale).

At a fine scale, biotite–pyrite has selectively replaced former mafic-dominated gneissic bands, and sericite–calcite has selectively altered plagioclase-rich bands. In leucocratic domains and bands, pyrite and secondary biotite occur as grain-boundary controlled disseminations replacing primary metamorphic biotite and former amphibole. These textures are most common in domains with lower gold grades. In domains with higher gold grades, stylolitic dissolution fabrics, crackle-breccia textures, shears, fractures, and veins with biotite–pyrite(–sericite) fills are more abundant.

At the deposit scale, sectional interpretation combined with statistical evaluation suggest that, for any given grade threshold, K-feldspar rich gneiss and pegmatite facies contain a higher proportion of gold than other facies within the quartzofeldspathic gneiss association (Fig. 52). Sulfides within the ore zones are dominated by pyrite (2–8%; grain size <0.2 mm), with accessory pyrrhotite, chalcopyrite, electrum, and telluride minerals, and trace minerals including, but not limited to, sphalerite, galena, and bornite. Free gold occurs mostly as fine-grained (typically 10–30 μm) inclusions within pyrite, and less commonly along biotite–sericite fractures cutting silicate minerals. Visible gold has been observed in a single drillcore from the Boston Shaker zone, and mineralized quartz veins are notably absent. The pyritic ores are enveloped by a disseminated pyrrhotite(–pyrite) halo that is locally more strongly developed in the hangingwall, particularly at Havana. Within the mineralized zone, relic pyrrhotite inclusions in pyrite suggest increasing, but variable, oxidation states.

Mineralized zones are enclosed within a subconcordant alteration envelope. The alteration envelope exhibits a mineralogical zonation, with central biotite ≥ sericite >> calcite(–siderite) zones passing outward through sericite > biotite > chlorite(–calcite) zones, into sericite–chlorite(–biotite–calcite) zones at the margins (Fig. 53). Outside the hydrothermal alteration envelope, prograde metamorphic minerals have altered to various assemblages of chlorite, sericite, calcite, epidote, and hematite. Reactivation of synmineralization shears was accompanied by local intensive sericite and/or chlorite alteration that has overprinted synmineralization alteration and assemblages. The overprint is texturally destructive, and appears to have been associated with local mobilization of gold, resulting in lower gold grades proximal to the shear. When combined with the sulfide percentage, the ratios of biotite, sericite, and chlorite have proven a reliable indicator of potential grade outcomes. The index (referred to herein as the ‘Tropicana Index’) has proved to be an effective tool in the planning and prioritization of resource delineation drilling prior to the receipt of assay results.

Strong to moderate biotite–sericite >> calcite alteration, spatially and temporally related to gold mineralization, is ascribed to a hydrothermal alteration event that post-dates the metamorphic thermal maximum (Doyle et al., 2007). Evidence for this event includes, but is not limited to:

- Mineralization-associated alteration assemblages that overprint high-grade metamorphic minerals
- Biotite–pyrite veins and fracture fills that crosscut and displace gneissic banding and transposed folds
- Mineralized veins and crackle breccia domains that overprint pegmatite divisions, interpreted as anatectic segregations formed during peak metamorphism (Doyle et al., 2008)

Gold mineralization is temporally related to shear planes (thrusts) post-dating the main gneissic fabric developed during peak (granulite-facies) metamorphism. Variation in the orientation of bounding and internal shears is attributed to the influence of lithological layering and pre-existing polyphase folding on these shears during mineralization. Fluids are interpreted to have passed

outward from controlling thrusts into a rheologically and chemically receptive K-feldspar rich gneissic package. Permeability created during brittle fragmentation was accompanied by synchronous partitioning of strain into pervasively biotite–sericite–pyrite-altered dissolution- and shear-planes that envelop more competent lithons. Sulfide and gold mineralization formed from higher temperature silica-undersaturated fluids buffered by the wall rock at variable oxidation. In combination, the alteration assemblages, the occurrence of chalcopyrite, and the trace element concentrations in pyrite suggest fluid temperatures exceeding 350˚C.

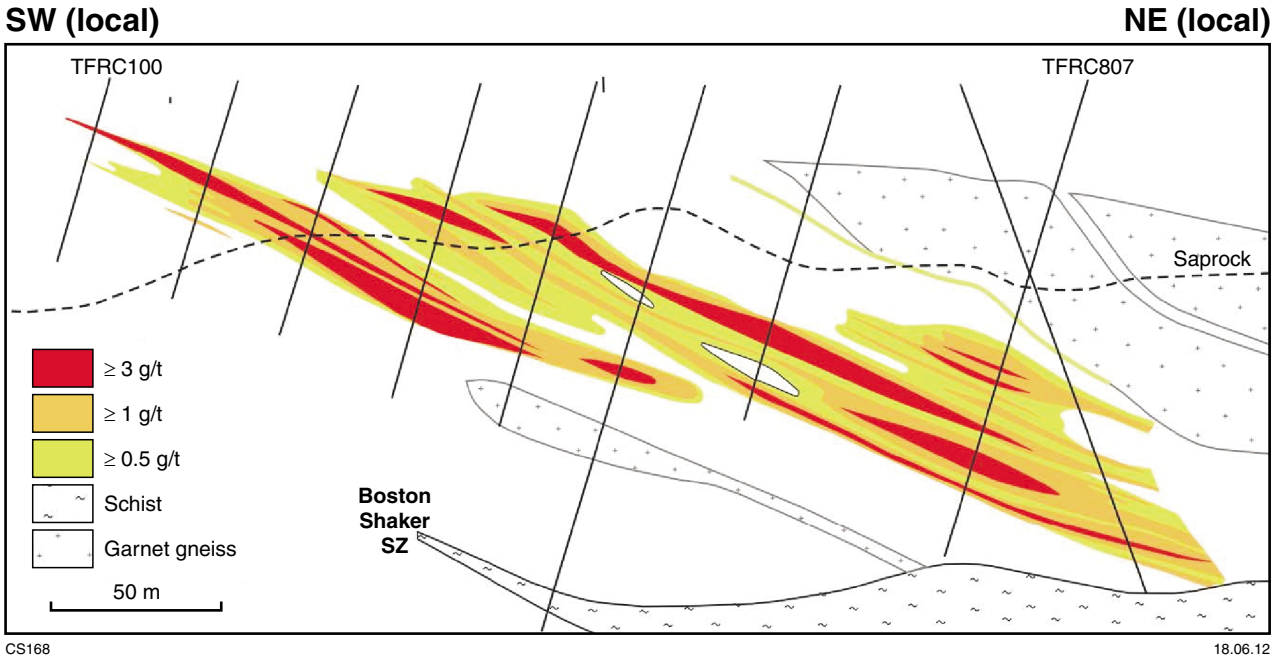

Figure 50. Cross section of the Tropicana zone parallel to plunge direction, looking north. Figure courtesy of AngloGold Ashanti.

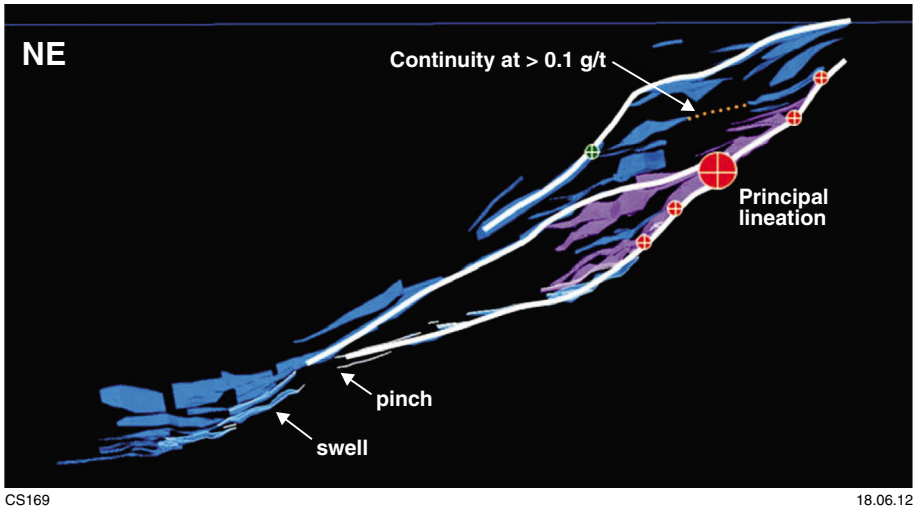

Figure 51. Schematic section of the Havana zone orthogonal to plunge direction, looking southeast through a 3D Vulcan model. Purple triangulation delineates the most continuous ≥3 g/t gold lode. Figure courtesy of AngloGold Ashanti.

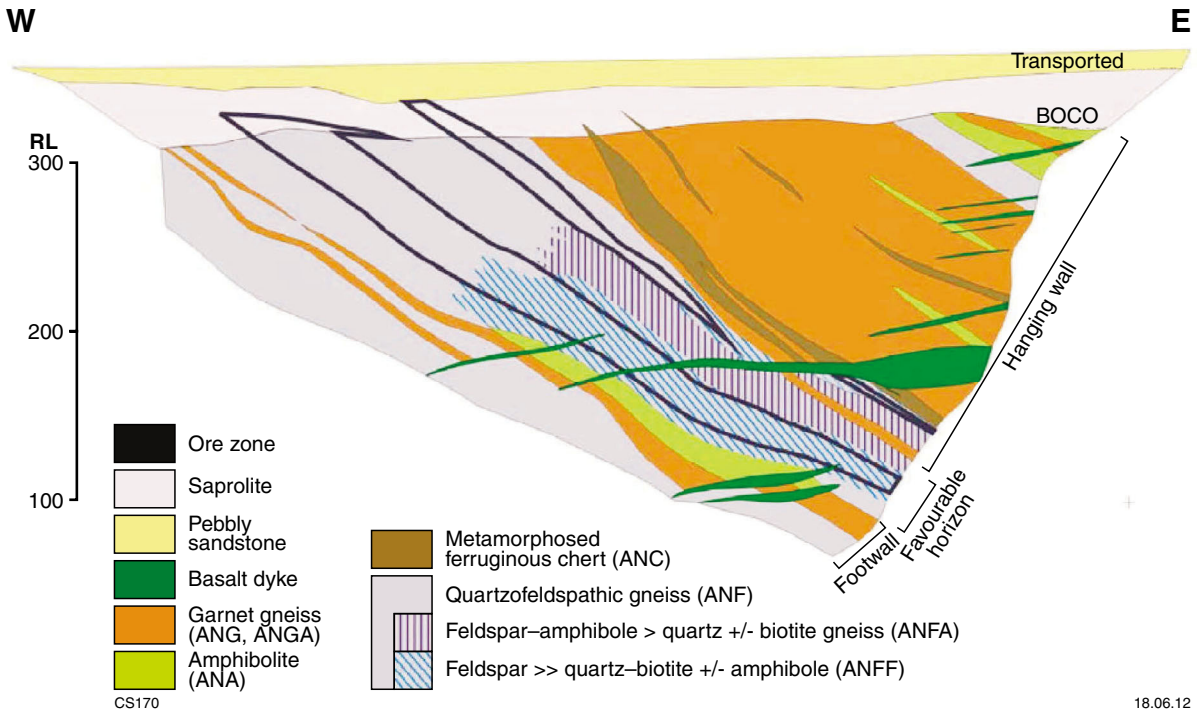

Figure 52. Geological cross section of the Havana zone (local grid 141650N), illustrating the principal facies associations and mineralized zones. Figure courtesy of AngloGold Ashanti.

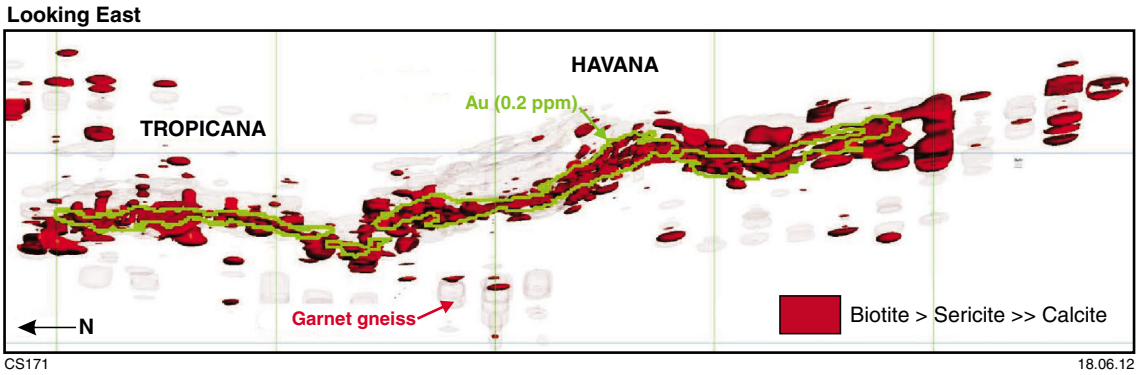

Figure 53. Leapfrog 3D model of biotite-dominant alteration and gold (looking east; local grid), Tropicana and Havana zones. Figure courtesy of AngloGold Ashanti.

Day 1

Stop 1. Havana South

This stop (MGA 649300E 6760100N) is located within an active exploration and mining area. Access is via drilling tracks and requires an escort by staff from the Tropicana Gold Project.

Use of hammers and removal of samples at this locality is strictly prohibited, as the exposures are located within the bounds of a registered archeological site.

Rubbly outcrop on a low ridgeline southeast of the Havana South orebody marks the position of a major shear zone (Crouching Tiger Shear Zone) that can be traced for several kilometres in RC and diamond drilling. Domains of sericite and chlorite schist 5–10 m wide locally contain lithons of lower-strain rock showing greater preservation of earlier deformation fabrics. Within schistose domains, the foliation dips moderately to the east-southeast, with an S–C intersection lineation plunging approximately 30° towards 110–130. S–C fabric relationships are contradictory, as both dextral and sinistral kinematics are identifiable, although dextral kinematics are more abundant.

Lithons locally show early tight folds that are refolded by a second generation of tight folds with similar fold axes, producing a Type 3 fold interference pattern. The main schistosity is overprinted by crenulation and kink bands with reverse kinematics.

Stop 2. Hat Trick Hill

The outcrop in the Hat Trick area is sufficiently good to allow the proposal of a detailed structural history, with some metamorphic constraints. At least seven deformation events have been identified in these rocks. D_1 produced centimetre-scale, isoclinal to open, asymmetric folds in a north–south orientation within metamorphosed BIF. Peak M_1 metamorphism at granulite facies was associated with D_1, and was followed by post-peak intrusion of monzonite or granite. D_2 folds are north–south orientated, open, and occur at the metre-scale. The onset of amphibolite-facies retrogression (M_2) may have begun during D_2. Northeast-trending, tight to open folds represent D_3, which refolded the orientation of L_1. D_4 produced east–west oriented, open, metre-scale folds that refold north–south F_2 folds, and form dome-and-basin interference patterns. Greenschist-facies retrogression (M_3) most likely began during D_4 and affected all rock types. Finally, three stages of shearing have been identified, which affect all previous folding events.

Locality 2.1. Hat Trick Hill

This locality (at MGA 654578E 6765600N) is accessible from the Tropicana exploration camp via active exploration tracks (4WD only) within the mining leases of the Tropicana Gold Project.

Use of hammers and removal of samples at this locality is strictly prohibited, as the exposures are located within the bounds of a registered archeological site.

A prominent hill 2.6 km northeast of the Tropicana Deposit provides a rare opportunity to view Archean basement rocks within this sand-covered region. Hat Trick Hill lies at the southern end of a 3 km long ridgeline that has been mapped in detail (Fox, 2010; Fig. 54). This section of the guide summarizes the deformation history described by Fox (2010).

The geology of the Hat Trick Hill area comprises chert, BIF, amphibolite, granulite, and felsic gneiss. Gently dipping BIF units cap many of the hills, and often coincide with hinge regions of open, upright antiforms and synforms. Banding within the BIF and chert may be parallel to original stratification, but has been strongly modified by metamorphism, isoclinal folding, and pegmatite intrusion. Evidence of early deformation within the BIF is recorded by asymmetrical, open to isoclinal folds (F_1). In some locations, F_1 folds are accompanied by an axial planar cleavage (S_1) that is subparallel to banding (bedding; S_0) along the limbs, and displays refraction between cherty and carbonate-rich bands in the hinges. F_1 folds plunge to the north and south (average 30°), and the hinge surfaces dip approximately 45° to the east. A strong mineral elongation lineation (L_1) is developed on the banding plane parallel to the F_1 fold axes. In BIF, L_1 is defined by quartz(–feldspar) grains that define a strong rodding, whereas felsic gneiss divisions display a weakly developed mineral-elongation lineation. The change in the plunge orientation of L_1 provides important constraints on the superimposed folding that resulted in both Type 1 and 2 fold-interference patterns.

Type 1 dome-and-basin fold interference patterns at the metre to decametre scale are well represented in the Hat Trick Hill area. At MGA 654578E 6765600N, F_1 recumbent isoclinal folds are refolded about a doubly plunging dome that is slightly asymmetrical with a steeper east-dipping limb. Structural measurements and field observations demonstrate that the domes have a dominant north–south elongation. Assessing the timing relations at this locality is problematic; however, mapping across the ridgeline suggests that north–south folds can be ascribed to F_2, whereas east–west folds are attributable to F_4. The plunge orientation of L_1 systematically changes from south to north. Discontinuous shears, traceable for 10 m or less, display small-scale (10–20 cm) dextral offsets of banding within the BIF.

Locality 2.2. Hat Trick ridge

Continue northeast from Locality 2.1 along exploration gridlines within the Tropicana Gold Project mining leases, to a ridge (MGA 655400E 6766400N).

The focal point for this locality are outcrop patterns that are reminiscent of Type 2 fold-interference patterns between F_1 and F_2 folds (Fig. 55), but which, on the basis of detailed mapping, are interpreted to record stacking of BIF slices on reverse faults. The western margin of the BIF units is marked by a high density of shears with S–C fabric relations that record dominant reverse kinematics. Banding (bedding) in the BIF exposures is typically subparallel to banding in adjacent granitic gneiss exposures, although there is local discontinuity along

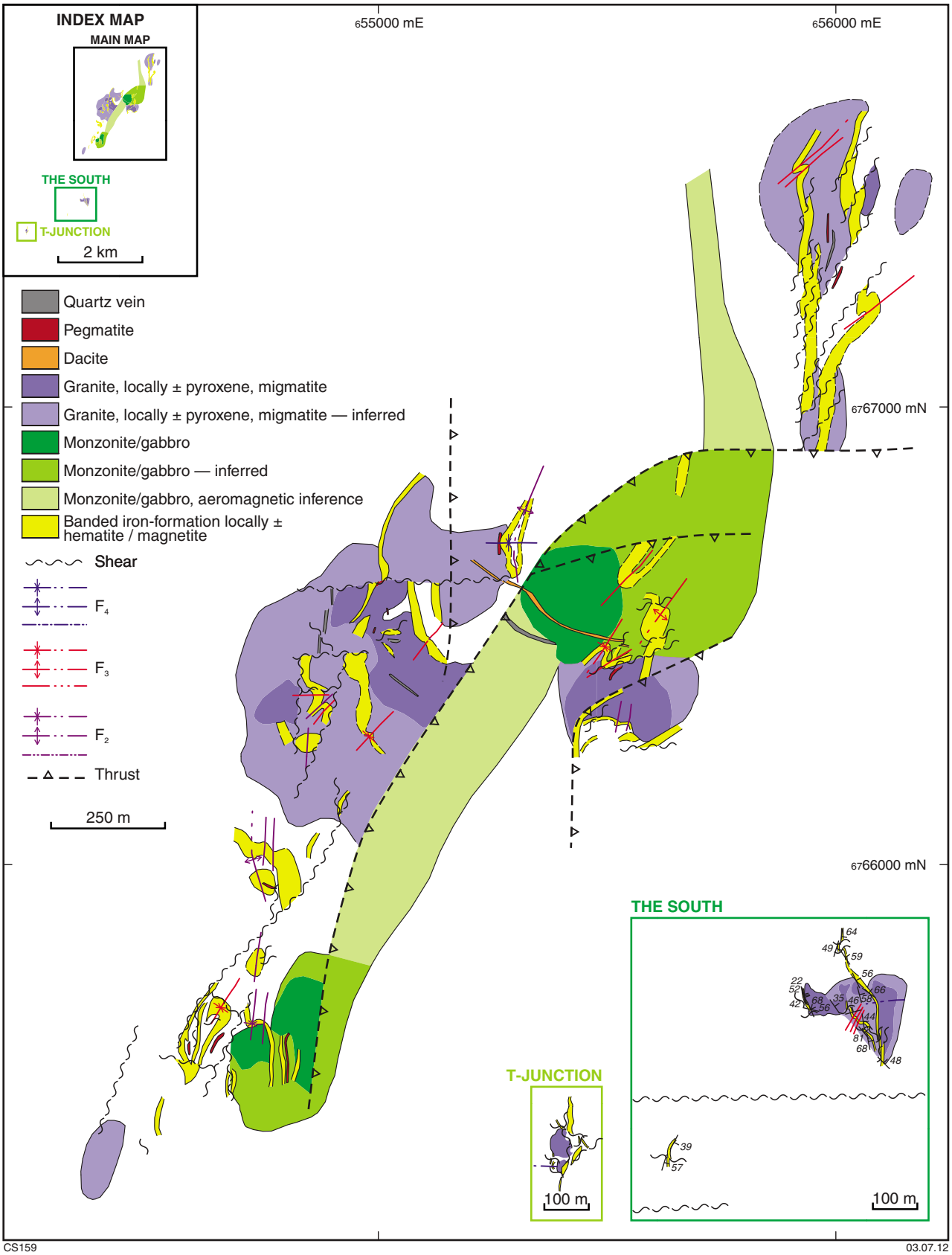

Figure 54. Interpretive geological map of the Hat Trick Hill area (after Fox, 2010).

sheared contacts. L_1 dominantly plunges to the southeast, and small-scale F_1 folds display a well-developed axial planar cleavage. F_2 folds and a weak stretching lineation defined by aligned magnetite plunge gently to the south. Combined, the minor fold vergence and reverse fault separation of the BIF units are inconsistent with refolding of a large-scale F_1 fold around northeast-trending F_2 folds.

Locality 2.3. Hat Trick ridge

This locality (MGA 655900E 6766900N) is accessible from the Tropicana exploration camp via active exploration tracks within the Tropicana Gold Project mining leases.

Lying at the northern end of Hat Trick ridge is an outcrop area of high structural complexity. Strings of BIF are interleaved with schist that locally contains lithons of granitic gneiss. Banding (bedding) within the BIF dips both to the west and to the east, marking the position of a northeast-oriented fold with a hinge surface dipping approximately 50° towards 110. Folds are ascribed to F_3 on the basis of rotation of L_1 around the northeast-trending axes. Gentle, upright F_4 folds are evident on the metre scale, and cause widespread warping of the outcrop pattern at this locality and throughout the Hat Trick area. In contrast, folds ascribed to F_3 are largely restricted to the northern parts of the ridge.

Day 2

Directions to Stop 3:

From the intersection of the Tropicana Camp Road and Rason Lake Road, turn left (north). Drive 14.8 km to rubbly hills located on the left-hand side of the road (at MGA 658154E 6774537N).

Stop 3. Mafic to ultramafic rocks — Archean greenstone?

The purpose of this stop is to examine mafic to ultramafic metamorphosed rocks that form low rises of rubbly outcrop. These rocks occur as pods within interpreted northwest-trending boudins surrounded by strongly sheared metagranite, which has intruded the mafic to ultramafic rocks. The metagranite contains coarse-grained quartz ribbons and recrystallized feldspar aggregates in a fine-grained, granular groundmass. The boudins are up to 100 m long, and contain a strong stretching lineation, plunging 5° towards 131 on the foliation wrapping around the mafic blocks. The mafic to ultramafic rocks are variably magnetic; magnetic susceptibility readings range from 0–300 x 10^{-5} SI units.

The mafic rocks are medium-grained metagabbros with localized layering of variable composition, ranging from pyroxene- or amphibole-rich with garnet to more felsic. A sample of metagabbro (GSWA 184379) from this locality consists of about 40% pyroxene, 40% plagioclase, 10% garnet, with epidote, chlorite, hornblende and actinolitic amphibole, minor quartz, titanite, and opaque oxide grains. The pyroxenes (dominantly clinopyroxene and lesser orthopyroxene) are partly overgrown and rimmed by amphibole and chlorite, although there is also relict hornblende overgrown by pyroxene. The later amphiboles are acicular and range from pleochroic green, to blue-green, to blue, with the latter indicative of a quite sodic composition. Large cracks in the garnets are filled with chlorite and locally, epidote. The plagioclase is overgrown with epidote and zoisite, and a small calcite vein is present. This rock may have been metamorphosed up to granulite facies, and subsequently retrogressed to amphibolite–greenschist facies.

A second sample of metagabbro (GSWA 184380) is composed mostly of plagioclase and pyroxene (mostly clinopyroxene but possibly minor orthopyroxene). The pyroxene is overgrown by blue-green, mostly acicular amphibole, although minor relict hornblende is also present. The plagioclase is overgrown by epidote and minor zoisite, and there is also minor titanite, opaque oxide grains, quartz, apatite, and possibly a little rutile. A foliation is defined by amphibole and epidote. This metagabbro may have been metamorphosed up to granulite facies (based on the presence of ?orthopyroxene), but is now indicative of amphibolite facies.

A metamafic rock (GSWA 184381) is dominated by pyroxene (both orthopyroxene and clinopyroxene) overgrown by hornblende and acicular blue-green amphibole. There is also some plagioclase in the sample, although it is almost completely overgrown by small grains of epidote. Opaque oxide is rimmed by titanite, and there is very minor (secondary?) quartz, and some largish grains of probable apatite. This sample is more mafic than both GSWA 184379 and 184380, also from this locality, but does not necessarily represent an ultramafic protolith. The sample is now an amphibolite.

Based on the field relationships evident just north of the Tropicana Deposit, where Archean metagranite (GSWA 182435) intrudes mafic and ultramafic rocks (Fig. 43a,b), the rocks at this locality are also likely to be Archean greenstones. Alternatively, they could represent the mafic components of Paleoproterozoic, co-magmatic, mingled and mixed felsic and mafic intrusions, which occur elsewhere in the Tropicana region (see below). However, these co-magmatic rocks do not contain an ultramafic component, unlike the mafic rocks at this locality, and there is no indication of mingling textures. The mafic and ultramafic rocks at this locality may be part of the same (greenstone) sequence as that at Hat Trick Hill (Fig. 40), and potentially form part of the Northern Foreland, or part of an Archean fragment rifted from the Yilgarn Craton (Fig. 25).

Directions to Stop 4:

Continue on the Rason Lake Road for 19.2 km, then turn sharp right onto a track towards Bobbie Point. Drive for 5.7 km, bear right, then drive 2 km to Bobbie Point on the northern side of the track (MGA 662415E 6792732N).

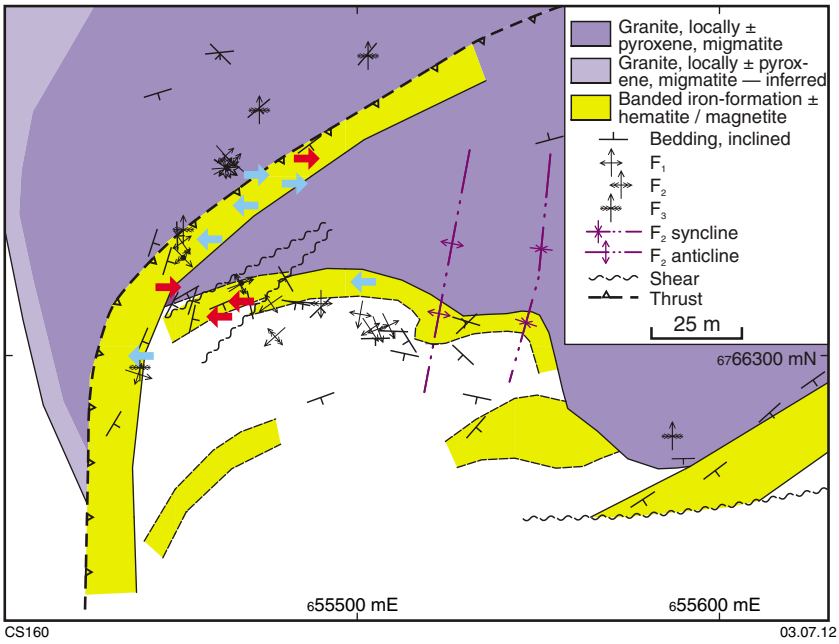

Figure 55. Detailed geological map of the Hat Trick Hill area, showing banded iron-formation (in yellow), granitic gneiss (in purple), and the main F_2 fold axes. Vergence is inconsistent, with red arrows denoting plunges to the north and blue arrows denoting plunges to the south (after Fox, 2010).

Stop 4. Bobbie Point Metasyenogranite

The Bobbie Point Metasyenogranite is well exposed over a series of rocky ridges in this area. The intrusion is also well defined in gravity data as a distinct, ellipsoidal, deep low, bound to the northwest by the Cundeelee Fault (Figs 40 and 41). The metasyenogranite has a weak to moderate, northeasterly trending foliation, but contains localized high-strain or mylonite zones. The Bobbie Point Metasyenogranite is also cut by dextral shear zones (Plate 2), and abundant thin quartz veins (Fig. 56a).

The metasyenogranite is pink, medium-grained, varies from seriate textured to equigranular, and contains rounded equant quartz phenocrysts and subhedral K-feldspars in a fine- to medium-grained groundmass. Clots of fine-grained mafic minerals are up to 12 mm in size (Fig. 56b). Elsewhere, the Bobbie Point Metasyenogranite varies from coarse to medium grained, is locally seriate textured, and is variably strained and mylonitized. To the northeast, south of McKay Creek, a localized S–C fabric in a steeply northwest-dipping mylonite zone with a subvertical mineral lineation suggests northwest-side up kinematics. To the east, steeply southeast-dipping mylonite zones with a strong, down-dip mineral lineation have a slaty appearance and well-developed strain gradients.

A sample from this locality (Bobbie Point) yielded a date of 1708 ± 15 Ma, interpreted as the age of magmatic crystallization of the syenogranite (GSWA 194737, Kirkland et al., 2010i), indicating emplacement during the early stages of the Biranup Orogeny. This metasyenogranite is one of the most isotopically evolved of the Biranup Zone metagranites and has εHf (-10 to -8) and whole-rock εNd (-15) signatures, consistent with a reworked Archean Yilgarn source (see 'Lu–Hf isotopes' section).

The dated sample is composed of 60–65% perthitic orthoclase, 30–35% quartz, 4% muscovite, and 1% magnetite, plus traces of leucoxene (possibly as a replacement of titanite), pyrite, and rare zircon. Less common larger grains and aggregates of quartz and perthitic orthoclase are up to 4 mm in diameter, although most grains are less than 2 mm. Some orthoclase grains are subhedral; quartz grains are anhedral and commonly exhibit undulose extinction. Some quartz grains preserve orthoclase along resorption channels that define a bipyramidal outline, suggesting shallow-level initial emplacement. Muscovite is fine grained and decussate, and is present as irregular lenses and along grain boundaries.

Directions to Stop 5:

Continue east on the same track for 17.4 km, then turn left. Drive 1.4 km, and bear left. Drive for another 1.1 km, bear left, then right. Drive for 11.8 km, bear left, and drive 1.3 km. Bear right and drive 400 m to two granite hills, located on the left-hand side of the road (MGA 675563E 6802915N).

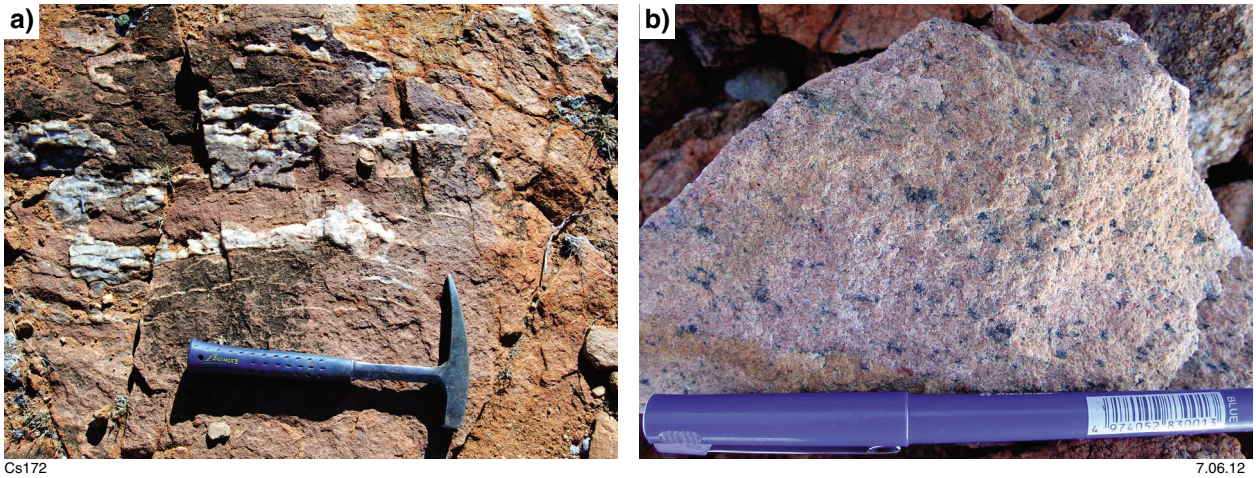

Figure 56. a) Quartz veins in Bobbie Point Metasyenogranite; Excursion 2, Stop 4, Bobbie Point; b) Paleoproterozoic Bobbie Point Metasyenogranite (GSWA 194737).

Stop 5. McKay Creek Metasyenogranite and related rocks

Well-exposed metasyenogranitic rocks in this area appear similar to the Bobbie Point Metasyenogranite, but contain a bit more biotite. However, dating of the McKay Creek Metasyenogranite has shown that it is significantly older, with an interpreted magmatic crystallization age of 1761 ± 10 Ma (GSWA 182424, preliminary data).

The metasyenogranite dated at this locality outcrops in two distinct, approximately 15 m high, bouldery hills (Fig. 57a) where it appears undeformed, although adjacent to these hills the same metasyenogranite has a weak to moderate, northeasterly trending, steeply dipping foliation similar to that in the Bobbie Point Metasyenogranite. East of the hills, the metagranite is more mafic, and appears to be mingled and mixed with a seriate-textured quartz metadiorite (hybrid?) with distinctive onion-skin weathering. The metadiorite contains small rounded inclusions of green, fine-grained, more mafic rock that has lobate contacts, which suggests mingling of a more mafic phase with the metadiorite. These rocks are cut by a syenogranitic dyke.

About 200 m farther east, strongly foliated metasyenogranite is also exposed. The strong foliation contains slaty horizons with chlorite alteration, and dips at 75° to the southeast. The northeasterly trending fabric is consistent with northeasterly trending shear zones, interpreted from aeromagnetic data, which cut tight folds to the northeast.

The metasyenogranite at this locality is medium-grained, equigranular, and rich in K-feldspar. The sample dated (GSWA 182424) was collected from the unfoliated outcrop, and comprises a visually estimated primary mineralogy of 38% quartz, 32% K-feldspar, 27% plagioclase, and 3% biotite. The feldspars are mostly less than 2 mm long, with clouding by clay and sericite(–clinozoisite) in plagioclase and clay clouding in K-feldspar. Much of the plagioclase is untwinned or poorly twinned, and the visually estimated mineralogy was made on the stained offcut, where the difference between K-feldspar and plagioclase is more obvious. Some K-feldspar is as much as 4 to 5 mm long, and some very fine grained plagioclase grains are enclosed within quartz grains. The quartz is interstitial, anhedral, and up to 4 mm in grain size, although some grains have a resorbed, almost bipyramidal habit, with feldspars in probable resorption channels. Biotite is fine grained and unoriented, and accessory oxide, apatite, and rare zircon occur in, and adjacent to, the biotite.

Metadiorite sampled to the east of the two hills (GSWA 182486) comprises a medium-grained matrix of interlocking plagioclase and K-feldspar with quartz, and smaller grains of abundant brown-green hornblende and opaque oxide. The feldspars are mostly altered to sericite, and minor epidote is also present. The more mafic phase (GSWA 182422) has a doleritic texture, is rich in plagioclase (partly altered to sericite), has minor pyroxene mostly overgrown by hornblende and minor chlorite, and also contains abundant opaque grains, and minor titanite and quartz.

Directions to Stop 6:

Retrace the track for 2.5 km, to a large rocky ridge on the north side of the track (MGA 677351E 6802223N).

Stop 6. Ridge near McKay Creek — Barren Basin metasedimentary rocks

The northeasterly trending ridge, about 1 km long and 40 m wide, at this locality is dominated by quartzite, metasandstone, and minor metasiltstone. These rocks contain well-preserved sedimentary features such as symmetrical ripples and planar cross-bedding, with the

latter indicating younging to the southeast (Fig. 57b,c). Bedding ranges from the centimetre to half-metre scale, and its orientation varies from vertical to steeply southeast-dipping. The metasedimentary rocks contain a weak, low angle cleavage dipping steeply to the northwest. The facing direction, bedding cleavage relationships, and intersection all indicate a northeasterly plunging anticline with its hinge to the northwest; i.e. this ridge is in the eastern limb of an upright anticline.

Across strike to the east is sparse rubbly outcrop of strongly foliated phyllitic schist. At the easternmost part of this section, just below a small rise of laterite, is a strongly deformed quartzite with a northeasterly trending, vertical foliation that contains a mineral lineation plunging 37° towards 028. This coincides with a minor shear zone interpreted in the aeromagnetic data (Plate 2; Fig. 42), which is parallel to the major northeasterly trending shear zones that occur in the vicinity of gold mineralization to the northeast (e.g. Hercules Prospect).

Preliminary geochronology of a quartzite sample (GSWA 182405) from this locality has yielded a maximum depositional age of 1990 ± 15 Ma, based on a weighted mean date from two analyses from a single zircon. A more conservative estimate of the maximum age of deposition can be based on the weighted mean date of 2641 ± 3 Ma for the next youngest 52 analyses. The full range of analyses (n = 58) yielded dates between 2735–2619 Ma, indicating a significant Neoarchean component compatible with Yilgarn Craton provenance. The sample dated is dominated by a micromosaic of quartz grains mostly less than 0.1 mm in diameter, with sparse subparallel elongate and blocky grains to 1 mm long with weak undulose extinction. Small blocky grains up to 0.3 mm long have been altered to clay (<1%), and there are sparse lenses of very fine grained quartz–sericite schist. These lenses are rarely up to 1 mm long, and may contain microcrystalline hematite(–leucoxene). Accessory leucoxene is disseminated, up to 0.3 mm long, and occurs with possible tourmaline. The sample has a weak macrolayering represented by weakly strained old grains and smaller recrystallized grains.

It is interesting to compare the dates from this quartzite with dates obtained from a quartz-pebble metaconglomerate that, together with an overlying quartzite, forms a distinct ridge, about 1.5 km long and 40 m wide, located about 6.5 km southeast of Bartlett Bluff (Fig. 57d; MGA 663584E 6774594N). The geochronology sample (GSWA 182416) is from a pebble metasandstone with sparse pebbles (about 3–4 cm) in a micaceous matrix with black iron-rich laminations. A preliminary date of 1752 ± 19 Ma, based on one analysis, is interpreted as a maximum age of deposition. A more conservative estimate of 1798 ± 24 Ma is based on the next six youngest analyses. Thirty-three analyses yielded dates of 2835–1794 Ma, including significant age components at c. 2635 and 1807 Ma.

These metasedimentary rocks have similar age components to metasedimentary rocks in the Barren Basin (e.g. Woodline Formation, Mount Barren Group), which also contain Archean age components. They are all interpreted as part of the Cycle 1 sediments related to basin formation along the margin of the Yilgarn Craton during rifting, prior to and during the Biranup Orogeny (see 'Barren Basin — Cycle 1 sediments' section). Quartzite mapped to the west at Lindsay Hill (van de Graaff and Bunting, 1977), adjacent to the Cundeelee Fault (Plate 2), is inferred to be another remnant of Barren Basin Cycle 1 sediments. A possible source for 1760–1750 Ma detrital maxima, which is common in these sediments, are the c. 1760 Ma granitic rocks of the Biranup Zone. This indicates mixing of sedimentary detritus from the Yilgarn Craton (i.e. from the northwest) with Biranup Zone granitic rocks (potentially from local sources, or from the opposite direction, or both).

Although this field guide does not include a stop at the metaconglomerate locality southeast of Bartlett Bluff (there is no track to it), it is included here to allow comparison to the metasedimentary rocks exposed at Stop 6. The pebbles in the metaconglomerate are subangular to subrounded, and range from large (5–10 cm long) and closely packed (clast-supported) to small (0.5 – 2 cm long) and more sparse (matrix-supported). They are commonly black and white and iron-rich, and have magnetic susceptibility measuring up to 80 x 10^{-5} SI units. There are distinctive iron-rich laminated layers throughout the succession, which are also magnetic; up to 130 x 10^{-5} SI units. These layers are also locally strongly lineated, plunging 32° towards 111. The matrix is quartz rich but also micaceous. Between the coarse metaconglomerate beds are 10–20 cm beds of finely laminated metasiltstone with iron-rich laminae. About 10 m across-strike to the east is a pale-grey quartzite interbedded with metagritstone and metasandstone. The quartzite is nonmagnetic. Bedding dips moderately to the east and is cut by a weak to moderate foliation, also dipping east but at a shallower angle (Fig. 57e). This indicates fold vergence (direction to the next antiform) to the east, and that this locality is in the overturned limb of a gently northeast-plunging antiform. There are no clear younging indicators to support this, although with more time graded or cross-bedding might be found. The pebbles are elongate within the foliation. The bedding and foliation are cut by steeply dipping quartz veins about 3 cm wide.

The sample dated (GSWA 182416) contains a strong schistosity and compositional layering, with quartz-rich and micaceous laminations partly stained with limonite, and minor opaque oxide that is visible in hand specimen. The thin section has approximately 35% muscovite, 5–7% opaque oxide grains, <1% leucoxene/anatase, accessory zircon, and rare patches of tourmaline. Muscovite lamellae from 0.1 – 3 mm wide are partly planar, with widely spaced crenulations at 40–80º to the schistosity, or are anastomosing around lenses of inequigranular quartz, including single crystal quartz grains up to 1.5 mm in diameter. Some of the micaceous lamellae have limonite staining. Some micaceous lamellae are interrupted by grains and lenses of medium to coarse-grained quartz, with roughly circular lenses up to 2 mm in diameter, and more irregular lenses up to 5 mm long. Aggregates of magnetite(–leucoxene/anatase) up to 1.5 mm long occur in many of the micaceous lamellae, but separate lenses of leucoxene/anatase also occur in quartz. Minor, partly pulled-apart grains and aggregates of zircon, to 0.4 mm

Figure 57. a) View of small bouldery hill of c. 1760 Ma McKay Creek Metasyenogranite; near McKay Creek, Excursion 2, Stop 5; b) well-developed symmetrical ripples in metasandstone near McKay Creek, Excursion 2, Stop 6; c) well-developed planar cross-beds in metasandstone indicating younging to the southeast; photo looking southeast, Excursion 2, Stop 4; d) view looking north of metaconglomerate ridge southeast of Bartlett Bluff (MGA 663584E 6774594N); e) bedding layers (horizontal in photo) and cleavage (lower left to upper right) in metaconglomerate southeast of Bartlett Bluff (MGA 663584E 6774594N).

long, occur mostly within the micaceous lamellae, whereas rare patches rich in microcrystalline tourmaline occur in quartz-rich lenses.

Camp off the track nearby.

Day 3

Directions to Stop 7:

Retrace the tracks past Bobbie Point to Rason Lake Road, and then southwards through to the intersection with the Tropicana Camp Road. Continue straight ahead for 2 km on Rason Lake Road, avoiding the right turn (the main road to the Tropicana airstrip). You are now on the track that leads to Plumridge Lakes Nature Reserve. Continue for 7.3 km to the turnoff to Pleiades Lakes (MGA 668821E 6758867N). Note that both the turnoff and first 5–6 km of track can be quite washed out. Continue following the track for 22.2 km, to Stop 7 (MGA 683549E 6770104N).

Stop 7. Pleiades Lakes — Paleoproterozoic metagranites

To the west of Pleiades Lakes is an area of reasonably good outcrop. This area is about 30 km east-northeast of the Tropicana Deposit and associated Archean rocks, and appears to be dominated by Paleoproterozoic metasyenogranitic and metagabbroic rocks (Plate 2; Fig. 40). The area is interpreted as lying to the east of a major, northeasterly trending, southeast-dipping thrust fault that in part separates these rocks from the inferred reworked Archean fragment that contains the Tropicana Deposit (Plate 2; Fig. 42). To the southeast is another major fault, which marks the boundary of the Mesoproterozoic Gwynne Creek Gneiss, which in turn is faulted against the Fraser Zone. The Pleiades Lakes exposures occur at the far northeastern extremity of a distinct, northeasterly trending zone about 150 km long and 2–8 km wide, which is defined in aeromagnetic data by its mottled appearance, caused by the presence of both high and low magnetic anomalies. These are mostly interpreted as remanence effects, but are in part considered due to the mixed and mingled nature of the magmatic rocks exposed in this area, some of which are magnetite rich (see below). For the most part, a major fault lies along the western side of this aeromagnetic feature.

At this locality, scattered outcrop on a low rise near the track comprises very weathered, moderately foliated, banded gneiss with pegmatite veins, intruded by fresher outcrops of easterly trending, metasyenogranitic dykes or sheets. The gneiss is possibly an orthogneiss as it appears to contain some K-feldspar megacrysts, although these megacrysts may be related to the pegmatites, and the outcrop is too weathered to see much detail. If interpreted as an orthogneiss, it may be the same megacrystic metagranite seen elsewhere at Pleiades Lakes (see below). The banding is folded into a steeply northwesterly plunging S-fold, which appears to pre-date the metasyenogranitic dykes. A foliation in the gneiss trends northwest and dips about 65° to the southwest, parallel to the axial plane of the fold. A lens of dark, dense, finely layered, strongly foliated rock approximately 10 m long by 4 m wide is surrounded by one of the felsic dykes, and by a weathered pavement of the gneiss (Fig. 58a). The lens is in the shape of a steeply northeast-plunging S-fold, and contains earlier, small-scale isoclinal folds with an axial-planar foliation.

The metasyenogranitic dykes are nonmagnetic, whereas the dark lens has magnetic susceptibility values ranging from 2000–6000 x 10^{-5}, and locally extending up to 8000 x 10^{-5} SI units, indicating a high magnetite content. This suggests that the lens is likely to be a raft of metamorphosed iron-formation. A sample of the dark iron-rich rock (GSWA 182407) has a magnetic susceptibility of 1200–2000 x 10^{-5} SI units, with the variation perhaps due in part to the layering. The sample contains about equal proportions of magnetite, metamorphic orthopyroxene, and quartz, about 10% plagioclase, and about 3–4% biotite. Iron-rich clots and schleiren are common in the metagranites west of Pleiades Lakes (see Excursion 2, Stops 6 and 7). If this lens is a raft of (Archean?) metamorphosed iron-formation, then it is feasible that these sediments locally affected the composition of the metagranites.

Geochronology sample GSWA 182426 was collected from a metasyenogranitic dyke about 10 m northwest of the dark, iron-rich lens. The metasyenogranite is pink, medium-grained, equigranular, and massive to moderately foliated. The sample yielded a preliminary date of 1671 ± 2 Ma, interpreted as the age of magmatic crystallization.

Directions to Stop 8:

Continue on the same track for 1.2 km (MGA 684468E 6770483N). From here traverse from approximately 150 m east to 200 m west.

Stop 8. Pleiades Lakes traverse — intrusive and structural relationships

This locality provides an opportunity to view various phases of mingled and mixed metagranitic and metagabbroic rocks, and to examine the heterogeneous nature of strain in these rocks. At the eastern end of this traverse are exposures of massive to foliated, coarse- to medium-grained, K-feldspar megacrystic metagranite (MGA 684613E 6770517N). The K-feldspar megacrysts are grey-blue to pink, have an average size of 2 cm, and are locally abundant. The groundmass is coarse to medium grained, and contains plagioclase, quartz, and dark mafic clots that are on average about 4 mm in size, and are composed dominantly of biotite. This metagranite appears to be mingled with a pink, equigranular metasyenogranite, and both contain pods of more mafic material. The contacts between the two granitic phases are either lobate, suggesting mingling, or sharp and vein-like, possibly reflecting a later pulse of the metasyenogranitic phase (Fig. 58b). The later phase is probably the same c. 1671 Ma metasyenogranitic veins seen at Stop 7. The dark mafic clots in the K-feldspar megacrystic metagranite

yielded moderate to high magnetic susceptibility readings that range from 200–1800 x 10^{-5} SI units, indicating the presence of magnetite in these clots.

The K-feldspar megacrystic metagranite yielded a preliminary date of 1689 ± 9 Ma, interpreted as the magmatic crystallization age (GSWA 182428; Fig. 58c). Two analyses yielded preliminary dates of 1800 and 1784 Ma, interpreted as the ages of inherited components. The date of 1689 ± 9 Ma indicates that the megacrystic metagranite is distinctly older than the metasyenogranitic dyke dated at Stop 7, which is consistent with the field relationships seen here (Fig. 58b). To the south of this locality, at Stop 9, is a similar K-feldspar megacrystic metagranite, although with a more syenogranitic composition, which yielded a preliminary date of 1694 ± 7 Ma (GSWA 182411). These dates, and the older dates from Bobbie Point (c. 1710 Ma; Excursion 2, Stop 4) and MacKay Creek (c. 1760 Ma; Excursion 2, Stop 5), show that granitic magmatism of dominantly alkaline composition affected this region from at least c. 1760 Ma through to c. 1670 Ma, although the c. 1760 Ma granites may represent an earlier, separate event. Most of these granitic magmas also show evidence for the presence of a co-magmatic mafic phase.

The sample dated at this locality (GSWA 182428) contains large, irregular mafic clots and irregularly disseminated coarse-grained K-feldspars. Visually estimated, the primary mineralogy for the area of the thin section has 45% plagioclase, 26% quartz, 15% biotite, 8% K-feldspar, 2% opaque oxide, and <1% each of garnet, apatite, titanite, epidote, and zircon. This indicates a granodioritic composition, although the proportion of K-feldspar is underestimated. The main mafic lenses are subparallel, although there is no obvious foliation defined by crystal fabrics. The plagioclase also contains patches of decussate muscovite and sericite (3–4%). The epidote and muscovite are metamorphic or secondary. The K-feldspar grains are perthitic microcline, are up to 12 mm long, and contain inclusions of plagioclase, quartz, and opaque oxide grains. Plagioclase grains are up to 6 mm, anhedral to subhedral, and are irregularly dusted with sericite, fine-grained muscovite, and epidote in various proportions. Interstitial quartz grains up to 8 mm long have undulose extinction, and are accompanied by sparse patches of recrystallized, new grains. Mafic lenses up to 15 mm long are largely composed of unoriented biotite, up to 4 mm in grain size, as well as finer-grained recrystallized biotite. Oxide, apatite, titanite, garnet, and epidote grains also occur in, and adjacent to, the mafic aggregates, with garnet and titanite grains up to 1 mm in size and zircons 0.1 – 0.25 mm long. Rare lenses of fine-grained quartz and decussate biotite, located adjacent to mafic lenses, may represent xenoliths, although this interpretation is uncertain. A single grain of pyrite was identified using low-angle incident light. Recrystallization of quartz and biotite has occurred; this, and the presence of metamorphic garnet and epidote, and low-temperature secondary muscovite and sericite, indicates that early amphibolite-facies metamorphism (quartz–feldspar–biotite–garnet) may have been followed by lower-temperature modification.

To the west, near the track (MGA 684468E 6770483N), is an area of scattered outcrop of a mafic intrusive rock mingled with the K-feldspar megacrystic metagranite (Fig. 58d). This has produced a hybrid rock that contains quartz and K-feldspar phenocrysts, ranging from about 3–10 mm in size, within a fine-grained matrix (Fig. 58e). The mafic intrusive has an igneous texture, and may be originally of noritic composition, as shown on the Plumridge 1:250 000 sheet (van de Graaff and Bunting, 1977). It is slightly magnetic, at 100–150 x 10^{-5} SI units. Just east of the track, the hybrid has a localized, subvertical, high-strain fabric trending north, and a mineral lineation plunging 52° towards 154.

Two samples of this hybrid rock (GSWA 182408 and 182409) have quartz and K-feldspar phenocrysts ranging from 3–10 mm within a fine-grained matrix. In thin section, GSWA 182408 has a doleritic texture defined by interlocking plagioclase, with interstitial relict clinopyroxene overgrown by fine-grained blue-green amphibole. Orthopyroxene may also be present. The remainder of the sample contains about 10% biotite, 5% opaque oxide, and minor epidote. GSWA 182409 is similar to 182408, but contains some larger feldspars (mostly plagioclase), and minor perthite. There is also about 10% biotite, 10% epidote, blue-green amphibole, and minor chlorite, all of which almost completely overgrow relict pyroxene grains. The feldspar grains are also overgrown by epidote or zoisite, with the remainder of the sample containing 5–7% opaque oxide, and 4–5% quartz.

West of the track, the hybrid rocks are cut by another metasyenogranite sheet or dyke, which has a strong fabric. Both the K-feldspar megacrystic metagranite and the metasyenogranite are folded into a north-northwesterly trending S-fold, which occurs on the limb of a larger fold. The larger fold is a northerly plunging, open to tight antiform that is part of an antiform–synform pair, traceable over approximately 200 m, from east to west. Both the strong foliation and the mineral lineation in these rocks are folded. To the west (at approximately MGA 684213E 6770510N), a ridge of strongly deformed to mylonitic K-feldspar megacrystic metagranite and metasyenogranite defines the western limb of the synform. The strong deformation has produced ‘rounded’ K-feldspar porphyroclasts up to 3 cm wide, a very strong, steeply dipping to vertical mineral lineation (Fig. 58f), and locally, dextral porphyroclasts, although most are symmetrical. The dextral shear sense indicates east-side down, with normal movement sense. However, the high-strain fabric is folded about upright folds, which would suggest a subhorizontal movement surface prior to folding. Centimetre-scale foliation-parallel quartz veins are present throughout these rocks.

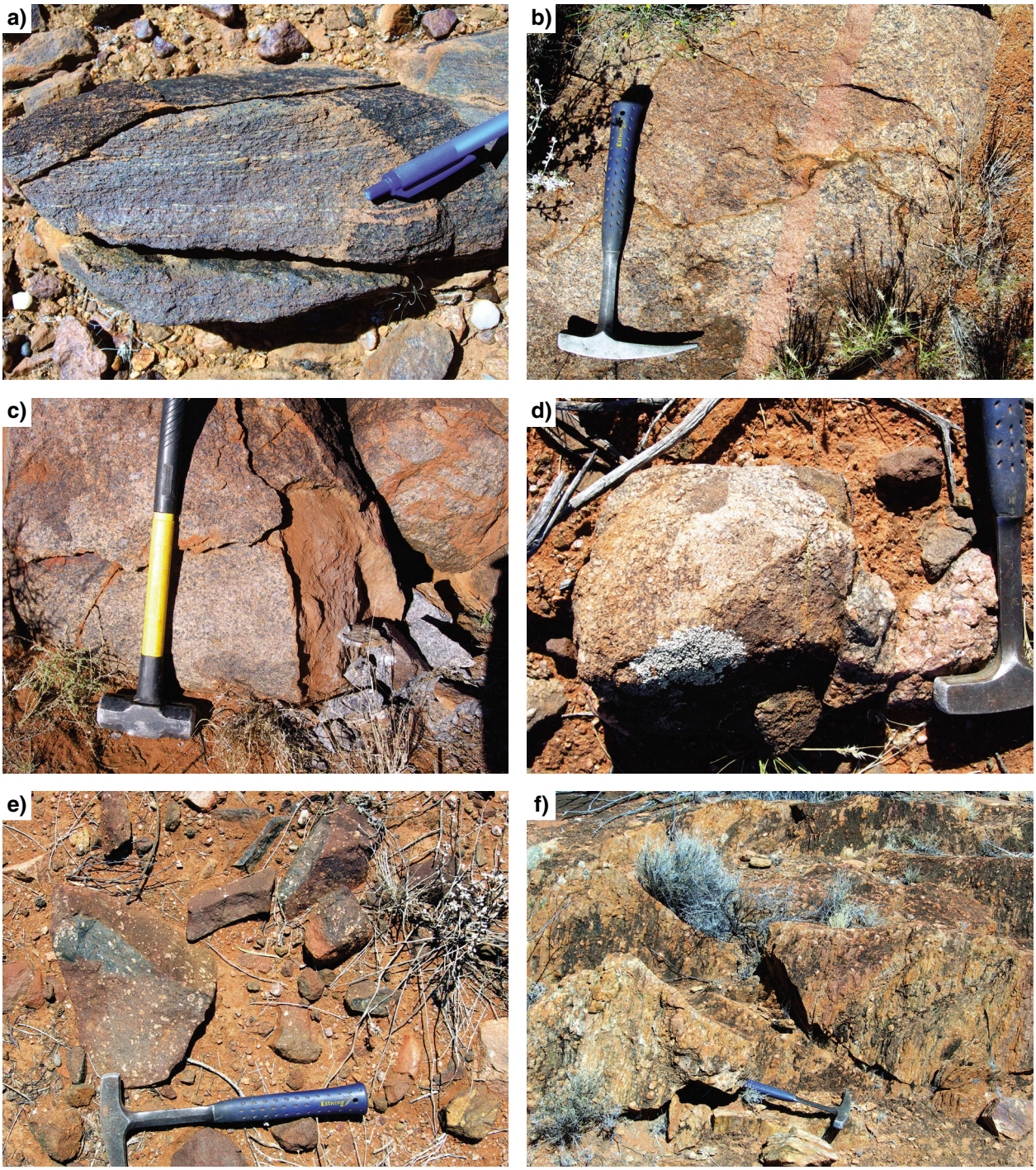

Figure 58. a) Sample of lens of dark, finely layered, iron-rich rock interpreted as metamorphosed iron-formation within metasyenogranitic dyke and orthogneiss; Pleiades Lakes, Excursion 2, Stop 7; b) late metasyenogranitic vein intruded into K-feldspar megacrystic metagranite; Pleiades Lakes, Excursion 2, Stop 8; c) geochronology sample site of K-feldspar megacrystic metagranite, GSWA 182428; Pleiades Lakes, Excursion 2, Stop 8; d) mingled K-feldspar megacrystic metagranite with a mafic phase; Pleiades Lakes, Excursion 2, Stop 8; e) hybrid rocks with K-feldspar and quartz phenocrysts in a fine-grained dark matrix; Pleiades Lakes, Excursion 2, Stop 8; f) strong, steeply plunging mineral lineation in K-feldspar megacrystic metagranite; Pleiades Lakes, Excursion 2, Stop 8.

Day 4

Directions to Stop 9:

Drive cross-country, approximately 300 m to the south (MGA 684379E 6769891N).

Stop 9. Pleiades Lakes — Paleoproterozoic metagranite

The purpose of this stop is to view small whalebacks and boulders of metasyenogranite, one of which was sampled for geochronology. The metasyenogranite is pink to grey, coarse grained, and seriate textured to porphyritic. It contains tabular feldspars up to 2 cm long, within a coarse-grained, seriate groundmass of feldspar, quartz, and biotite. Quartz phenocrysts are typically mauve in colour, and biotite occurs in clots up to 4 mm in diameter that also locally contain magnetite. These clots sometimes form millimetre- to centimetre-scale, wispy, irregular schlieren that are strongly magnetic (Fig. 59a). The metasyenogranite also contains strongly magnetic mafic pods that appear to have disaggregated and dispersed as mafic clots throughout the rock. The metasyenogranite is moderately magnetic, although quite variable, with the mafic clots producing the highest magnetic susceptibility readings of 100–800 x 10^{-5} SI units. In contrast, the schleiren are strongly magnetic, but also quite variable; most have readings around 1200 x 10^{-5}, but can extend up to 3170 x 10^{-5} SI units.

A sample of the metasyenogranite (Fig. 59b; GSWA 182411) has yielded a preliminary date of 1694 ± 7 Ma, interpreted as the age of magmatic crystallization of the syenogranite. Visually estimated, the primary mineralogy of this sample consists of 37% microcline, 33% quartz, 14–15% plagioclase, 9% biotite, 4% magnetite, 1% garnet, and <1% titanite, accompanied by minor apatite and sparse zircons up to 0.2 mm. Microcline occurs partly as megacrysts up to 10 mm long, with anhedral plagioclase up to 6 mm, and minor, strained, old grains of quartz with undulose extinction up to 4 mm long. There are also abundant smaller microcline and plagioclase grains up to 2 mm in grain size, although the very fine grained recrystallized feldspars are less abundant than recrystallized, fine-grained micromosaic quartz. Lenses of decussate or weakly foliated biotite are disseminated, and often contain some of the magnetite, garnet, titanite, apatite, and zircon. Garnet grains are 0.5 – 1.5 mm in size, and occur with or without inclusions of biotite, parallel to adjacent biotite. Separate grains and aggregates of magnetite are also disseminated. Sparse patches of sericite or epidote(–sericite–biotite) occur within some plagioclase grains, and sparse exsolved plagioclase in microcline also contains rare sericite. The petrology indicates that this rock underwent amphibolite-facies metamorphism, which was followed by low-temperature alteration.

Directions to Stop 10:

Continue southwards cross-country for approximately 2.5 km (to MGA 684553E 6768114N).

Stop 10. Mylonite and ultramylonite zones

This stop is in an area of good outcrop spread over several ridges. At this locality, K-feldspar megacrystic metagranite is interlayered (or mingled) with metagabbro. The metagabbro is fine grained (average grain size 2 mm), and although foliated, has a relict igneous texture. It is moderately magnetic, up to about 200 x 10^{-5} SI units. Metagabbro sample GSWA 18242 comprises interlocking plagioclase and minor perthite, with pyroxene grains overgrown by complex mixtures of fibrous or blue-green amphibole, epidote, opaque oxide, reddish biotite, and ?chlorite. Some of the opaque oxide is rimmed by amphibole. As metagranite sample GSWA 182430 was cut perpendicular to the lineation, it does not show the mylonitic fabric. The porphyroclasts comprise K-feldspar, microcline, or perthite, and there is minor, coarse muscovite within the fabric. The matrix is very fine grained, and consists of feldspar and quartz, plus abundant, tiny, aligned biotite flakes. At the angle the section was cut, the feldspar and quartz appear to have recrystallized with recovery textures.

The K-feldspar megacrystic metagranite has a mylonitic to ultramylonitic, east-trending, moderately to steeply south-dipping foliation, and a very strong mineral lineation plunging 28° towards 103 (Fig. 59c). K-feldspar porphyroclasts are mostly rounded due to the intense deformation (Fig. 59d). No clear sense of shear is discernible due to the strong flattening and rounding of the porphyroclasts. Some layers contain rounded K-feldspar porphyroclasts in a dark, fine-grained matrix, which is interpreted as an ultramylonite fabric with extreme grain-size reduction.

These rocks occur close to easterly trending thrust faults interpreted from the aeromagnetic data (Fig. 42), and it is possible that the high-strain fabric seen here is related to the same deformation event. The timing of deformation is unknown, but could be the same event that produced the east-northeasterly trending shear zones that offset mineralization in the Tropicana Deposit.

Directions to Stop 11:

Retrace the route back to the track, turn left, and retrace back to the Plumridge Lakes Nature Reserve Track intersection; turn left (east). Drive for 36.5 km (to MGA 686531E 6734284N), then make your way cross-country to Gwynne Creek, approximately 1.5 km to the east (MGA 687717E 6734294N).

Stop 11. Gwynne Creek Gneiss — Mesoproterozoic Arid Basin

The Gwynne Creek Gneiss is interpreted to be separated from rocks of the Biranup Zone by a major, northeasterly trending fault, and from the undercover, denser, more magnetic rocks of the Fraser Zone by a similar fault (Plate 2). The gneiss is interpreted to be part of the Arid Basin Cycle 2 sediments, and, given its position along the northwestern margin of the Fraser Zone, may be part of

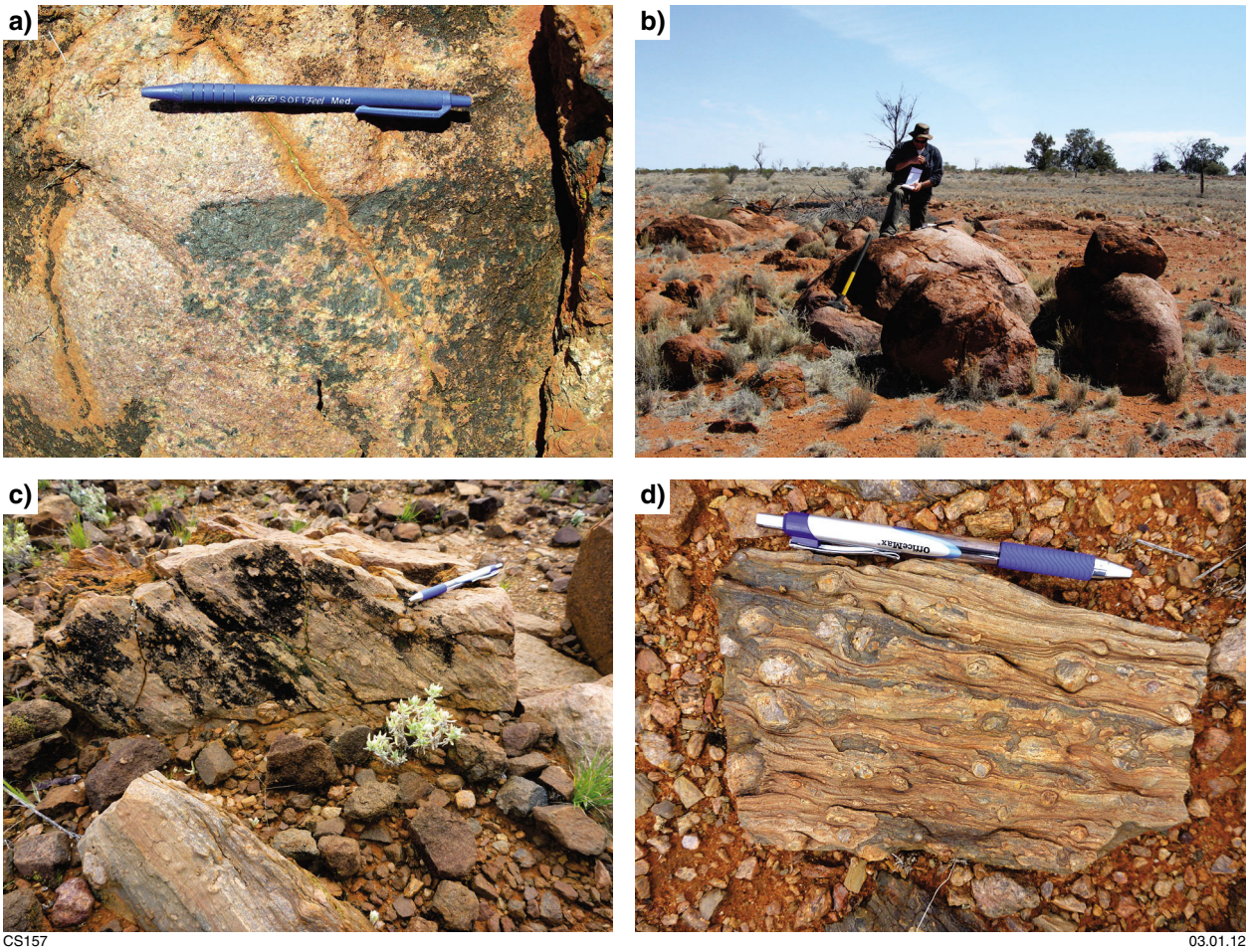

Figure 59. a) Strongly magnetic mafic schleiren in metasyenogranite; Pleiades Lakes, Excursion 2, Stop 9; b) geochronology sample site of metasyenogranite, GSWA 182411; Pleiades Lakes, Excursion 2, Stop 9; c) strong mineral lineation in mylonitic K-feldspar megacrystic metagranite; Pleiades Lakes, Excursion 2, Stop 10; d) ultramylonite fabric, showing intense rounding of K-feldspar megacrysts; Pleiades Lakes, Excursion 2, Stop 10.

the same sequence of metasedimentary rocks that outcrop in the Fraser Range to the southwest (Plate 1; Fig. 27; see 'Fraser Zone' section). Dating of detrital zircons from the Gwynne Creek Gneiss is consistent with this interpretation.

The Gwynne Creek Gneiss is dominated by psammitic gneiss interlayered with thinner layers of semipelitic gneiss, and also includes layered, finely laminated quartzofeldspathic gneiss with layer-parallel leucosome, and minor metagranitic, metamafic, and meta-ultramafic rocks. The paragneissic rocks are intruded by late, coarse to very coarse, K-feldspar rich pegmatites.

Preliminary geochronology from a semipelitic gneiss (Fig. 15b) sampled approximately 10 km to the northeast of this locality indicates that the metasedimentary rocks of the Gwynne Creek Gneiss have a maximum depositional age of 1483 ± 12 Ma (based on one analysis), with a more conservative estimate based on six grains of 1533 ± 11 Ma (GSWA 182432). This rock also includes a significant c. 1675 Ma detrital component, and smaller age components at c. 1607 and 1739 Ma. Interbedded psammitic gneiss, sampled close to the semipelitic gneiss, yielded preliminary dates spanning 1681–1395 Ma. Ten analyses yielded a concordia age of 1297 ± 7 Ma, interpreted as the age of metamorphism.

Garnet–biotite quartzofeldspathic migmatitic gneiss, from approximately 9 km to the northeast of this locality, yielded a concordia age of 1657 ± 5 Ma (GSWA 194735, Kirkland et al., 2010g), which is interpreted as representing detrital material from a migmatitic precursor, based on the maximum depositional age described above. Two analyses of dark-coloured overgrowths in two zircon grains yielded an age of 1270 ± 11 Ma, interpreted to date zircon growth during metamorphism. Three analyses of bright rims (in cathodoluminescence images) from three grains yielded an age of 1193 ± 26 Ma, interpreted to reflect the timing of zircon growth during a metamorphic event. The bright rims heal brittle fractures transecting entire zircon crystals, including the dark overgrowths,

thereby constraining the timing of brittle deformation in this rock to between 1270 and 1193 Ma (Kirkland et al., 2011a).

The geochronology indicates that deposition of the Gwynne Creek Gneiss took place after the Biranup Orogeny, and that a substantial component of the detritus was sourced from rocks of the Biranup Zone. This interpretation is consistent with other Cycle 2 sediments, such as those in the Fraser Range. Mafic sills or dykes and localized intrusions of ultramafic rocks throughout the metasedimentary succession are probably related to the c. 1300 Ma Fraser Zone intrusions. Interpreted metamorphic dates of 1297 ± 7 Ma and 1270 ± 11 Ma indicate minimum depositional ages, and most likely date high-temperature metamorphism and leucosome formation in the Gwynne Creek Gneiss during Stage I of the Albany–Fraser Orogeny. The younger date of 1193 ± 26 Ma indicates that these rocks were also affected during Stage II, possibly after a period of uplift and brittle deformation. These interpretations are consistent with field relationships, as described below.

The approximately 16 km long, north–south section of Gwynne Creek and adjoining areas provide good exposure of the Gwynne Creek Gneiss and its dominantly northeasterly trending structures. The metasedimentary rocks contain a well-developed gneissic layering with localized, layer-parallel leucosome. This layering (S_1) is folded into small-scale, tight to isoclinal (F_1) folds containing an axial-planar foliation (S_2) that is for the most part parallel to the main layering, and which defines the main fabric in these rocks (Fig. 60a). This fabric trends to the northeast, and dips moderately to the east-southeast or southeast. The S_1 layering is also locally boudinaged. F_1 folds plunge gently, either to the south or to the northeast, but are refolded into gently to moderately, northeasterly plunging, tight to isoclinal, inclined folds with southeast-dipping axial planes (F_2; Fig. 60b). At this locality, a sequence of (F_2) S-folds are the dominant folds exposed. A mineral lineation is variably plunging to the northeast and the southwest, and is locally coincident with an intersection lineation between the main layering (S_1) and the axial-planar foliation (S_2). Both sets of folds are cut by pegmatite veins and small, late, brittle faults (Fig. 60c).

At the northern end of this creek section, in an embayment to the west, is an occurrence of silica caprock associated with a meta-ultramafic rock that is not exposed, but was described from drillholes during GSWA mapping in the 1970s (van de Graaff and Bunting, 1977). A petrographic report described a sample from the drillcore (GSWA 37527) as an ultramafic hornblende granulite, comprising about 60% pale-green hornblende, 30% orthopyroxene, 10% clinopyroxene, and very minor plagioclase, accessory tremolite, and hematite.

A mafic lens, about 1 m wide, within the psammitic gneiss is bound by a small brittle fault on its northwestern side, and is interpreted as an altered and metamorphosed mafic dyke. A sample of this mafic rock (GSWA 182401) has an unusual appearance in thin section, and comprises abundant anhedral opaque oxide with fine-grained coronas of blue-green amphibole locally intergrown with chlorite.

Figure 60. a) Layer-parallel, small-scale isoclinal F_1 folds, folding thin leucosome layers and fabric (S_1); Gwynne Creek Gneiss, Excursion 2, Stop 11; b) view of F_2 synformal fold hinge refolding small-scale F_1 folds and S_1 fabric; Gwynne Creek Gneiss, Excursion 2, Stop 11; c) pair of small, late, brittle faults. One fault is adjacent to the hammer; the other is delineated by the sharp contact to the right. Gwynne Creek Gneiss, Excursion 2, Stop 11.

Some of this amphibole is quite blue and is probably reibeckite. Another amphibole is pleochroic pale-green to very bright emerald green, and is locally intergrown with fibrous amphibole. Some of the opaque oxide grains have rims of small garnets, and there are also sparse, small, euhedral garnets throughout the matrix. There appears to be some relict pyroxene (orthopyroxene?), which is very altered and overgrown with fine amphibole and chlorite. These are set within a matrix of interlocking plagioclase, some of which may be anorthite (no albite twinning). The sample also possibly includes rare titanite and accessory apatite.

Semipelitic gneiss (GSWA 184399; sampled adjacent to the track turnoff to this locality) is fine to medium grained, and has a strong to mylonitic foliation. It comprises about 10–15% biotite and 8–10% garnet, with the remainder containing K-feldspar, plagioclase, and quartz, with accessory epidote, opaque oxide, and zircon. Biotite is pale to medium brown, and is aligned in the foliation. Garnet is clear, partly overgrown, and is locally wrapped by the foliation, or has pressure shadows. The quartz and feldspars have mostly lobate or ragged grain boundaries, although some grains show recovery textures and 120° junctions. The thin section also contains textures in the form of droplets and veinlets, interpreted as due to partial melting.

Psammitic gneiss (GSWA 184400; sampled to the north along Gwynne Creek) is similar to the semipelitic gneiss (GSWA 184399), but contains less biotite, more quartz, and no garnet. Biotite has a localized decussate texture, or is aligned within the foliation, and comprises about 5% of the section. This sample also includes 40–50% quartz, and a mixture of K-feldspar and plagioclase, all with lobate grain boundaries; minor sericite alteration is present on the feldspars. Minor opaque oxide grains, and accessory epidote and rounded zircon are also present.

From here, return to the track and drive north back towards Tropicana. This is the end of the excursion.

References

Adams, M 2011, Structural and geochronological evolution of the Malcolm Gneiss, Nornalup Zone, Albany–Fraser Orogen, Western Australia: Curtin University, Perth, Western Australia, BSc Honours thesis (unpublished).

Adams, M 2012, Structural and geochronological evolution of the Malcolm Gneiss, Nornalup Zone, Albany–Fraser Orogen, Western Australia: Record 2012/4, 132p.

Aitken, RA 2010, Moho geometry gravity inversion experiment (MoGGIE): a refined model of the Australian Moho, and its tectonic and isostatic implications: Earth and Planetary Science Letters, v. 297, p. 71–83.

Barley, ME, Brown, SJA, Krapež, B and Kositcin, N 2008, Physical volcanology and geochemistry of a Late Archaean volcanic arc: Kurnalpi and Gindalbie Terranes, Eastern Goldfields Superterrane, Western Australia: Precambrian Research, v. 161, p. 53–76.

Barquero-Molina, M 2010, Kinematics of bidirectional extension and coeval NW-directed contraction in orthogneisses of the Biranup Complex, Albany Fraser Orogen, southwestern Australia: Geological Survey of Western Australia, Report 109, 205p.

Beeson, J, Delour, CP and Harris, LB 1988, A structural and metamorphic traverse across the Albany Mobile Belt, Western Australia: Precambrian Research, v. 40–41, p. 117–136, doi:10.1016/0301-9268(88)90064-2.

Beeson, J, Harris, LB and Delour, CP 1995, Structure of the western Albany Mobile Belt (south-western Australia): evidence for overprinting by Neoproterozoic shear zones of the Darling Mobile Belt: Precambrian Research, v. 75, p. 47–63, doi:10.1016/0301-9268(95)00017-Y.

Black, LP, Harris, LB and Delour, CP 1992, Reworking of Archaean and Early Proterozoic components during a progressive, Middle Proterozoic tectonothermal event in the Albany Mobile Belt, Western Australia: Precambrian Research, v. 59, p. 95–123.

Blewett, RS, Czarnota, K and Henson, PA 2010, Structural-event framework for the eastern Yilgarn Craton, Western Australia, and its implications for orogenic gold: Precambrian Research, v. 183, p. 203–209.

Bodorkos, S and Clark, DJ 2004a, Evolution of a crustal-scale transpressive shear zone in the Albany Fraser Orogen, SW Australia: 1. P–T conditions of Mesoproterozoic metamorphism in the Coramup Gneiss: Journal of Metamorphic Geology, v. 22, no. 8, p. 691–711, doi: 10.1111/j.1525-1314.2004.00543.x.

Bodorkos, S and Clark, DJ 2004b, Evolution of a crustal-scale transpressive shear zone in the Albany Fraser Orogen, SW Australia: 2. Tectonic history of the Coramup Gneiss and a kinematic framework for Mesoproterozoic collision of the West Australian and Mawson cratons: Journal of Metamorphic Geology, v. 22, no. 8, p. 713–731, doi: 10.1111/j.1525-1314.2004.00544.x.

Bodorkos, S and Wingate, MTD 2008a, 184120: monzogranitic gneiss, Pallinup River; Geochronology Record 700: Geological Survey of Western Australia, 4p.

Bodorkos, S and Wingate, MTD 2008b, 184127: porphyritic monzodiorite, Powell Point; Geochronology Record 704: Geological Survey of Western Australia, 4p.

Bodorkos, S and Wingate, MTD 2008c, 184128: leucocratic tonalitic gneiss, Powell Point; Geochronology Record 705: Geological Survey of Western Australia, 4p.

Bodorkos, S and Wingate, MTD 2008d, 184314: leucocratic granodioritic gneiss, Lort River – Ashdale Road; Geochronology Record 710: Geological Survey of Western Australia, 4p.

Bunting, JA, De Laeter, JR and Libby, WG 1976, Tectonic subdivisions and geochronology of the northeastern part of the Albany–Fraser Province, Western Australia, *in* Annual report for the year 1975: Geological Survey of Western Australia, Perth, Western Australia, p. 117–126.

Campbell, IH, Griffiths, RW and Hill, RI 1989, Melting in an Archaean mantle plume: heads it's basalts, tails it's komatiites: Nature, v. 339, p. 697–699.

Campbell, IH, McCall, GJH and Tyrwhitt, DS 1970, The Jimberlana norite, Western Australia — a smaller analogue of the Great Dyke of Rhodesia: Geological Magazine, v. 107, p. 1–12.

Cassidy, KF, Champion, DC, Krapež, B, Barley, ME, Brown, SJA, Blewett, RS, Groenewald, PB and Tyler, IM 2006, A revised geological framework for the Yilgarn Craton, Western Australia: Geological Survey of Western Australia, Record 2006/8, 8p.

Champion, DC and Cassidy, KF 2007, An overview of the Yilgarn and its crustal evolution, *in* Proceedings *edited by* FP Bierlein and CM Knox-Robinson: Geoscience Australia; Kalgoorlie '07, Kalgoorlie, Western Australia, 25 September 2007; Record 2007/14, p. 8–13.

Champion, DC and Sheraton, JW 1997, Geochemistry and Nd isotope systematics of Archaean granites of the Eastern Goldfields, Yilgarn Craton, Australia: implications for crustal growth processes: Precambrian Research, v. 83, p. 109–132.

Clark, DJ 1999, Thermo-tectonic evolution of the Albany–Fraser Orogen, Western Australia: University of New South Wales, Sydney, New South Wales, PhD thesis (unpublished).

Clark, DJ, Kinny, PD, Post, NJ and Hensen, BJ 1999, Relationships between magmatism, metamorphism and deformation in the Fraser Complex, Western Australia: constraints from new SHRIMP U–Pb zircon geochronology: Australian Journal of Earth Sciences, v. 46, p. 923–932.

Clark, DJ, Hensen, BJ and Kinny, PD 2000, Geochronological constraints for a two-stage history of the Albany–Fraser Orogen, Western Australia: Precambrian Research, v. 102, no. 3, p. 155–183.

Clark, WC 1995, Granite petrogenesis, metamorphism and geochronology of the western Albany–Fraser Orogen, Albany, Western Australia: Curtin University of Technology, Perth, Western Australia, BSc Honours thesis (unpublished).

Collins, WJ, Belousova, EA, Kemp, AIS and Murphy, J 2011, Two contrasting Phanerozoic orogenic systems revealed by hafnium isotope data: Nature Geoscience, v. 4, p. 333–337.

Condie, KC and Myers, JS 1999, Mesoproterozoic Fraser Complex: geochemical evidence for multiple subduction-related sources of lower crustal rocks in the Albany–Fraser Orogen, Western Australia: Australian Journal of Earth Sciences, v. 46, p. 875–882.

Cruse, T 1991, The sedimentology, depositional environment and Ediacaran fauna of Mondurup and Barnett Peaks, Stirling Range Formation, Western Australia: University of Western Australia, Perth, Western Australia, BSc Honours thesis (unpublished).

Cruse, T and Harris, LB 1994, Ediacaran fossils from the Stirling Range Formation, Western Australia: Precambrian Research, v. 67, p. 1–10.

Czarnota, K, Champion, DC, Goscombe, B, Blewett, RS, Cassidy, KF, Henson, PA and Groenewald, PB 2010, Geodynamics of the eastern Yilgarn Craton: Precambrian Research, v. 183, p. 175–202.

Dawson, GC, Krapež, B, Fletcher, IR, McNaughton, N and Rasmussen, B 2003, 1.2 Ga thermal metamorphism in the Albany–Fraser Orogen of Western Australia: consequence of collision or regional heating by dyke swarms?: Journal of the Geological Society, London, v. 160, p. 29–37.

Dawson, GC, Krapež, B, Fletcher, IR, McNaughton, NJ and Rasmussen, B 2002, Did late Palaeoproterozoic assembly of proto-Australia involve collision between the Pilbara, Yilgarn and Gawler Cratons? Geochronological evidence from the Mount Barren Group in the Albany–Fraser Orogen of Western Australia: Precambrian Research, v. 118, p. 195–220.

De Waele, B and Pisarevsky, SA 2008, Geochronology, paleomagnetism and magnetic fabric of metamorphic rocks in the northeast Fraser Belt, Western Australia: Australian Journal of Earth Sciences, v. 55, p. 605–621.

Doepel, JJG (compiler) 1973, Norseman, Western Australia: Geological Survey of Western Australia, 1:250 000 Geological Series Explanatory Notes, 40p.

Doepel, JJG 1975, Albany–Fraser Province, *in* The geology of Western Australia: Geological Survey of Western Australia, Memoir 2, p. 94–102.

Doyle, MG, Gibbs, D, Savage, J and Blenkinsop, TG 2009, Geology of the Tropicana Gold Project, Western Australia, *in* Smart science for exploration and mining: Economic Geology Research Unit, James Cook University; 10th Biennial SGA Meeting of The Society for Geology Applied to Mineral Deposits, Townsville, Queensland, 17 August 2009; Proceedings Volume 1, p. 50–52.

Doyle, MG, Kendall, BM and Gibbs, D 2007, Discovery and characteristics of the Tropicana Gold District, *in* Proceedings *edited by* FP Bierlein and CM Knox-Robinson: Geoscience Australia; Kalgoorlie '07 Conference, Kalgoorlie, Western Australia, 25 September 2007; Record 2007/14, p. 186–190.

Doyle, MG, Kendall, BM, Gibbs, D and Kent, M 2008, Tropicana Deposit: a new gold province in Western Australia, *in* New generation advances in geoscience: Geological Society of Australia; Australian Earth Sciences Convention (AESC) 2008, Perth, Western Australia, 21 July 2008; Abstracts 89, p. 85.

Elias, M and Bunting, JA 1982, Wiluna, W.A.: Geological Survey of Western Australia, 1:250 000 Geological Series Explanatory Notes, 20p.

Evans, T 1999, Extent and nature of the 1.2 Ga Wheatbelt dyke swarm, Yilgarn Craton, Western Australia: University of Western Australia, Perth, Western Australia, BSc Honours thesis (unpublished).

Fasano, G and Franceschini, A 1987, A multidimensional version of the Kolmogorov–Smirnov test: Monthly Notes of the Royal Astronomical Society, v. 225, p. 155–170.

Fitzsimons, ICW 2003, Proterozoic basement provinces of southern and southwestern Australia and their correlation with Antarctica: Geological Society of London Special Publication, v. 206, p. 93–130.

Fitzsimons, ICW and Buchan, C 2005, Geology of the western Albany–Fraser Orogen, Western Australia — a field guide: Geological Survey of Western Australia, Record 2005/11, 32p.

Fitzsimons, ICW, Kinny, PD, Wetherley, S and Hollingsworth, DA 2005, Bulk chemical controls on metamorphic monazite growth in pelitic schists and implications for U–Pb age data: Journal of Metamorphic Geology, v. 23, p. 261–277.

Fletcher, IR, Libby, WG and Rosman, KJR 1987, Sm–Nd dating of the 2411 Ma Jimberlana dyke, Yilgarn Block, Western Australia: Australian Journal of Earth Sciences, v. 34, p. 523–525.

Fletcher, IR, Myers, JS and Ahmat, AL 1991, Isotopic evidence on the age and origin of the Fraser Complex, Western Australia: a sample of Mid-Proterozoic lower crust: Chemical Geology: Isotope Geoscience, v. 87, p. 197–216.

Flint, RB and Daly, SJ 1993, Coompana Block, *in* The Geology of South Australia *edited by* JF Drexel, WV Preiss and AJ Parker: Geological Survey of South Australia, South Australia, Bulletin 54, p. 168–169.

Fox, LJ 2010, Geology of the Hat Trick Prospect in the Tropicana Project area, Western Australia: James Cook University, Townsville, Queensland, BSc Honours thesis (unpublished), 104p.

French, JE, Heaman, LM and Chacko, T 2002, Feasibility of chemical U–Th–total Pb baddeleyite dating by electron microprobe: Chemical Geology, v. 188, p. 85–104.

Gee, RD, Baxter, JL, Wilde, SA and Williams, IR 1981, Crustal development in the Yilgarn Block, *in* Archaean Geology *edited by* JE Glover and DI Groves: Geological Society of Australia; Second International Archaean Symposium, Perth, Western Australia, Special Publication 7, p. 43–56, 14p.

Geological Survey of Western Australia 2007, South Yilgarn geological exploration package: Geological Survey of Western Australia, Record data package 2007/13.

Geological Survey of Western Australia 2011, East Albany–Fraser and southeast Yilgarn, 2011 update: Geological Survey of Western Australia, Geological Exploration Package.

Geoscience Australia 1998, Australian crustal elements (national geoscience dataset): Geoscience Australia, Canberra, Australian Capital Territory, viewed 29 August 2011, <http://www.ga.gov.au/meta/ANZCW0703002384.html>.

Giddings, JW 1976, Precambrian palaeomagnetism in Australia I: basic dykes and volcanics from the Yilgarn Block: Tectonophysics, v. 30, p. 91–108.

Giles, D, Betts, PG and Lister, GS 2004, 1.8–1.5 Ga links between the North and South Australian Cratons and the Early–Middle Proterozoic configuration of Australia: Tectonophysics, v. 380, p. 27–41.

Goleby, BR, Blewett, RS, Korsch, RJ, Champion, DC, Cassidy, KF, Jones, LEA, Groenewald, PB and Henson, PA 2004, Deep seismic reflection profiling in the Archaean northeastern Yilgarn Craton, Western Australia: implications for crustal architecture and mineral potential: Tectonophysics, v. 388, p. 119–133.

Griffin, TJ 1989, Explanatory notes on the Widgiemooltha 1:250 000 geological sheet, Western Australia (2nd edition): Geological Survey of Western Australia, Record 1989/4, 81p.

Griffin, WL, Wang, X, Jackson, SE, Pearson, NJ, O'Reilly, SY, Xu, X and Zhou, X 2002, Zircon chemistry and magma genesis, SE China: in-situ analysis of Hf isotopes, Pingtan and Tonglu igneous complexes: Lithos, v. 61, p. 237–269.

Hall, CE, Jones, SA and Bodorkos, S 2008, Sedimentology, structure and SHRIMP zircon provenance of the Woodline Formation, Western Australia: implications for the tectonic setting of the West Australian Craton during the Paleoproterozoic: Precambrian Research, v. 162, p. 577–598, doi:10.1016/j.precamres.2007.11.001.

Hawkesworth, CJ, Dhuime, B, Pietranik, AB, Cawood, PA, Kemp, AIS and Storey, CD 2010, The generation and evolution of the continental crust: Journal of the Geological Society, v. 167, no. 2, p. 229–248.

Howard, HM, Smithies, RH, Kirkland, CL, Evins, PM and Wingate, MTD 2009, Age and geochemistry of the Alcurra Suite in the western Musgrave Province and implications for orthomagmatic Ni–Cu–PGE mineralization during the Giles Event: Geological Survey of Western Australia, Record 2009/16, 16p.

Jones, SA 2006, Mesoproterozoic Albany–Fraser Orogen-related deformation along the southeastern margin of the Yilgarn Craton: Australian Journal of Earth Sciences, v. 53, p. 213–234.

Kelsey, DE, Clark, C and Hand, M 2008, Thermobarometric modelling of zircon and monazite growth in melt-bearing systems: examples using model metapelitic and metapsammitic granulites: Journal of Metamorphic Geology, v. 26, p. 199–212.

Kemp, AIS, Foster, GL, Schersten, A, Whitehouse, MJ, Darling, J and Storey, CD 2009, Concurrent Pb–Hf isotope analysis of zircon by laser ablation multi-collector ICP-MS, with implications for the crustal evolution of Greenland and the Himalayas: Chemical Geology, v. 261, p. 244–260.

Kemp, AIS, Wilde, SA, Hawkesworth, CJ, Coath, CD, Nemchin, AA, Pidgeon, RT, Vervoort, JD and DuFrane, SA 2010, Hadean crustal evolution revisited: new constraints from Pb–Hf isotope systematics of the Jack Hills zircons: Earth and Planetary Science Letters, v. 296, p. 45–56.

Kendall, BM, Doyle, MG and Gibbs, D 2007, Tropicana: the discovery of a new gold province in Western Australia: NewGenGold Conference, Perth, Western Australia, 15 November 2007; Proceedings, p. 85–95.

Kinny, PD and Maas, R 2003, Lu–Hf and Sm–Nd isotope systems in zircon: Reviews in Mineralogy and Geochemistry, v. 53, no. 1, p. 327–341.

Kirkland, CL, Whitehouse, MJ and Slagstad, T 2009a, Fluid-assisted zircon and monazite growth within a shear zone: a case study from Finnmark, Arctic Norway: Contributions to Mineralogy and Petrology, v. 158, no. 5, p. 637–657.

Kirkland, CL, Wingate, MTD, Spaggiari, CV and Pawley, MJ 2009b, 194721: metagabbronorite, Harris Lake; Geochronology Record 853: Geological Survey of Western Australia, 4p.

Kirkland, CL, Spaggiari, CV, Wingate, MTD, Smithies, RH and Pawley, MJ 2010a, New geochronology from the Albany–Fraser Orogen: implications for Mesoproterozoic magmatism and reworking, *in* Geological Survey of Western Australia Annual Review 2008–09: Geological Survey of Western Australia, Perth, Western Australia, p. 58–65.

Kirkland, CL, Wingate, MTD, Spaggiari, CV and Pawley, MJ 2010b, 194719: metasyenogranite, Symons Hill; Geochronology Record 848: Geological Survey of Western Australia, 5p.

Kirkland, CL, Wingate, MTD, Spaggiari, CV and Pawley, MJ 2010c, 194722: siliciclastic schist, Harris Lake; Geochronology Record 850: Geological Survey of Western Australia, 6p.

Kirkland, CL, Wingate, MTD, Spaggiari, CV and Pawley, MJ 2010d, 194731: psammitic gneiss, Ponton Creek; Geochronology Record 860: Geological Survey of Western Australia, 4p.

Kirkland, CL, Wingate, MTD, Spaggiari, CV and Pawley, MJ 2010e, 194732: metagranodiorite, Ponton Creek; Geochronology Record 855: Geological Survey of Western Australia, 4p.

Kirkland, CL, Wingate, MTD, Spaggiari, CV and Pawley, MJ 2010f, 194733: porphyritic metamonzogranite, Ponton Creek; Geochronology Record 854: Geological Survey of Western Australia, 4p.

Kirkland, CL, Wingate, MTD, Spaggiari, CV and Pawley, MJ 2010g, 194735: quartzofeldspathic gneiss, Gwynne Creek; Geochronology Record 867: Geological Survey of Western Australia, 5p.

Kirkland, CL, Wingate, MTD, Spaggiari, CV and Pawley, MJ 2010h, 194736: metasyenogranite, Bartlett Bluff; Geochronology Record 849: Geological Survey of Western Australia, 4p.

Kirkland, CL, Wingate, MTD, Spaggiari, CV and Pawley, MJ 2010i, 194737: metasyenogranite, Bobbie Point; Geochronology Record 866: Geological Survey of Western Australia, 4p.

Kirkland, CL, Wingate, MTD, Spaggiari, CV and Pawley, MJ 2010j, 194720: rapakivi metadiorite, Harris Lake; Geochronology Record 852: Geological Survey of Western Australia, 4p.

Kirkland, CL, Wingate, MTD, Spaggiari, CV and Pawley, MJ 2010k, 194723: metamonzogranite, Harris Lake; Geochronology Record 851: Geological Survey of Western Australia, 4p.

Kirkland, CL, Wingate, MTD, Spaggiari, CV and Pawley, MJ 2010l, 194724: metasyenogranite, Harris Lake; Geochronology Record 856: Geological Survey of Western Australia, 4p.

Kirkland, CL, Spaggiari, CV, Pawley, MJ, Wingate, MTD, Smithies, RH, Howard, HM, Tyler, IM, Belousova, EA and Poujol, M 2011a, On the edge: U–Pb, Lu–Hf, and Sm–Nd data suggests reworking of the Yilgarn Craton margin during formation of the Albany–Fraser Orogen: Precambrian Research, v. 187, p. 223–247, doi:10.1016/j.precamres.2011.03.002.

Kirkland, CL, Wingate, MTD and Spaggiari, CV 2011b, 184334: migmatitic granitic gneiss, Quagi Beach; Geochronology Record 992: Geological Survey of Western Australia, 4p.

Kirkland, CL, Wingate, MTD and Spaggiari, CV 2011c, 194707: metamonzogranite, Mount Andrew Track; Geochronology Record 990: Geological Survey of Western Australia, 4p.

Kirkland, CL, Wingate, MTD and Spaggiari, CV 2011d, 194708: leucosome in metamonzogranite, Mount Andrew Track; Geochronology Record 989: Geological Survey of Western Australia, 5p.

Kirkland, CL, Wingate, MTD and Spaggiari, CV 2011e, 194709: metagranite, Cave Rock; Geochronology Record 985: Geological Survey of Western Australia, 4p.

Kirkland, CL, Wingate, MTD and Spaggiari, CV 2011f, 194710: metagranite, southwest of Boingaring Rocks; Geochronology Record 996: Geological Survey of Western Australia, 4p.

Kirkland, CL, Wingate, MTD and Spaggiari, CV 2011g, 194712: metasyenogranite, west of Boingaring Rocks; Geochronology Record 997: Geological Survey of Western Australia, 4p.

Kirkland, CL, Wingate, MTD and Spaggiari, CV 2011h, 194714: psammitic gneiss, Gnamma Hill; Geochronology Record 999: Geological Survey of Western Australia, 6p.

Kirkland, CL, Wingate, MTD and Spaggiari, CV 2011i, 194715: leucosome in psammitic gneiss, Gnamma Hill; Geochronology Record 1000: Geological Survey of Western Australia, 4p.

Kirkland, CL, Wingate, MTD, Spaggiari, CV and Tyler, IM 2011j, 194773: granitic rock, Eucla No. 1 drillhole; Geochronology Record 1001, Geological Survey of Western Australia, 4p.

Kirkland, CL, Spaggiari, CV, Wingate, MTD, Smithies, RH, Belousova, EA, Murphy, R and Pawley, MJ 2011k, Inferences on crust–mantle interaction from Lu–Hf isotopes: a case study from the Albany–Fraser Orogen: Geological Survey of Western Australia, Record 2011/12, 25p.

Kositcin, N, Brown, SJA, Barley, ME, Krapež, B, Cassidy, KF and Champion, DC 2008, SHRIMP U–Pb zircon age constraints on the Late Archaean tectonostratigraphic architecture of the Eastern Goldfields Superterrane, Yilgarn Craton, Western Australia: Precambrian Research, v. 161, p. 5–33.

Krapež, B and Barley, ME 2008, Late Archaean synorogenic basins of the Eastern Goldfields Superterrane, Yilgarn Craton, Western Australia. Part III. Signatures of tectonic escape in an arc–continent collision zone: Precambrian Research, v. 161, p. 183–199.

Krapež, B, Barley, ME and Brown, SJA 2008, Late Archaean synorogenic basins of the Eastern Goldfields Superterrane, Yilgarn Craton, Western Australia. Part I. Kalgoorlie and Gindalbie Terranes: Precambrian Research, v. 161, p. 135–153.

Love, GJ 1999, A study of wall-rock contamination in a tonalitic gneiss from King Point, near Albany, Western Australia: Curtin University of Technology, Perth, Western Australia, BSc Honours thesis (unpublished).

Muhling, PC and Brakel, AT (compilers) 1985, Mount Barker – Albany, Western Australia: Geological Survey of Western Australia, 1:250 000 Geological Series Explanatory Notes, 21p.

Myers, JS 1985, The Fraser Complex: a major layered intrusion in Western Australia, *in* Professional papers for 1983: Geological Survey of Western Australia, Report 14, p. 57–66.

Myers, JS 1990a, Albany–Fraser Orogen, *in* Geology and mineral resources of Western Australia: Geological Survey of Western Australia, Memoir 3, p. 255–263.

Myers, JS 1990b, Yilgarn Craton — mafic dyke swarms, *in* Geology and mineral resources of Western Australia: Geological Survey of Western Australia, Memoir 3, p. 126–127.

Myers, JS 1995a, Geology of the Albany 1:1 000 000 sheet: Geological Survey of Western Australia, 1:1 000 000 Geological Series Explanatory Notes, 10p.

Myers, JS 1995b, Geology of the Esperance 1:1 000 000 sheet (2nd edition): Geological Survey of Western Australia, 1:1 000 000 Geological Series Explanatory Notes, 10p.

Myers, JS, Shaw, RD and Tyler, IM 1996, Tectonic evolution of Proterozoic Australia: Tectonics, v. 15, p. 1431–1146.

Nelson, DR 1995a, 112128: muscovite–biotite–sillimanite paragneiss, Point Malcolm; Geochronology Record 499: Geological Survey of Western Australia, 4p.

Nelson, DR 1995b, 83657A: porphyritic biotite monzogranite, Esperance Harbour jetty; Geochronology Record 100: Geological Survey of Western Australia, 4p.

Nelson, DR 1995c, 83659: recrystallized leucogranite, Observatory Point; Geochronology Record 102: Geological Survey of Western Australia, 4p.

Nelson, DR 1995d, 83662: biotite–hornblende monzogranite gneiss, Poison Creek; Geochronology Record 86: Geological Survey of Western Australia, 4p.

Nelson, DR 1995e, 83663: granodiorite gneiss, Israelite Bay; Geochronology Record 74: Geological Survey of Western Australia, 4p.

Nelson, DR 1995f, 83667: porphyritic biotite granite, Balladonia Rock; Geochronology Record 76: Geological Survey of Western Australia, 4p.

Nelson, DR 1995g, 83690: biotite granodiorite gneiss, Bald Rock; Geochronology Record 78: Geological Survey of Western Australia, 4p.

Nelson, DR 1995h, 83697: biotite monzogranite gneiss, Mount Burdett; Geochronology Record 81: Geological Survey of Western Australia, 4p.

Nelson, DR 1995i, 83700A: hornblende–biotite syenogranite gneiss, Coramup Hill Quarry; Geochronology Record 82: Geological Survey of Western Australia, 4p.

Nelson, DR 1996a, 112168: fine-grained sandstone, No Tree Hill; Geochronology Record 491: Geological Survey of Western Australia, 4p.

Nelson, DR 1996b, 112170: metasandstone, Barrens Beach; Geochronology Record 492: Geological Survey of Western Australia, 3p.

Nelson, DR 2001, 168963: mylonitized syenogranite, Mountain Well; Geochronology Record 182: Geological Survey of Western Australia, 4p.

Nelson, DR 2005a, 178070: amphibolite, Haig Cave; Geochronology Record 596: Geological Survey of Western Australia, 4p.

Nelson, DR 2005b, 178071: recrystallized biotite microtonalite, Haig Cave; Geochronology Record 597: Geological Survey of Western Australia, 4p.

Nelson, DR 2005c, 178072: tonalitic gneiss, Haig Cave; Geochronology Record 598: Geological Survey of Western Australia, 4p.

Nelson, DR, Myers, JS and Nutman, AP 1995, Chronology and evolution of the Middle Proterozoic Albany–Fraser Orogen, Western Australia: Australian Journal of Earth Sciences, v. 42, p. 481–495.

Nemchin, AA and Pidgeon, RT 1998, Precise conventional and SHRIMP baddeleyite U–Pb age for the Binneringie Dyke, near Narrogin, Western Australia: Australian Journal of Earth Sciences, v. 45, p. 673–675.

Oorschot, CW 2011, P–T–t evolution of the Fraser Zone, Albany–Fraser Orogen, Western Australia: Geological Survey of Western Australia, Record 2011/18, 101p.

Pawley, MJ, Romano, SS, Hall, CE, Wyche, S and Wingate, MTD 2009, The Yamarna shear zone: a new terrane boundary in the northeastern Yilgarn Craton?, *in* Geological Survey of Western Australia Annual Review 2007–08: Geological Survey of Western Australia, Perth, Western Australia, p. 27–33.

Pawley, MJ, Wingate, MTD, Kirkland, CL, Wyche, S, Hall, CE, Romano, SS and Doublier, MP in press, Adding pieces to the puzzle: episodic crustal growth and a new terrane in the northeast Yilgarn Craton, Western Australia: Australian Journal of Earth Sciences, vol. 59, no. 5.

Pisarevsky, SA, Wingate, MTD and Harris, LB 2003, Late Mesoproterozoic (ca 1.2 Ga) paleomagnetism of the Albany–Fraser Orogen: no pre-Rodinia Australia–Laurentia connection: Geophysical Journal International, v. 155, p. F6–F11.

Rämö, OT (editor) 2005, Granitic systems. Ilmari Haapala volume: Lithos, v. 80, no. 1–4, 402p.

Rasmussen, B, Bengtson, S, Fletcher, IR and McNaughton, N 2002, Discoidal impressions and trace-like fossils more than 1200 million years old: Science, v. 296, p. 1112–1115.

Rasmussen, B and Fletcher, IR 2004, Zirconolite: a new U–Pb chronometer for mafic igneous rocks: Geology, v. 32, p. 785–789.

Rasmussen, B, Fletcher, IR, Bengtson, S and McNaughton, N 2004, SHRIMP U–Pb dating of diagenetic xenotime in the Stirling Range Formation, Western Australia: 1.8 billion year minimum age for the Stirling biota: Precambrian Research, v. 133, p. 329–337.

Shaw, RD, Wellman, P, Gunn, P, Whitaker, AJ, Tarlowski, C and Morse, M 1996, Guide to using the Australian Crustal Elements Map: Australian Geological Survey Organisation, Record 1996/30, 44p.

Sheraton, JW, Black, LP and Tindle, AG 1992, Petrogenesis of plutonic rocks in a Proterozoic granulite-facies terrane — the Bunger Hills, East Antarctica: Chemical Geology, v. 97, p. 163–198, doi:10.1016/0009-2541(92)90075-G.

Sofoulis, J 1958, The geology of the Phillips River Goldfield, W.A.: Geological Survey of Western Australia, Bulletin 110, 240p.

Sofoulis, J 1966, Widgiemooltha, WA SH 51-14: Geological Survey of Western Australia: 1:250 000 Geological Series Explanatory Notes, 25p.

Spaggiari, CV, Bodorkos, S, Barquero-Molina, M, Tyler, IM and Wingate, MTD 2009, Interpreted bedrock geology of the south Yilgarn and central Albany–Fraser Orogen, Western Australia: Geological Survey of Western Australia, Record 2009/10, 84p.

Swager, CP 1997, Tectono-stratigraphy of late Archaean greenstone terranes in the southern Eastern Goldfields, Western Australia: Precambrian Research, v. 83, p. 11–42.

Thom, R and Chin, RJ (compilers) 1984, Bremer Bay, Western Australia: Geological Survey of Western Australia, 1:250 000 Geological Series Explanatory Notes, 20p.

Thom, R, Lipple, SL and Sanders, CC (compilers) 1977, Ravensthorpe, Western Australia: Geological Survey of Western Australia, 1:250 000 Geological Series Explanatory Notes, 38p.

Thom, R, Chin, RJ and Hickman, AH (compilers) 1984a, Newdegate, Western Australia: Geological Survey of Western Australia, 1:250 000 Geological Series Explanatory Notes, 24p.

Thom, R, Hickman, AH and Chin, RJ 1984b, Newdegate, WA Sheet SI50-8: Geological Survey of Western Australia, 1:250 000 Geological Series.

Turek, A 1966, Rubidium–strontium isotopic studies in the Kalgoorlie–Norseman area, Western Australia: Australian National University, Canberra, Australian Capital Territory, PhD thesis (unpublished).

Tyler, IM 2005, Australia: Proterozoic, *in* Encyclopedia of Geology *edited by* RC Selley, LRM Cocks and IR Plimer: Elsevier, Oxford, UK, Volume 1, p. 208–221.

Vallini, DA, Rasmussen, B, Krapež, B, Fletcher, IR and McNaughton, NJ 2002, Obtaining diagenetic ages from metamorphosed sedimentary rocks: U–Pb dating of unusually coarse xenotime cement in phosphatic sandstone: Geology, v. 30, p. 1083–1086.

Vallini, DA, Rasmussen, B, Krapež, B, Fletcher, IR and McNaughton, N 2005, Microtextures, geochemistry and geochronology of authigenic xenotime constraining the cementation history of a Paleoproterozoic metasedimentary sequence: Sedimentology, v. 52, p. 101–122.

van de Graaff, WJE and Bunting, JA (compilers) 1975, Neale, Western Australia: Geological Survey of Western Australia, 1:250 000 Geological Series Explanatory Notes, 23p.

van de Graaff, WJE and Bunting, JA (compilers) 1977, Plumridge, Western Australia: Geological Survey of Western Australia, 1:250 000 Geological Series Explanatory Notes, 28p.

van de Graaff, WJE, Bunting, JA and Lamberts, IT (compilers) 1975, Neale, WA Sheet SH51-4: Geological Survey of Western Australia, 1:250 000 Geological Series.

Wade, BP, Payne, JL, Hand, M and Barovich, KM 2007, Petrogenesis of ca 1.50 Ga granitic gneiss of the Coompana Block: filling the 'magmatic gap' of Mesoproterozoic Australia: Australian Journal of Earth Sciences, v. 54, p. 1089–1102.

Wallace, LM, Ellis, S and Mann, P 2008, Tectonic block rotation, arc curvature, and backarc rifting: Insights into these processes in the Mediterranean and the western Pacific: IOP Conference Series: Earth and Environmental Science, v. 2, no. 1 (012010), doi: 10.1088/1755-1307/2/1/012010.

Webb, AW, Thomson, BP, Blissett, AH, Day, SJ, Flint, RB and Parker, AJ 1982, Geochronology of the Gawler Craton, South Australia: Department of Mines and Energy, South Australia, Report 82/86.

Wetherley, S 1998, Tectonic evolution of the Mount Barren Group, Albany–Fraser Province, Western Australia: University of Western Australia, Perth, Western Australia, PhD thesis (unpublished).

Wingate, MTD 2007, Proterozoic mafic dykes in the Yilgarn Craton, *in* Proceedings *edited by* FP Bierlein and CM Knox-Robinson: Geoscience Australia; Kalgoorlie '07 conference, Kalgoorlie, Western Australia, 25 September 2007; Record 2007/14, p. 80–84.

Wingate, MTD and Bodorkos, S 2007a, 177909: monzogranite gneiss, Yardilla Bore; Geochronology Record 659: Geological Survey of Western Australia, 4p.

Wingate, MTD and Bodorkos, S 2007b, 177910: metamorphosed quartz sandstone, Peters Dam; Geochronology Record 660: Geological Survey of Western Australia, 6p.

Wingate, MTD and Bodorkos, S 2007c, 179644: foliated monzogranite, Mount Andrew; Geochronology Record 676: Geological Survey of Western Australia, 4p.

Wingate, MTD, Campbell, IH and Harris, LB 2000, SHRIMP baddeleyite age for the Fraser Dyke Swarm, southeast Yilgarn Craton, Western Australia: Australian Journal of Earth Sciences, v. 47, p. 309–313.

Wingate, MTD, Pirajno, F and Morris, PA 2004, Warakurna large igneous province: a new Mesoproterozoic large igneous province in west-central Australia: Geology, v. 32, no. 2, p. 105–108.

Wingate, MTD, Morris, PA, Pirajno, F and Pidgeon, RT 2005, Two large igneous provinces in late Mesoproterozoic Australia, *in* Supercontinents and Earth Evolution Symposium 2005 *edited by* MTD Wingate and SA Pisarevsky: Geological Society of Australia; Fremantle, Western Australia, 26 September 2005; Abstracts 81, p. 151.

Witt, WK 1997, Geology of the Ravensthorpe and Cocanarup 1:100 000 sheets: Geological Survey of Western Australia, 1:100 000 Geological Series Explanatory Notes, 26p.

Witt, WK 1998, Geology and mineral resources of the Ravensthorpe and Cocanarup 1:100 000 sheets: Geological Survey of Western Australia, Report 54, 152p.

Wyche, S, Kirkland, CL, Riganti, A, Pawley, MJ, Belousova, EA and Wingate, MTD in press, Isotopic constraints on stratigraphy in the central and eastern Yilgarn Craton, Western Australia: Australian Journal of Earth Sciences, vol. 59, no. 5.

Appendix

Field trip logistics

Logistics

These field excursions are designed on a safari-style, self-drive, self-cater basis; i.e. participants are responsible for their own transport (see notes below regarding vehicle suitability), camping equipment, food, and water. Although this guide provides location details and driving directions, which can be used by anyone wishing to independently follow the excursion routes, it is also recommended that travelers take topographic maps and a GPS for navigation.

The excursions involve several nights of camping. In most of the camping areas, there are no facilities of any kind available. It is important that participants bring enough food and water to last the duration of each excursion, as there is no extra time allocated to stop in towns for shopping. Note also that the route during Excursion 2 does not pass through any towns at all. Opportunities to refuel at Fraser Range Station (Excursion 1) and at the Tropicana camp (Excursion 2) are by prior arrangement only; please note that only diesel is available. We strongly recommend participants fully refuel their vehicles, carry extra fuel if necessary, and stock up on supplies before each excursion,

Health and safety

Many of the areas visited during the two excursions are in remote country, and extra care is required to minimize risks to health and safety. Although every effort is made to minimize such risks, all participants are ultimately responsible for their own safety. GSWA cannot be held responsible for any financial losses, damage to equipment, or personal injuries incurred on these field excursions.

Excursion 2 includes a visit to the mining leases of AngloGold Ashanti, by prior arrangement only. Visitors are required to undergo an induction before viewing drillcore.

Road conditions and vehicle suitability

The field excursion routes cover a mixture of sealed roads, gravel roads, and dirt tracks, with minimal off-road driving. Creek crossings, rocky ground, and moderately dense scrub will be encountered during the course of the field trip, and possible hazards include: damage to vehicles (differentials, sumps, radiators etc.), tyre punctures, spinifex fires, and bogs (sand and mud). Suitable four-wheel drive (4WD) vehicles are required, and need to be fitted or supplied with fire extinguishers, first-aid kits, and all repair and recovery equipment typically required during off-road driving, including tyre changing and repair, and bog recovery equipment. If vehicles are not fitted with long-range fuel tanks, care must be taken to properly store any portable fuel tanks (e.g. jerry cans). All drivers should be suitably certified or experienced in off-road (4WD) driving.

Convoy procedure

This section applies to all GSWA-led excursions, which can involve large numbers (as many as 20) of vehicles travelling for long distances. Normal convoy etiquette applies, as follows:

- Each day will begin with a meeting at which the day's itinerary will be discussed.
- The convoy speed will be determined by the slowest vehicle, noting that many of the participants are already restricted by their employers to speeds lower than State speed limits.
- Each vehicle will travel with headlights on whilst on main roads and tracks.
- Each driver will maintain safe travel distances between them and the vehicles in front and behind, and will be considerate of local traffic.
- At each turnoff, intersection, or obstacle, each driver will wait until they have made clear visual (and acknowledged) contact with the vehicle behind; each driver will acknowledge to a waiting vehicle in front that they have observed the turnoff (e.g. by flashing headlights).
- UHF radio equipment should be fitted or carried by each vehicle; a frequency/channel will be agreed upon at the beginning of the trip and maintained throughout the excursion. A limited number of hand-held UHF radios will be available for those who do not have UHF sets.
- Regular vehicle counts will be performed.
- Should a vehicle become detached from the convoy and unable to communicate via UHF radio, a series of rendezvous points have been identified. The vehicle is to return to the appropriate rendezvous point and wait to be reunited with the convoy. These rendezvous points are:

Excursion 1

Day 1:

AM: corner of Farrell's Road and South Coast Highway — 33°44′18.2″S, 121°17′53.7″E

PM: intersection of the Coolgardie–Esperance Highway and Telegraph Track — 32°21′16.4″S, 121°45′34.0″E

Day 2:

AM: Stop 2 — MGA 492094E 6395845N

PM: intersection of the Mount Andrew Track and Telegraph Track — MGA 481033E 6411397N

Day 3:

AM: Stop 5, Gnamma Hill — MGA 471530E 6439471N

PM: Fraser Range Station — MGA 480565E 6456426N

Day 4:

AM(1): intersection of the Symon's Hill Track and track to Stop 8 — MGA 529791E 651812N

AM(2): track junction before Stop 9 — MGA 547044E 6533286N

PM(1): Stop 9 — MGA 546153E 6534950N

PM(2): intersection of north–south track with Trans-Australian Railway — MGA 543409E 6566785N

Excursion 2

Travel from Kalgoorlie to Tropicana:

AM(1): Pinjin, right-hand turnoff to Tropicana — MGA 472830E 6671045N

AM(2): Argus Corner (about 3 hours from Kalgoorlie) — 30°10′05″S, 123°37′45″E

PM(1): Start of Tropicana Road — MGA 629731E 6729068N

Day 1:

PM: Stop 2, Hat Trick Hill — MGA 654578E 6765600N

Day 2:

AM: intersection of the Rason Lake Road and Bobbie Point Track — MGA 657631E 6790252N

PM: Stop 5, McKay Creek area — MGA 675563E 6802915N

Day 3:

AM: intersection of the Rason Lake Road and Tropicana Camp Road — MGA 663957E 6762255N

PM: Stop 8, Pleiades Lakes area — MGA 684468E 6770483N

Day 4:

AM: Stop 7, Pleiades Lakes area — MGA 683549E 6770104N

PM: Start of Plumridge Lakes Nature Reserve — MGA 681534E 6753770N

Travel from Tropicana to Kalgoorlie:

AM(1): intersection of the Tropicana Road with Argus Corner Road — MGA 629731E 6729068N

PM(1): Argus Corner (about 5 hours from Tropicana) — 30°10′05″S, 123°37′45″E

PM 2: Pinjin, left-hand turnoff onto Pinjin–Kurnalpi Road — MGA 472830E 6671045N

Climatic conditions

These field excursions were designed to be run in September, when daytime maximum temperatures can be expected to be between 15 and 25º C (Excursion 1), and between 18 to 28º C (Excursion 2). Night-time minimum temperatures can be expected to drop to between 0º and 10°C (Excursion 1), and between 8º and 13°C (Excursion 2). Strong winds and rain are possibilities. A UV hazard is likely, and participants are expected to take their own precautions against sunburn. In spring, hayfever may also be of concern to susceptible participants and these people should take their own precautions (medication). If using this field guide to travel at other times of the year, please check expected weather conditions. Note that summer temperatures can be extreme.

Walking and hiking

Some of the excursion stops require short hikes (typically less than 1 km) over rocky ground. Appropriate protective clothing should be worn, including hiking or safety boots.

Stop 1 of Excursion 1 is on a coastal rock platform east of Esperance, overlooking the Southern Ocean. Although the outcrop is above the high-water mark, participants should be vigilant and keep an outlook for waves sweeping over the rock platforms. Tide predictions can be found on the Bureau of Meteorology Website at <http://www.bom.gov.au/oceanography/tides/>.

Camping

The excursion involves several nights of camping. Participants are responsible for bringing their own camping equipment, including swags, tents, and food. Potential hazards involved in collecting firewood and around open fires are to be noted and appropriate care taken. All rubbish is to be removed. All participants are requested to exercise appropriate care and discretion with respect to ablutions, and all waste is to be buried and tissues disposed of by burning (noting bushfire hazards in doing so, particularly in high winds). Please be aware of the potential to become disoriented and detached from the camp whilst seeking privacy for ablutions. If you get lost, stay where you are and wait for your absence to be noticed. Always carry a box of matches or a lighter in case you need to light a signal fire.

Other potential hazards involved with camping in the Albany–Fraser region include snake bites, and scorpion, centipede, spider, and other insect bites or stings.

Note that wild camels represent a threat, and should never be approached.

Radio schedules and safety checks

All GSWA vehicles are equipped with, or will carry, UHF and HF radios, satellite phones, GPS vehicle tracking systems, and EPIRBs. It is a requirement for all GSWA field staff to communicate with GSWA's Perth Radio Room or an identified Safety Officer twice each day (morning and afternoon). During the excursion, the excursion leaders will report on the well-being of the entire excursion group, but each participant should also maintain their own safety schedules if they have such procedures in place.

RECORD 2011/23

THE GEOLOGY OF THE EAST ALBANY–FRASER OROGEN — A FIELD GUIDE

Spaggiari et al.

This Record is published in digital format (PDF) and is available as a free download from the DMP website at <http://www.dmp.wa.gov.au/GSWApublications>.

Further details of geological products produced by the Geological Survey of Western Australia can be obtained by contacting:

Information Centre
Department of Mines and Petroleum
100 Plain Street
EAST PERTH WESTERN AUSTRALIA 6004
Phone: (08) 9222 3459 Fax: (08) 9222 3444
http://www.dmp.wa.gov.au/GSWApublications

SHEET INDEX

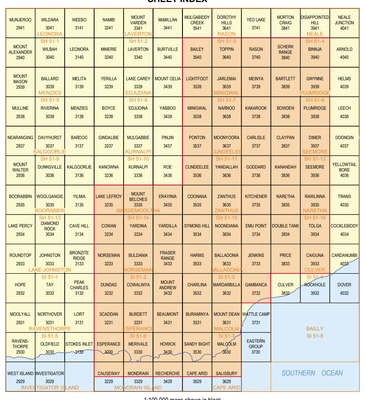

1:100 000 maps shown in black

1:250 000 maps shown in brown

Search for current GSWA map products online <http://www.dmp.wa.gov.au/GSWApublications>

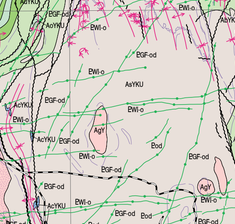

Fault, major
- exposed
- thrust, exposed, triangle on upthrown side
- strike-slip, exposed, showing relative dextral horizontal displacement
- strike-slip, exposed, showing relative sinistral horizontal displacement
- thrust, concealed, triangle on upthrown side
- concealed

Fault
- exposed
- normal, exposed, tick on downthrown side
- thrust, exposed, triangle on upthrown side
- reverse, exposed, triangle on upthrown side
- strike-slip, exposed, showing relative dextral horizontal displacement
- strike-slip, exposed, showing relative sinistral horizontal displacement
- concealed

Fault or shear, major
- exposed
- strike-slip, exposed, showing relative dextral horizontal displacement
- strike-slip, exposed, showing relative sinistral horizontal displacement
- concealed

Fault or shear
- exposed
- normal, exposed, tick on downthrown side
- strike-slip, exposed, showing relative dextral horizontal displacement
- strike-slip, exposed, showing relative sinistral horizontal displacement
- concealed

Fold, showing axial trace
- unspecified
- anticline, exposed
- syncline, exposed
- overturned anticline, exposed
- overturned syncline, exposed
- antiformal syncline, exposed
- antiform, exposed
- synform, exposed

Bedding
- trend of bedding

Igneous layering
- trend of igneous layering

Metamorphic foliation
- trend of metamorphic foliation

Gneissic layering
- trend of gneissic layering

Fracture pattern

Aeromagnetic trend line

Formed road

Track

Railway, operating

Townsite
- population 10 000–15 000
- less than 1 000

Homestead

Roadhouse

Mine, proposed

ESPERANCE
Scaddan
Coonana
Balladonia
TROPICANA

Mineralization site on this map has been extracted from GSWA's MINEDEX database. For clarity, other sites have been omitted. Full details of site numbers, site locations, site status, mineralization, and commodities can be obtained from the MINEDEX database, accessed at <http://www.dmp.wa.gov.au/minedex>.

SEE PLATE 1A FOR GEOLOGICAL REFERENCE

PLATE 2

Compiled by CV Spaggiari 2009–11 (Albany–Fraser), MJ Pawley 2010–11 (Yilgarn); southeast Yilgarn extracted from Geological Survey of Western Australia 2005 and 2008, 1:500 000 scale interpreted bedrock geology

Geology by CV Spaggiari 2006–11, CL Kirkland 2008–11, and MJ Pawley 2008 (Albany–Fraser); MP Doublier, CM Doyle, B Goscombe, PB Groenewald, CE Hall, S Jones, MGM Painter, MJ Pawley, SS Romano, and S Wyche 1998–08 (east Yilgarn); TJ Griffin 1980–84, AH Hickman 1979–81, and P McGoldrick 1988–90 (southeast Yilgarn)

Cartography by AK Jones

Edited by K Greenberg and SK Martin

Published by the Geological Survey of Western Australia

This map is published in digital format (PDF) and is available online at <http://www.dmp.wa.gov.au/GSWApublications>.
Copies of this map are available from the Information Centre, Department of Mines and Petroleum,
100 Plain Street, East Perth, WA 6004.
Phone (08) 9222 3459 Fax (08) 9222 3444
Website <http://www.dmp.wa.gov.au/gswa> Email geological.survey@dmp.wa.gov.au

The recommended reference for this map is:
Spaggiari, CV and Pawley, MJ 2012, Interpreted pre-Mesozoic bedrock geology of the east Albany–Fraser Orogen and southeast Yilgarn Craton (1:500 000), *in* The geology of the east Albany–Fraser Orogen — a field guide *compiled by* CV Spaggiari, CL Kirkland, MJ Pawley, RH Smithies, MTD Wingate, MG Doyle, TG Blenkinsop, C Clark, DW Oorschot, LJ Fox, and J Savage: Geological Survey of Western Australia, Record 2011/23, Plate 1.

Government of **Western Australia**
Department of **Mines and Petroleum**

HON. NORMAN MOORE, M.L.C.
MINISTER FOR MINES AND PETROLEUM

Geological Survey of Western Australia

RICK ROGERSON
EXECUTIVE DIRECTOR

SCALE 1:500 000

5 000 0 10 20 30 40 50
Metres Kilometres

UNIVERSAL TRANSVERSE MERCATOR PROJECTION
HORIZONTAL DATUM: GEOCENTRIC DATUM OF AUSTRALIA 1994
VERTICAL DATUM: AUSTRALIAN HEIGHT DATUM

Grid lines indicate 20 000 metre interval of the Map Grid Australia Zone 51

GDA

The Map Grip Australia (MGA) is based on the Geocentric Datum of Australia 1994 (GDA94)
GDA94 positions are compatible within one metre of the datum WGS84 positions

GEOLOGICAL SURVEY OF WESTERN AUSTRALIA

RECORD 2011/23 PLATE 1

INTERPRETED PRE-MESOZOIC BEDROCK GEOLOGY OF THE EAST ALBANY–FRASER OROGEN AND SOUTHEAST YILGARN CRATON

June 2012

PROTEROZOIC–PHANEROZOIC

PALEOZOIC

CARBONIFEROUS–PERMIAN

318–270 Ma — CPpo-sepg — **PATERSON FORMATION:** conglomerate (including diamictite), sandstone, and siltstone; largely glacigene

EPBN-od — **Beenong Dyke Suite:** mafic dykes; northwesterly trending; interpreted from aeromagnetic data
EPNB-od — **Nindibillup Dyke Suite:** mafic dykes; west-northwesterly trending, variably magnetic; some exceeding 400 km long; mostly interpreted from aeromagnetic data
EPNW-od — **Cosmo Newbery Dyke Suite:** northwest-trending mafic dykes; interpreted from aeromagnetic data; concealed where dashed

Eo — Mafic intrusive rock
Eod — Dolerite dyke, sill, or plug; fine- to medium-grained dolerite and gabbro; concealed where dashed

PROTEROZOIC

MESOPROTEROZOIC

Albany–Fraser Orogeny Stage II (1215–1140 Ma)

1200–1140 Ma — Esperance Supersuite — EEP-g, EEP-gm
EEP-g — Granitic rock; undeformed to moderately deformed
EEP-gm — Monzogranite; undeformed to moderately deformed; includes magnetite-rich varieties

c. 1210 Ma — Giovenangrup–Fraser Dyke Suite — EGF-od — Dolerite and gabbro dykes; east-northeast- to northeast-trending; mostly interpreted from aeromagnetic data; concealed where dashed

1321–1150 Ma — Erg-mh — **MOUNT RAGGED FORMATION:** psammitic schist and quartzite interbedded with thin layers of pelitic rocks

Albany–Fraser Orogeny Stage I (1345–1260 Ma)

1330–1280 Ma — Recherche Supersuite — ERE-mg, ERE-mgm
ERE-mg — Metagranite; heterogeneous; even grained or porphyritic; moderately to strongly deformed; may include intrusions of **Esperance Supersuite**
ERE-mgm — Monzogranitic gneiss; may contain remnants of **Biranup Zone** rocks

PALEOPROTEROZOIC–MESOPROTEROZOIC

1480–1345 Ma — Egk-xmtn-mo, Emm-xmh-mws
Egk-xmtn-mo — **GWYNNE CREEK GNEISS:** psammitic gneiss with minor semipelitic layers; includes minor metagranitic, metamafic, and meta-ultramafic rocks
Emm-xmh-mws — **MALCOLM METAMORPHICS:** interbedded psammitic and pelitic schist; mafic amphibolitic schist; minor calc-silicate rocks; may include granitic dykes and intrusions

Exmg-mwMD — Metagranitic and metamafic rocks, undivided; may include metasedimentary rocks

Biranup Orogeny (1710–1620 Ma)

1700–1620 Ma — EmgBR, Exmg-mogBR, Exmgn-mogBR, Exmgn-mdnBR, Exmgni-mhnBR
EmgBR — Metagranite
Exmg-mogBR — K-feldspar megacrystic metagranite and metasyenogranite, mingled with metagabbroic rocks; hybrid rocks; may include remnants of Archean rocks
Exmgn-mogBR — Granitic gneiss intruded by coarse pegmatite; undivided; may include interleaved Fraser Zone rocks
Exmgn-mdnBR — Granitic and metasedimentary gneisses dominant; includes intrusions of **Recherche** and **Esperance Supersuites**; may include remnants of Archean rocks
Exmgni-mhnBR — Migmatitic, monzogranitic to syenogranitic gneisses dominant; commonly garnet-bearing; may include remnants of Archean rocks

c. 1708 Ma — Ebt-mgr — **BOBBIE POINT METASYENOGRANITE:** metasyenogranite; weakly foliated to mylonitic; includes minor mingled mafic rocks and minor banded iron-formation rafts

c. 1760 Ma — Ekc-xmgr-mgi — **McKAY CREEK METASYENOGRANITE:** metasyenogranite, mingled with metagabbro; localized hybrids of metagranodiorite and metadiorite; may include intrusions of **BOBBIE POINT METASYENOGRANITE** and remnants of Archean rocks

c. 2410 Ma — Widgiemooltha Dyke Suite — EWl-o — Dolerite and gabbro; includes cumulate and granophyric differentiates; concealed where dashed

2700–1650 Ma — ÆmgBR, ÆmgnBR, ÆmgnBR, ÆxmgssBR, ÆxmwoBR
ÆmgBR — Metagranitic rocks dominant; may include remnants of Archean rocks
ÆmgnBR — Metagranitic and gneissic rocks dominant, locally with mafic amphibolite lenses; may include remnants of Archean rocks
ÆmgnBR — Migmatitic, monzogranitic to syenogranitic granitic gneisses dominant; most are garnet-bearing; may include remnants of Archean rocks
ÆxmgssBR — Foliated metagranitic rocks with lenses of mafic amphibolite; may include remnants of Archean rocks
ÆxmwoBR — Mafic amphibolite dominant; intruded by foliated metagranitic rocks; may include remnants of Archean rocks

2800–1330 Ma — ÆxmnAFON, ÆxmgnAFON, ÆxmgAFON
ÆxmnAFON — Meta banded iron-formation, metagabbro, and metaleucogabbro; may include metagranite and **Biranup Zone** intrusions
ÆxmgnAFON — Granitic gneiss; quartzofeldspathic gneiss, locally with garnet; amphibolite; metagranite; minor meta banded iron-formation; may include **Biranup Zone** intrusions
ÆxmgAFON — Metagranitic and metamafic rocks; Archean granite and greenstone and Proterozoic granitic and mafic rocks deformed and metamorphosed during the **Albany–Fraser Orogeny**

2900–2660 Ma — AxmiAFON, AxmogAFON, AmoAFON, AxmbAFON, AmbAFON, AxmuAFON
AxmiAFON — Meta banded iron-formation, metachert, metasedimentary rocks, and amphibolite
AxmogAFON — Metagabbro and meta-ultramafic rocks; intruded by metagranite
AmoAFON — Meta-igneous mafic intrusive rock, undivided
AxmbAFON — Greenstones, undivided; may include iron formation
AmbAFON — Metamafic volcanic rocks, undivided
AxmuAFON — Meta-ultramafic rocks, quartzite, metaconglomerate, and metasandstone

AmgmY, AmgnY, AmgssY, AgY, AgmY

AmgmY — Biotite metamonzogranite; medium to coarse grained
AmgnY — Granitic gneiss, locally migmatitic; includes local mafic bands and enclaves
AmgssY — Foliated metagranite, locally gneissic; may include amphibolite lenses; includes deeply weathered rock
AgY — Granitic rock, undivided; metamorphosed
AgmY — Monzogranite; common biotite and rare local hornblende; minor granodiorite and syenogranite; fine to coarse grained; equigranular to porphyritic; massive to weakly foliated; metamorphosed

AmnYKA — Gneiss; protolith unknown

AsYKA — Siliciclastic sedimentary rock, undivided; includes sandstone, siltstone, shale, and chert; metamorphosed

2686–2666 Ma [1,4] — AmfYKA, AfYKA
AmfYKA — Felsic metavolcaniclastic rock
AfYKA — Felsic volcanic and volcaniclastic rock; metamorphosed; commonly deeply weathered and kaolinized

AmwoYKA — Amphibolite

2696 Ma [3] — AoYKA — Mafic intrusive rock, undivided; metamorphosed; includes deeply weathered rocks

2715–2692 Ma [4] — AbYKA — Fine to very fine grained mafic rock, minor ultramafic rock, undivided; metamorphosed; commonly deeply weathered

AoYKA — Ultramafic rock; may include pyroxenite and serpentinite; metamorphosed

AuYKA — Ultramafic volcanic rock; metamorphosed

AmtYKU — Quartzofeldspathic gneiss

AsYKU — Sedimentary rock, undivided; includes sandstone, siltstone, shale, and chert; metamorphosed; commonly deeply weathered

AcYKU — Chert and banded iron-formation; undivided; metamorphosed

2714–2704 Ma [4] — AfYKU — Felsic volcanic and volcaniclastic rock; metamorphosed; commonly deeply weathered and kaolinized

AoYKU — Mafic intrusive rock, undivided; metamorphosed; includes deeply weathered rocks

AbYKU, AbsYKU

AbYKU — Fine to very fine grained mafic rock, minor ultramafic rock, undivided; metamorphosed; commonly deeply weathered
AbsYKU — Pyroxene spinifex-textured basalt; locally variolitic and/or pillowed; metamorphosed

ARCHEAN

AuYKU — Ultramafic volcanic rock; metamorphosed

Abtoxs — **TOBIN FORMATION:** wacke, lithic sandstone, siltstone, abundant chert and banded iron-formation, and minor felsic volcaniclastic rocks; metamorphosed

2699–2682 Ma [4,7] — Abp-xf-v — **TOPPIN HILL FORMATION:** felsic volcanic and volcaniclastic rocks, with minor siliciclastic sedimentary rocks; metamorphosed

AmqtYYA — Quartzofeldspathic gneiss, locally strongly foliated

AmwYYA — Meta-igneous mafic rock; undivided

AoYYA — Igneous mafic intrusive rock, undivided; metamorphosed

AmbYYA, Axb-ogIYA, AbYYA
AmbYYA — Metamafic volcanic rock, undivided
Axb-ogIYA — Mafic volcanic rock with minor gabbro; metamorphosed
AbYYA — Mafic volcanic rock; metamorphosed

Mingliwel Suite

2769–2765 Ma [4] — AMN-mgn — Granitic gneiss

AmqYBU — Quartzofeldspathic gneiss derived from felsic volcanic and/or sedimentary rock

c. 2774 Ma — Ahj-fdvd — **HANNS JASPER FORMATION:** dacitic volcaniclastic sandstone; crystal and lithic rich; metamorphosed

AmdYBU, AsYBU
AmdYBU — Metasedimentary rock, undivided; includes metamorphosed sandstone, siltstone, shale, and chert
AsYBU — Siliciclastic rocks, undivided; metamorphosed

AmcYBU, AcYBU
AmcYBU — Metachert
AcYBU — Chemical sedimentary rock, undivided; metamorphosed

AmfdYBU — Meta-andesite

AmwYBU — Meta-igneous mafic rock; undivided

AmoYBU, AoYBU
AmoYBU — Metamafic intrusive rock
AoYBU — Igneous mafic intrusive rock, undivided; metamorphosed

AmbYBU, AbYBU
AmbYBU — Metamafic volcanic rock, undivided
AbYBU — Mafic volcanic rock, undivided; metamorphosed

AmoYBU — Meta-igneous ultramafic intrusive rock, undivided

AmuYBU — Meta-ultramafic rock, undivided; includes talc–chlorite(–carbonate) and tremolite–chlorite schist

c. 1620 Ma — Efd-mhng — **FLY DAM FORMATION:** interbedded psammitic to pelitic gneiss with leucosomes; pelitic layers garnet- and biotite-rich

Edgy Suite — c. 1665 Ma — EEY-xmgg-mog — Metagranodiorite, metadiorite and metagabbro, granitic gneiss, lenses of metasedimentary rocks, and pegmatite; may include remnants of other **Biranup Zone units**

c. 1750 Ma — Ewo-mt — **WOODLINE FORMATION:** quartz metasandstone, quartz metaconglomerate, and metasiltstone

c. 1305–1290 Ma — EmogFR, Exmog-mgnFR
EmogFR — Metagabbroic rocks; may include felsic granulite, metagranitic and metasedimentary rocks; undivided
Exmog-mgnFR — Metagabbroic and metamafic rocks; may include metagranite and metasedimentary rocks, mafic and felsic granulite

1305–1290 Ma — EFM-xmog-mgn — **FRASER RANGE METAMORPHICS:** sheeted and mostly strongly deformed metagabbro, metagranite, and minor metasedimentary rocks; includes hybrid rocks and mafic and felsic granulite

1335–1290 Ma — EFM-xmdn-mhn, EFM-xmhn-mno

FRASER RANGE METAMORPHICS
EFM-xmdn-mhn — Sedimentary gneiss; psammitic, semipelitic, and locally calc-silicate layers; commonly interlayered with bands of amphibolite, or mafic and felsic granulite
EFM-xmhn-mno — Sedimentary gneiss; interlayered psammitic to pelitic, amphibolite- to granulite- facies gneiss, commonly interlayered with bands of amphibolite, or mafic and felsic granulite

Exmt-mqAFOB — Quartzite and metasandstone, interbedded with metasiltstone; locally interbedded with metaconglomerate and pebbly metasandstone

2700–2630 Ma — AmgmBR, AmgrBR
AmgmBR — Metamonzogranite; foliated
AmgrBR — Metasyenogranite; mostly homogeneous; weakly to strongly foliated; local folded mafic amphibolite lenses; sparse leucosomes

2710–1330 Ma — ÆmuxmgnMO — **MUNGLINUP GNEISS:** granitic gneiss, heterogeneous, and minor metamafic rocks; Archean granite and greenstone and Proterozoic granitic and mafic rock deformed and metamorphosed during the **Albany–Fraser Orogeny**

GUNBARREL BASIN

ALBANY–FRASER OROGEN

RAGGED BASIN

Fraser and Nornalup Zones

ALBANY–FRASER OROGEN

ARID BASIN

MADURA PROVINCE

Biranup Zone

ALBANY–FRASER OROGEN

BARREN BASIN

Biranup Zone

Biranup Zone

Northern Foreland

ALBANY–FRASER OROGEN

YILGARN CRATON

Kalgoorlie Terrane

Yilgarn Craton

Kurnalpi Terrane

Burtville Terrane

REDUCED-TO-POLE AEROMAGNETIC IMAGE

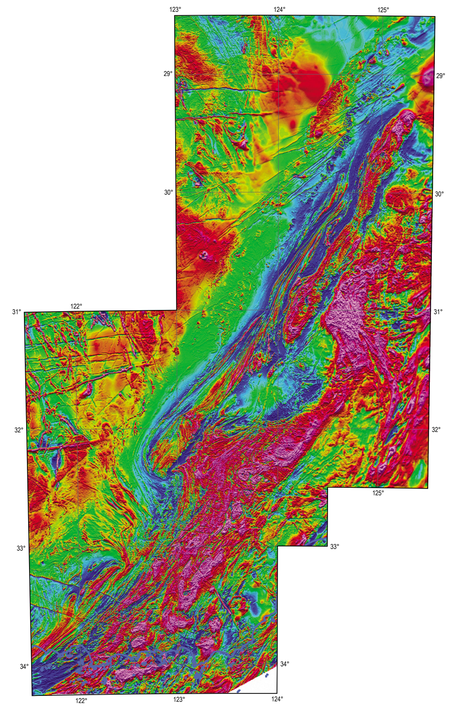

SCALE 1:3 000 000
0 200
Kilometres

BOUGUER GRAVITY IMAGE

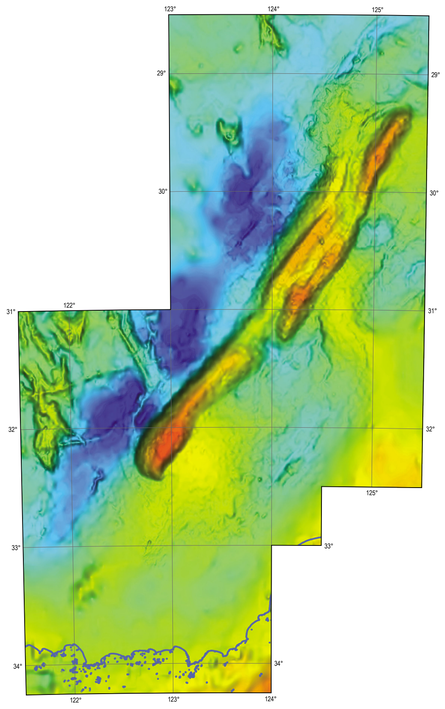

SCALE 1:3 000 000
0 200
Kilometres

RADIOMETRIC TERNARY IMAGE

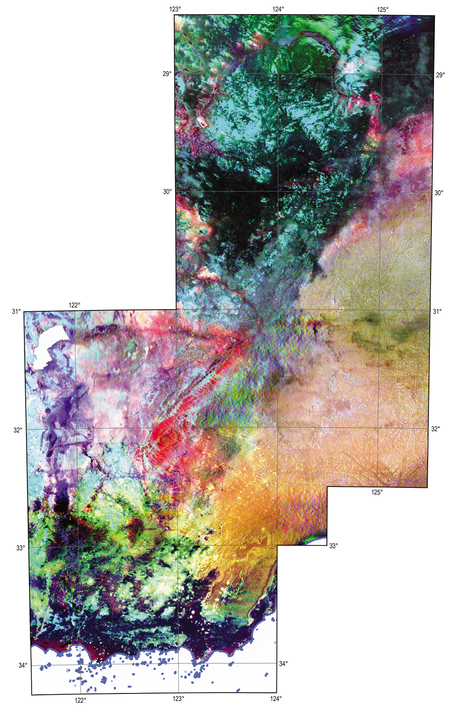

SCALE 1:3 000 000
0 200
Kilometres

SRTM IMAGE

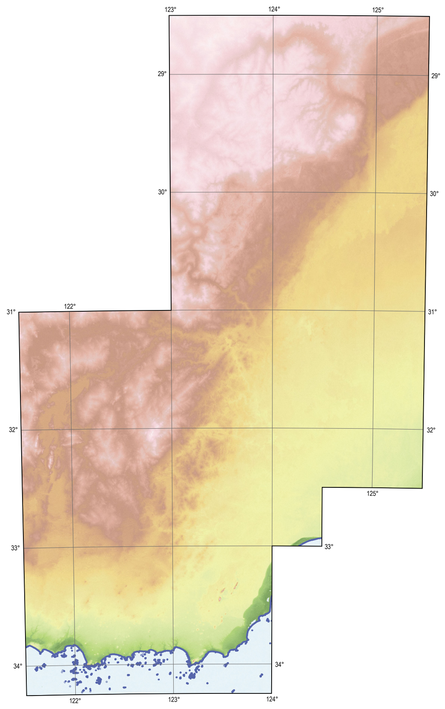

SCALE 1:3 000 000
0 200
Kilometres

SHEET INDEX

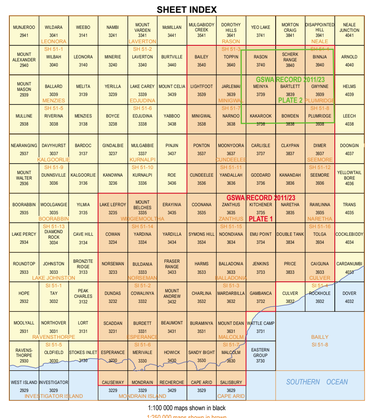

1:100 000 maps shown in black
1:250 000 maps shown in brown

Search for current GSWA map products online <http://www.dmp.wa.gov.au/GSWApublications>

DATA DICTIONARY

Theme	Data Currency	Organization
Geology *	2011	Geological Survey of Western Australia, Department of Mines and Petroleum
Mineral sites *	JAN 2012	Geological Survey of Western Australia, Department of Mines and Petroleum

* DMP data can be viewed interactively via GeoVIEW.WA <http://www.dmp.wa.gov.au/geoview>, and related datasets can be downloaded from the GSWA Data and Software Centre <http://www.dmp.wa.gov.au/datacentre>.

Compiled by CV Spaggiari 2009–11 (Albany–Fraser), MJ Pawley 2010–11 (east Yilgarn); southeast Yilgarn extracted from Geological Survey of Western Australia 2005 and 2008, 1:500 000 scale interpreted bedrock geology

Geology by CV Spaggiari 2006–11, CL Kirkland 2008–11, and MJ Pawley 2008 (Albany–Fraser); CM Doyle and S Jones 2005, MP Doublier, CE Hall, MJ Pawley, SS Romano, and S Wyche 1998–08 (east Yilgarn); TJ Griffin 1980–84, AH Hickman 1979–81, and P McGoldrick 1988–90 (southeast Yilgarn)

Geochronology from GSWA data (published and in preparation) and interpreted from external sources (listed below). Some GSWA geochronology may come from samples obtained on adjoining sheets. GSWA geochronology data are available online at <http://www.dmp.wa.gov.au/geochron>.

Geochronology by:

1) Cassidy, KF 2007, GA Sample 989670S0B: Geoscience Australia's geochronology database, July 2007 data release.
2) Durphy, JM et al. 2003, Geoscience Australia, Record 2003/15, p. 95–99.
3) Krapež, B et al. 2000, Tectonophysics v. 322, p. 89–133.
4) Kositcin, N et al. 2008, Precambrian Research v. 161, p. 5–33.
5) Fletcher, IR et al. 2001, Geoscience Australia, Record 2001/47, p. 44–47.
6) Sircombe, KN et al. 2007, Geoscience Australia, Record 2007/1, p. 169–174.
7) Sircombe, KN et al. 2007, Geoscience Australia, Record 2007/1, p. 175–180.
8) Fletcher, IR et al. 2001, Geoscience Australia, Record 2001/47, p. 27–30.

Cartography by AK Jones

Edited by K Greenberg and SK Martin

Published by the Geological Survey of Western Australia

This plate is published in digital format (PDF) and is available online at <http://www.dmp.wa.gov.au/GSWApublications>. Copies of this plate are available from the Information Centre, Department of Mines and Petroleum, 100 Plain Street, East Perth, WA 6004.
Phone (08) 9222 3459 Fax (08) 9222 3444
Website <http://www.dmp.wa.gov.au/gswa> Email geological.survey@dmp.wa.gov.au

The recommended reference for this plate is:
Spaggiari, CV and Pawley, MJ 2012, Interpreted pre-Mesozoic bedrock geology of the east Albany–Fraser Orogen and southeast Yilgarn Craton (1:500 000), *in* The geology of the east Albany–Fraser Orogen — a field guide *compiled by* CV Spaggiari, CL Kirkland, MJ Pawley, RH Smithies, MTD Wingate, MG Doyle, TG Blenkinsop, C Clark, CW Oorschot, LJ Fox, and J Savage: Geological Survey of Western Australia, Record 2011/23, Plate 1A.

Government of **Western Australia**
Department of **Mines and Petroleum**

HON. NORMAN MOORE, M.L.C.
MINISTER FOR MINES AND PETROLEUM

Geological Survey of Western Australia

RICK ROGERSON
EXECUTIVE DIRECTOR

SCALE 1:500 000
5 000 0 10 20 30 40 50
Metres Kilometres

UNIVERSAL TRANSVERSE MERCATOR PROJECTION
HORIZONTAL DATUM: GEOCENTRIC DATUM OF AUSTRALIA 1994
VERTICAL DATUM: AUSTRALIAN HEIGHT DATUM

Grid lines indicate 20 000 metre interval of the Map Grid Australia Zone 51

GDA

The Map Grip Australia (MGA) is based on the Geocentric Datum of Australia 1994 (GDA94)
GDA94 positions are compatible within one metre of the datum WGS84 positions

GEOLOGICAL SURVEY OF WESTERN AUSTRALIA
RECORD 2011/23 PLATE 1A

GEOPHYSICAL AND REMOTE SENSING IMAGERY AND REFERENCE FOR PLATE 1, EAST ALBANY–FRASER OROGEN AND SOUTHEAST YILGARN CRATON

June 2012

PHANEROZOIC — PALEOZOIC — CARBONIFEROUS–PERMIAN

318–270 Ma — CPpα-sepg — **PATERSON FORMATION:** conglomerate (including diamictite), sandstone, and siltstone; largely glacigene

Cosmo Newbery Dyke Suite

ᵽPNW-od — Northwest-trending mafic dykes; interpreted from aeromagnetic data; concealed where dashed

ᵽod — Dolerite dyke, sill, or plug; fine- to medium-grained dolerite and gabbro; concealed where dashed

PROTEROZOIC — MESOPROTEROZOIC

Albany–Fraser Orogeny Stage II (1215–1140 Ma)

1200–1140 Ma — Esperance Supersuite — ᵽEP-g — Granitic rocks; undeformed to moderately deformed

c. 1210 Ma — Gnowangerup–Fraser Dyke Suite — ᵽGF-od — Dolerite and gabbro dykes; east-northeast- to northeast-trending; mostly interpreted from aeromagnetic data

Albany–Fraser Orogeny Stage I (1345–1260 Ma)

1330–1280 Ma — Recherche Supersuite — ᵽRE-mg — Metagranite; heterogeneous; even grained or porphyritic; moderately to strongly deformed; may include intrusions of **Esperance Supersuite**

1305–1290 Ma — ᵽmogFR, ᵽxmog-mgnFR

ᵽmogFR — Metagabbroic rocks; may include felsic granulite, metagranitic and metasedimentary rocks; undivided

ᵽxmog-mgnFR — Metagabbroic and metamafic rocks; may include metagranite and metasedimentary rocks, mafic and felsic granulite

1480–1300 Ma — ᵽgk-xmtn-mo — **GWYNNE CREEK GNEISS:** psammitic gneiss with minor semipelitic layers; includes minor metagranitic, metamafic, and meta-ultramafic rocks

PALEOPROTEROZOIC

Biranup Orogeny (1710–1620 Ma)

1700–1620 Ma — ᵽmgBR, ᵽxmg-mogBR, ᵽxmgn-mogBR

ᵽmgBR — Metagranite

ᵽxmg-mogBR — K-feldspar megacrystic metagranite and metasyenogranite, mingled with metagabbroic rocks; hybrid rocks; may include remnants of Archean rocks

ᵽxmgn-mogBR — Granitic gneiss intruded by coarse pegmatite; undivided; may include interleaved **Fraser Zone** rocks

1708 Ma — ᵽbt-mgr — **BOBBIE POINT METASYENOGRANITE:** metasyenogranite; weakly foliated to mylonitic; includes minor mingled mafic rocks and minor banded iron-formation rafts

c. 1750 Ma — ᵽxmt-mtqAFOB — Quartzite and metasandstone, interbedded with metasiltstone; locally interbedded with metaconglomerate and pebbly metasandstone

1760 Ma — ᵽkc-xmgr-mgi — **McKAY CREEK METASYENOGRANITE:** metasyenogranite, mingled with metagabbro; localized hybrids of metagranodiorite and metadiorite; may include intrusions of **BOBBIE POINT METASYENOGRANITE** and remnants of Archean rocks

ARCHEAN–PROTEROZOIC — NEOARCHEAN–PALEOPROTEROZOIC

2700–1650 Ma — AᵽmgBR — Metagranitic rocks dominant; may include remnants of Archean rocks

c. 2410 Ma — Widgiemooltha Dyke Suite — ᵽWI-o — Dolerite and gabbro; includes cumulate and granophyric differentiates

2800–1330 Ma — Aᵽxmin-mogAFON, Aᵽxmgn-mwαAFON, Aᵽxmg-moAFON

Aᵽxmin-mogAFON — Meta banded iron-formation, metagabbro and metaleucogabbro; may include metagranite and **Biranup Zone** intrusions

Aᵽxmgn-mwαAFON — Granitic gneiss; quartzofeldspathic gneiss, locally with garnet; amphibolite; metagranite; minor banded meta iron-formation; may include **Biranup Zone** intrusions

Aᵽxmg-moAFON — Metagranitic and metamafic rocks; Archean granite and greenstone and Proterozoic granitic and mafic rocks deformed and metamorphosed during the **Albany–Fraser Orogeny**

Axmog-mαeAFON — Metagabbro and meta-ultramafic rocks; intruded by metagranite

ARCHEAN — NEOARCHEAN

AmgnY, AgY (c. 2706 Ma[1])

AmgnY — Granitic gneiss, locally migmatitic; includes local mafic bands and enclaves

AgY — Granitic rock, undivided; metamorphosed

Atb-xs-c — **TOBIN FORMATION:** wacke, lithic sandstone, siltstone, abundant chert and banded iron-formation, and minor felsic volcaniclastic rocks; metamorphosed

2699–2682 Ma[2 3] — Atp-xf-s — **TOPPIN HILL FORMATION:** felsic volcanic and volcaniclastic rocks, with minor siliciclastic sedimentary rocks; metamorphosed

AmwYYA — Meta-igneous mafic rock; undivided

AmbYYA — Metamafic volcanic rock, undivided

Tectonic units: GUNBARREL BASIN; ALBANY–FRASER OROGEN; Fraser and Nornalup Zones; ARID BASIN; Biranup Zone; BARREN BASIN; Biranup Zone; ALBANY–FRASER OROGEN; Northern Foreland; ALBANY–FRASER OROGEN; Yamarna Terrane; YILGARN CRATON

Fault, major
- thrust, exposed, triangle on upthrown side
- strike-slip, exposed, showing relative dextral horizontal displacement
- strike-slip, exposed, showing relative sinistral horizontal displacement
- thrust, concealed, triangle on upthrown side

Fault
- exposed
- thrust, exposed, triangle on upthrown side
- strike-slip, exposed, showing relative dextral horizontal displacement
- strike-slip, exposed, showing relative sinistral horizontal displacement
- concealed

Fault or shear, major
- exposed
- concealed

Fault or shear
- exposed
- concealed

Shear zone, major
- exposed
- strike-slip, exposed, showing relative sinistral horizontal displacement
- concealed

Shear zone
- exposed
- strike-slip, exposed, showing relative dextral horizontal displacement
- strike-slip, exposed, showing relative sinistral horizontal displacement
- concealed

Fold, showing axial trace
- antiform, exposed
- synform, exposed
- unspecified

Bedding
- trend of bedding

Metamorphic foliation
- trend of metamorphic foliation

Gneissic layering
- trend of gneissic layering

Fracture pattern

Aeromagnetic trend line

Track

MINERAL SITES

MINERALIZATION STYLE
- Orthomagmatic mafic and ultramafic
- Vein and hydrothermal
- Regolith hosted

COMMODITY GROUP
- Precious metal
- Steel alloy metal

COMMODITY

Commodity	Symbol
Chromium	Cr
Copper	Cu
Gold	Au
Heavy minerals	HM
Nickel	Ni
Palladium	Pd
Platinum	Pt

SITE NAME

Mine, deposit, prospect, or occurrence...... Ninja

Mineralization sites on this map have been extracted from GSWA's MINEDEX database. For clarity, names have been shown only for selected sites. Full details of site numbers, site locations, site status, mineralization, and commodities can be obtained from the MINEDEX database, accessed at <http://www.dmp.wa.gov.au/minedex>.

SHEET INDEX

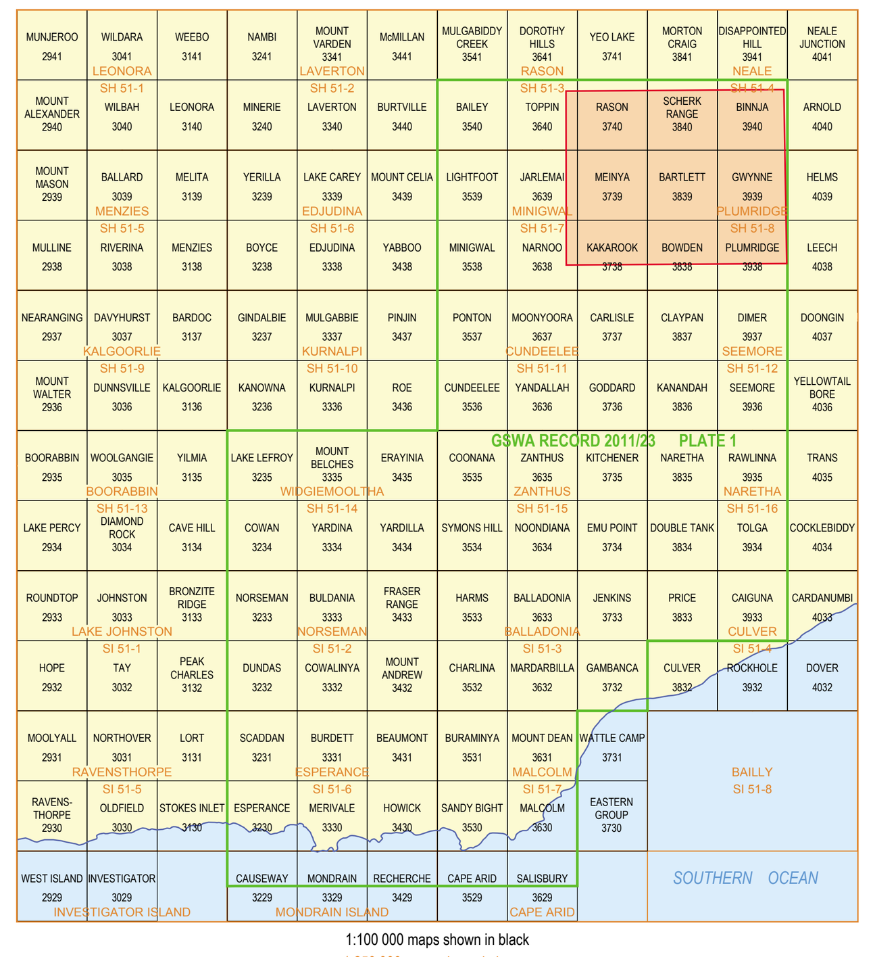

1:100 000 maps shown in black
1:250 000 maps shown in brown
Search for current GSWA map products online <http://www.dmp.wa.gov.au/GSWApublications>

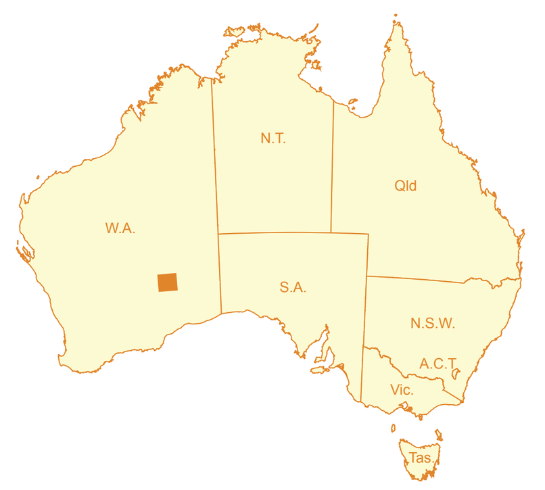

Compiled by CV Spaggiari 2009–11 (Albany–Fraser) and MJ Pawley 2010–11 (east Yilgarn)
Geology by CV Spaggiari and CL Kirkland 2008–11, and MJ Pawley 2008 (Albany–Fraser); CM Doyle and S Jones 2005, MJ Pawley and SS Romano 2008 (east Yilgarn)

Geochronology from GSWA data (published and in preparation) and interpreted from external sources (listed below). Some GSWA geochronology may come from samples obtained on adjoining map sheets. GSWA geochronology data are available online at <http://www.dmp.wa.gov.au/geochron>.

Geochronology by:
(1) Cassidy, KF 2007, GA Sample ID 98967050B: Geoscience Australia's geochronology database, July 2007 data release.
(2) Sircombe, KN et al. 2007, Geoscience Australia, Record 2007/1, p. 169–174.
(3) Sircombe, KN et al. 2007, Geoscience Australia, Record 2007/1, p. 175–180.

Cartography by AK Jones
Edited by K Greenberg and SK Martin
Published by the Geological Survey of Western Australia

This map is published in digital format (PDF) and is available online at <http://www.dmp.wa.gov.au/GSWApublications>.
Copies of this map are available from the Information Centre, Department of Mines and Petroleum,
100 Plain Street, East Perth, WA 6004.
Phone (08) 9222 3459 Fax (08) 9222 3444
Website <http://www.dmp.wa.gov.au/gswa> Email geological.survey@dmp.wa.gov.au

The recommended reference for this map is:
Spaggiari, CV and Pawley, MJ 2012, Interpreted pre-Mesozoic bedrock geology of the Tropicana region of the east Albany–Fraser Orogen (1:250 000), *in* The geology of the east Albany–Fraser Orogen — a field guide *compiled by* CV Spaggiari, CL Kirkland, MJ Pawley, RH Smithies, MTD Wingate, MG Doyle, TG Blenkinsop, C Clark, CW Oorschot, LJ Fox, and J Savage: Geological Survey of Western Australia, Record 2011/23, Plate 2.

DATA DICTIONARY

Theme	Data Currency	Organization
Geology *	2011	Geological Survey of Western Australia, Department of Mines and Petroleum
Mineral sites *	JAN 2012	Geological Survey of Western Australia, Department of Mines and Petroleum

* DMP data can be viewed interactively via GeoVIEW.WA <http://www.dmp.wa.gov.au/geoview>, and related datasets can be downloaded from the GSWA Data and Software Centre <http://www.dmp.wa.gov.au/datacentre>.

Government of **Western Australia**
Department of **Mines and Petroleum**
HON. NORMAN MOORE, M.L.C.
MINISTER FOR MINES AND PETROLEUM

Geological Survey of Western Australia
RICK ROGERSON
EXECUTIVE DIRECTOR

SCALE 1:250 000
2 500 Metres 0 5 10 15 20 25 Kilometres

UNIVERSAL TRANSVERSE MERCATOR PROJECTION
HORIZONTAL DATUM: GEOCENTRIC DATUM OF AUSTRALIA 1994
VERTICAL DATUM: AUSTRALIAN HEIGHT DATUM
Grid lines indicate 20 000 metre interval of the Map Grid Australia Zone 51

GDA — The Map Grip Australia (MGA) is based on the Geocentric Datum of Australia 1994 (GDA94)
GDA94 positions are compatible within one metre of the datum WGS84 positions

GEOLOGICAL SURVEY OF WESTERN AUSTRALIA

RECORD 2011/23 PLATE 2

INTERPRETED PRE-MESOZOIC BEDROCK GEOLOGY OF THE TROPICANA REGION OF THE EAST ALBANY–FRASER OROGEN

June 2012